DEVELOPMENT OF STATISTICAL METHODS FOR MONITORING INSECT ABUNDANCE

Emily Beth Dennis

A Thesis submitted for the degree of

Doctor of Philosophy in

the subject of Statistics

School of Mathematics, Statistics and Actuarial Science

University of Kent

May 2015

Abstract

During a time of habitat loss, climate change and loss of biodiversity, efficient analytical tools are vital for population monitoring. This thesis concerns the modelling of butterflies, whose populations are undergoing various changes in abundance, range, phenology and voltinism. In particular, three-quarters of UK butterfly species have shown declines in their distribution, abundance, or both over a ten-year period. As the most comprehensively monitored insect taxon, known to respond rapidly and sensitively to change, butterflies are particularly valuable, but devising methods that can be fitted to large data sets is challenging and they can be computer intensive.

We use occupancy models to formulate occupancy maps and novel regional indices, which will allow for improved reporting of changes in butterfly distributions. The remainder of the thesis focuses on models for count data. We show that the popular N-mixture model can sometimes produce infinite estimates of abundance and describe the equivalence of multivariate Poisson and negative-binomial models.

We then present a variety of approaches for modelling butterfly abundance, where complicating features are the seasonal nature of the counts and variation among species. A generalised abundance index is very efficient compared to generalised additive models, which are currently used for annual reporting, and new parametric descriptions of seasonal variation produce novel and meaningful parameters relating to phenology and survival. We develop dynamic models which explicitly model dependence between broods and years. These new models will improve our understanding of the complex processes and drivers underlying changes in butterfly populations.

Acknowledgements

I would firstly like to express my gratitude to my academic supervisors, Professor Byron Morgan and Professor Martin Ridout, for their continuous support and insight, as well as Dr Stephen Freeman, Dr David Roy and Dr Tom Brereton for their advice and expertise. It has been a pleasure working with you all. My particular thanks to Byron for your continued guidance, enthusiasm and encouragement, for being an inspiring mentor, and for accommodating my move to the west. My particular thanks also to Stephen and David, for introducing me to the study of butterflies and suggesting a PhD at the University of Kent.

I am grateful to the Engineering and Physical Sciences Research Council (EPSRC), the School of Mathematics, Statistics and Actuarial Science at the University of Kent, and the National Centre for Statistical Ecology (NCSE) for funding my PhD research. I would also like to thank Professor David Elston and Dr Diana Cole for being examiners of my thesis.

Many thanks to the Centre for Ecology & Hydrology/Butterfly Conservation for providing UKBMS and BNM data, and special thanks to the great number of volunteer recorders who give up their time to contribute to these data sets, without which the research presented in this thesis would not have been possible. The UKBMS is operated by CEH, BC and the British Trust for Ornithology and funded by a multi-agency consortium including the Countryside Council for Wales, Defra, the Joint Nature Conservation Committee, Forestry Commission, Natural England, the Natural

Environment Research Council, and Scottish Natural Heritage. Thanks also to Thibaut Couturier for supplying the Hermann's tortoise data.

Thanks to all of my family and friends, with particular thanks to my parents for their unwavering love and support. Most of all thanks to my partner James, for knowing me so well and bringing me happiness.

Contents

List of Figures

List of Tables

List of electronic appendices

Dynamic occupancy maps

We provide dynamic occupancy maps for Wall Brown, Ringlet and Silver-washed Fritillary, based on the occupancy models fitted with varying detection probability in Section 2.4.3.

List of supplementary `R` files

We provide `R` code for the models developed in Chapters 3, 5 and 6.

Chapter 3

`Nmixture_model.r` - contains the likelihood functions for the N-mixture model, for any number of sampling visits, using the multivariate Poisson and negative-binomial formulation, and standard Royle (2004a) formulation.

`Simulation_for_Nmixture.r` - contains code to simulate example data and fit the N-mixture model, using the two different approaches.

Chapter 5

`GAI_model.r` - contains functions for the GAI likelihood, and functions to optimise the concentrated likelihood, including the iterative approach.

`Simulation_for_GAI.r` - contains code to fit the GAI to an example of simulated data.

Chapter 6

`Dynamic_model.r` - contains functions for the dynamic model likelihood, as well as functions to optimise the concentrated likelihood.

`Simulation_for_Dynamic.r` - contains code to simulate example data and fit the dynamic model.

Chapter 1

Introduction

Global biodiversity is acknowledged to be under significant decline (Barnosky et al. 2011), which is projected to continue without greater action to limit anthropogenic climate change (Thomas, C. D. et al. 2004; Pereira et al. 2010). The importance of biodiversity is widely recognised for its multi-faceted rôle in controlling our ecosystems (Chapin III et al. 2000; Díaz et al. 2006). Land-use change, climate change and other human-induced factors have been recognised as important causes of recent declines in biodiversity (Chapin III et al. 2000; Rands et al. 2010).

At a time of climate change and major loss of biodiversity, efficient tools for monitoring populations are paramount. Within statistical ecology various types of data may be collected (King 2014), but in this thesis we focus primarily upon count data, as well as presence/absence records, where individuals within a population may not be identified.

Animal abundance indices, typically derived from count data, are required as a vital source for robust biodiversity indices to help monitor, understand and predict future responses to changes in climate and land-use. Indices contribute to the assessment of progress made towards targets to reduce biodiversity loss at both national (Defra 2013) and global scales (Butchart et al. 2010; Convention on Biological Diversity 2006). In 1993 the Convention on Biological Diversity (CBD; Glowka et al. 1994) came into force as an international treaty which aimed for the conservation and

sustainable use of biological resources. In response to the Convention the UK set up the UK Biodiversity Action Plan (UKBAP; Ruddock et al. 2007) and the use of biodiversity indicators was recommended to measure and communicate progress in reaching biodiversity targets.

1.1 Butterflies

Insects are an important component of our ecosystems and account for a major proportion of the world's biodiversity (Gaston 1991), but many groups are not well monitored. Given the sparsity of data available for many insect taxa, wide scale studies and contributions towards biodiversity goals, such as the UKBAP, are mainly based upon a limited selection of indicator taxa, chiefly butterflies, but also other taxa such as moths, Odonata (dragonflies and damselflies) and bees.

Butterflies are the most comprehensively monitored insect taxon and are hence the most practical insects to study. Butterflies are increasingly recognised as a valuable environmental indicator for changes in biodiversity and phenology because as ectotherms they respond rapidly and sensitively to changes in climate and habitat and act as a representative for other species, particularly other insects (Thomas 2005; Pearman and Weber 2007).

A growing number of participatory schemes for monitoring insects, predominantly butterflies, have been developed (Table 1.1). This thesis will focus on modelling British butterfly data, however butterfly monitoring schemes exist in many countries and continue to be established, hence the methods we develop will have wider applicability. In the UK, abundance indices for butterflies form one of 25 indicators employed by UK government for the assessment of general trends in biodiversity (Defra 2013). Butterfly indicators for the UK and Europe are discussed further by van Swaay et al. (2008) and Brereton et al. (2011b). Monitoring schemes for other insect taxa also exist, for example for moths, dragonflies and bees (Table 1.2). A key element of such schemes is the high level of volunteer participation

Table 1.1: Butterfly monitoring schemes in Europe and beyond. The year that the scheme was established and recent estimate of the number of transects monitored per year are taken from van Swaay and Warren (2012), except where otherwise specified.

Location	Year	Number of transects
Andorra	2004	6
Belgium - Flanders	1991	10
Estonia	2004	11
Finland	1999	65-67
France	2005	611-723
Germany	2005	400
Ireland	2007	190
Israel*	2009	40
Lithuania	2009	14
Luxemburg	2010	30
North America**	Variable	Unknown
Norway	2009	9-18
Russia - Bryansk area	2009	2-14
Slovenia	2007	9-14
Spain - Catalonia	1994	60-70
Sweden	2010	90
Switzerland	2003	90-95
The Netherlands	1990	430
Ukraine	1990	159
United Kingdom***	1976	> 1200

*`http://eubon-ipt.gbif.org/resource.do?r=butterflies-monitoring-scheme-il`

** `http://www.nab-net.org/goal-1`

*** Brereton et al. (2014)

Table 1.2: Sources of count data for other insect taxa in the UK.

Taxon	Scheme	References
Moths	Rothamsted Insect Survey	http://www.rothamsted.ac.uk/insect-survey/ Conrad et al. (2006)
	Garden Moth Scheme	Bates et al. (2013)
Odonata	British Dragonfly Monitoring Scheme	http://www.british-dragonflies.org.uk/content/british-dragonfly-monitoring-scheme
Bees	BeeWalk	http://bumblebeeconservation.org/get-involved/surveys/beewalk/
Aphids	Rothamsted Insect Survey	http://www.rothamsted.ac.uk/insect-survey/

required to gather such large quantities of data. The volunteers are often referred to as citizen scientists (Silvertown 2009; Devictor et al. 2010).

In this thesis we model data for UK butterflies from two different schemes, which are described in Section 1.3. Both data sets consist of citizen science records, but the two schemes require different levels of commitment and effort: count data require greater expertise and commitment, whereas opportunistic records are likely to be made by the general public.

In addition to monitoring schemes which consist of count data, opportunistic recording schemes exist for a variety of taxa, for example in the UK the data for many of these schemes is overseen by the Biological Records Centre, which forms part of the National Biodiversity Network (NBN, `https://data.nbn.org.uk/`). Observation records of this type generally require less commitment from citizen scientists as records are opportunistic. These data are used to study changes in species' distributions, and in this thesis we study distribution data for British butterflies, which we describe in Section 1.3.2.

1.1.1 Changes in abundance and distribution

Over a ten-year period, three-quarters of UK butterfly species have shown declines in distribution, population, or both (Fox et al. 2011a). A recent Red List for the 62 resident and regularly breeding butterflies in Britain showed an increase in the number of species classified as threatened, indicating that four species are Regionally Extinct (Black-veined White, Large Copper, Mazarine Blue and Large Tortoiseshell), 19 are threatened (two Critically Endangered, eight Endangered and nine Vulnerable), and a further 11 species are classified as Near Threatened (Fox et al. 2011c). Excluding the four species extinct from Britain, and including Cryptic Wood White (which was not considered in Fox et al. (2011c)), there are considered to be 59 butterfly species that occur regularly in the UK.

According to the European Red List, across Europe populations of 31% of butterfly species are thought to be declining, with 9% of species classified as threatened and 10% as Near Threatened (van Swaay et al. 2010), but

this may be an underestimate for some species (van Swaay et al. 2011). Analysis of distribution data by Thomas, J. A. et al. (2004) suggested that in Britain butterflies are declining more rapidly than birds and plants.

In response to climate change and habitat loss and deterioration, habitat-specialist species have experienced declines in abundance and distribution, whereas changes for generalists are more variable (Warren et al. 2001). Under recent climate change, distributional shifts have been documented for many species. The Comma, for example, has spread northwards by more than 200 km since 1990 (Thomas and Lewington 2010), an expansion which has been accompanied by an increase in abundance, despite previous decline (Asher et al. 2001). Some butterfly species have expanded northwards and to higher latitudes in response to warmer climates (Parmesan et al. 1999). Northward shifts in range margin have also been found for some moths (Fox et al. 2011b), Odonata (Hickling et al. 2005) and many other taxonomic groups (Hickling et al. 2006).

Despite many species expanding their range northwards, there is also evidence of retractions in range (Thomas et al. 2006). One example species is Grayling, which although widespread in coastal areas, has been mostly lost from inland sites due to loss of suitable habitat and has also shown declines in abundance (Asher et al. 2001). Franco et al. (2006) attributed site extinctions of four butterfly species with southern limits in Britain to both climate warming and habitat loss. Hill et al. (2002) assessed distributional changes for British butterflies, predicting that with limited opportunity to expand northwards, and possible retraction at southern margins, northerly distributed species are likely to fare worse under climate change. Species with southern distributions have the potential to shift northwards, leading to either similar or increased range sizes, depending on whether southern sites are lost. Dapporto and Dennis (2013) reported that the most negative distribution trends for UK butterflies were associated with so-called mid generalists, whereas specialist species benefit from conservation measures.

Warren et al. (2001) and Dapporto and Dennis (2013) suggest that changes in abundance and distributions tend to have strong positive correla-

tion, however Mair et al. (2012) found that for British butterflies northward shifts in range margin were not always accompanied by increases in overall distribution or abundance. An in-depth discussion of possible drivers of changes in the distributions of UK butterflies is given by Asher et al. (2001).

Butterfly populations are known to fluctuate with weather conditions (Pollard and Yates 1993). Pollard (1988) studied associations between butterfly populations and weather, and mainly concluded a causal link between warm summers and population values. This association was confirmed for a longer dataset by Roy et al. (2001), who predicted increases for the majority of species under future warmer climates. However relationships with winter weather are disputed (Roy et al. 2001; Dennis and Sparks 2007; Isaac et al. 2011b).

1.1.2 Changes in phenology

Increasing temperatures under recent climate change have given rise to advances in phenology, the seasonal timing of events such as timing of flowering, breeding or emergence, for various taxa (Walther et al. 2002; Parmesan 2007).

A number of studies have compared phenological changes for butterflies with changes in climate. Sparks and Yates (1997) studied historical phenological records for 12 British butterflies and suggested that "climate warming of the order of 3°C could advance butterfly appearance by two to three weeks". Analysis for 35 species over a longer time period predicted that a warming of the order of 1°C could lead to advances of 2-10 days for most butterflies (Roy and Sparks 2000). Botham et al. (2008) found that species that fly earlier in the year have shown the greatest advances in their flight periods, which may be explained by proportionally greater increases in spring temperatures compared to summer temperatures. Increases in the duration of flight periods were also found. There is also evidence for advances in flight period for butterflies in Spain (Stefanescu et al. 2003), California, USA (Forister and Shapiro 2003) and Sweden (Karlsson 2014). Spatial variation in phenology has also been found, with a tendency for

some (but not all) species' flight period to be earlier in the south relative to the north (Roy and Asher 2003). Analyses by Diamond et al. (2011) and Altermatt (2010b) also suggest that species' traits, such as overwintering stage and diet, may influence changes in species' phenology in response to climate change.

Phenological studies for butterflies have typically involved measures such as mean first appearance, mean peak appearance and mean length of the flight period, which could present bias, for example through observer behaviour. The date of first appearance may be influenced by variation in abundance (Roy and Sparks 2000), variation in voltinism, or an increase in the number of monitored sites (van Strien et al. 2008).

Hodgson et al. (2011) utilised generalised additive models (GAMs) to model both spatial and temporal variation in species' seasonal pattern, and hence observe phenological changes, such as variation in the number of generations per year, which we will discuss in Section 1.1.3. Suitable models for phenology might improve the estimation and prediction of changes, and assist the study of potential implications of phenological changes, such as phenological mismatch. For example, Hindle et al. (2014) suggest the possibility of phenological mismatch between the emergence of Marbled White and the species' main nectar source.

1.1.3 Voltinism

As is true of many insects, butterfly life-cycles vary from one adult generation per year (univoltine), two per year (bivoltine), or more than two per year (multivoltine). The majority of UK butterflies are univoltine, with 11 bivoltine species and a further few species with complex/multivoltine life-cycles, such as Small Heath and Speckled Wood (Pollard and Yates 1993). Voltinism is known to vary with climatic conditions (Pollard and Yates 1993), hence for some species the number of annual broods can vary with space and time. For example, Common Blue exhibit two broods in southern Britain, reducing to a single brood in the north (Asher et al. 2001; Hodgson et al. 2011).

Given advances in flight period, which prolong the length of the season, some species are showing increases in voltinism by additional generations. Some species have also shown increases in the relative size of subsequent generations. Altermatt (2010a) evaluated changes in voltinism for 263 butterfly and moth species in Central Europe. Kernel density estimates of occurrence record dates were used to identify peaks in the seasonal pattern, although second and subsequent generations were pooled. For 72% of species the second/subsequent generations had become more pronounced. Additionally, 44 univoltine or bivoltine species were found to have gained an additional brood relative to before 1980. Increases in voltinism have also been found for Finnish moths (Pöyry et al. 2011) and Hodgson et al. (2011) also found that the number of peaks in the seasonal pattern varied with space and/or time for 7 out of 15 UK butterfly species considered.

Many phenological studies for butterflies have not considered the timing of separate broods, although Botham et al. (2008) split the data for bivoltine but not multivoltine species. Some studies have taken metrics over the whole flight period (for example Roy and Sparks 2000), whereas others have only considered the first brood (Karlsson 2014), or excluded multivoltine species from the analysis (for example Roy and Asher 2003; Stefanescu et al. 2003).

1.1.4 Modelling butterfly abundance

Here we provide background to the work in this thesis by exploring pre-existing models for butterfly abundance. A key challenge when modelling the abundance of insects such as butterflies is the seasonal nature of the data. Counts are usually only made of the most visible adult stage of the life-cycle, but typically for multiple visits within the flight period. For each brood within a given season, counts generally increase from zero and then decrease to zero corresponding to the emergence and death of adult butterflies. Methods for modelling this type of data need to account for such seasonal variation, in addition to potential between-year variation.

A range of models have been proposed to describe the pronounced within-year variation in counts. In the calculation of abundance indices

for UK butterflies, generalised additive models (GAMs) are used (Rothery and Roy 2001) to describe the seasonal variation non-parametrically. A spline is fitted to data from multiple sites to estimate a seasonal pattern for each year. Brewer (2008) explored the use of generalised estimating equations for describing within-season correlation in data for Small Heath.

Empirical methods, such as GAMs, can only estimate relative abundance, and provide no additional demographic information. The model defined by Zonneveld (1991) and related to that of Manly (1974) estimates abundance, mortality rate, day of peak emergence and the variance in emergence, and is implementable via the Insect Count Analyzer (INCA; 2011). The model is based upon a differential equation that describes the variation in counts over a season, where the associated integral requires numerical integration. The strong assumptions of the model have been highlighted (Haddad et al. 2008; Gross et al. 2007; Calabrese 2012), namely that emergence is logistically distributed and death rate is constant. Calabrese (2012) generalised the Zonneveld (1991) model to allow for asymmetric emergence patterns and age-dependent death rate, but found that the newly associated parameters were not consistently identifiable from count data alone. Consequently, as discussed in a review of methods for monitoring butterflies (Nowicki et al. 2008), the Zonneveld (1991) model remains difficult to apply and has not been widely adopted, and Nowicki et al. (2008) suggest that "finding an effective way to estimate longevity with transect counts seems impossible".

Soulsby and Thomas (2012) developed a model also based on a differential equation for describing the seasonal variation in counts, but allowed only for discrete, non-overlapping generations and claimed the methods are not applicable to data for species observed only in small numbers. Survival was also assumed to be constant, and model estimation required potentially complicated step-wise numerical integration for non-constant survival.

Butterfly abundance has also been studied in the context of smaller-scale mark-release-recapture (MRR) studies. For example Nowicki et al. (2009) studied the influence of density-dependence on the butterfly populations of

two species, surveyed intensively for 12 years. Nowicki et al. (2008) review MRR sampling as a method for modelling butterfly abundance, but in this thesis we focus on modelling butterfly abundance from counts of unmarked individuals since optimal methods are needed for these data, which are readily available from large-scale, long-term monitoring programs.

1.2 Thesis motivation and aims

This thesis primarily aims to develop new statistical methods for modelling the abundance and distribution of butterflies. Climate change is predicted to become an increasingly important cause of biodiversity decline and new statistical methods are needed to model and predict species' complex responses. The majority of studies are based on a single or small number of species, or limited timespan, and feasibility of application to a greater dataset is unclear. We focus on developing methods that will be broadly applicable to many species, despite much variation, for example in abundance, life-cycle and habitat preferences.

Given the efforts of many volunteer contributors, huge sources of data are available for UK butterflies, hence statistical techniques are required to exploit the information fully. The previous approach used for deriving UK butterfly abundance indices, for example, was not able to make use of all data collected. Consequently this thesis develops new methods, which can be applied to all data collected for multiple species, across many years and sites, with relative efficiency and accuracy. This has particular relevance for the analysis of data from long-term monitoring schemes where efficient methods will lead to faster outputs and feedback of results to recorders and policy makers. The provision of feedback to recorders is essential for the motivation and retention of participants in citizen science projects.

In addition to improving efficiency, we aim to develop models which may address the "lack of mechanistic understanding about factors driving butterfly population dynamics' over large spatial and temporal scales' (Isaac et al. 2011b). By considering both within- and between-year varia-

tion in populations, we aim to describe the underlying processes determining changes in abundance, demography and phenology, rather than solely describe the count data empirically. Predicting variation in seasonal patterns using GAMs, as in Hodgson et al. (2011), allows for changes in phenology and voltinism to be visualised, but not simply quantified. We aim to develop parametric approaches for modelling seasonal variation in butterfly abundance, with the aim of producing estimates of meaningful and relevant parameters. Limited focus has previously been placed on explicitly modelling bi- or multi-voltine data, and how climate change may affect different broods and their dependence.

In this thesis we develop robust and flexible frameworks for modelling butterfly count data, which can be modified according to the purpose of a particular study or application. In doing so, further application of the models may provide new insights relevant to the monitoring and conservation of seasonal insects, such as butterflies.

We also develop recommendations for optimal modelling of the spatial distribution of UK butterflies. Modelling of UK butterfly occupancy has to date been fairly limited and is needed to provide more accurate assessments of change. Suitable methods for modelling spatio-temporal variation can enhance the study of changes in distribution and range dynamics in the monitoring of responses to changes in climate and habitat.

The development of new models that are suitable for describing count data requires knowledge about common models in this area, and their potential relevance for butterflies. Hence we additionally consider performance of the N-mixture model (Royle 2004a), which models abundance and detectability from repeated counts made at a set of sites. The N-mixture model is a popular tool for modelling abundance, and is hence of interest for conservation and management. Although not directly applicable for typical butterfly count data, due to their seasonal variability in numbers, we see that the N-mixture model links with aspects of the models developed for butterfly data in this thesis. Furthermore, future application to insects may be possible with adaptation of the model.

We develop a variety of modelling approaches with the aim of introducing new models that are both more efficient and more informative, and applicable to all species, with possible adaptation where required. We suggest avenues for further work throughout this thesis. The topic of each chapter could be explored in greater depth, but had this been done the full range of different models proposed in this thesis would not have been realised.

1.3 Data for UK butterflies

In this thesis methods are applied to count and observation data for UK butterflies, which are summarised in Table 1.3, and described in further detail in this section. As mentioned in Section 1.3.3, in this thesis we do not study the WCBS data. Latin names for the UK butterfly species mentioned and/or studied in this thesis are given in Table 1.4.

1.3.1 UK Butterfly Monitoring Scheme

Count data for UK butterflies are principally gathered through the UK Butterfly Monitoring Scheme (UKBMS), an intensive, wide-scale system of weekly transect walks which began in 1976. The scheme design allows for counts to be made throughout the season for butterfly activity, during which abundance will vary according to different seasonal patterns of emergence. Recorders make counts of observed butterflies within a set limit (an estimated distance of five metres ahead and to the sides of the recorder) along a fixed line transect route under favourable conditions. Counts are taken weekly during the main butterfly flight period from the beginning of April until the end of September, within specified periods of the day and when weather conditions are suitable for butterfly activity. Transects are typically 2-4 km long and divided into a maximum of 15 sections which correspond to different habitat or management units, though in this thesis we aggregate counts for all sections within a transect. The UKBMS transect method (Pollard Walks) is described in depth by Pollard and Yates (1993),

Table 1.3: Summary of the primary sources of data for UK butterflies.

Scheme	Description	Chapter(s)
UK Butterfly Monitoring Scheme (UKBMS)	Long-term network of over 1200 self-selected sites each monitored weekly (April-September) under standardised conditions. Established in 1976. Counts are used to report trends in abundance annually (Brereton et al. 2014). Over 17 million butterflies have been counted (Botham et al. 2013a).	4, 5 and 6
Butterflies for the New Millennium (BNM)	Ad-hoc observation records submitted by the public. Formally created in 1995. Consists of over 7.5 million observation records (Asher et al. 2011). Used for mapping species distributions (Asher et al. 2001) and estimating simple trends (Fox et al. 2011a).	2
Wider Countryside Butterfly Survey (WCBS)	A reduced-effort scheme launched fully in 2009 (Brereton et al. 2011a). At least two visits are made per year to randomly-selected 1 km squares. Aims to reduce bias within UKBMS towards sites of specific interest and improve recording of wider countryside species. Combined with UKBMS data in recent reporting (Brereton et al. 2014).	-

Table 1.4: Latin names of the UK butterfly species mentioned and/or studied in this thesis, grouped by taxonomic family. Species that are extinct in the UK (Section 1.1.1) are denoted by *.

Taxonomic family	Species	Latin name
Hesperiidae	Small Skipper	*Thymelicus sylvestris*
Lycaenidae	Adonis Blue	*Polyommatus (Lysandra) bellargus*
	Brown Argus	*Aricia agestis*
	Brown Hairstreak	*Thecla betulae*
	Chalkhill Blue	*Polyommatus (Lysandra) coridon*
	Common Blue	*Polyommatus icarus*
	Green Hairstreak	*Callophrys rubi*
	Holly Blue	*Celastrina argiolus*
	Large Blue	*Phengaris (Maculinea) arion*
	Large Copper*	*Lycaena dispar*
	Mazarine Blue*	*Polyommatus (Cyaniris) semiargus*
	Purple Hairstreak	*Favonius quercus*
	Small Blue	*Cupido minimus*
Nymphalidae	Comma	*Polygonia c-album*
	Dark Green Fritillary	*Argynnis aglaja*
	Large Tortoiseshell*	*Nymphalis polychloros*
	Marsh Fritillary	*Euphydryas aurinia*
	Painted Lady	*Vanessa (Cynthia) cardui*
	Red Admiral	*Vanessa atalanta*
	Silver-washed Fritillary	*Argynnis paphia*
	Small Tortoiseshell	*Aglais urticae*
	White Admiral	*Limenitis camilla*
Pieridae	Black-veined White*	*Aporia crataegi*
	Brimstone	*Gonepteryx rhamni*
	Cryptic Wood White	*Leptidea juvernica*
	Green-veined White	*Pieris napi*
	Small White	*Pieris rapae*
Satyridae	Gatekeeper	*Pyronia tithonus*
	Grayling	*Hipparchia semele*
	Marbled White	*Melanargia galathea*
	Ringlet	*Aphantopus hyperantus*
	Scotch Argus	*Erebia aethiops*
	Small Heath	*Coenonympha pamphilus*
	Speckled Wood	*Pararge aegeria*
	Wall Brown	*Lasiommata megera*

and has been shown to provide a good representation of large-scale trends in abundance for most species (Isaac et al. 2011a). Two reduced-effort methods are also used to aid the monitoring of a small number of habitat-specialist species: adult timed counts and larval web counts (Brereton et al. 2014), but in this thesis we do not consider these data.

The main objective of the UKBMS is to provide data for assessment of the status and trends in the abundance of UK butterfly species for both conservation and research purposes. Abundance estimates derived from the UKBMS data play an important rôle in acting as indicators for trends in biodiversity, habitat change and climate change (Brereton et al. 2011b). In 2013, population trends could be calculated for 56 of the 59 butterfly species regularly found in the UK, to demonstrate whether the overall abundance of each species has changed over time (Brereton et al. 2014).

The scheme began in 1976 with 34 sites, but the network has grown steadily to over 1000 sites recorded each year (1212 sites in 2013, of which 130 were monitored using reduced effort methods, Brereton et al. 2014). A large network of recorders has contributed to the UKBMS, making around a quarter of a million weekly visits in total to almost 2000 sites and counting over 17 million butterflies (Botham et al. 2013a). Ideally, an annual index of abundance for each site may be calculated as the sum of the weekly counts; the scheme design is for a count to be made in each of 26 weeks. Inevitably, some weeks of the transect season are missed due to unsuitable weather conditions or recorder unavailability, for example due to illness or holidays, and hence fewer than 26 counts per year are typically made at each site, and require suitable interpolation.

Past and present methods for deriving indices of abundance from UKBMS data will be reviewed in Chapter 4.

1.3.2 Butterflies for the New Millennium

The Butterflies for the New Millenium (BNM) database was formed in 1995 and consists of over 7.5 million ad-hoc observation records submitted mostly by volunteer members of the public (Asher et al. 2011). The dataset also

consists of historical records prior to 1995, but the scheme has grown significantly since it was formally created as the BNM in 1995. The BNM provides a much greater geographical coverage of the UK compared to the UKBMS data, for which around 1200 self-selected sites are monitored intensively each year (Brereton et al. 2014). The majority of BNM records arise from opportunistic recording following no structured format, compared to the UKBMS which follows a standardized scheme design.

The BNM data are used for mapping species distributions across the UK. In particular, broad trends between multi-year survey periods have been studied (Warren et al. 2001; Fox et al. 2007, 2011a), and atlases are also produced from BNM records (Asher et al. 2001). Asher et al. (2011) assessed the proportional change in species' national distributions between 1995-9 and 2005-9. The change in range for each species was calculated as the percentage change in species occupancy between the two time periods, where occupancy was derived in terms of the number of occupied 10 km squares at which the species has been recorded in both time periods.

Similar analyses have been made for changes in the distributions of UK moths and dragonflies (Hickling et al. 2005; Fox et al. 2011b). Hickling et al. (2005) studied British Odonata species using data at a 10 km resolution from the Biological Records Centre for two ten-year periods (1960-1970 and 1985-1995). Fox et al. (2011b) presents initial results from the National Moth Recording Scheme, which was set up in 2007 and also worked at a 10 km resolution. Despite being collected in an unstandardised manner, records from the BNM scheme are available in large numbers and are hence likely to hold much information that may not currently be being put to optimal use.

Pagel et al. (2014) present a hierarchical model that describes temporal variation in range size and abundance by combining BNM data with UKBMS data for Gatekeeper, but the approach may not be readily applicable to species without considerable data available.

1.3.3 Wider Countryside Butterfly Survey

A new reduced-effort scheme, the Wider Countryside Butterfly Survey (WCBS), was piloted in 2007 and fully launched in 2009 (Brereton et al. 2011a). The scheme aims to reduce the current bias in the UKBMS arising from uneven sampling of wider countryside species, due to the self-selection of sites. In particular the UKBMS sites are biased towards sites of specific interest and rich in butterflies, such as protected areas. Protected areas have been shown to support greater populations than non-protected areas (Gillingham et al. 2014) and potentially facilitate range expansions (Thomas et al. 2012).

The WCBS involves making at least two visits within July and August to a randomly-selected 1 km square. The sampling design is broadly similar to that adopted for the Breeding Bird Survey (BBS) which is coordinated by the British Trust for Ornithology (BTO) and hence provides an opportunity for BTO recorders to monitor butterflies in addition to birds (Risely et al. 2011). Roy et al. (2014) found comparable trends from the two schemes in a study of 26 butterfly species between 2009 and 2013 when both schemes were operating, although changes were greater on WCBS transects for 17 of the species considered. The WCBS data have recently been used in conjunction with UKBMS data in the annual reporting of wider countryside species (Brereton et al. 2014), using the two-stage GAM approach described in Section 4.1.3 of this thesis.

In this thesis we focus on UKBMS and BNM data, however the WCBS could be incorporated with the UKBMS data in the methods presented, to reduce the current sampling bias by covering both protected areas and the wider countryside.

1.4 Thesis structure

This thesis consists of five core chapters.

In Chapter 2 we explore the performance of occupancy models applied to opportunistic distribution records for UK butterflies. Due to the unstan-

dardised nature of the BNM, only records of species' presence are made, and hence there is a lack of information on where species are absent, therefore a benchmarking approach is taken (Kéry et al. 2010b). The production of annual maps of occupancy probability and associated errors is demonstrated. These maps are also visualised as dynamic maps which change each year. Furthermore we derive novel occupancy indices, which we produce for different regions of the UK, as well as the UK as a whole.

In Chapter 3 we consider the N-mixture model, which is a widely used method for estimating the abundance of a population in the presence of unknown detection probability, from only a set of counts subject to spatial and temporal replication (Royle 2004a). We show that particularly when detection probability and the number of sampling occasions are small, infinite estimates of abundance can arise. We explain the equivalence of N-mixture and multivariate Poisson and negative-binomial models, which provides new approaches for fitting these models. The methods in Chapter 3 are illustrated by a simulation study and an analysis of data on Hermann's tortoise *Testudo hermanni*. The work in Chapter 3 has been published in *Biometrics* (Dennis et al. 2015b), as an open-source paper. Aspects of the models fitted in Chapter 3 have links with the models in the later chapters of the thesis.

Chapters 4-6 focus on modelling the relative abundance of butterflies from count data, namely from the UKBMS. In Chapter 4 we describe past and recent models developed for butterfly abundance. We detail a two-stage approach that uses Generalised Additive Models (GAMs) to describe the annual seasonal variation in count data for butterflies. This approach is published in *Methods in Ecology and Evolution* (Dennis et al. 2013), and is currently the adopted method for analysing national butterfly data in the UK, contributing to annual national reports (Botham et al. 2013b; Brereton et al. 2014). In addition the methods in (Dennis et al. 2013) are in wider use in Europe and North America. These methods provide foundations for comparison with the new models in this thesis.

In the latter part of Chapter 4 we describe a 'stopover' model approach

for describing butterfly count data which estimates relevant parameters, such as times of emergence within the season and survival. This method was published in Matechou et al. (2014), for which I performed the application to UKBMS data. The stopover model is revisited in the later chapters of this thesis, where further applications are made, as well as modifications of the model.

Chapter 5 presents a novel generalised abundance index (GAI) within a general framework which encompasses both parametric and non-parametric approaches for describing seasonal variation in butterfly counts. We show how the use of concentrated likelihood techniques leads to very efficient model fitting, compared to previous modelling techniques which can be highly time consuming. The work in this chapter has been submitted to the *Annals of Applied Statistics* (Dennis et al. 2014).

Chapter 6 builds on the models in Chapter 5 to produce dynamic models, which describe data from all years simultaneously. Novel estimates of annual productivity are produced. We extend the model to bivoltine species, where productivities are estimated separately for each brood, and extended indices which indicate contributions from different broods are devised. We illustrate the incorporation of relevant covariates within the model. The work in this chapter has been submitted for publication in *Journal of Agricultural, Biological, and Environmental Statistics* (Dennis et al. 2015a).

Associated `R` code is provided as an electronic appendix to this thesis. These files are listed and briefly described on page xx of this thesis.

Chapter 2

Occupancy modelling

The study of species distributions is an important and continually growing area in ecological research, allowing the investigation of factors affecting species occurrence, as well as analysis of changes in species' range and distribution. Given the changes in distribution of UK butterflies, such as those described in Chapter 1, this chapter is motivated by a need to devise suitable methods to analyse and understand these changes. As in the case of UK butterflies, for BNM data the primary source of distribution data available often consists of opportunistic, citizen-science type records (Hochachka et al. 2012), for which typical occupancy models requiring presence-absence data are not directly suitable (MacKenzie et al. 2003).

This chapter investigates the performance of occupancy models in the context of modelling the distribution of UK butterflies from opportunistic records. In Section 2.1 we provide a general review of the methods suggested in recent literature for modelling occupancy in situations where typical presence-absence records are not available. In Section 2.2 we describe the two potential modelling approaches that we will consider, namely a presence-only model (Royle 2004a) and a presence-absence model, which requires the presence records of other "benchmark" species for absence information (Kéry et al. 2010b). In Sections 2.3 and 2.4 we apply these methods to BNM data and compare their performance. This includes a demonstration of the use of standard error maps to accompany maps of occupancy and

we also explore the effects of varying benchmarking and detection probability. In Section 2.4.4 we develop occupancy indices on a national and regional basis, before concluding this chapter with a discussion.

2.1 Background

The BNM scheme consists of opportunistic observation records of UK butterflies, used for mapping species distributions (see Chapter 1). Despite the large source of information available from the BNM, modelling of UK butterfly distributions, particularly on a large scale, has to date been limited, possible due to the difficulties proposed in modelling ad-hoc data. Static maps of observations inform changes in distribution and range, which contribute to monitoring and conservation efforts, for example by studying broad trends between multi-year survey periods. However, simple analyses such as these generally ignore annual changes in distribution. Furthermore, maps of observation locations in their raw form can only display the range at which a species is detected, which may not necessarily correlate well with the actual underlying distribution. In this chapter we investigate the performance of occupancy models for providing new and improved descriptions of UK butterfly distributions.

Accurate estimation and modelling of distributions is important for assessing levels of change, be it contractions in response to degradation of habitats or expansions in response to climate warming, which may open up new locations for colonization (Warren et al. 2001). Effective modelling may also be beneficial for the assessment of the performance of conservation efforts for declining species.

Numerous approaches to species distribution modelling have been proposed (Elith et al. 2006; Warton and Aarts 2013), although many do not explicitly estimate the probability of occurrence of a species, in particular by not formally accounting for imperfect detection. In a review of 108 recently published articles that use MaxEnt, a popular machine-learning procedure for modelling presence-only data (Phillips et al. 2006), Yack-

ulic et al. (2013) found that 36% discarded absence information by using a presence-only framework and only 14% mentioned detection probability. Ignoring imperfection detection can influence estimates of occupancy (Kéry 2011; Guillera-Arroita et al. 2014b; Lahoz-Monfort et al. 2014), which is demonstrated with occupancy maps by Kéry et al. (2013).

Royle et al. (2012) proposed a model (with the `maxlike` package in `R`) for estimating occupancy without the need for absence information, but under certain model assumptions. The paper provides a critical review of MaxEnt, which does not directly estimate the probability of occurrence. The two methods are applied to data from the North American Breeding Bird Survey and compared to estimates from a presence-absence approach. Estimates from MaxEnt were found to under-estimate prevalence when compared with estimates from the presence-absence data, which were similar to estimates from the presence-only model.

In further applications, Maxlike has also generally been compared to MaxEnt. Merow and Silander (2014) discuss similarities between Maxlike and MaxEnt and suggest that Maxlike can perform well for large data sets, but note that there can be high variability in estimates of an intercept parameter. Hastie and Fithian (2013) criticise the parametric assumptions of Maxlike, in particular the assumption of a linear logistic form. Higa et al. (2015) showed that Maxlike is sensitive to spatial bias in sampling effort. Despite it's potential fragility, Maxlike has been adopted successfully for multiple applications (Sarre et al. 2013; Flockhart et al. 2013), and was preferred to MaxEnt by Fitzpatrick et al. (2013).

Yackulic et al. (2013) highlight potential flaws and assumptions associated with the use of MaxEnt and recommend the use of a presence-absence framework where possible. Point process models offer another approach for modelling presence-only data (Warton and Shepherd 2010; Chakraborty et al. 2011), and have been shown to have equivalence or relation to other methods (Aarts et al. 2012; Renner and Warton 2013; Fithian et al. 2013), however only relative occurrence can be estimated by Maxent and these approaches (Guillera-Arroita et al. 2014a).

When presence-absence information with replicate observations is available, site-occupancy models are recommended (Kéry 2011; Yackulic et al. 2013), as they provide for inference on a defined parameter for occupancy, as well as allowing for imperfect detection. Van Strien et al. (2013) discuss the biases associated with opportunistic citizen science data which can be addressed with the aid of occupancy models, namely geographical bias in the distribution of surveyed locations, observation bias via variation in observer effort, and reporting bias where observers may not record all species observed. To our knowledge, comparison of Maxlike with site-occupancy models has been limited, most likely because the presence-only model is typically needed when only presence information is available. Ferrer-Paris et al. (2014) fitted both Maxlike and site-occupancy models, but to data from different time scales.

Nowicki et al. (2008) advocate the use of occupancy models for modelling butterfly distributions, but the BNM data in their raw form contain only presence information. However, site-occupancy models (MacKenzie et al. 2003) which require presence-absence data can be applied to opportunistic observations by employing recorded sightings of other, "benchmark" species to provide the absence (non-detection) records (Kéry et al. 2010b; Hill 2011). The sightings of other species therefore provide information on where the target species has not been recorded, and can also be used to estimate detection probability by forming repeated visits within a period of temporal closure, where the occupancy status does not change. So, for example, at a particular site a record of $1, -, 0, 0$, would represent the scenario where i) the target species was observed at the site on the first occasion in the season, ii) the site was not visited on occasion 2 (or no species were detected if the site was visited), iii) at least one other species (other than the target species) was observed at the site on occasions 3 and 4. Some within-season replication is required in order to separate detection probability from occupancy probability, but not necessarily at all sites.

A benchmarking approach will be optimal when all detected species have been recorded, although this may not always be the case for opportunistic

data, for example species of particular interest may be recorded, rather than every common species that was observed. Estimates based on records of only one-species or short lists (where only a selection of species are recorded if observed) have shown imprecision (van Strien et al. 2010), and Kéry et al. (2010b) advise that all observed species are recorded. However variation in the length of the lists of species observed at each site has been accounted for by Szabo et al. (2010) and van Strien et al. (2013).

Site-occupancy models with benchmarking have been applied to opportunistic records of various taxa including dragonflies, butterflies and birds (van Strien et al. 2010, 2011; Kéry et al. 2010a,b). Van Strien et al. (2013) found that estimates of distribution trends from occupancy models fitted to opportunistic data for butterfly and dragonfly species in the Netherlands were reliable compared with trends from monitoring data. A recent simulation study also favoured occupancy models for estimating robust distribution trends from opportunistic data (Isaac et al. 2014). An alternative method defined by Hill (2011), which is known as *Frescalo*, also performed well for Isaac et al. (2014). Here recorder intensity is described by the proportion of benchmark species observed at similar sites within the neighbourhood surrounding a given location.

Previous applications of site-occupancy models using benchmarking have frequently involved fitting dynamic occupancy models (MacKenzie et al. 2003; Royle and Kéry 2007), but in this chapter, for comparison with the presence-only model, we apply standard site-occupancy models separately to data for each year. Kéry et al. (2013) demonstrated the use of dynamic occupancy models for mapping the range of the European crossbill *Loxia curvirostra*, but in other studies the focus tends to have been placed upon solely temporal change in occupancy (via time series), or spatial change within a single year. Although there have been many applications of site-occupancy models using benchmarking, in this chapter we have the specific aim of modelling butterfly distributions from the BNM data, in order to produce appropriate maps and indices, to aid the monitoring of species' distributions and ranges.

For UK butterflies, we are interested in estimating spatial occupancy for a given species for each year. Despite the controversy concerning the use of Maxlike, we nonetheless test the performance of this method for BNM data, and make a comparison with fitting occupancy models, using benchmarking to obtain absence information. In Section 2.3.1 we explore whether varying the chosen benchmark species affects output from the occupancy models.

Upon identifying a favoured method (Maxlike or occupancy models using benchmarking), we will then create new dynamic maps which change annually, as well as devise concise summaries of regional changes in the form of novel occupancy indices. Analyses of BNM data have generally been at a coarse scale, such as 10 km, however Cowley et al. (1999) showed that sampling at the 10 km scale may under-emphasize local declines in abundance. Hence in this analysis we will work at a finer 1 km scale to predict spatial occupancy for UK butterflies, given that most BNM records are at this scale (or finer). Thus the set of all UK 1 km squares at which butterflies have been recorded form the sites for this occupancy study, and we estimate occupancy for all 1 km squares in the UK (excluding Northern Ireland).

2.2 Methods

We now outline two modelling approaches, namely the presence-only approach and the site-occupancy model approach, which we will use by benchmarking.

2.2.1 Presence-only model

Royle et al. (2012) present a method for the estimation of the probability of occurrence, ψ, from presence-only data using a conventional likelihood approach. The data are assumed to have been collected under random sampling and the probability of species detection is assumed constant.

Under presence-absence sampling, at each sampled location, x, a random variable, y, is observed as zero or one according to the species true presence

or absence (assuming perfect detection). In this instance we can assume

$$y(x) \sim \text{Bernoulli}(\psi(y \mid x)),$$

where $\psi(y \mid x) = \Pr(y(x) = 1)$, is the probability that location x is occupied.

For presence-only data, the target species is observed present at all sampled locations, $x_1, \ldots, x_n$, and hence $y = 1$ with probability 1, for all x_i. Hence x_i represent a sample from all possible spatial values $\mathcal{X}$ which is biased towards locations at which the species of interest is present. Using $\pi()$ and $\psi()$ to represent probability distributions for x and y, respectively, then using Bayes rule, as described in Royle et al. (2012), gives

$$\pi(x \mid y = 1) = \frac{\psi(y = 1 \mid x)\pi(x)}{\psi(y = 1)}.$$

Here $\psi(y = 1)$ is the marginal probability that a location is occupied, which can be expressed by

$$\psi(y = 1) = \sum_{x \in \mathcal{X}} \psi(y = 1 \mid x)\pi(x).$$

Given that $\pi(x)$ describes the possible values of x, under random sampling $\pi(x)$ will be constant. Hence, at a given location x_i, where $i = 1, \ldots, n$,

$$\begin{aligned}\pi(x_i \mid y_i = 1) &= \frac{\psi(y_i = 1 \mid x_i, \boldsymbol{\beta})\pi(x_i)}{\sum_{x \in \mathcal{X}} \psi(y = 1 \mid x; \boldsymbol{\beta})\pi(x)} \\ &= \frac{\psi(y_i = 1 \mid x_i, \boldsymbol{\beta})}{\sum_{x \in \mathcal{X}} \psi(y = 1 \mid x; \boldsymbol{\beta})},\end{aligned}$$

where the occupancy probabilities depend on parameters, $\boldsymbol{\beta}$. For a presence-only sample at n locations, the likelihood to be maximised is

$$\mathrm{L}_{PO}(\boldsymbol{\beta}; \{x_i\}) = \prod_{i=1}^{n} \frac{\psi(y_i = 1 \mid x_i; \boldsymbol{\beta})}{\sum_{x \in \mathcal{X}} \psi(y = 1 \mid x; \boldsymbol{\beta})}.$$

The parameters $\boldsymbol{\beta}$ typically describe a relationship with covariates, for example using a logit link, as

$$\text{logit}(\psi(y_i = 1 \mid x_i; \boldsymbol{\beta}))) = \beta_0 + \sum_{m=1}^{M} \beta_m w_{i,m},$$

where β_0 is an intercept and $\beta_1, \ldots, \beta_M$ are coefficients for each of the M site-specific covariates, $w_{i,m}$. The model currently excludes inference on

detection probability, p, which cancels out from $\mathrm{L}_{PO}(\boldsymbol{\beta})$ when assumed to be constant. However it may be possible for detection probability to vary with covariates independent of those that determine occupancy (Yackulic et al. 2013). In this chapter we denote the presence-only model by PO.

2.2.2 Site-occupancy model

Unlike the PO model, the site-occupancy model (MacKenzie et al. 2003) requires non-detection records, as well as replication with a period of closure, where the occupancy status of the species at each site does not change. As described in Section 2.1, for opportunistic records non-detection records can be created from detections of benchmark species (Kéry et al. 2010b).

For records made at S sites, each surveyed T times, and an encounter history $\mathbf{y}_i = \{y_{i,j}; j = 1, 2, \ldots, T\}$ for the ith site, the individual encounter history probability is given as

$$\Pr(\mathbf{y}_i \mid z_i = 1) = \prod_{j=1}^{T} p_{i,j}^{y_{i,j}} (1 - p_{i,j})^{1-y_{i,j}},$$

where z_i is an indicator for whether the site is occupied and $p_{i,j}$ represents the detection probability for site i and visit j. For example, if $\mathbf{y}_i = 101$, then $\Pr(\mathbf{y}_i = 101 \mid z_i = 1) = p_{i,1}(1 - p_{i,2})p_{i,3}$. The multinomial likelihood is then the product of all such probabilities over the set of S sites

$$\mathrm{L}_{PA}(\boldsymbol{\beta}, \boldsymbol{p}; \{\mathbf{y}_i\}) = \prod_{i=1}^{S} \{\Pr(\mathbf{y}_i \mid z_i = 1)\psi_i + I(\mathbf{y}_i = 0)(1 - \psi_i)\},$$

where the occupancy probability, ψ_i, is a function of M site-specific covariates, $w_{i,m}$, so that $\mathrm{logit}(\psi_i) = \beta_0 + \sum_{m=1}^{M} \beta_m w_{i,m}$. Detection probability can similarly vary with site-specific covariates, as well as covariates that vary within the season, for example to describe variation in observation effort, or factors that might affect a species' detectability. The likelihood is zero-inflated to account for the sampling of potentially unoccupied sites. Hence $I(\mathbf{y}_i = 0)$ denotes an indicator function which is satisfied if the encounter history for the ith site is entirely zero, i.e. $I(\mathbf{y}_i = 0) = 1; I(\mathbf{y}_i > 0) = 0$. The corresponding probability that the site is unoccupied, when $\mathbf{y}_i = 0$, is $(1 - \psi_i)$. Here we denote site-occupancy models by PA.

2.2.3 Assessing model performance

In this chapter we will apply the PO and PA models to BNM data. We compare average occupancy estimates across space between the two models, at locations at which the species of interest was observed, and at all considered locations, as well as the average standard error at these locations. We use Akaike's Information Criterion (AIC) to compare the performance of variations of the PA model.

In addition we estimate receiver operator characteristic (ROC) curves for each model (Fielding and Bell 1997), which are frequently employed to assess the accuracy of species' distribution models (Yackulic et al. 2013; Liu et al. 2011). Many methods for assessing how well a model estimates presence and absence require a threshold value to be chosen in order to convert continuous occupancy estimates to binary presence-absence predictions, for comparison with observed presence and absence (Liu et al. 2011). ROC curves are threshold independent, since this approach plots sensitivity against '1-specificity' for all possible thresholds of occurrence. Sensitivity and specificity are best described using a so-called confusion matrix (Table 2.1). Sensitivity is the probability that a presence is correctly predicted, $a/(a+c)$ and '1-specificity' is the probability that a true absence is incorrectly predicted as a presence, $b/(b+d)$, where predictions are classified as presence or absence for each possible threshold value.

Data are typically partitioned such that a proportion of the records are used for model-fitting (calibration data), and the remainder are retained as an independent sample for testing the model, by comparing model predic-

Table 2.1: A confusion matrix for observed and predicted presence/absence patterns (Fielding and Bell 1997).

		Observed	
		Present	Absent
Predicted	Present	a	b
	Absent	c	d

tions with true observations as just described. In this chapter we randomly partition as in Phillips et al. (2006), such that 70% of the records were taken as calibration data and the remaining 30% were reserved for testing the models. Various alternative methods of data partitioning are described by Fielding and Bell (1997), for example k-fold partitioning.

The area under the ROC curve (AUC) provides a single threshold-independent measure of accuracy, but should be interpreted with caution (Lobo et al. 2008), especially for small samples (Hanczar et al. 2010), which may be relevant when assessing results for specialist or localised species. The AUC can be interpreted as the probability that a random presence and a random absence would be correctly predicted by the model (Phillips et al. 2006). An ROC curve requires both presence and absence information, therefore we use records from benchmark species to define absences from which to ascertain correct/incorrect prediction. Hence the ROC curves in this chapter consider species detections against random points (Yackulic et al. 2013; Phillips et al. 2006).

2.2.4 Indexing occupancy

As described in Section 2.1, trends in distribution for UK butterflies have been typically based on studying broad trends between multi-year survey periods. We are interested in devising suitable indices for occupancy from the model output. It is possible that changes in species' occupancy will vary regionally, for example a species may be expanding at the northern edge of it's range, but be contracting or being lost from sites at the southern edge. Hence in this chapter we also explore approaches for devising occupancy indices for different regions of the UK. In this section we describe two main approaches for indexing occupancy, which will be tested for BNM data in Section 2.4.4.

A weighted index

Intuitively, for each year, we use the weighted mean of the estimated occupancy probabilities to create an index for occupancy in a given year k. We use the reciprocals of the associated variances as the weighting. Hence the index, I, in a given year k, may be estimated by

$$I_k = \frac{\sum_{i=1}^{n_k} \psi_{i,k}\sigma_{i,k}^{-2}}{\sum_{i=1}^{n_k} \sigma_{i,k}^{-2}},$$

where the occupancy probability, $\psi_{i,k}$ and standard error $\sigma_{i,k}$ are estimated from the PA model for location i of n_k points in the region of interest in year k. In doing so, occupancy estimates with smaller associated standard errors will have a higher contribution to the estimated index.

As defined by Meier (1953), the estimated associated variance, V_k, of the index is

$$V_k = \frac{1}{\sum_{i=1}^{n_k} \sigma_{i,k}^{-2}} \left\{ 1 + 4 \sum_{i=1}^{n} \frac{1}{q_{i,k}} \frac{\sigma_{i,k}^{-2}}{\sum_{i=1}^{n_k} \sigma_{i,k}^{-2}} \left(1 - \frac{\sigma_{i,k}^{-2}}{\sum_{i=1}^{n_k} \sigma_{i,k}^{-2}} \right) \right\},$$

where $q_{i,k}$ is the number of replicate visits made at site i in year k.

A simple average index

As an alternative to a weighted index, we can simply take the average occupancy estimate in the region of interest, such that each point effectively has the same weighting. In this case

$$I_k = \frac{1}{n_k} \sum_{i=1}^{n_k} \psi_{i,k},$$

where the associated variance of the index may be estimated by

$$V_k = \frac{1}{n_k^2} \sum_{i=1}^{n_k} \sigma_{i,k}^2.$$

In Section 2.4.4 we test these two approaches for indexing occupancy from BNM data for the regions defined in Section 2.3. Additionally we assess the effects of defining the points within each region of interest by taking all squares within the region, or by taking only those at which observations

have been made. We discuss the advantages and disadvantages in each case.

Finally, we will describe multiple ways to derive occupancy indices for the UK as a whole, given the estimation of regional indices, and then compare trend estimates with reported estimates of changes in distribution and abundance.

2.3 Application

In this section we describe the methodology for applying the two models of Section 2.2 to BNM data. We compare the PO and PA approaches for three illustrative UK butterfly species, using data from the BNM between 1995 and 2009. Historical records made prior to the scheme's formation in 1995 also exist, but are fewer in numbers and so are not considered here. Records from the BNM data with a precise location (1 km^2 or less) and exact date were extracted. Therefore 1 km squares are the definition of a site in this model and we assume that different records in the same sample unit do not refer to different locations that vary greatly (van Strien et al. 2011). For some standardisation to create a period of temporal closure within each year when the occupancy status of each site does not change, the data were restricted to be approximately within the main period for butterfly flight (beginning of April to the end of September).

Ringlet and Wall Brown have relatively large ranges across the UK. Ringlet has shown expansions in range and increases in abundance, whereas Wall Brown has experienced losses from much of inland England, with an increasingly coastal distribution (Asher et al. 2001; Fox et al. 2011a). Population numbers of Wall Brown are also in decline, and this species was classified as Near Threatened in the most recent Red List (Fox et al. 2011c). Wall Brown and Ringlet are both wider-countryside species, with Wall Brown mainly found in grasslands whereas the Ringlet favours damp situations with tall grassland, such as in woodland areas.

The third species, Silver-washed Fritillary, is a habitat-specialist, found

in woodlands and limited mostly to southern England, this species has started to show slight increases in range and abundance. Given the fairly limited distribution of Silver-washed Fritillary, for this species the models were fitted to a smaller region, limited to being below 100 m above the northing of the most northerly observation of Silver-washed Fritillary (between 1995 and 2009) at 506000 m. More detailed accounts of each species, including changes in their distributions, can be found in Asher et al. (2001) and Thomas and Lewington (2010).

The PO and PA models were fitted using the `maxlike` (Royle et al. 2012) and `unmarked` (Fiske and Chandler 2011) packages in `R` (R Core Team 2015), respectively. The PA models were fitted with absence information obtained from selected benchmark species which we describe in Section 2.3.1. Each model was fitted to data separately for each year from 1995 to 2009. Northing, easting, minimum February temperature (since February was on average the coldest winter month), and average monthly rainfall (mm, April-September) were considered as potential covariates for occupancy with both linear and quadratic effects (we show that AIC values are higher when only linear effects are used). The weather-related covariates were taken from historic weather-station data (Met Office 2015), which were smoothed using a thin-plate spline (Green and Silverman 1994), using the `fields` package (Nychka et al. 2014) in `R`, to get weather covariates at a scale of 1 km^2. Selected land cover variables were also considered, but as linear effects only. Percentage land cover was used from a 1 km resolution land cover map from 2007 (Morton et al. 2014). The data consist of 10 land cover classes, but, as given in Table 2.2, in this chapter we used five combined classes to minimise the complexity of the models. Extensive covariate selection was not performed and the covariates used may not be optimal, but allow for a direct comparison of the two models. All covariates were standardised to have zero mean and unit variance.

For simplicity in the model comparison, detection probability was assumed constant in the PA model. However, we later explore the effects of allowing non-constant detection probability in Section 2.4.3. As butterfly

Table 2.2: Land cover classes for UK land cover data for 2007 from (Morton et al. 2014), where the five combined classes are those used in this chapter.

Land cover class	Combined class
Broadleaf woodland	Woodland
Coniferous woodland	
Arable	Arable
Improved grassland	Grassland
Semi-natural grassland	
Mountain, heath and bog	Mountain
Saltwater	-
Freshwater	-
Coastal	-
Built-up areas and gardens	Urban

numbers vary within the season according to their life-cycle, we anticipate that the probability of detecting a species will be influenced by the population size according to the time within the season. Hence we use the proportion of observations made of the species of interest each week, over all sites and years, as a proxy for the seasonal variation in population size. We use this as a linear covariate for detection probability, p, in Section 2.4.3.

In Section 2.4.4 we explore novel regional occupancy indices as described in Section 2.2.4, based upon output from the PA model. These new indices provide a summary of the annual changes in a species' occupancy, rather than the single percentage-change values that are typically used as measures of change. Indices were calculated for the UK as a whole and each of the regions displayed in Figure 2.1.

2.3.1 Generating non-detection records for BNM data

In order to fit the PA model (Section 2.2.2) to BNM data, we use a benchmarking approach as described in Section 2.1, where the observations of

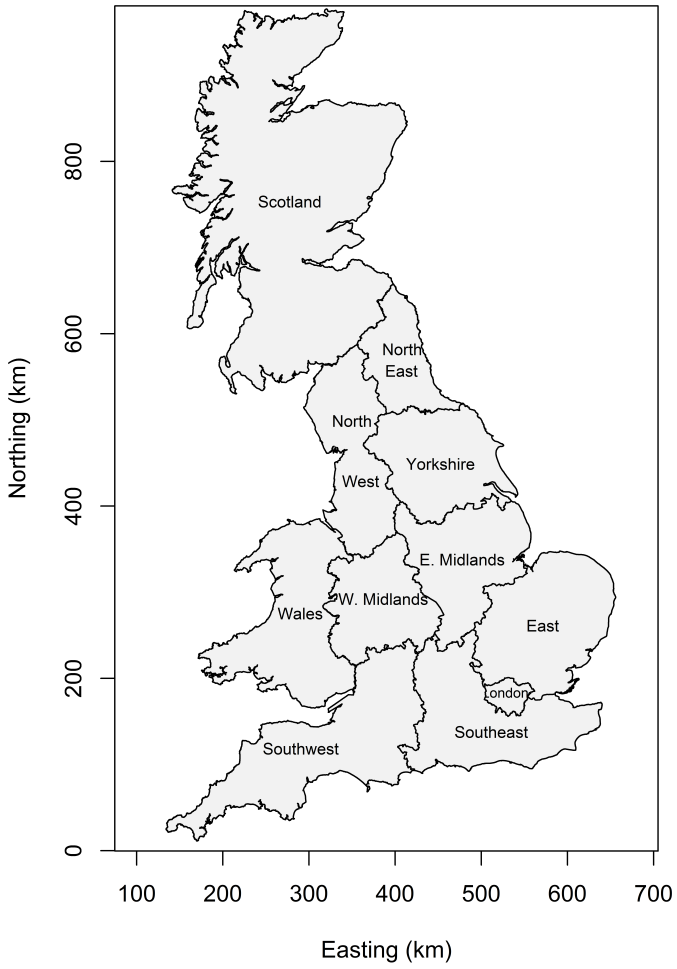

Figure 2.1: Regions used for regional occupancy indices.

non-target, benchmark species are used to generate non-detection records, and hence form detection histories, $\{\mathbf{y}_i\}$, for each site.

Throughout this chapter, including the comparisons with PO, we used the observations of the ten species occupying the most 10 km grid squares (based on a table of distribution trends given by Fox et al. 2011a) to produce non-detection records, in order to create detection histories for the PA models. This judgement was loosely based upon the assumption that if a very common species is detected during a visit, it is likely that the recorder would have also recorded a less or equally common species if it was also observed. However we additionally assess the effects of using more bench-

mark species in Section 2.4.2, by fitting the PA model with the 20 species occupying the most 10 km grid squares, as well as for all 51 species for which BNM data were available.

Detections of the benchmark species outside the first and last month that the target species was observed in a given year were disregarded, in order to prevent non-detection records being created outside of the target species' flight period, when the target species is mostly likely not present and hence not detectable. Observations were treated as weekly to provide a maximum of 26 replicates within a season, although in 87% of cases fewer than 5 replicates were made at each location within a given year, based on data for the ten benchmark species. The average number of visits made to each 1 km square in a given year has increased slightly over time, from approximately 2.9 in 1995 to 3.4 in 2009.

2.3.2 Model performance for BNM data

We estimate occupancy from each model (PO and PA) and display the output using occupancy maps. Corresponding maps of estimated standard error are used to display the associated uncertainty, using the Delta method to produce estimates on the untransformed scale (using the `deltamethod` function in the `msm` package (Jackson 2011) in `R`). To obtain ROC curves, the BNM data were randomly partitioned as described in Section 2.2.3. As a check, ROC curves were created for ten random partitions but were generally very similar for each partition.

2.4 Results

2.4.1 Model comparison

Model output from multiple years suggests the PO model is less reliable than the PA model for these data. Tables 2.3 and 2.4 demonstrate that the average prediction from the PO model (AO_{ALL}) is often very low, with more realistic average estimates produced by the PA model, which is particularly

significant for Ringlet which is known to have a relatively large range in the UK. Furthermore average occupancy estimates at the observed locations (AO_{OBS}) of Wall Brown and Ringlet are higher for the PA model than the PO model.

Average standard errors from PA are always larger than from PO (with the exception of 1999 for Silver-washed Fritillary where they are equivalent to three decimal places), but this might be expected given the lower occupancy estimates from PO, and despite this estimates from PA are more reliable than from PO based on the estimated occupancy probabilities. Similar results are found for Silver-washed Fritillary, although in this instance the PO model did not converge for 6 out of 15 years (Table 2.5), a frequency which rose to 13 out of 15 years when the model was not fitted to a limited range (below a northing of 506000 m). AUC values are consistently higher from the PA model. Example ROC curves for each species are given in Figure 2.2, demonstrating the slightly better discrimination capabilities of the PA model.

For 2009, parameter estimates for Wall Brown from the PA and PO model are all of the same sign and similar magnitude, whereas for Ringlet and Silver-washed Fritillary there is greater variability in the parameter estimates between the two models (Table 2.6). In particular for Ringlet, when the PO model underestimates occupancy in 2009, there are differences between the intercept terms of the two models, with a larger estimate and standard error for the PO model. In most cases standard errors are small relative to the regression parameter estimates, implying that the chosen covariates are significant. The optimal covariate selection is likely to vary between species, and potentially across different years, and may be identified using model selection, but as previously stated in this chapter the covariates were selected for demonstration and comparison of the two models.

The PA model was also fitted with only linear effects on each covariate (i.e without quadratic effects on northing, easting, minimum temperature and rainfall), but the AIC values were consistently lower when the quadratic effects were included (Figure 2.3). We note that the AIC differences are

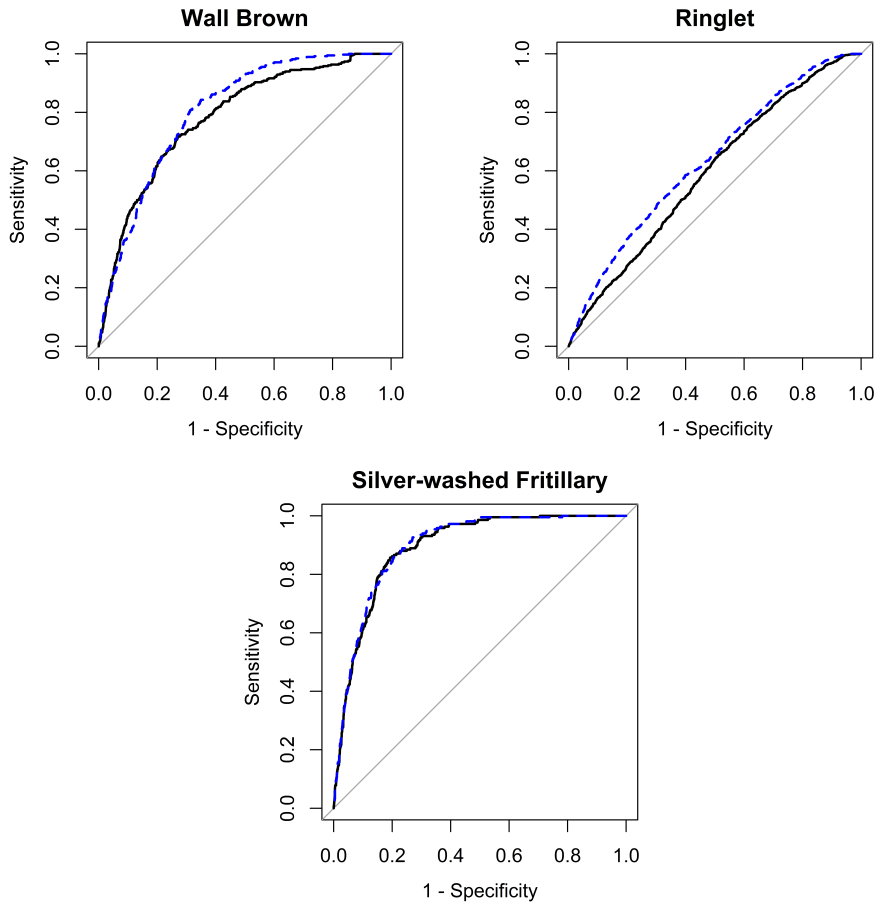

Figure 2.2: ROC curves for a single random partition for each species, for the PO (solid black) and PA (dashed blue) models.

large, but this might be expected given the large amounts of data being modelled.

Figures 2.4-2.9 display occupancy maps and corresponding standard errors for the PA and PO models for each species in 2009. Predicted occupancy from PA in 2009 for Wall Brown and Ringlet shows higher estimates of occupancy corresponding to locations of the observations (Figures 2.4 and 2.6), but much lower estimates from the PO model (Figures 2.5 and 2.7). This is particularly evident for Ringlet. Standard errors from the PA model for Ringlet are greater in Scotland, which might be expected given the more limited sampling in this area (see Section 2.4.2).

Estimates of spatial occupancy for Silver-washed Fritillary in 2009 are similar from the two models, with the exception of southern Wales which

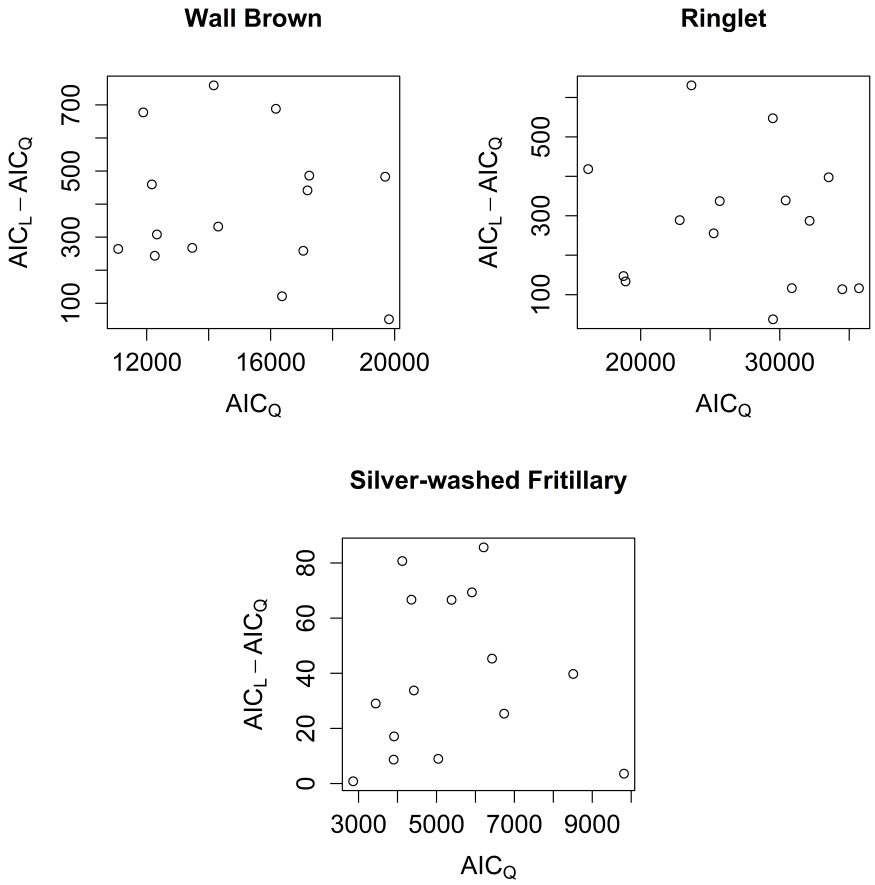

Figure 2.3: AIC comparison for fitting the PA model with (Q) and without (L) quadratic effects (on northing, easting, minimum temperature and rainfall), for Wall Brown, Ringlet & Silver-washed Fritillary.

has greater estimates of occupancy from the PA model, despite minimal records in this area. Further investigation may be required to distinguish whether this prediction reflects the true distribution, or is a consequence of the sparser recording in this region.

In this chapter occupancy maps have only been presented for a single year, but dynamic maps, which visualise annual changes in distribution by displaying occupancy maps for each year in sequence, are provided as an electronic appendix to this thesis.

Despite the reasonable performance of PO in some instances, Tables 2.3-2.5 demonstrate that the PO model shows varied success in providing realistic estimates across multiple years. As a consequence of the unrelia-

bility of the PO model for these data, in the following sections we consider only the PA model.

Table 2.3: Comparison of the PO and PA models for Wall Brown data. AO_{ALL} and AO_{OBS} are the average estimated occupancy probability from all points and from all points at which Wall Brown was observed, respectively. ASE is the average standard error of the estimated occupancy probability from all points and AUC is the average AUC value from 10 partitions.

	AO_{OBS}		AO_{ALL}		ASE		AUC	
Year	PO	PA	PO	PA	PO	PA	PO	PA
1995	0.52	0.70	0.21	0.38	0.024	0.032	0.557	0.724
1996	0.34	0.58	0.13	0.32	0.018	0.028	0.683	0.742
1997	0.26	0.69	0.11	0.44	0.018	0.036	0.572	0.744
1998	0.39	0.52	0.17	0.30	0.021	0.025	0.657	0.713
1999	0.94	0.52	0.59	0.31	0.020	0.028	0.645	0.721
2000	0.98	0.63	0.64	0.33	0.010	0.028	0.557	0.732
2001	0.33	0.53	0.15	0.38	0.021	0.036	0.581	0.681
2002	0.26	0.52	0.11	0.32	0.018	0.035	0.675	0.706
2003	0.28	0.52	0.11	0.28	0.014	0.026	0.590	0.731
2004	0.21	0.59	0.07	0.30	0.013	0.023	0.727	0.753
2005	0.26	0.54	0.09	0.28	0.014	0.024	0.727	0.757
2006	0.28	0.51	0.09	0.25	0.013	0.023	0.737	0.759
2007	0.19	0.39	0.06	0.19	0.011	0.022	0.666	0.750
2008	0.29	0.48	0.07	0.22	0.012	0.023	0.766	0.811
2009	0.30	0.44	0.08	0.17	0.010	0.017	0.729	0.799

Table 2.4: Comparison of the PO and PA models for Ringlet data. AO_{ALL} and AO_{OBS} are the average estimated occupancy probability from all points and from all points at which Ringlet was observed, respectively. ASE is the average standard error of the estimated occupancy probability from all points and AUC is the average AUC value from 10 partitions.

	AO_{OBS}		AO_{ALL}		ASE		AUC	
Year	PO	PA	PO	PA	PO	PA	PO	PA
1995	0.81	0.82	0.42	0.53	0.021	0.035	0.706	0.725
1996	0.03	0.63	0.01	0.46	0.013	0.038	0.649	0.684
1997	0.84	0.77	0.52	0.55	0.023	0.025	0.596	0.678
1998	0.88	0.70	0.58	0.53	0.020	0.030	0.583	0.663
1999	0.04	0.77	0.02	0.58	0.021	0.028	0.610	0.660
2000	0.22	0.72	0.10	0.53	0.020	0.038	0.647	0.688
2001	0.18	0.71	0.08	0.55	0.022	0.036	0.603	0.674
2002	0.07	0.75	0.03	0.60	0.022	0.031	0.609	0.667
2003	0.19	0.70	0.10	0.59	0.023	0.036	0.611	0.661
2004	0.41	0.72	0.24	0.59	0.024	0.030	0.603	0.643
2005	0.13	0.76	0.07	0.65	0.021	0.042	0.591	0.622
2006	0.01	0.81	0.01	0.71	0.021	0.027	0.611	0.645
2007	0.19	0.74	0.10	0.62	0.020	0.034	0.615	0.648
2008	0.14	0.77	0.07	0.61	0.015	0.032	0.613	0.642
2009	0.06	0.71	0.03	0.59	0.022	0.028	0.600	0.633

Table 2.5: Comparison of the PO and PA models for Silver-washed Fritillary data. AO_{ALL} and AO_{OBS} are the average estimated occupancy probability from all points and from all points at which Silver-washed Fritillary was observed, respectively. ASE is the average standard error of the estimated occupancy probability from all points and AUC is the average AUC value from 10 partitions. Instances where the PO model did not converge are identified by the gaps.

	AO_{OBS}		AO_{ALL}		ASE		AUC	
Year	PO	PA	PO	PA	PO	PA	PO	PA
1995	0.25	0.58	0.02	0.12	0.007	0.019	0.860	0.904
1996	0.37	0.54	0.04	0.11	0.010	0.017	0.867	0.894
1997	-	0.55	-	0.12	-	0.017	-	0.904
1998	-	0.50	-	0.08	-	0.013	-	0.907
1999	0.47	0.52	0.05	0.07	0.011	0.011	0.917	0.929
2000	-	0.51	-	0.07	-	0.013		0.914
2001	-	0.49	-	0.06	-	0.013		0.908
2002	0.28	0.47	0.02	0.07	0.005	0.013	0.910	0.919
2003	0.30	0.50	0.03	0.08	0.005	0.012	0.892	0.913
2004	0.37	0.55	0.04	0.10	0.008	0.015	0.906	0.914
2005	-	0.54	-	0.12	-	0.017	-	0.898
2006	0.28	0.56	0.04	0.15	0.006	0.017	0.868	0.879
2007	-	0.51	-	0.09	-	0.013	-	0.901
2008	0.35	0.51	0.03	0.10	0.006	0.014	0.879	0.895
2009	0.45	0.53	0.05	0.09	0.008	0.012	0.896	0.901

Table 2.6: Parameter estimates for each model and species for 2009, where MLE is the maximum likelihood estimate and SE is the associated standard error.

	Wall Brown				Ringlet				Silver-washed Fritillary			
Parameter	MLE_{PA}	SE_{PA}	MLE_{PO}	SE_{PO}	MLE_{PA}	SE_{PA}	MLE_{PO}	SE_{PO}	MLE_{PA}	SE_{PA}	MLE_{PO}	SE_{PO}
intercept	-1.639	0.092	-3.032	0.126	0.624	0.083	-3.588	0.686	-1.716	0.581	-4.312	0.540
north	-2.241	0.235	-2.837	0.302	-0.910	0.121	-0.564	0.056	-4.538	0.619	-2.303	0.538
$north^2$	1.106	0.121	0.987	0.126	-0.857	0.092	0.023	0.042	-1.696	0.311	-0.740	0.286
east	6.186	0.300	6.833	0.336	-0.197	0.190	1.041	0.096	3.457	1.603	-3.221	1.504
$east^2$	-0.014	0.082	-0.126	0.081	0.213	0.083	-0.185	0.036	-2.184	0.421	-0.357	0.394
tmin	1.070	0.130	0.968	0.122	-0.950	0.109	0.010	0.048	0.885	0.269	1.090	0.263
$tmin^2$	-0.203	0.050	-0.078	0.052	0.272	0.042	0.052	0.019	0.045	0.054	0.198	0.051
rain	6.711	0.345	6.082	0.362	-0.375	0.210	0.207	0.090	3.930	1.700	-4.760	1.607
$rain^2$	-1.993	0.120	-2.429	0.138	0.020	0.075	-0.243	0.039	0.199	0.408	-1.570	0.427
woodland	-1.081	0.108	-1.434	0.186	0.770	0.074	0.220	0.032	1.189	0.123	1.031	0.125
grassland	-0.865	0.144	-2.040	0.266	0.247	0.082	-0.219	0.045	0.041	0.198	-0.295	0.194
arable	-1.033	0.156	-2.428	0.293	0.549	0.093	-0.343	0.051	-0.026	0.230	-0.709	0.226
urban	-1.004	0.094	-1.305	0.167	-0.150	0.050	-0.121	0.029	-0.386	0.158	-0.443	0.154
mountain	-1.468	0.178	-2.673	0.278	-0.011	0.106	-0.591	0.060	0.043	0.139	-0.067	0.135

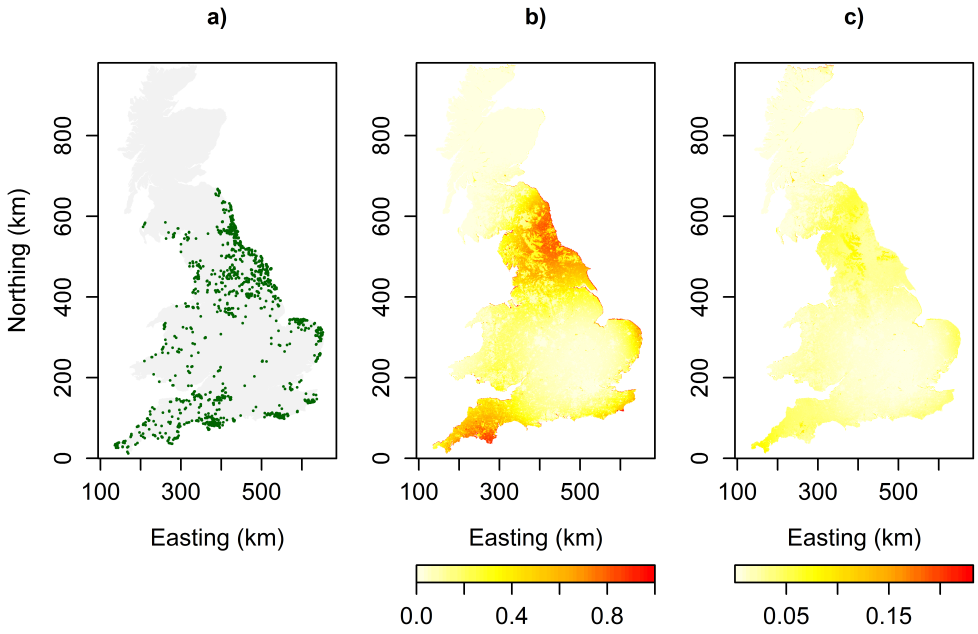

Figure 2.4: PA model output for Wall Brown in 2009: a) observations b) estimated occupancy probability c) standard error.

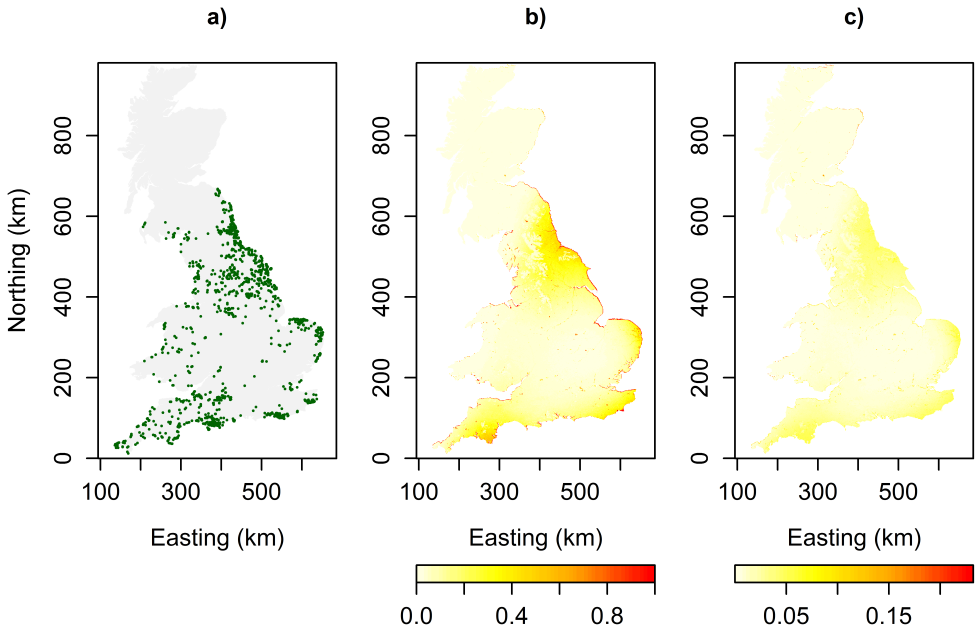

Figure 2.5: PO model output for Wall Brown in 2009: a) observations b) estimated occupancy probability c) standard error.

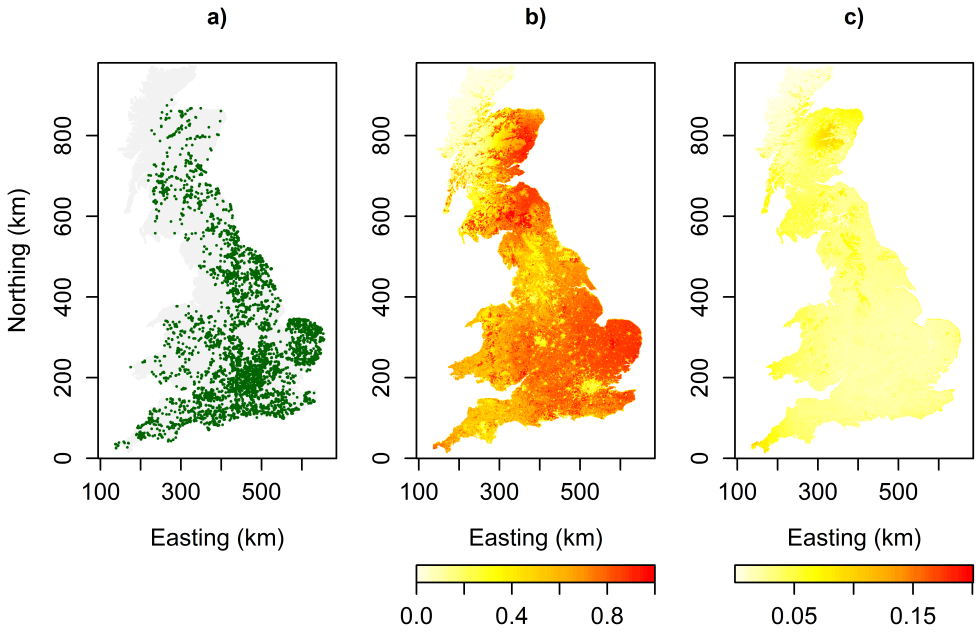

Figure 2.6: PA model output for Ringlet in 2009: a) observations b) estimated occupancy probability c) standard error.

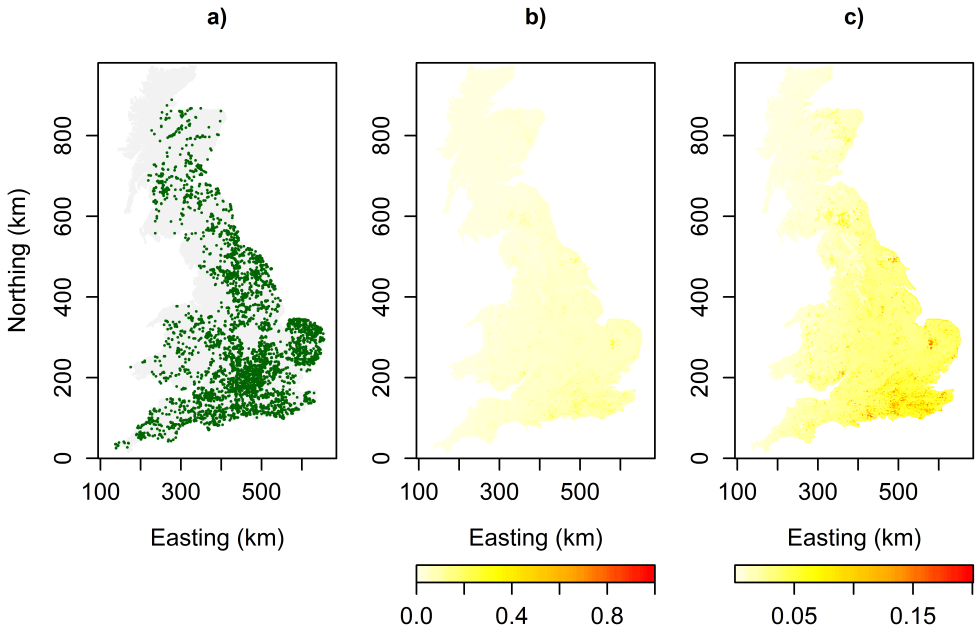

Figure 2.7: PO model output for Ringlet in 2009: a) observations b) estimated occupancy probability c) standard error.

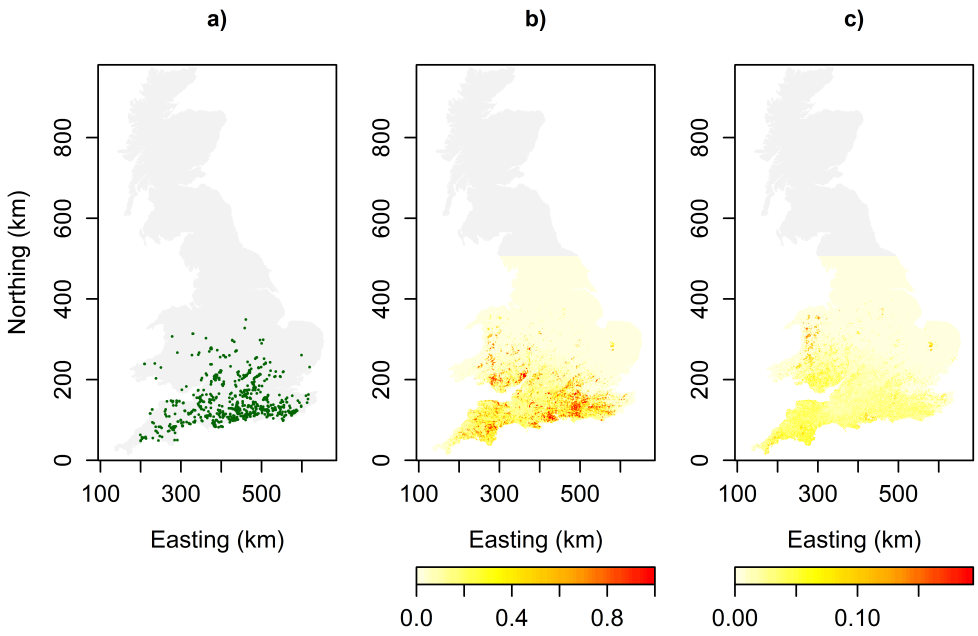

Figure 2.8: PA model output for Silver-washed Fritillary in 2009: a) observations b) estimated occupancy probability c) standard error.

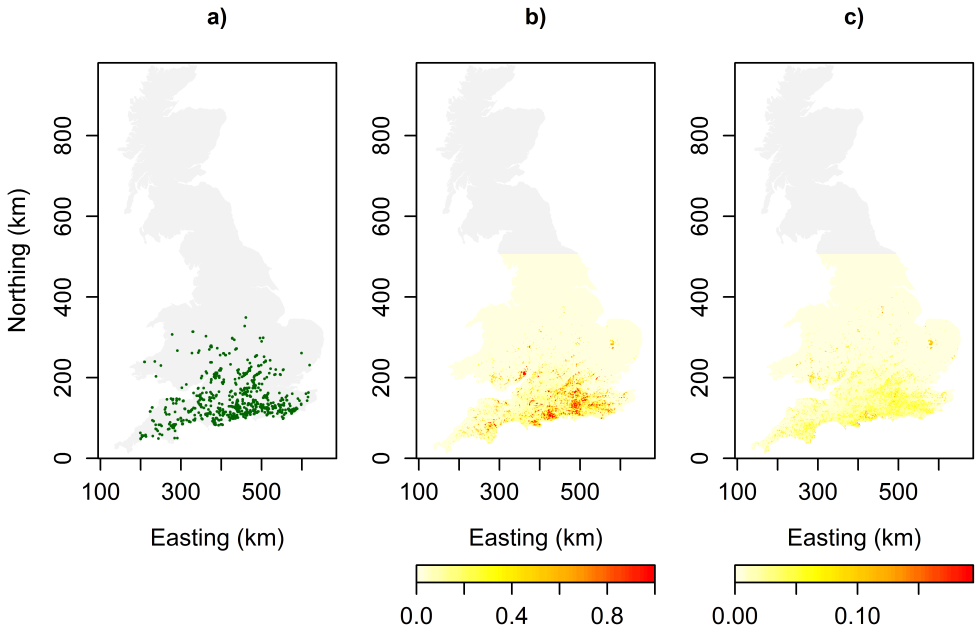

Figure 2.9: PO model output for Silver-washed Fritillary in 2009: a) observations b) estimated occupancy probability c) standard error.

2.4.2 Optimal benchmarking

By increasing the number of benchmark species used, we can anticipate increases in the number of sites and/or the number of replicated visits per site. Observations were made at an average of 15552, 17085 and 17659 locations per year for 10, 20 and all benchmark species, respectively. There is a minimal difference in the mean number of replicates per site and year for varying numbers of benchmark species (2.73, 2.85 and 2.83 respectively). Figure 2.10 shows similar patterns in the location of observations, in 2000, from varying numbers of benchmark species. Regardless of the number of benchmark species used, some areas shows limited coverage, such as Scotland, large areas of Wales, East Anglia and North Devon.

Tables 2.7-2.9 show that varying the number of benchmark species has minimal effect on the average occupancy estimates from the PA model. These minor differences may be anticipated given that the majority of records are likely to arise from observations of more common species, hence as increasingly scarce species are included in the benchmarking, the effect on the model results is limited. This may not be true for particular areas

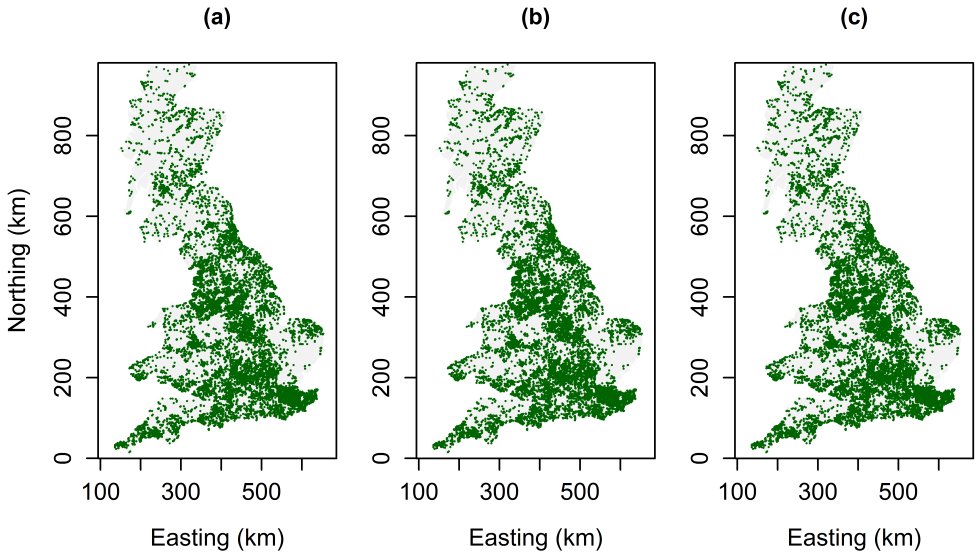

Figure 2.10: Locations of BNM records from a) 10, b) 20 and c) all benchmarking species in 2000.

with poorer coverage and/or with species which may have restricted ranges but be relatively widespread within that range, for example Scotch Argus in Scotland.

To assess the effect of varying the benchmarking effort on an area with more limited sampling coverage, in Table 2.10 we present estimated occupancy probabilities for Scotland for Ringlet. Neither of the other species' ranges extends significantly into Scotland. With the exception of 2003, there are minimal differences in the mean occupancy probabilities from varying benchmarking for Ringlet in Scotland, suggesting that using 10 species may be sufficient in this case.

There were only small differences in computation time from increasing the number of benchmark species used, however as discussed in Section 2.1, it is possible that as increasingly rare species are included, the likelihood of a common species, such as Ringlet, being recorded may decrease. Analysis of the species composition and number of species recorded, often referred to as list length, could help determine whether all observed species are typically recorded.

Table 2.7: Variation in benchmarking for Wall Brown. AO_{ALL} and AO_{OBS} are the mean estimated occupancy probability from all points and from all points at which Wall Brown was observed, respectively. ASE is the average standard error of the estimated occupancy probability from all points.

	AO_{OBS}			AO_{ALL}			ASE		
Year	10	20	all	10	20	all	10	20	all
1995	0.70	0.69	0.69	0.38	0.37	0.37	0.032	0.031	0.030
1996	0.58	0.57	0.57	0.32	0.31	0.31	0.028	0.027	0.027
1997	0.69	0.67	0.67	0.44	0.43	0.42	0.036	0.036	0.035
1998	0.52	0.50	0.50	0.30	0.29	0.29	0.025	0.024	0.023
1999	0.52	0.52	0.51	0.31	0.30	0.30	0.028	0.027	0.025
2000	0.63	0.62	0.61	0.33	0.32	0.31	0.028	0.026	0.026
2001	0.53	0.52	0.52	0.38	0.37	0.36	0.036	0.036	0.035
2002	0.52	0.50	0.50	0.32	0.31	0.30	0.035	0.032	0.031
2003	0.52	0.50	0.50	0.28	0.28	0.28	0.026	0.025	0.024
2004	0.59	0.58	0.57	0.30	0.29	0.29	0.023	0.022	0.022
2005	0.54	0.52	0.52	0.28	0.27	0.27	0.024	0.023	0.023
2006	0.51	0.50	0.49	0.25	0.24	0.23	0.023	0.022	0.021
2007	0.39	0.38	0.38	0.19	0.18	0.18	0.022	0.021	0.020
2008	0.48	0.46	0.46	0.22	0.20	0.20	0.023	0.022	0.022
2009	0.44	0.43	0.43	0.17	0.17	0.17	0.017	0.016	0.016

Table 2.8: Variation in benchmarking for Ringlet. AO_{ALL} and AO_{OBS} are the mean estimated occupancy probability from all points and from all points at which Ringlet was observed, respectively. ASE is the average standard error of the estimated occupancy probability from all points.

	AO_{OBS}			AO_{ALL}			ASE		
Year	10	20	all	10	20	all	10	20	all
1995	0.82	0.82	0.81	0.53	0.53	0.52	0.035	0.035	0.034
1996	0.63	0.63	0.62	0.46	0.46	0.45	0.038	0.038	0.040
1997	0.77	0.77	0.77	0.55	0.55	0.55	0.025	0.025	0.024
1998	0.70	0.69	0.69	0.53	0.53	0.53	0.030	0.029	0.029
1999	0.77	0.77	0.77	0.58	0.58	0.58	0.028	0.028	0.027
2000	0.72	0.71	0.71	0.53	0.52	0.52	0.038	0.037	0.035
2001	0.71	0.71	0.71	0.55	0.55	0.55	0.036	0.035	0.034
2002	0.75	0.74	0.73	0.60	0.59	0.58	0.031	0.029	0.029
2003	0.70	0.74	0.73	0.59	0.69	0.69	0.036	0.026	0.027
2004	0.72	0.71	0.70	0.59	0.58	0.57	0.030	0.029	0.029
2005	0.76	0.75	0.74	0.65	0.64	0.62	0.042	0.042	0.036
2006	0.81	0.80	0.80	0.71	0.70	0.70	0.027	0.026	0.026
2007	0.74	0.73	0.73	0.62	0.61	0.60	0.034	0.033	0.032
2008	0.77	0.76	0.75	0.61	0.59	0.59	0.032	0.030	0.029
2009	0.71	0.70	0.70	0.59	0.57	0.57	0.028	0.028	0.027

Table 2.9: Variation in benchmarking for Silver-washed Fritillary. AO_{ALL} and AO_{OBS} are the mean estimated occupancy probability from all points and from all points at which Silver-washed Fritillary was observed, respectively. ASE is the average standard error of the estimated occupancy probability from all points.

	AO_{OBS}			AO_{ALL}			ASE		
Year	10	20	all	10	20	all	10	20	all
1995	0.58	0.57	0.57	0.12	0.12	0.12	0.019	0.019	0.019
1996	0.54	0.55	0.54	0.11	0.11	0.11	0.017	0.017	0.017
1997	0.55	0.55	0.55	0.12	0.12	0.12	0.017	0.017	0.017
1998	0.50	0.50	0.50	0.08	0.08	0.08	0.013	0.013	0.013
1999	0.52	0.52	0.51	0.07	0.07	0.07	0.011	0.011	0.011
2000	0.51	0.51	0.50	0.07	0.07	0.07	0.013	0.014	0.014
2001	0.49	0.49	0.49	0.06	0.07	0.07	0.013	0.014	0.014
2002	0.47	0.47	0.46	0.07	0.07	0.07	0.013	0.013	0.013
2003	0.50	0.50	0.50	0.08	0.08	0.08	0.012	0.012	0.012
2004	0.55	0.54	0.54	0.10	0.10	0.10	0.015	0.015	0.015
2005	0.54	0.53	0.53	0.12	0.12	0.11	0.017	0.017	0.017
2006	0.56	0.56	0.55	0.15	0.15	0.15	0.017	0.017	0.017
2007	0.51	0.51	0.50	0.09	0.09	0.09	0.013	0.013	0.013
2008	0.51	0.51	0.50	0.10	0.10	0.09	0.014	0.014	0.014
2009	0.53	0.52	0.52	0.09	0.09	0.09	0.012	0.012	0.012

Table 2.10: Variation in benchmarking for Ringlet in Scotland. AO_{ALL} and AO_{OBS} are the mean estimated occupancy probability from all points in Scotland and from all points in Scotland at which Ringlet was observed, respectively. ASE is the average standard error of the estimated occupancy probability from all points in Scotland.

	AO_{OBS}			AO_{ALL}			ASE		
Year	10	20	all	10	20	all	10	20	all
1995	0.51	0.52	0.50	0.27	0.28	0.26	0.044	0.044	0.041
1996	0.45	0.46	0.44	0.40	0.40	0.37	0.054	0.055	0.059
1997	0.85	0.86	0.86	0.32	0.33	0.33	0.022	0.021	0.020
1998	0.62	0.64	0.64	0.32	0.32	0.31	0.036	0.034	0.032
1999	0.74	0.76	0.74	0.44	0.44	0.42	0.034	0.033	0.032
2000	0.67	0.67	0.65	0.40	0.39	0.36	0.048	0.047	0.043
2001	0.56	0.57	0.56	0.33	0.33	0.32	0.044	0.041	0.039
2002	0.71	0.71	0.70	0.38	0.37	0.36	0.036	0.034	0.032
2003	0.57	0.77	0.75	0.48	0.79	0.78	0.057	0.023	0.026
2004	0.76	0.76	0.75	0.46	0.46	0.44	0.035	0.034	0.032
2005	0.72	0.73	0.69	0.50	0.51	0.47	0.064	0.064	0.049
2006	0.88	0.88	0.88	0.72	0.72	0.70	0.028	0.027	0.028
2007	0.61	0.61	0.60	0.48	0.47	0.45	0.048	0.045	0.042
2008	0.60	0.60	0.60	0.41	0.39	0.38	0.041	0.037	0.034
2009	0.62	0.62	0.61	0.41	0.41	0.40	0.033	0.032	0.031

2.4.3 Detection probability

In this section we explore the effects of allowing seasonal variation in detection probability, as described in Section 2.3. Figure 2.11 shows how the proportion of observations made per week varies throughout the season for each species, according to the species' life-cycle. Wall Brown is a bivoltine species, hence the curve exhibits two peaks, whereas Ringlet and Silver-washed Fritillary are both univoltine with a single peak in the proportion of observations made per week.

The PA model with varying detection probability has smaller AICs, however there are generally only minimal differences in average occupancy estimates (Tables 2.11-2.13). Figure 2.12 shows the estimated detection probabilities for 2009, which reflect the seasonal variation of the covariate used.

Figure 2.13 plots the average detectability over the season for each year and species. Based on simple linear regressions applied to average detection probabilities in Figure 2.13, the average detection has increased significantly ($p \leq 0.05$) for Wall Brown and Silver-washed Fritillary, but not Ringlet, which is reflected in Figure 2.13. Increases in detection probability could be a result of changes in observer effort. Averaged over the season and multiple years, detection probability is similar for the three species (0.16 to two decimal places for all three species).

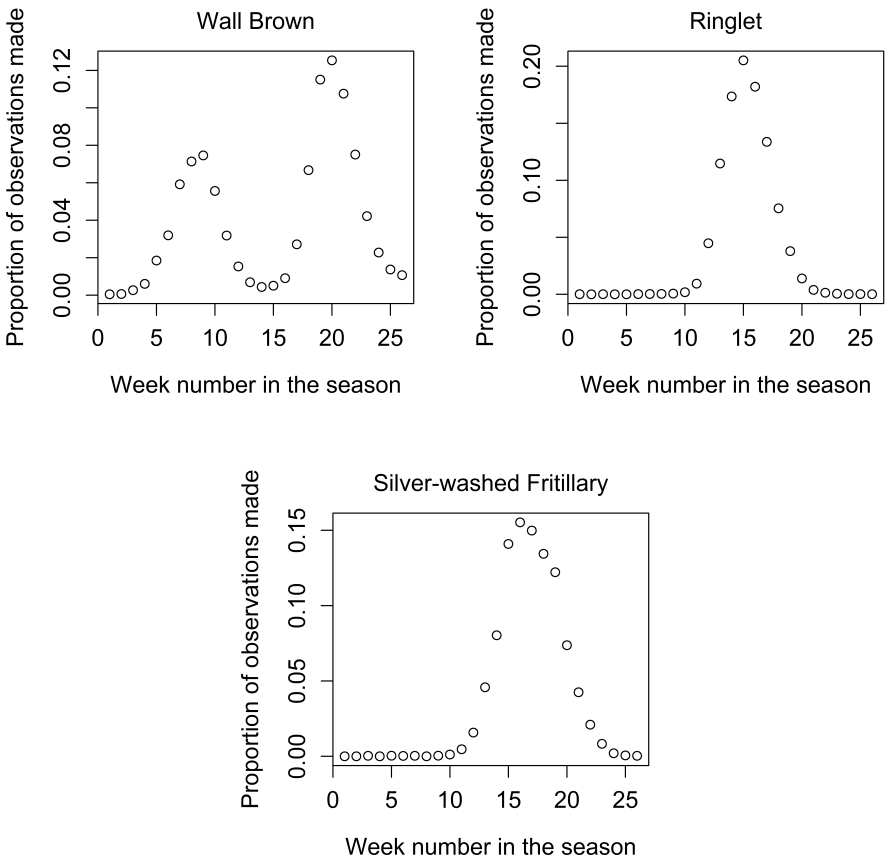

Figure 2.11: Proportion of observations made per week across all locations and years, for Wall Brown, Ringlet and Silver-washed Fritillary.

Table 2.11: Comparison of the PA model with detection probability constant or varying linearly with α, the proportion of observations made per week, for Wall Brown. AO_{ALL} and AO_{OBS} are the mean estimated occupancy probability from all points and from all points at which Wall Brown was observed, respectively. ASE is the average standard error of the occupancy probability from all points and AIC the Akaike Information Criterion.

	AO_{OBS}		AO_{ALL}		ASE		AIC	
Year	$p(.)$	$p(\alpha)$	$p(.)$	$p(\alpha)$	$p(.)$	$p(\alpha)$	$p(.)$	$p(\alpha)$
1995	0.70	0.68	0.38	0.36	0.032	0.028	12261	10151
1996	0.58	0.56	0.32	0.31	0.028	0.027	11889	11595
1997	0.69	0.63	0.44	0.41	0.036	0.036	13471	11785
1998	0.52	0.47	0.30	0.27	0.025	0.022	17054	15200
1999	0.52	0.53	0.31	0.31	0.028	0.024	19817	17260
2000	0.63	0.60	0.33	0.31	0.028	0.026	16366	14525
2001	0.53	0.50	0.38	0.35	0.036	0.033	12328	10783
2002	0.52	0.50	0.32	0.30	0.035	0.032	14308	12742
2003	0.52	0.50	0.28	0.27	0.026	0.023	17246	15605
2004	0.59	0.56	0.30	0.28	0.023	0.021	19697	16857
2005	0.54	0.53	0.28	0.27	0.024	0.023	16169	14067
2006	0.51	0.54	0.25	0.26	0.023	0.022	17190	14823
2007	0.39	0.39	0.19	0.19	0.022	0.022	12164	11344
2008	0.48	0.46	0.22	0.20	0.023	0.022	11080	10166
2009	0.44	0.42	0.17	0.16	0.017	0.015	14162	12220

Table 2.12: Comparison of the PA model with detection probability constant or varying linearly with α, the proportion of observations made per week, for Ringlet. AO_{ALL} and AO_{OBS} are the mean estimated occupancy probability from all points and from all points at which Ringlet was observed, respectively. ASE is the average standard error of the occupancy probability from all points and AIC the Akaike Information Criterion.

	AO_{OBS}		AO_{ALL}		ASE		AIC	
Year	$p(.)$	$p(\alpha)$	$p(.)$	$p(\alpha)$	$p(.)$	$p(\alpha)$	$p(.)$	$p(\alpha)$
1995	0.82	0.74	0.53	0.48	0.035	0.030	16225	11112
1996	0.63	0.59	0.46	0.42	0.038	0.033	18766	14651
1997	0.77	0.66	0.55	0.48	0.025	0.024	23647	14470
1998	0.70	0.67	0.53	0.53	0.030	0.029	25683	16160
1999	0.77	0.68	0.58	0.52	0.028	0.026	29500	19208
2000	0.72	0.67	0.53	0.48	0.038	0.030	22808	14338
2001	0.71	0.67	0.55	0.53	0.036	0.033	18914	12839
2002	0.75	0.70	0.60	0.57	0.031	0.029	25251	15666
2003	0.70	0.66	0.59	0.53	0.036	0.027	30870	20910
2004	0.72	0.70	0.59	0.59	0.030	0.027	32148	21666
2005	0.76	0.69	0.65	0.57	0.042	0.030	29520	18441
2006	0.81	0.75	0.71	0.67	0.027	0.026	33521	21852
2007	0.74	0.72	0.62	0.61	0.034	0.031	30433	21272
2008	0.77	0.73	0.61	0.61	0.032	0.032	34502	20901
2009	0.71	0.70	0.59	0.58	0.028	0.025	35699	23998

Table 2.13: Comparison of the PA model with detection probability constant or varying linearly with α, the proportion of observations made per week, for Silver-washed Fritillary data. AO_{ALL} and AO_{OBS} are the mean estimated occupancy probability from all points and from all points at which Silver-washed Fritillary was observed, respectively. ASE is the average standard error of the occupancy probability from all points and AIC the Akaike Information Criterion.

	AO_{OBS}		AO_{ALL}		ASE		AIC	
Year	$p(.)$	$p(\alpha)$	$p(.)$	$p(\alpha)$	$p(.)$	$p(\alpha)$	$p(.)$	$p(\alpha)$
1995	0.58	0.55	0.12	0.12	0.019	0.018	3910	3123
1996	0.54	0.52	0.11	0.11	0.017	0.017	4420	3773
1997	0.55	0.53	0.12	0.11	0.017	0.016	5047	4161
1998	0.50	0.48	0.08	0.07	0.013	0.012	4356	3613
1999	0.52	0.49	0.07	0.07	0.011	0.010	4121	3455
2000	0.51	0.49	0.07	0.07	0.013	0.013	3441	2905
2001	0.49	0.48	0.06	0.06	0.013	0.013	2862	2566
2002	0.47	0.47	0.07	0.07	0.013	0.013	3900	3390
2003	0.50	0.49	0.08	0.08	0.012	0.012	5386	4661
2004	0.55	0.51	0.10	0.09	0.015	0.014	5910	4665
2005	0.54	0.51	0.12	0.11	0.017	0.016	6212	5157
2006	0.56	0.53	0.15	0.14	0.017	0.016	9813	7792
2007	0.51	0.50	0.09	0.09	0.013	0.013	6738	5721
2008	0.51	0.50	0.10	0.10	0.014	0.014	6426	5778
2009	0.53	0.51	0.09	0.09	0.012	0.011	8512	6803

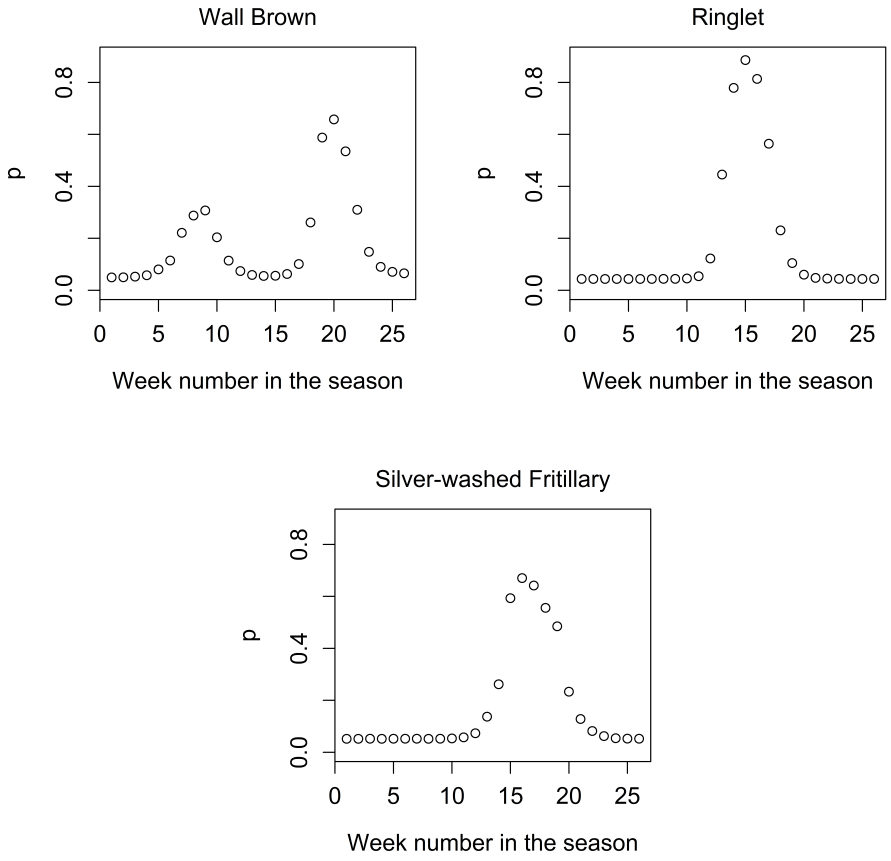

Figure 2.12: Estimated detection probability throughout the season for each species in 2009.

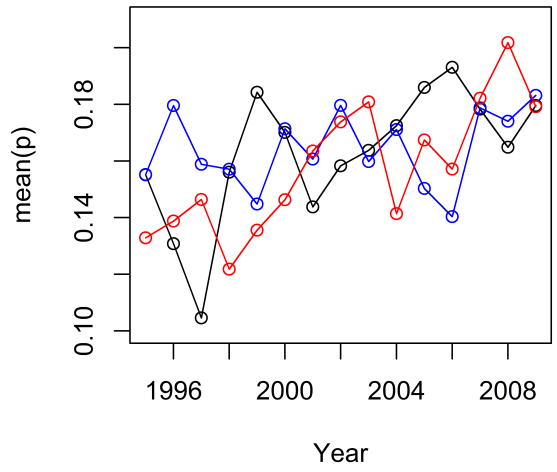

Figure 2.13: Mean estimated detection probability (over the season) per year for Wall Brown (black), Ringlet (blue) and Silver-washed Fritillary (red).

2.4.4 Occupancy indices

In this section we present novel occupancy indices, as outlined in Section 2.2.4. The regions used are shown in Figure 2.1. Given the results in Section 2.4.3, we use the PA model with varying detection probability.

Figures 2.14-2.16 display regional indices for the three species, derived using varying approaches. For Silver-washed Fritillary the range was limited in the model fitting (Section 2.3) hence regional indices are not available for Scotland and Northwest England. In each figure, plots a) and b) compare using the weighted index versus the simple index, as described in Section 2.2.4, based on all locations in each region. Although using the standard errors of the occupancy estimates as a weighting seems intuitive, the resulting indices are generally more variable. In the case of particularly large/small occupancy estimates, associated estimated standard errors are likely to be small and/or poorly estimated, and consequently this can produce problems with the weighted indices, where the more extreme values have higher weightings which influence the indices. For example the index for Wall

Brown in Scotland is zero for the weighted index, but is more realistically slightly larger than zero for the simple index (Figure 2.14), a feature which similarly occurs for some regions for Silver-washed Fritillary in Figure 2.16. For Ringlet the index for Scotland fluctuates significantly for the weighted index compared to the simple index (Figure 2.15).

In plot c) of each Figure 2.14-2.16, we plot simple regional occupancies based on using only locations at which records have been made in that year. Using all possible points as in plots a) and b) relies on predictions of occupancy in unsampled locations, however using only sampled locations, as in plots c), could produce results that are biased given the unstandardised sampling design of the BNM. Furthermore, when using the recorded locations for each year, there is variation in the sample of points contributing to the indices for each year, as a result of the unstandardised manner of the data. For Wall Brown there are minimal differences between Figures 2.14b and 2.14c for most regions, although the estimated index for Scotland is much lower when all locations are used, which is likely to be more realistic given the limited distribution of Wall Brown in Scotland. For Ringlet and Silver-washed Fritillary there are also only minimal differences between Figures 2.15b and 2.15c and Figures 2.16b and 2.16c, although for Silver-washed Fritillary in Wales there is some variation.

Although using only sampled locations removes any bias from using predictions at unsampled locations, these illustrative results suggest that there may be bias when sampling is uneven, particularly for some regions such as Scotland and Wales, which were shown to be undersampled in Figure 2.10. This issue may be more prevalent for rare, localised species which were not studied in this preliminary development of the indices. Further work is needed, but using a simple index from all locations may be the most suitable approach for deriving occupancy indices.

Figure 2.17a shows indices for the UK as a whole for each species. For Wall Brown and Ringlet, the indices derived from either taking the average of the occupancy estimates for all points in the UK (black lines) are similar to those calculated by taking a geometric mean of the regional indices in plot

b) of Figures 2.14 and 2.15. However for Silver-washed Fritillary, which has a more limited range in the UK, the index derived using a geometric mean is much lower, although taking only regions with an index of above 0.05 produces an index more similar to the simple index for all locations (black line). The indices of abundance in Figure 2.17b show similar patterns to the occupancy indices, despite having a different scale and representing changes in abundance, from UKBMS data, rather than changes in occupancy from BNM data.

Table 2.14 compares estimated percentage trends from the UK occupancy indices (black lines in Figure 2.17) created from the PA model, with distribution and abundance trends reported in Fox et al. (2011a). The predicted trends from the PA model are of the same sign as the reported trends, but for Wall Brown and Ringlet the values are of a greater magnitude, implying that changes in distribution may be greater than previously suggested. Given the regional indices presented in this section, novel estimates of regional trends in distribution could also be made.

In this section we have proposed innovative indices for studying variation in occupancy, but wider application is needed to identify the optimal approach, which may vary for different species. We discuss some possible avenues for further work in the discussion of this chapter. The indices in this section have been presented without associated error estimates. Estimates of error were made as described in Section 2.2.4, but resulted in very small values. This is likely to be a result of the large number of points contributing to the indices.

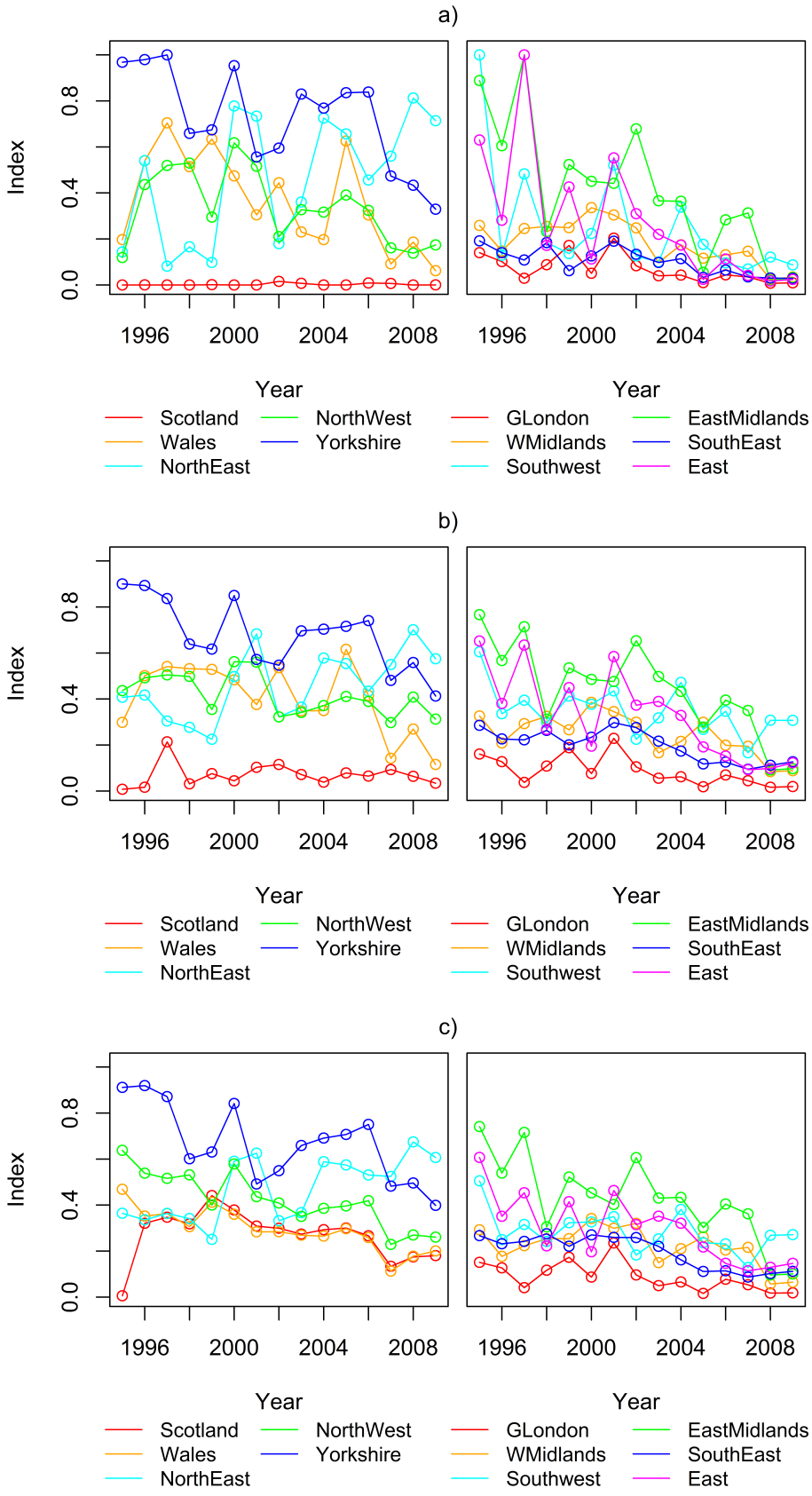

Figure 2.14: Regional occupancy indices for Wall Brown from the PA model. a) weighted index for all locations b) simple index for all locations c) simple index for only recorded locations.

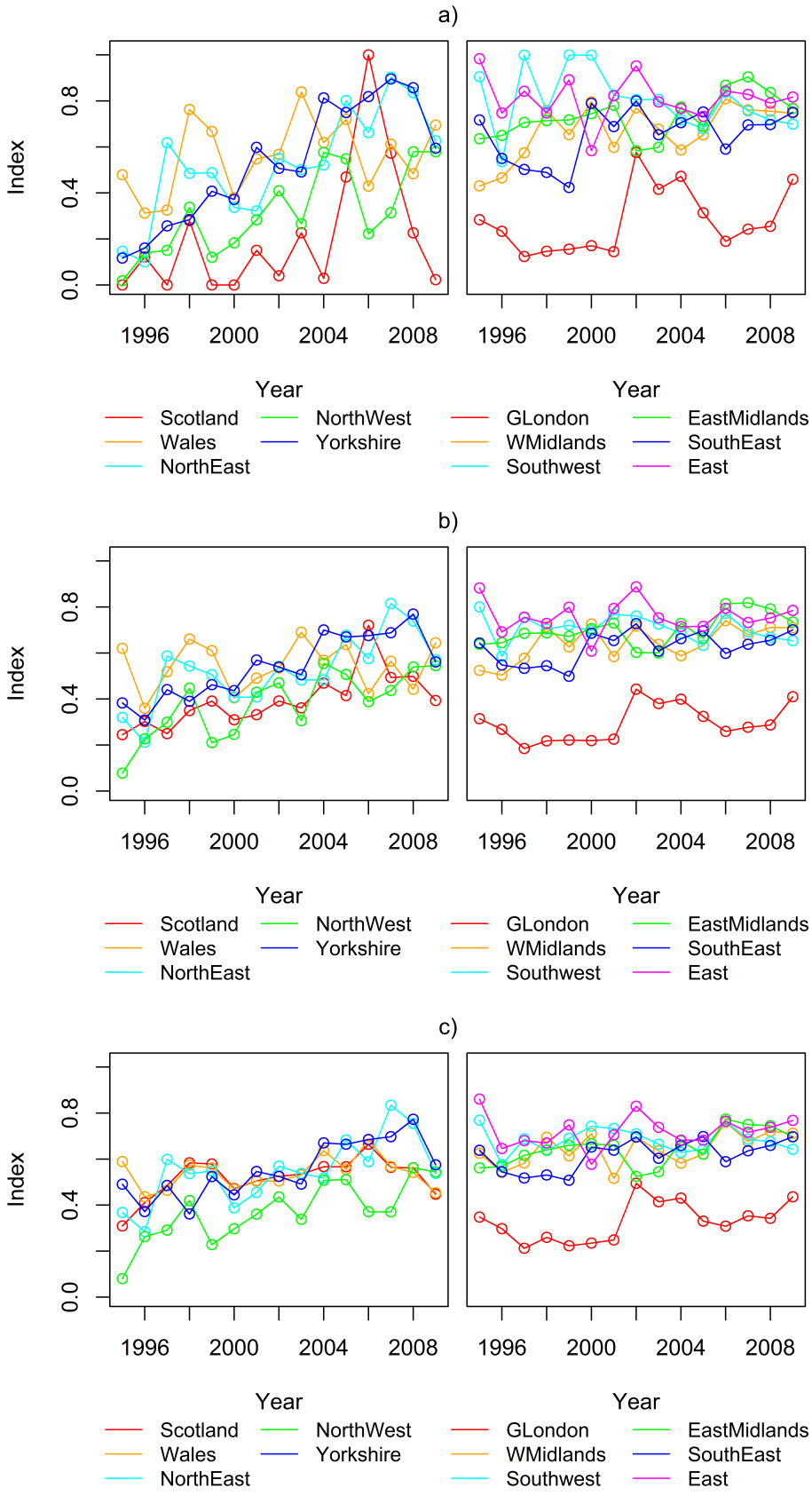

Figure 2.15: Regional occupancy indices for Ringlet from the PA model. a) weighted index for all locations b) simple index for all locations c) simple index for only recorded locations.

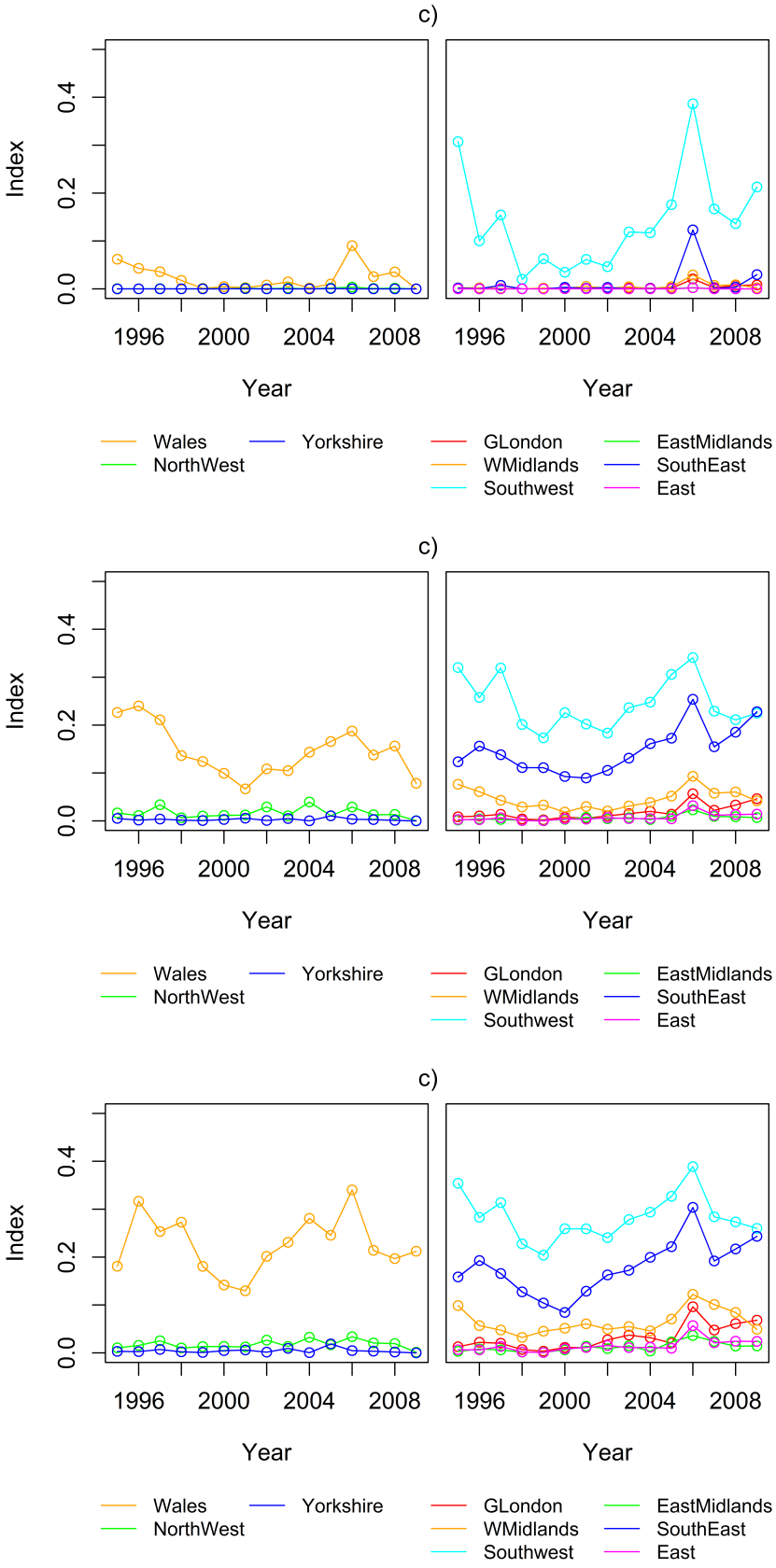

Figure 2.16: Regional occupancy indices for Silver-washed Fritillary from the PA model. a) weighted index for all locations b) simple index for all locations c) simple index for only recorded locations.

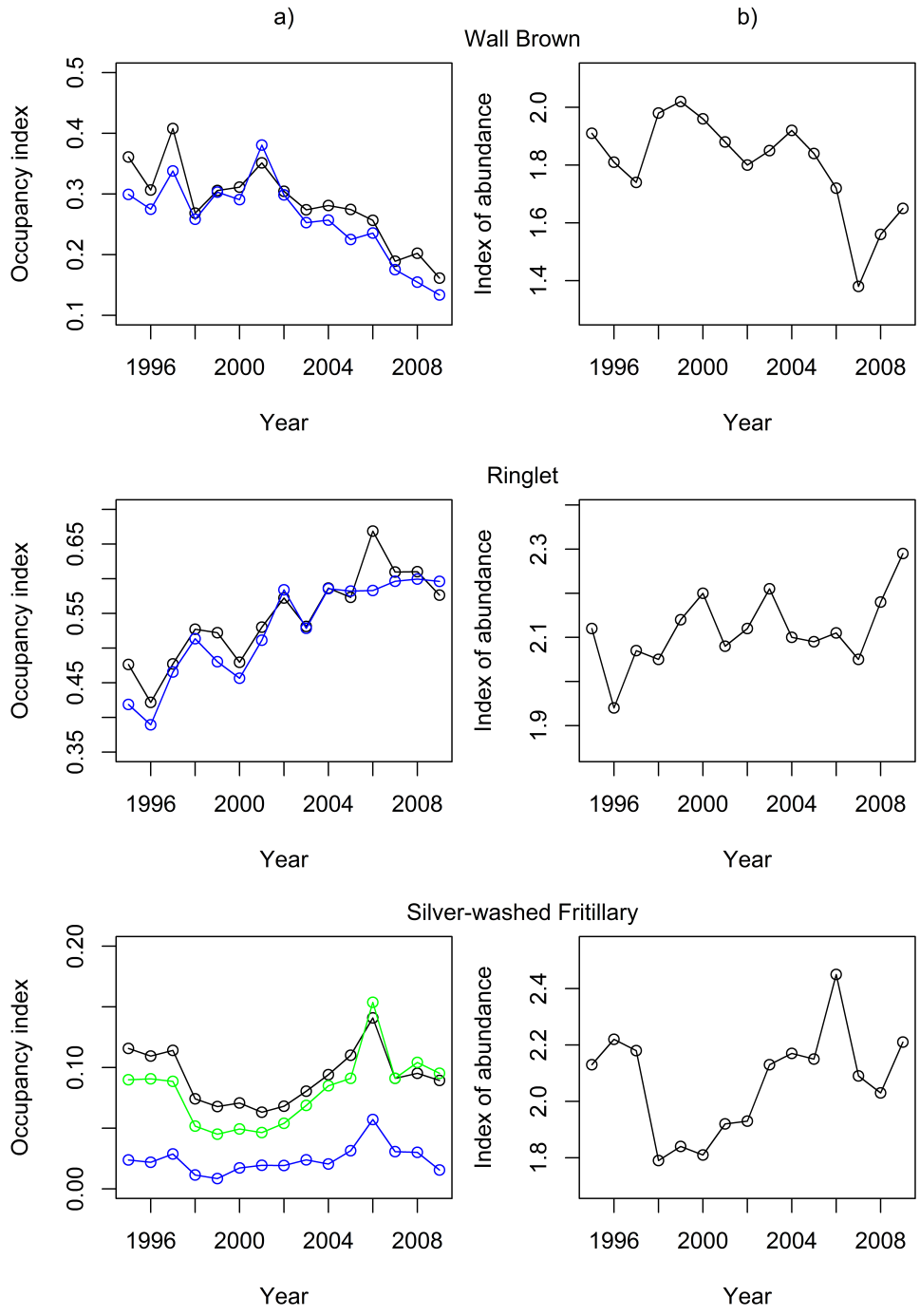

Figure 2.17: a) UK occupancy indices for each of the three species based on an index calculated for the UK (black), a geometric mean of all regions (blue), or a geometric mean of regions with a minimum occupancy index of at least 0.05 (green). The simple index approach based on all locations was used. b) Index of abundance for each species, generated from UKBMS data using the two-stage GAM approach.

Table 2.14: Comparison of trends in occupancy and abundance. Trends for PA represent percentage change of the linear trend of the UK occupancy index from the PA model (black lines in Figure 2.17a). RDT and RAT are the distribution and abundance trends reported in Fox et al. (2011a). Significant trends are represented by $*p \leq 0.05$, $**p \leq 0.01$ and $***p \leq 0.001$, but were not reported for RDT.

	Series trend (%)				
Species	PA		RDT	RAT	
Wall Brown	-46	***	-21	-37	*
Ringlet	37	***	8	25	*
Silver-washed Fritillary	4		12	38	

2.5 Discussion

This chapter has investigated the performance of occupancy models when applied to unstandardised, opportunistic distribution data for UK butterflies. Using a site-occupancy model with benchmarking (PA model) was found to be superior to the presence-only Maxlike model (PO model) for estimating spatial occupancy from BNM data.

Despite performing comparably to the PA model in some instances, the PO model did not produce consistent results for each year for the three species considered. As highlighted by Royle et al. (2012), a key assumption of the PO model is that the data arise from a random sample of presence locations which could be an inappropriate assumption for ad-hoc data. For example there could be bias in the records towards locations with a high butterfly density or known to have specific species present. The presence-only model may be suitable in some other contexts, particularly where detection can more reasonably be assumed as constant and sampling to be random.

The PO model was particularly unreliable for Silver-washed Fritillary. In the scenarios where the model-fitting did not converge, a feature which could also present itself for other species not assessed here, it is possible

that convergence might be achieved by wider testing of suitable covariates or starting values, however this may be futile given that the PA model had no difficulty in fitting to these data.

The findings in this chapter provide a basis for devising recommendations for new modelling of the BNM data with occupancy models. Modelling of the UK butterfly distributions has previously been limited, particularly in the context of wide-scale application for monitoring many species over multiple years. Further application, particularly to a wider set of species and scenarios, may lead to a new framework for modelling the distributions of UK butterflies, which will benefit the study and assessment of changes in distribution, both in terms of contractions and expansions. As for the methods in Chapters 5 and 6, which model butterfly abundance, the optimal approach for modelling occupancy may vary according to species and study aim. An area for future study is the modelling of local changes in occupancy (and abundance), for example at sites of particular conservation interest.

The creation of dynamic maps provides an up-to-date tool for visualising and monitoring changes in a species' distribution, and could benefit the motivation and retention of the citizen scientists that contribute to the BNM database. Furthermore, Kéry et al. (2013) highlighted the importance of providing associated error maps, providing a demonstration for European crossbill *Loxia curvirostra* in Switzerland, and stating that "quantifying and honestly communicating the uncertainty in species distribution maps is a greatly under-appreciated but very important issue", although of course it is important to remember that the errors themselves are only estimates. The dynamic maps were created for illustration, and in future suitable code could be developed to generate dynamic maps easily, for potential presentation on websites that can be easily accessed.

This chapter has only illustrated the potential of using occupancy models to estimate spatial occupancy for UK butterflies, and further analysis is needed. Appropriate model selection is required to identify the most suitable covariates for both occupancy and detection probability, which is likely

to vary among species, and will influence the resulting occupancy estimates and associated maps and indices. Here only variables for aggregated land cover classes were considered, whereas more specific subclasses may be important, particularly for habitat specialist species, such as those restricted to or favouring chalk and limestone grassland, for example Chalkhill Blue and Adonis Blue (Asher et al. 2001). Incorporating information on specific plant distributions could be valuable for species with specific or favoured foodplants (Asher et al. 2001), for example Purple Hairstreak is restricted to oak trees, whereas Adonis Blue favours Horseshoe Vetch *Hippocrepis comosa*. Variables linked to species' host plants have been shown to relate to butterfly distributions by Dennis et al. (2005).

Here we considered only linear or quadratic covariate relationships. A quadratic relationship was assumed for some covariates, such as those related to weather, as a linear relationship may be too limiting, but quadratic effects allow for variations at extremes, for example a species may favour temperatures that are neither too warm or too cold. Other non-linear relationships could be accounted for, as in Maxent (Elith et al. 2011; Merow et al. 2013). For example, splines could be incorporated, as used to describe variation in detection by Strebel et al. (2014).

In this analysis we allowed detection probability to vary with a species' seasonal variation in abundance by using the proportion of observations made per week as a covariate. A similar metric was used for predicting phenology by Bishop et al. (2013), although a spline may also provide a flexible modelling approach for detectability (Strebel et al. 2014). Other applications of occupancy models to opportunistic data for taxa such as butterflies have used date as a covariate for detection probability, but have limited the analysis to a single brood for bi- or multivoltine species (van Strien et al. 2013).

There may be many other influences on detection probability, for example weather-based covariates could be included if available, or covariates to account for spatial variation in detection, such as land cover type or latitude. Given the incorporation of suitable covariates, relationships could be

inspected to advance the study of factors that influence changes in species' range and distribution, although for opportunistic data sets such as the BNM, suitable covariates for detection probability may not typically be available. We anticipate that for taxa such as butterflies, within-season variation in detection arising from variation in the number of adult butterflies may outweigh variation in detection from other factors, although investigating the effects of the number of species recorded is an avenue for further work (van Strien et al. 2013).

Royle and Nichols (2003) developed a model that incorporates heterogeneity in detection probability as a result of variation in abundance, and in doing so estimates of site abundance can be obtained from presence-absence data, which are typically cheaper and easier to obtain than count data, such as for the UKBMS. Although in this chapter we have shown detection probability to vary with abundance, the Royle-Nichols model requires abundance to be constant within a period of closure, which is unlikely for butterflies due to the seasonal variability. Nowicki et al. (2008) and Bried and Pellet (2011) suggest that a situation where samples are made on the same day may be an exception, but this would not be applicable for opportunistic data such as from the BNM. Similar issues apply for fitting the N-mixture model in Chapter 3 to count data for butterflies, due to a lack of closure between repeated visits. Nowicki et al. (2008) point out that abundance estimates from the Royle-Nichols model are also likely to be biased for large population numbers with low individual detection probabilities, which was supported by Bried and Pellet (2011) who found that presence-absence did not reliably estimate abundance for a sparse butterfly species.

The choice of benchmark species in the PA model could be fine-tuned. For example, rather than taking the most prevalent species, considering whether particular habitats are covered by the selected benchmark species may improve the approach. Adopting a regional approach to benchmarking would also be worth consideration, since the expected list of species likely to be found will vary regionally, for example species found in Scotland will vary considerably compared to those found in southern England. Hill (2011)

adopted a regional benchmarking approach for analysing the occurrence of bryophytes, but a much higher level of species richness was available than for UK butterfly species. In many applications, the full list of observed species is used, and the length of the list of species observed at each site on a particular visit may be used as a measure of observation and reporting effort in the form of a covariate for detection probability (Szabo et al. 2010; van Strien et al. 2013).

There may be benefit in accounting for spatial autocorrelation in occupancy probability (Johnson et al. 2012), for example Bled et al. (2011) explicitly account for relative distances between sites as well as the influence of local density on occupancy. However these approaches may be computationally draining for multi-species, multi-year analyses, particularly at fine spatial scales over potentially large ranges.

Combining multiple sources of information has received growing interest (Schaub and Kéry 2012). A preliminary investigation of combining UKBMS data, treating the counts as presence-absence data, with BNM data produced no appreciable benefit in occupancy estimation. Pagel et al. (2014) modelled temporal variation in range size and abundance by combining BNM and UKBMS data at the 10 km scale, but discuss the potential limitations for widespread application.

Within the BNM there are under-sampled areas in some regions of the UK. Incorporation of data from other schemes (UKBMS and WCBS) may reduce this issue, or alternatively a post-stratification of sites may be possible to reduce bias from under-sampled areas or land cover types (Van Turnhout et al. 2008), as suggested in van Strien et al. (2013).

The benchmarking approach has the benefit of multi-year dynamic models for presence-absence data already being available (MacKenzie et al. 2006), which can be fitted using a hierarchical perspective (Royle and Kéry 2007; Royle and Dorazio 2008). Dynamic occupancy models are an avenue for further work which may provide the opportunity to study temporal changes in the distribution of UK butterflies better, with relevant extinction and colonisation probability parameters, which were each mapped by Kéry

et al. (2013). However, as pointed out by van Strien et al. (2013), fitting such occupancy models to large data sets can be computationally intensive, particularly in a Bayesian framework. Bled et al. (2011) developed dynamic occupancy models to study the direction of spread of invasive species, which could be applied to range expansion, but may require a coarser scale than 1 km^2.

Recent developments of occupancy models allow the closure assumption to be relaxed, and the arrival and departure times of a species to be described, providing estimates of phenology (Kendall et al. 2013; Chambert et al. 2015). Roth et al. (2014) demonstrated a method for estimating arrival and departure dates based on occupancy models, and estimated the length of the flight period for two butterfly species. Adaptation of these models may be possible for bi- or multivoltine species. Although in this case the arrival and departure of the species, rather than individuals, is modelled. In Section 4.2 we describe stopover models that estimate emergence and departure (death) from count data, where survival can also be estimated, which are then applied further in Chapters 5 and 6.

The novel regional indices developed in this chapter allow for the study of occupancy trends in regions of particular interest and how changes in occupancy might vary spatially over a species' range, for example to determine whether behaviour is related between certain regions. National indices may also provide new perspectives of distribution trends for UK butterflies, which have previously only been reported in terms of percentage change over multi-year periods. Indices for groups of particular species may be derived by taking the geometric mean of the indices for each species (Buckland et al. 2005; Brereton et al. 2011b), on a UK, country or now regional basis.

The regions used in this chapter were chosen arbitrarily for demonstration, and alternative methods for choosing appropriate regions may be preferred. There is much potential to derive alternative spatial indices, for example using a clustering mechanism, or by alternative regions, for example by land cover type, or for urban areas. The fitted models could also be used to derive occupancy indices for specific areas or sites of interest. Har-

rison et al. (2014) displayed changes in the abundance of farmland birds for each 100 km square in the UK on a map. The regional occupancy indices described in this chapter could be visualised in a similar way.

Opportunistic schemes are commonly used to form atlases for various taxa around the world and these methods are likely to be applicable to other species groups. In the UK alone, 39 recording schemes exist for mapping the distributions of invertebrates, overseen by the Biological Records Centre (BRC), in addition to schemes for birds and plants (Thomas 2005).

Chapter 3

N-mixture models

Estimating the abundance of a population is an important component of ecological research. The N-mixture model (Royle 2004a) is widely used to estimate animal abundance from only a set of counts. In this chapter we explore computational aspects of fitting the N-mixture model. In particular, we show that especially when detection probability and/or the number of sampling occasions are small, infinite estimates of abundance can arise. We also explain and exploit the equivalence of N-mixture and multivariate Poisson and negative-binomial models, which provides powerful new approaches for fitting these models. This chapter is based on Dennis et al. (2015b), from which all tables and figures in the chapter have been taken.

3.1 Background

N-mixture models can be used to estimate animal abundance from counts, subject to both spatial and temporal replication, whilst accounting for imperfect detection (Royle 2004a). Whereas alternative sampling methods for obtaining estimates of abundance exist, such as capture-recapture, distance, removal and multiple-observer sampling, these may be expensive in effort or cost, or impractical for some species and scenarios. A benefit of the N-mixture model is the reasonably low comparative cost and effort required for data collection, which does not require individuals to be identified. This is especially true of many citizen-science based monitoring programs.

Consequently, since development by Royle (2004a), many applications and extensions of the N-mixture model have been made. These include applications to various taxa, including birds (Kéry et al. 2005), mammals (Zellweger-Fischer et al. 2011) and amphibians (Dodd and Dorazio 2004; McIntyre et al. 2012). In addition, covariates have often been used to examine spatial patterns in abundance and detection (Kéry 2008) and hence create maps of spatial abundance (Royle et al. 2005). Dénes et al. (2015) review extensions that have been made to the N-mixture model, and we describe many of these in the discussion of the chapter.

Despite the popularity of the N-mixture model, only limited studies have made comparisons with estimates derived via alternative methods or undertaken simulation studies of performance (for example Hunt et al. 2012; Couturier et al. 2013; Yamaura 2013). A potential issue for fitting the model using classical inference is the need to specify an upper bound, K, to approximate an infinite summation in the likelihood. We found this matter was rarely mentioned in publications. For example, McIntyre et al. (2012) used simulated data to support their amphibian study, highlighting the benefit of more sampling occasions, particularly when detection probability was low, however the value of K used was not provided. When software such as `unmarked` (Fiske and Chandler 2011) written in `R` (R Core Team 2015) and PRESENCE (Hines 2011) is used for model fitting, it is possible that only default values of the bound K are employed. Yamaura (2013) performed simulations for the N-mixture model under various scenarios, but noted that the choice of K did not influence the results. However, in an application to Goldcrest data, Knape and Korner-Nievergelt (2015) found that estimates of abundance were sensitive to K, and suggested that in some cases abundance and detection may not be separable. Couturier et al. (2013) suggest bias could be induced by the choice of K for low detection probabilities and we revisit the data from this study in Section 3.7.

In this chapter we explore the effect that K can have on parameter estimates. We investigate computational aspects of fitting N-mixture models, in particular via a simulation study for scenarios where detection probabil-

ity is low and/or the number of sampling occasions is small. This may be of particular importance for the study of cryptic species, and may have implications for sample design: many applications to date have made only three visits, whereas in Royle (2004a) simulations were tested for five visits and an application made to data with ten visits. When only one sampling visit is made, it is well known that in the absence of covariates the N-mixture model reduces to a thinned Poisson distribution, with only one estimable parameter, the product of mean abundance and detection probability, a feature which underlies aspects of the work which follows.

The N-mixture model is described in Section 3.2. In Section 3.3 we explain the equivalence of the Poisson N-mixture model with a multivariate Poisson distribution. We use this formulation to show that infinite estimates of abundance may arise, and provide a simple diagnostic to identify such cases. The multivariate Poisson formulation has the advantage of not requiring a constant K to be set. Section 3.4 provides the probability function in the bivariate negative-binomial case. In Section 3.5 we show how the choice of K in the N-mixture model interacts with the occurrence of infinite estimates of abundance, and how incorrect conclusions may arise. An automatic method for choosing K is provided. Section 3.6 provides moment estimates and evaluates the use of two diagnostic tests for the negative-binomial case for when infinite estimates of abundance may arise. Section 3.7 provides an application to real data on Hermann's tortoise *Testudo hermanni*, and the chapter ends with discussion in Section 3.8. Appendix A assesses the performance of method-of-moments estimation compared to maximum likelihood from the N-mixture model.

3.2 The N-mixture model

Under the study design in Royle (2004a), a set of counts is made during sampling visits $j = 1, 2, \ldots, T$ at $i = 1, 2, \ldots, S$ locations (sites). In this chapter we assume that visits are equally spaced over time, and hence time, occasion and visit are interchangeable. The population is assumed to be

closed during the period of sampling, for example with respect to mortality, recruitment and movement, and each individual is assumed to have the same detection probability p. Each count $y_{i,j}$ at site i and time j is then assumed to be an independent binomial random variable,

$$y_{i,j} \sim \text{Bin}(N_i, p),$$

where N_i is the unknown population size at site i. To fit the model using classical inference, we assume the N_i to be independent random variables with probability density function $f(N; \boldsymbol{\theta})$, and then maximise the likelihood

$$\text{L}(p, \boldsymbol{\theta}; \{y_{i,j}\}) = \prod_{i=1}^{S} \left[\sum_{N_i=\kappa_i}^{\infty} \left\{ \prod_{j=1}^{T} \text{Bin}(y_{i,j}; N_i, p) \right\} f(N_i; \boldsymbol{\theta}) \right], \tag{3.1}$$

where $\kappa_i = \max_j y_{i,j}$. In this chapter we shall consider both Poisson and negative-binomial mixing distributions for N. As noted by Royle (2004a), numerical maximisation of (3.1) requires the replacement of the infinite summation over N_i by a sum with upper limit K. The value of K may be selected by fitting the model for a succession of increasing values and selecting K when the parameter estimates appear to stabilise (Royle 2004a).

In this chapter we will show that the N-mixture model can produce unrealistically large estimates of abundance. We describe this feature by using the equivalence of the N-mixture model with multivariate Poisson and negative-binomial models, which we will first describe for the Poisson case in the next section.

3.3 Equivalence of the Poisson N-mixture model with a multivariate Poisson model

The number of individuals observed at a site at time j can be written as the convolution of independent random variables, corresponding to those seen only once, those seen twice etc. This natural feature of the N-mixture model can be formalised as we now show.

Let $\mathcal{S}$ denote the set of non-empty subsets of $\{1, \ldots, T\}$, and let the random variable $X_{i,s}\,(s \in \mathcal{S})$ denote the number of individuals seen at site

i only on occasions s. For example, $X_{i,124}$ denotes the individuals seen at site i on occasions 1, 2 and 4 only. Then, if we let $\mathcal{S}_j$ denote those elements of $\mathcal{S}$ that include a given occasion j, we can decompose $y_{i,j}$ as

$$y_{i,j} = \sum_{s \in \mathcal{S}_j} X_{i,s}.$$

For example, with $T = 3$, we have

$$\begin{aligned} y_{i,1} &= X_{i,1} + X_{i,12} + X_{i,13} + X_{i,123} \\ y_{i,2} &= X_{i,2} + X_{i,12} + X_{i,23} + X_{i,123} \\ y_{i,3} &= X_{i,3} + X_{i,13} + X_{i,23} + X_{i,123}. \end{aligned}$$

Conditional on N_i, the joint distribution of the set of random variables $X_{i,s}\,(s \in \mathcal{S})$ is multinomial, with index N_i and probabilities $\pi_{i,s} = p^{|s|}(1-p)^{T-|s|}$, where $|s|$ denotes the number of elements in the set s. When $N_i \sim \text{Pois}(\lambda)$, the $X_{i,s}\,(s \in \mathcal{S})$ are independent Poisson random variables, with

$$\mathbb{E}\left(X_{i,s}\right) = \lambda p^{|s|}(1-p)^{T-|s|},$$

see Johnson et al. (1997, p146). The thinned Poisson is the case $T = 1$.

It follows that the joint distribution of $(y_{i,1}, \ldots, y_{i,T})$ is multivariate Poisson (Johnson et al. 1997, Chapter 37), with

$$\mathbb{E}(y_{i,j}) = \sum_{s \in \mathcal{S}_j} \mathbb{E}(X_{i,s}) = \sum_{s \in \mathcal{S}_j} \lambda p^{|s|}(1-p)^{T-|s|}.$$

There are $\binom{T-1}{k-1}$ subsets $s \in \mathcal{S}_j$ such that $|s| = k$ $(k = 1, \ldots, T)$. Hence

$$\mathbb{E}(y_{i,j}) = \sum_{k=1}^{T} \binom{T-1}{k-1} \lambda p^k (1-p)^{T-k} = \lambda p.$$

Similarly, if we let $\mathcal{S}_{j,u}$ denote the elements of $\mathcal{S}$ that include both occasions j and u then

$$\text{cov}(y_{i,j}, y_{i,u}) = \sum_{s \in \mathcal{S}_{j,u}} \text{var}(X_{i,s}) = \sum_{s \in \mathcal{S}_{j,u}} \lambda p^{|s|}(1-p)^{T-|s|}.$$

There are $\binom{T-2}{k-2}$ subsets $s \in \mathcal{S}_{j,u}$ such that $|s| = k$ $(k = 2, \ldots, T)$. Hence, for $j \neq u$,

$$\text{cov}(y_{i,j}, y_{i,u}) = \sum_{k=2}^{T} \binom{T-2}{k-2} \lambda p^k (1-p)^{T-k} = \lambda p^2,$$

and $\text{corr}(y_{i,j}, y_{i,u}) = p$ $(j \neq u)$.

This result is a special case of Johnson et al. (1997, Equation 37.88), which is stated there without proof.

3.3.1 Example: T=2, Poisson case

Cormack (1989) mentions this case in closed-population capture-recapture modelling of data from one site only.

Suppressing site dependence, we have

$$y_1 = X_1 + X_{12} \qquad \text{and} \qquad y_2 = X_2 + X_{12}$$

where X_1, X_2, X_{12} are independent with $X_1, X_2 \sim \text{Pois}(\theta_1)$, where $\theta_1 = \lambda p(1-p)$ and $X_{12} \sim \text{Pois}(\theta_0)$, where $\theta_0 = \lambda p^2$. Note that small p would result typically in small values for X_{12}, and as p tends to zero y_1 and y_2 become independent, so that the model reverts to a thinned Poisson.

The counts (y_1, y_2) follow a bivariate Poisson distribution with $\text{corr}(y_1, y_2) = p$, and the bivariate Poisson probability is

$$\begin{aligned}\Pr(y_1, y_2; \lambda, p) &= \sum_{u=0}^{\min(y_1,y_2)} \left[\frac{e^{-\lambda p^2}(\lambda p^2)^u e^{-2\lambda p(1-p)}}{u!(y_1-u)!(y_2-u)!} \{\lambda p(1-p)\}^{y_1+y_2-2u} \right] \\ &= \{p(1-p)\}^{y_1+y_2} \sum_{u=0}^{\min(y_1,y_2)} \frac{e^{-\lambda(2p-p^2)}\lambda^{y_1+y_2-u}}{(1-p)^{2u}u!(y_1-u)!(y_2-u)!}.\end{aligned} \tag{3.2}$$

Including site dependence, the likelihood is

$$\text{L}(p, \lambda; \{y_{i,j}\}) = e^{-(2\theta_1+\theta_0)} \prod_{i=1}^{S} \left\{ \frac{\theta_1^{y_{i,1}+y_{i,2}}}{y_{i,1}!y_{i,2}!} \sum_{u=0}^{\min(y_{i,1},y_{i,2})} \binom{y_{i,1}}{u} \binom{y_{i,2}}{u} u! \left(\frac{\theta_0}{\theta_1^2}\right)^u \right\}. \tag{3.3}$$

For $T = 2$ the expressions of (3.1) and (3.3) are identical, but the likelihood of (3.3) may be maximised without requiring selection of a value K. □

3.3.2 Multivariate Poisson distribution

For general T, let $\mathcal{X}_i$ denote the set of all possible values $x_{i,s}$ of the random variables $X_{i,s},\ s \in \mathcal{S}$ such that

$$y_{i,j} = \sum_{s \in \mathcal{S}_j} x_{i,s}, \qquad j = 1, \ldots, T.$$

Because the random variables $X_{i,s}$ are independent, the joint probability function of $(y_{i,1}, \ldots, y_{i,T})$ is

$$\Pr(y_{i,1}, \ldots, y_{i,T}) = \sum_{\mathcal{X}_i} \prod_{s \in \mathcal{S}} \Pr(X_{i,s} = x_{i,s}),$$

and

$$\prod_{s \in \mathcal{S}} \Pr(X_{i,s} = x_{i,s}) = \prod_{s \in \mathcal{S}} \frac{\exp\left\{-\lambda p^{|s|}(1-p)^{T-|s|}\right\}\left\{\lambda p^{|s|}(1-p)^{T-|s|}\right\}^{x_{i,s}}}{x_{i,s}!}.$$

There are $\binom{T}{k}$ elements $s \in \mathcal{S}$ such that $|s| = k$, for $k = 1, \ldots, T$. Hence

$$\begin{aligned}\prod_{s \in \mathcal{S}} \exp\left\{-\lambda p^{|s|}(1-p)^{T-|s|}\right\} &= \exp\left\{-\lambda \sum_{k=1}^{T} p^k (1-p)^{T-k}\right\} \\ &= \exp\left[-\lambda\left\{1-(1-p)^T\right\}\right].\end{aligned}$$

Therefore, we can write

$$\begin{aligned}\Pr(y_{i,1}, \ldots, y_{i,T}; \lambda, p) = \sum_{\mathcal{X}_i} \prod_{s \in \mathcal{S}} &\frac{\left\{p^{|s|}(1-p)^{T-|s|}\right\}^{x_{i,s}}}{x_{i,s}!} \\ &\times \exp\left[-\lambda\left\{1-(1-p)^T\right\}\right] \lambda^{\sum_{s \in \mathcal{S}} x_{i,s}}. \qquad (3.4)\end{aligned}$$

We can check that the case $T = 2$ is given in (3.2). An associated `R` program, which is provided as an electronic appendix to this thesis, contains the functions required to optimised the multivariate Poisson (and negative-binomial) formulation of the N-mixture model and incorporates efficient construction of $\mathcal{X}_i$.

3.3.3 Performance of the multivariate Poisson model

For illustration, we investigate performance of the multivariate Poisson model via simulation from the fitted model. We assess output for the cases $T = 2, 3, 4$ based upon 1000 simulations where $\lambda = 2, 5, 10$, $p = 0.1, 0.25$ and $S = 20$. The chosen parameter values were guided by those used in Royle (2004a). The model was fitted using the `optim` function in the `R` software package (R Core Team 2015) using the default Nelder-Mead algorithm and a tolerance value of 1×10^{-12}. The results were checked with those from using several other `optim` algorithms, including simulated annealing and quasi-Newton.

We observe that estimates for λ were very large in some cases (the maximum estimate from 1000 simulations was 1.36×10^{13} when $\lambda = 5$, $p = 0.25$ and $T = 2$). Figure 3.1 shows that non-positive values of a covariance diagnostic,

$$\text{cov}^*(y_1, y_2) = \overline{y_1 y_2} - \{(\overline{y_1} + \overline{y_2})/2\}^2, \tag{3.5}$$

can identify the high estimates of λ from fitting the bivariate Poisson. Here $\overline{y_1 y_2}$ denotes the mean of the product $y_1 y_2$ over S sites. Note that this (intraclass) estimate is appropriate as $\mathbb{E}[y_1] = \mathbb{E}[y_2]$. A proof that a local maximum of the likelihood occurs at $p = 0$ when $\text{cov}^*(y_1, y_2) \leq 0$ is given in the next section. In unpublished work, Professor Peter Jupp, of the University of St Andrews, has proved that for the case $T = 2$ there are no other maxima when the diagnostic is satisfied. Further work is required for a general proof for $T > 2$. Hence, in these instances when $\hat{p} = 0$, in order to have finite $\widehat{\lambda p}$, $\hat{\lambda}$ is actually infinite and the large range of high estimates of abundance obtained in practice, as in Figure 3.1, is partly an artefact of the optimisation routine stopping prematurely when the likelihood is flat.

For more than two visits, which corresponds to $T > 2$, the appropriate

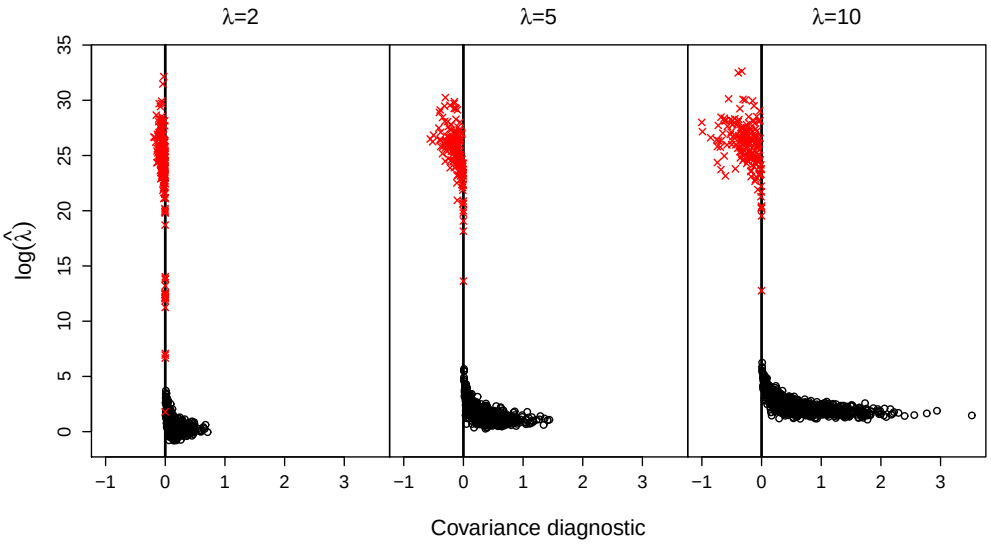

Figure 3.1: $\text{Log}(\hat{\lambda})$ from the bivariate Poisson model plotted against the covariance diagnostic, $\text{cov}^*(y_1, y_2)$ from (3.5), based upon 1000 simulated datasets for $S = 20$, $\lambda = 2, 5, 10$ and $p = 0.25$. Values at which the covariance diagnostic is negative are shown by red crosses.

covariance diagnostic can be estimated as

$$\text{cov}^*(y_1, \ldots, y_T) = \frac{2}{T(T-1)} \left(\overline{y_1 y_2} + \cdots + \overline{y_{T-1} y_T}\right) - \left(\frac{\overline{y_1} + \cdots + \overline{y_T}}{T}\right)^2, \tag{3.6}$$

where the first term consists of the average of the means of all $T(T-1)/2$ pairwise products. Our conjecture that the diagnostic extends for $T > 2$ is supported by Figure 3.2 which compares the covariance diagnostic (3.6) with $\hat{\lambda}$ from the multivariate Poisson model for $T = 3$, when $\lambda = 2, 5, 10$.

Performance of the covariance diagnostic is demonstrated further in Table 3.1, which shows close correspondence between the proportion of simulations where the diagnostic is negative and the proportion where $\hat{\lambda}$ is large ($\hat{\lambda} > 500$). Table 3.1 also shows the prevalence of infinite estimates of $\hat{\lambda}$, particularly as λ, T and p decrease. In fact for the case where $\lambda = 2$, $p = 0.1$ and $T = 2$, a finite value of $\hat{\lambda}$ was not achievable in over half of 1000 simulations.

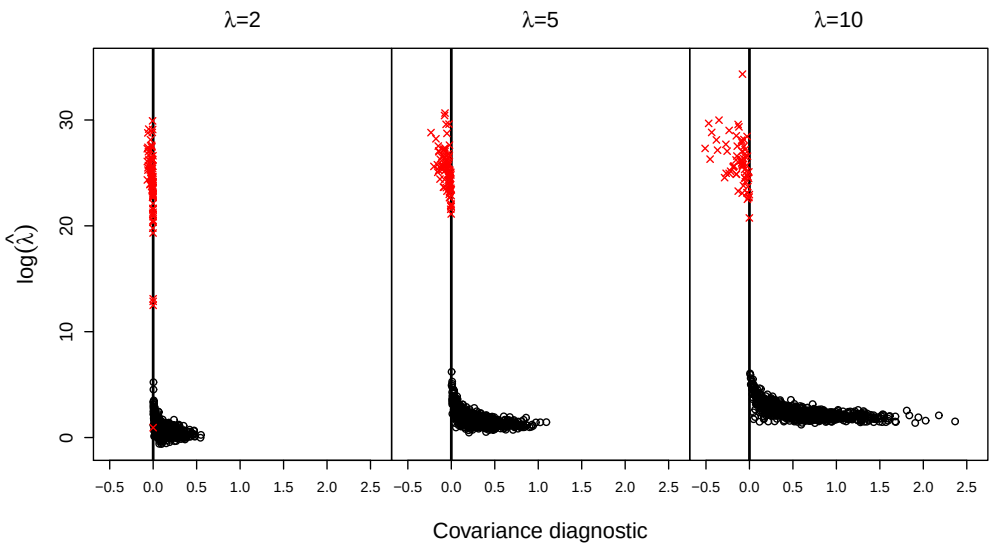

Figure 3.2: Log($\hat{\lambda}$) from the multivariate Poisson model with $T = 3$ plotted against the covariance diagnostic, cov*(y_1, y_2, y_3) from (3.6), based upon 1000 simulated datasets for $S = 20$, $\lambda = 2, 5, 10$ and $p = 0.25$. Values at which the covariance diagnostic is negative are shown by red crosses.

Table 3.1: Performance of the covariance diagnostic for the multivariate Poisson model for various scenarios of λ, p and T for $S = 20$ sites. EPN is the proportion of simulations when the sample covariance diagnostic was negative. EPD is the proportion of simulations where the estimate of $\hat{\lambda} > 500$.

		$T = 2$		$T = 3$		$T = 4$	
λ	p	EPN	EPD	EPN	EPD	EPN	EPD
2	0.10	0.505	0.505	0.351	0.351	0.276	0.276
2	0.25	0.225	0.224	0.090	0.089	0.033	0.033
5	0.10	0.427	0.427	0.362	0.361	0.219	0.222
5	0.25	0.167	0.167	0.084	0.084	0.017	0.020
10	0.10	0.398	0.398	0.317	0.318	0.251	0.256
10	0.25	0.180	0.181	0.066	0.066	0.038	0.038

Proof that when $T = 2$ a local maximum of the likelihood occurs at $p = 0$ when $\mathbf{cov}^*(y_1, y_2) \leq 0$

It is convenient here to set $\theta_0 = \lambda p^2, \theta_2 = \lambda p$. It can be proved that $\hat{\theta_2} = \frac{\sum_i (y_{i,1}+y_{i,2})}{2S}$, as noted in Holgate (1964). For observation $(y_{i,1}, y_{i,2})$, we write

$$g_i(\theta_0) = \sum_{m=0}^{u_i} \frac{\theta_0^m (\hat{\theta_2} - \theta_0)^{y_{i,1}+y_{i,2}-2m}}{m!(y_{i,1}-m)!(y_{i,2}-m)!}, \quad \text{where} \quad u_i = \min(y_{i,1}, y_{i,2}).$$

The profile log-likelihood function for θ_0 is then given by

$$\ell(\theta_0) = S(\theta_0 - 2\hat{\theta_2}) + \sum_{i=1}^{S} \log(g_i(\theta_0)) \quad \text{and}$$

$$\frac{d\ell}{d\theta_0} = S + \sum_{i=1}^{S} \frac{g_i'(\theta_0)}{g_i(\theta_0)}.$$

We deduce that

$$\frac{g_i'(0)}{g_i(0)} = \frac{1}{\hat{\theta_2}^2}\{y_{i,1}y_{i,2} - \hat{\theta_2}(y_{i,1} + y_{i,2})\}.$$

Thus

$$\left.\frac{d\ell}{d\theta_0}\right|_{\theta_0=0} = S + \frac{1}{\hat{\theta_2}^2}\left\{\sum_{i=1}^{S} y_{i,1}y_{i,2} - \hat{\theta_2}\sum_{i=1}^{S}(y_{i,1} + y_{i,2})\right\},$$

and

$$\left.\frac{d\ell}{d\theta_0}\right|_{\theta_0=0} \leq 0 \equiv \frac{1}{S}\sum_i y_{i,1}y_{i,2} \leq \hat{\theta}_2^2$$

$$\equiv \mathrm{cov}^*(y_1, y_2) \leq 0.$$

3.4 Explicit form for the bivariate negative-binomial case

The Poisson distribution may be replaced by a mixed-Poisson distribution, for which $\lambda \sim g(\lambda; \boldsymbol{\theta})$, when the probability of (3.2) becomes

$$\Pr(y_1, y_2; p, \boldsymbol{\theta})$$

$$= \{p(1-p)\}^{y_1+y_2} \sum_{u=0}^{\min(y_1,y_2)} \frac{1}{(1-p)^{2u}u!(y_1-u)!(y_2-u)!}$$

$$\times \int_0^\infty e^{-\lambda(2p-p^2)}\lambda^{y_1+y_2-u} g(\lambda; \boldsymbol{\theta})\mathrm{d}\lambda.$$

For the negative-binomial distribution, the mixing distribution is gamma with parameters $\boldsymbol{\theta} = (\alpha, \beta)$ and

$$g(\lambda; \alpha, \beta) = \frac{\beta^\alpha}{\Gamma(\alpha)} \lambda^{\alpha-1} e^{-\beta\lambda}, \text{ for } \lambda \geq 0, \tag{3.7}$$

which results in the NB-2 form (Hilbe 2011, p187). In this case

$$\begin{aligned}\int_0^\infty e^{-\lambda(2p-p^2)} \lambda^{y_1+y_2-u} g(\lambda; \alpha, \beta) \mathrm{d}\lambda \\ &= \frac{\beta^\alpha}{\Gamma(\alpha)} \int_0^\infty \left\{ e^{-\lambda(2p-p^2+\beta)} \times \lambda^{y_1+y_2-u+\alpha-1} \right\} \mathrm{d}\lambda \\ &= \frac{\beta^\alpha \Gamma(y_1+y_2-u+\alpha)}{\Gamma(\alpha)(2p-p^2+\beta)^{y_1+y_2-u+\alpha}},\end{aligned}$$

where we have used the fact that

$$\int_0^\infty \lambda^a e^{-b\lambda} \mathrm{d}\lambda = \frac{\Gamma(a+1)}{b^{a+1}} \qquad (a > -1, b > 0).$$

Therefore the joint probability for the bivariate negative-binomial model is given by

$$\begin{aligned}\Pr(y_1, y_2; p, \alpha, \beta) &= \frac{\beta^\alpha \{p(1-p)\}^{y_1+y_2}}{\Gamma(\alpha)} \\ &\times \sum_{u=0}^{\min(y_1,y_2)} \frac{\Gamma(y_1+y_2-u+\alpha)}{u!(y_1-u)!(y_2-u)!(1-p)^{2u}(2p-p^2+\beta)^{y_1+y_2-u+\alpha}}.\end{aligned} \tag{3.8}$$

In the parametrisation of (3.7), the mean and variance of the gamma distribution are α/β and α/β^2, respectively. If we now write $\lambda = \alpha/\beta$ for the expected value of the Poisson mean, then the variance is λ^2/α and the coefficient of variation of the Poisson mean is $1/\sqrt{\alpha}$. The Poisson model arises as the limit $\alpha, \beta \to \infty$, maintaining $\lambda = \alpha/\beta$.

In terms of the parameters α and λ, $\beta = \alpha/\lambda$ and we can write (3.8) as

$$\begin{aligned}\Pr(y_1, y_2; \lambda, p, \alpha) &= \frac{\alpha^\alpha \{p(1-p)\}^{y_1+y_2}}{\lambda^\alpha \Gamma(\alpha)} \\ &\times \sum_{u=0}^{\min(y_1,y_2)} \frac{\Gamma(y_1+y_2-u+\alpha)}{u!(y_1-u)!(y_2-u)!(1-p)^{2u}} \left\{ \frac{\lambda}{\lambda p(2-p)+\alpha} \right\}^{y_1+y_2-u+\alpha}.\end{aligned} \tag{3.9}$$

The case for $T > 2$ follows in the same way, by integrating the expression of (3.4), to give the multivariate negative-binomial probability as

$$\Pr(y_{i,1},\ldots,y_{i,T};\lambda,p,\alpha)=\frac{\alpha^{\alpha}}{\lambda^{\alpha}\Gamma(\alpha)}\sum_{\mathcal{X}_i}\prod_{s\in\mathcal{S}}\frac{\left\{p^{|s|}(1-p)^{T-|s|}\right\}^{x_{i,s}}\Gamma(\sum_{s\in\mathcal{S}}x_{i,s}+\alpha)}{x_{i,s}!\left\{1-(1-p)^{T}+\frac{\alpha}{\lambda}\right\}^{\sum_{s\in\mathcal{S}}x_{i,s}+\alpha}}.$$

The expression $y_{i,j}=\sum_{s\in\mathcal{S}_j}X_{i,s}$ also applies to the negative binomial case, but the $\{X_{i,s}\}$ are no longer independent.

3.5 The effect of the choice of K on fitting the N-mixture model

3.5.1 Incorrect estimates due to the choice of K

We now consider how the choice of K for computing the Poisson N-mixture likelihood of (3.1) interacts with the occurrence of infinite estimates of λ. Output is obtained for 1000 simulations based on the parameter values used in Royle (2004a), where $\lambda=5$, $p=0.25$ and $S=20,50$, but for number of sampling occasions $T=2,3,4,5$. The models were again fitted using `optim` in the `R` software package using the default Nelder-Mead algorithm and a tolerance value of 1×10^{-12}. The parameters p and λ were constrained to be in range via logit and log link functions, respectively. Each simulated dataset was fitted with $K=100,500,1000$.

We see that large finite estimates of abundance can arise, in particular where the number of sampling occasions T is small (Figure 3.3). Specifically, a proportion of simulations result in a second peak in the sampling distribution for $\hat{\lambda}$ and the value at which this is found increases with the value of K. Fitting the multivariate Poisson model to simulated data created under comparable scenarios for $T=2,3,4$ also produced a second peak in the sampling distribution for λ, but as described in Section 3.3.3, the estimates were substantially greater in the absence of the limiting value K in the N-mixture model. An increase in the number of sampling occasions reduces the incidence of high estimates of λ, which become rare for $T>3$, as more information is available as T increases. For $T=5$ very few high estimates of λ occurred in the 1000 simulations. Figure 3.4 demonstrates that an increase in the number of sites also reduces the proportion of high values.

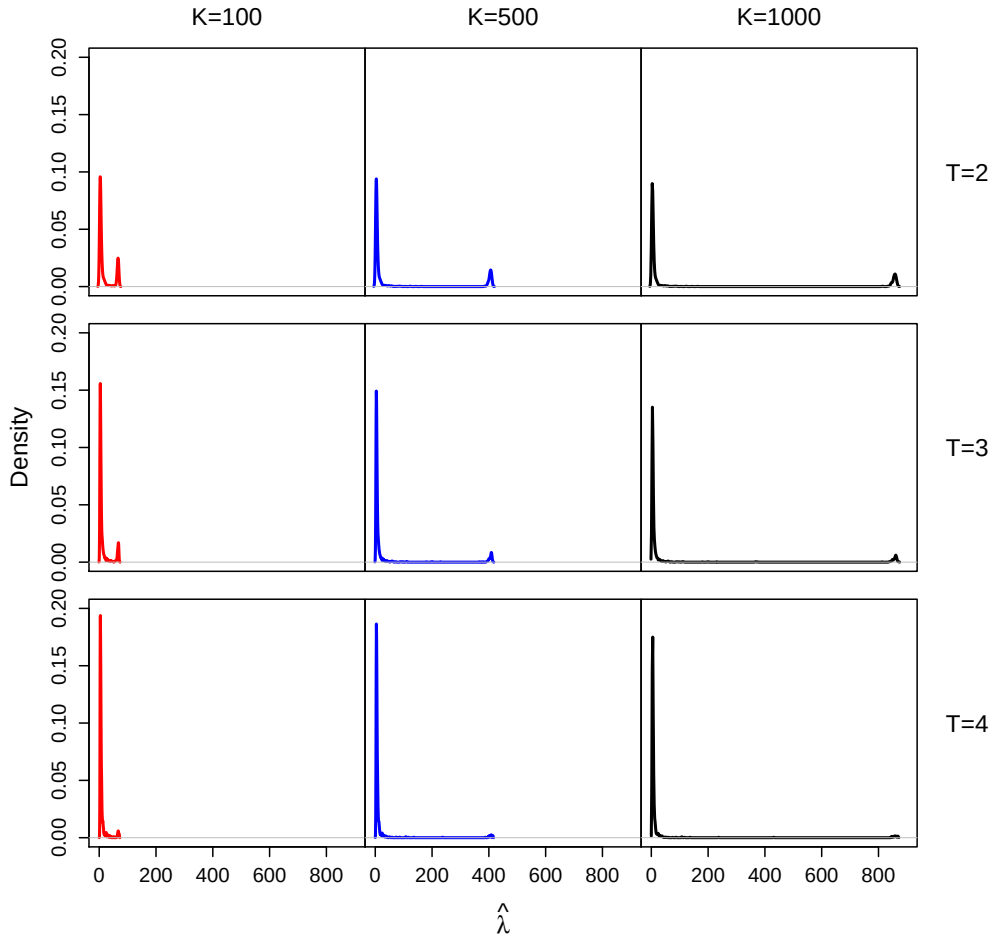

Figure 3.3: Kernel density estimates of $\hat{\lambda}$ from the Poisson N-mixture model when $S = 20$, $\lambda = 5$ and $p = 0.25$, based upon 1000 simulated datasets for $T = 2, 3, 4$ and $K = 100, 500, 1000$.

Thus when the N-mixture model is fitted by maximising the likelihood of (3.1), when $\hat{\lambda}$ should be infinite, λ is estimated as large as possible for a given value of K, and $\hat{p}$ is restricted to be as close to zero as possible. The occurrence of large finite estimates of λ is similar to analogous findings of Wang and Lindsay (2005) in the context of species richness estimation.

Figure 3.5a illustrates the effect of K for a single simulated dataset, with $\hat{\lambda}$ increasing linearly with K. The corresponding relationships from different simulations and parameter values are found to be very similar. The heuristic reason for this, and the fact that the green line in Figure 3.5a lies below the line of unit slope through the origin, is that for large λ the

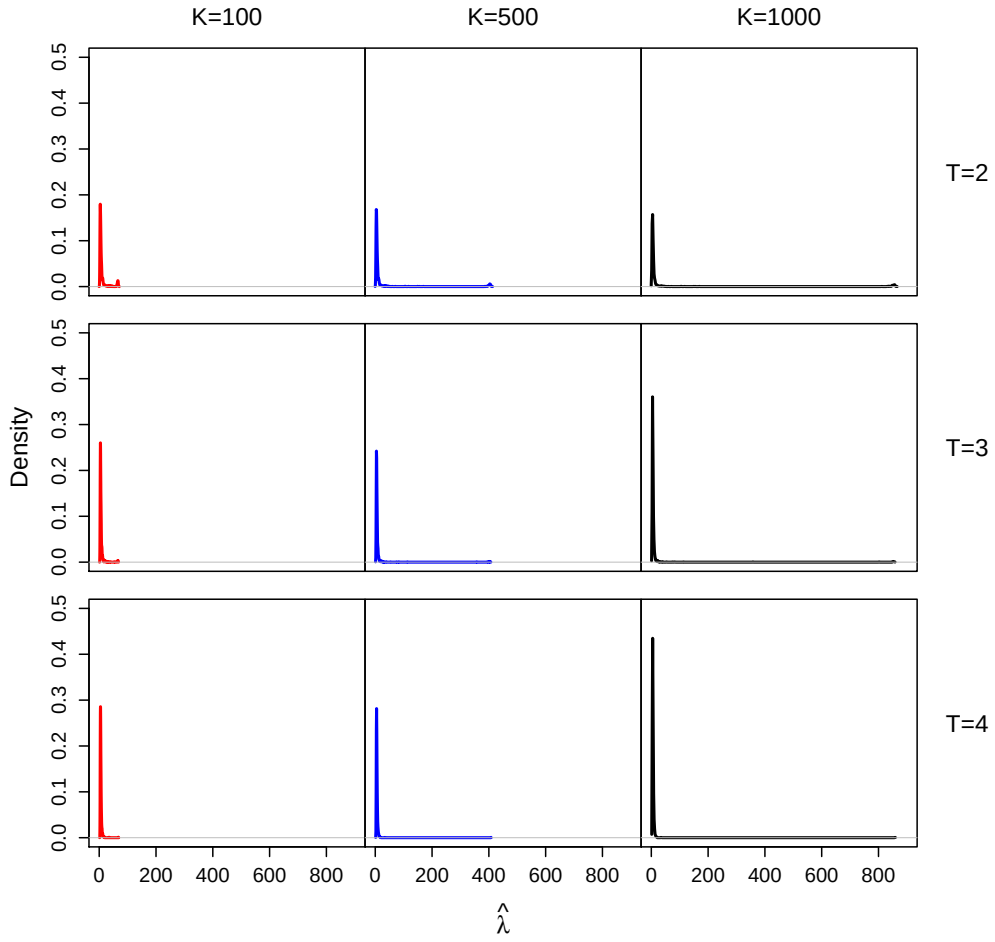

Figure 3.4: Kernel density estimates of $\hat{\lambda}$ from the Poisson N-mixture model when $S = 50$, $\lambda = 5$ and $p = 0.25$, based upon 1000 simulated datasets for $T = 2, 3, 4$ and $K = 100, 500, 1000$.

Poisson distribution is approximately Normal, N(λ,λ). For values of K in the approximate range $\lambda \pm 2\sqrt{\lambda}$, the effect of K is to lose a large fraction of this probability, and hence reduce the likelihood. Therefore it would not be possible to estimate λ values that correspond to reduced values of the likelihood and thus in practice $K > \hat{\lambda}$.

For a negative-binomial mixing distribution, we find that where $\hat{\lambda}$ is infinite for the Poisson distribution, the green solid line in Figure 3.5a is unchanged for the negative binomial. However, for a different simulation (blue lines), when the sample covariance diagnostic (3.5) is positive, for a Poisson mixing distribution, $\hat{\lambda} = 6.64$ for increasing K, but for a negative binomial

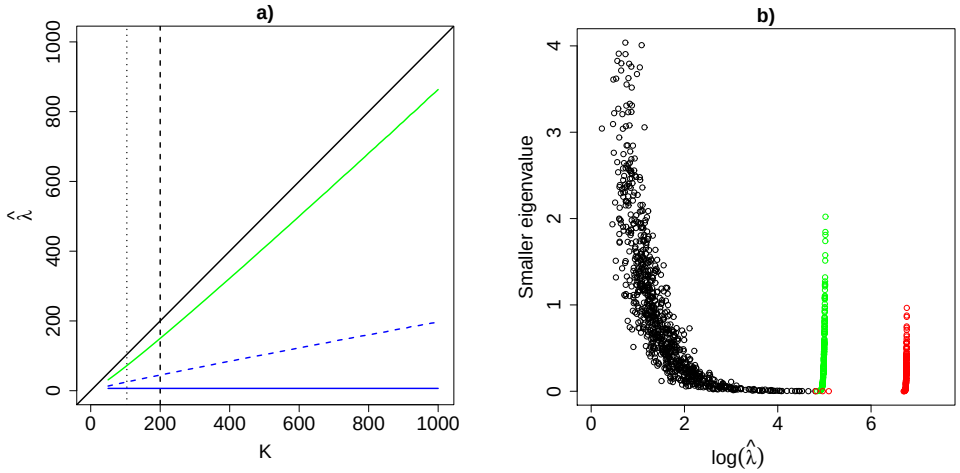

Figure 3.5: a) $\hat{\lambda}$ plotted against increasing K for a single simulation (green), with default values of K for `unmarked` ($K = \max(\text{count}) + 100$, dotted) and PRESENCE ($K = 200$, dashed) also shown. $\hat{\lambda}$ is plotted against increasing K for a different simulation in blue, with a comparison of λ estimates for a Poisson (solid) and negative-binomial (dashed) mixing distribution. b) A plot of $\log(\hat{\lambda})$ versus the smaller eigenvalue of the estimated Hessian at the maximum-likelihood estimate for $K = 200$ & 1000 (black), $K = 200$ (green) and $K = 1000$ (red) based upon 1000 simulated datasets. The parameter values used were $T = 2$, $S = 20$, $\lambda = 5$ and $p = 0.25$.

mixing distribution $\hat{\lambda}$ increases with K, although with a smaller slope than that of the Poisson line for the alternate simulation (shown in green). Hence we have seen here that the single covariance diagnostic is not sufficient in identifying infinite estimates of λ when a negative-binomial mixing distribution is used. We encounter this latter case, where estimates of λ are stable from the Poisson but not from the negative-binomial distribution, again in Section 3.7, when we consider a real dataset. An additional diagnostic for the negative-binomial case is given and explored in Section 3.6.

Figure 3.5b shows that as the value of $\hat{\lambda}$ increases, the smaller eigenvalue of the Hessian matrix of the log likelihood evaluated at the maximim-likelihood estimate, estimated within `optim` using the default Nelder-Mead algorithm and a tolerance value of 1×10^{-12}, decreases towards zero. The model becomes near singular (Catchpole et al. 2001), with only the prod-

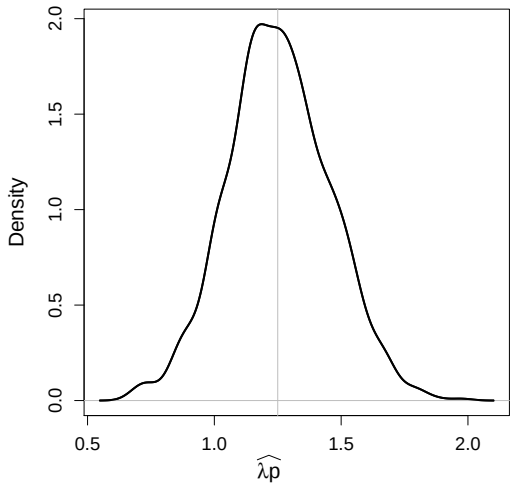

Figure 3.6: Kernel density estimate for $\widehat{\lambda p}$ from the Poisson N-mixture model, for $K = 200$ when $T = 2$, $S = 20$, $\lambda = 5$ and $p = 0.25$.

uct λp being estimable, corresponding to the thinned Poisson situation. As similarly demonstrated in Figure 3.3, estimates of λ made with different values of K are equivalent for finite $\hat{\lambda}$, but differ when $\hat{\lambda}$ should be infinite, and hence approaches K. The spread of non-zero eigenvalues when $\hat{\lambda}$ is close to K is reduced for larger K (Figure 3.5b). The artificial truncation of the range of λ by K is responsible for the non-zero values of the smaller eigenvalue for the largest values of $\hat{\lambda}$ (Figure 3.5b).

The sampling distribution of the product $\widehat{\lambda p}$ appears to be unbiased (Figure 3.6), hence when finite estimation of $\hat{\lambda}$ is impossible, only a single thinned-Poisson parameter λp is estimable, the rectangular hyperbola for which is shown in Figure 3.7a. Figure 3.7b illustrates the log-log transform of Figure 3.7a, rotated 135° about the axis to examine possible differences for an increasing number of visits, T. The main distribution shows similar spread for different values of T but fewer small estimates of λ as more visits are made. For cases where $\hat{\lambda}$ is truncated by K, estimates of λ do not vary with T, as found also when the green line of Figure 3.5a did not vary for alternative parameter values.

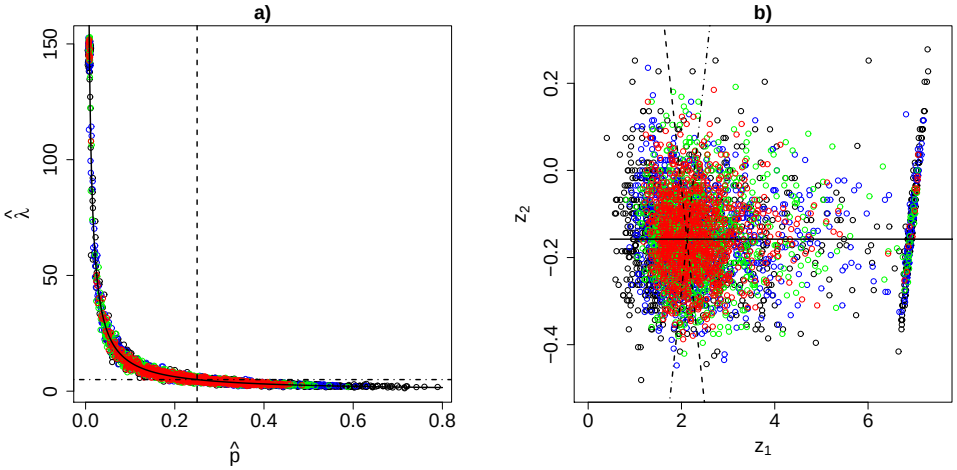

Figure 3.7: (a) A plot of $\hat{\lambda}$ versus $\hat{p}$ and (b) $\log(\hat{\lambda})$ versus $\log(\hat{p})$ rotated 135° clockwise about the origin, when $T = 2$ (black), $T = 3$ (blue), $T = 4$ (green) and $T = 5$ (red) for $K = 200$, $S = 20$, $\lambda = 5$ and $p = 0.25$. $z_1 = -\frac{1}{\sqrt{2}}\log\hat{p} + \frac{1}{\sqrt{2}}\log\hat{\lambda}$ and $z_2 = -\frac{1}{\sqrt{2}}\log\hat{p} - \frac{1}{\sqrt{2}}\log\hat{\lambda}$. In a) the solid line represents the hyperbola for λp and the straight lines correspond to the known values of p (dashed) and λ (dot-dash). In b) the straight lines represent the rotated logarithms of λp (solid), p (dashed) and λ (dot-dash).

3.5.2 Automatic choice of K

For the Poisson case the covariance diagnostic identifies when infinite values of $\hat{\lambda}$ arise. When the diagnostic is not satisfied, K may be selected automatically, for example by ensuring that the Poisson or negative-binomial upper tail probability is $< 10^{-10}$, so that the value of K will adapt for successive iterations according to the estimate of λ. This approach was also suggested by Guillera-Arroita et al. (2012). We have found this to be a simple and preferable alternative to fitting the model for successively larger values of K until estimates appear to stabilise.

3.6 Moment estimation for a mixed-Poisson N-mixture model

Suppose we have an N-mixture model in which N_i follows a mixed-Poisson distribution, as in Section 3.4, with

$$\mathbb{E}(N_i) = \lambda \qquad \text{and} \qquad \text{var}(N_i) = \sigma^2, \quad \text{with } \sigma^2 \geq \lambda.$$

Conditional on N_i, the random variables $y_{i,1}, \ldots, y_{,i,T}$ are independent binomial variables, with

$$y_{i,v}|N_i \sim \text{Bin}(N_i, p), \qquad v = 1, \ldots, T.$$

Therefore, conditional on N_i

$$\begin{aligned} \mathbb{E}(y_{i,v}|N_i) &= N_i p \\ \mathbb{E}(y_{i,v}^2|N_i) &= N_i p(1-p) + N_i^2 p^2 \\ \mathbb{E}(y_{i,v}, y_{i,w}|N_i) &= N_i^2 p^2 \qquad (v \neq w), \end{aligned}$$

and the corresponding unconditional expectations are

$$\mathbb{E}(y_{i,v}) = \lambda p \tag{3.10}$$

$$\mathbb{E}(y_{i,v}^2) = \lambda p(1-p) + (\lambda^2 + \sigma^2)p^2 \tag{3.11}$$

$$\mathbb{E}(y_{i,v}, y_{i,w}) = (\lambda^2 + \sigma^2)p^2 \qquad (v \neq w). \tag{3.12}$$

It follows that

$$\text{cov}(y_{i,v}, y_{i,w}) = \sigma^2 p^2 \qquad \text{and} \qquad \text{corr}(y_{i,v}, y_{i,w}) = \sigma^2 p/\lambda.$$

3.6.1 Moment estimation

We have the following moment estimates for $\mathbb{E}(y_{i,v})$, $\mathbb{E}(y_{i,v}^2)$ and $\mathbb{E}(y_{i,v}y_{i,w})$, respectively:

$$\begin{aligned} m_1 &= \frac{1}{ST}\sum_{j=1}^{T}\sum_{i=1}^{S} y_{i,j} \\ m_2 &= \frac{1}{ST}\sum_{j=1}^{T}\sum_{i=1}^{S} y_{i,j}^2 \\ m_{12} &= \frac{2}{ST(T-1)}\sum_{j=1}^{T}\sum_{s=j+1}^{T}\sum_{i=1}^{S} y_{i,j}y_{i,s}. \end{aligned}$$

Equating these to the expectations given by (3.10)-(3.12) yields the following moment estimators of the parameters λ, p and σ^2

$$\begin{aligned} \tilde{p} &= (m_1 - m_2 + m_{12})/m_1 \\ \tilde{\lambda} &= m_1/\tilde{p} \\ \tilde{\sigma}^2 &= (m_{12} - m_1^2)/\tilde{p}^2. \end{aligned}$$

Because $\sigma^2 \geq 0$, we require

$$m_{12} - m_1^2 \geq 0, \tag{3.13}$$

for a valid set of moment estimates. This is the same diagnostic as the covariance diagnostic given previously in (3.6), but derived via moments.

We also require $0 < p \leq 1$. The lower bound yields the new diagnostic

$$m_1 - m_2 + m_{12} > 0 \tag{3.14}$$

for a finite (moment) estimate of λ. The upper bound yields

$$m_1 - m_2 + m_{12} \leq m_1$$

or

$$m_{12} \leq m_2,$$

which is a consequence of the Cauchy-Schwarz inequality and not a useful diagnostic, as we found via simulation that it always holds. The bound $m_1 - m_2 + m_{12} > 0$ given above to ensure $\tilde{p} > 0$ and hence $\tilde{\lambda}$ finite, gives a new diagnostic.

If we adopt a method-of-moments (MOM) approach for the bivariate Poisson distribution, p is estimated by the sample correlation of the counts, as observed also by Royle (2004b), and λ is estimated by dividing $(\overline{n_1 + n_2})/2$ by this estimate of p. For more than two visits ($T > 2$), p can be estimated by the mean of all sample correlations between counts for different sampling occasions. Then $\tilde{\lambda}$ is the sample mean of all counts divided by this estimate of p. This generalises Holgate's (1964) work, which considered $T = 2$ only. In Appendix A of this chapter we assess the performance of MOM estimation as a simple method for parameter estimation compared to maximum likelihood for the N-mixture model.

3.6.2 Performance of the multivariate negative-binomial model

Given the proposed diagnostics for the mixed-Poisson case in Section 3.6.1, here we assess the performance of the multivariate negative-binomial model. Simulated data were fitted as in Section 3.3.3 but for the negative-binomial case, with $\lambda = 2, 5, 10$ and $\alpha = 1.25, 5$. We again assume that $\hat{\lambda} > 500$ equates to infinite $\hat{\lambda}$. If both (3.13) and (3.14) are negative, $\hat{\lambda}$ is very likely to be infinite and the mean proportion with $\hat{\lambda} > 500$ from 21 scenarios is 0.921 (Table 3.2). However performance of the diagnostics when one or more of the two diagnostics is negative is less clear. Additionally, $\hat{\lambda}$ may occasionally be infinite despite both diagnostics being positive and on average $\hat{\lambda} > 500$ for approximately 8.5% of simulations when both diagnostics are positive. We see fewer instances of infinite $\hat{\lambda}$ for large T and p. Performance for the bivariate cases where $p = 0.25$ and $\alpha = 1.25, 5$ are illustrated in Figures 3.8 and 3.9, and similarly for the multivariate case with $T = 3$ in Figures 3.10 and 3.11. We see that neither singly nor in combination do the diagnostics perform as well as the single diagnostic for the Poisson case.

Table 3.2: Performance of the covariance diagnostic for the multivariate negative-binomial model for various scenarios of λ, p, α and T for $S = 20$ sites. EP_1, EP_3 and EP_5 are the proportion of simulations where both diagnostics are negative, one or more diagnostic is negative, or both diagnostics are positive, respectively. EP_2, EP_4 and EP_6 are the corresponding proportions of those where $\hat{\lambda} > 500$.

λ	p	α	T	EP_1	EP_2	EP_3	EP_4	EP_5	EP_6
2	0.10	1.25	2	0.192	0.938	0.3	0.853	0.388	0.072
2	0.10	1.25	3	0.093	0.925	0.271	0.841	0.426	0.131
2	0.10	5.00	2	0.199	0.92	0.296	0.804	0.274	0.113
2	0.10	5.00	3	0.104	0.904	0.264	0.822	0.293	0.126
2	0.25	1.25	2	0.046	0.913	0.229	0.777	0.571	0.07
2	0.25	1.25	3	0.002	1	0.138	0.681	0.71	0.048
2	0.25	5.00	2	0.064	0.953	0.184	0.826	0.411	0.097
2	0.25	5.00	3	0.011	1	0.103	0.748	0.473	0.047
5	0.10	1.25	2	0.088	0.966	0.347	0.813	0.472	0.121
5	0.10	1.25	3	0.023	1	0.333	0.757	0.52	0.113
5	0.10	5.00	2	0.139	0.935	0.305	0.803	0.282	0.128
5	0.10	5.00	3	0.064	0.906	0.252	0.829	0.343	0.143
5	0.25	1.25	2	0.006	1	0.217	0.71	0.746	0.068
5	0.25	1.25	3	0	-	0.137	0.533	0.843	0.047
5	0.25	5.00	2	0.038	0.763	0.193	0.741	0.555	0.05
5	0.25	5.00	3	0.002	0.5	0.108	0.694	0.678	0.028
10	0.10	1.25	2	0.032	0.969	0.342	0.813	0.596	0.139
10	0.10	1.25	3	0.005	1	0.325	0.775	0.65	0.097
10	0.10	5.00	2	0.116	0.931	0.322	0.835	0.378	0.108
10	0.10	5.00	3	0.027	0.926	0.302	0.844	0.437	0.105
10	0.25	1.25	2	0	-	0.193	0.674	0.806	0.069
10	0.25	1.25	3	0	-	0.125	0.472	0.87	0.029
10	0.25	5.00	2	0.01	0.9	0.156	0.756	0.726	0.054
10	0.25	5.00	3	0.001	1	0.09	0.656	0.817	0.026

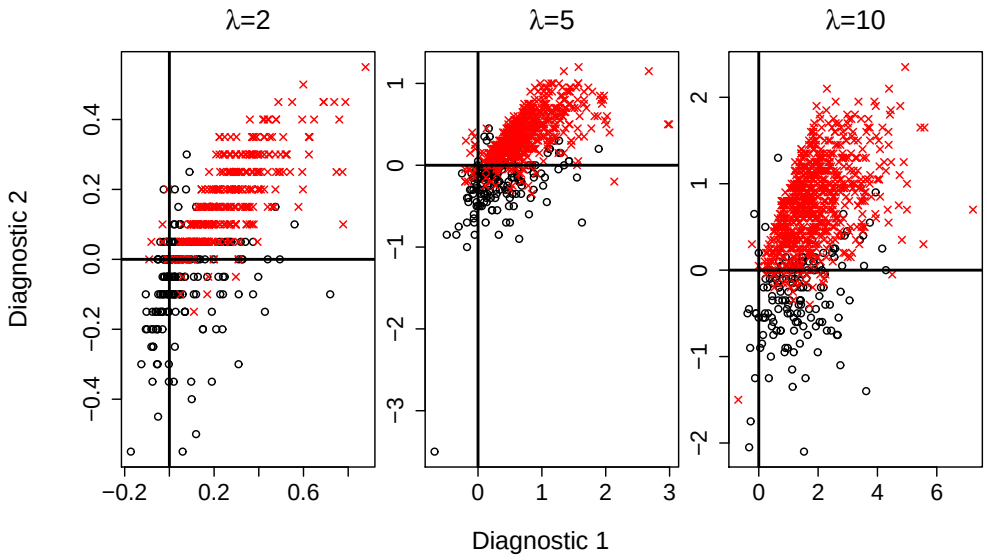

Figure 3.8: Diagnostic 1 (3.13) versus diagnostic 2 (3.14) from the bivariate negative-binomial model, based upon 1000 simulated datasets for $S = 20$, $\lambda = 2, 5, 10$, $\alpha = 5$ and $p = 0.25$. Values are which $\hat{\lambda} > 500$ and $\hat{\lambda} \leq 500$ are shown by black circles and red crosses, respectively.

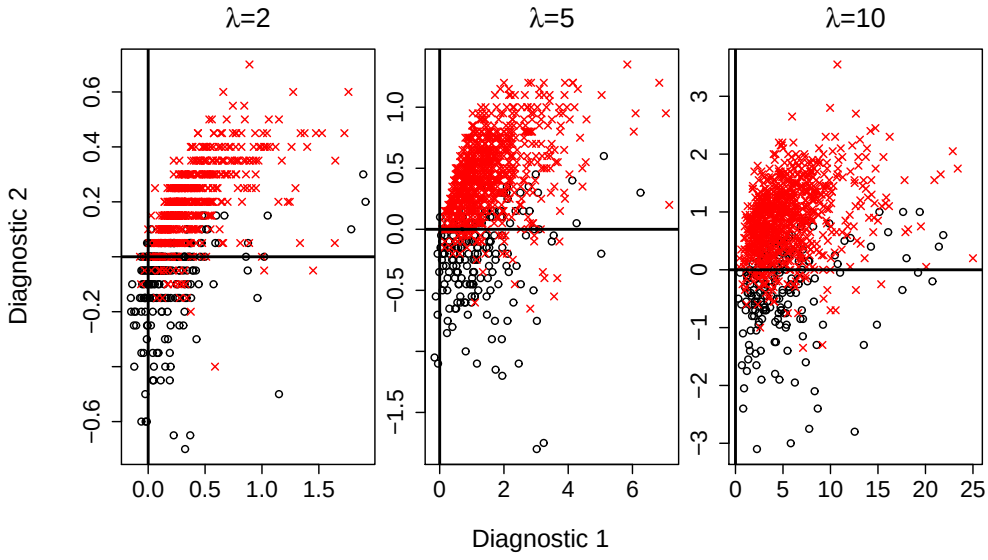

Figure 3.9: Diagnostic 1 (3.13) versus diagnostic 2 (3.14) from the bivariate negative-binomial model, based upon 1000 simulated datasets for $S = 20$, $\lambda = 2, 5, 10$, $\alpha = 1.25$ and $p = 0.25$. Values where $\hat{\lambda} > 500$ and $\hat{\lambda} \leq 500$ are shown by black circles and red crosses, respectively.

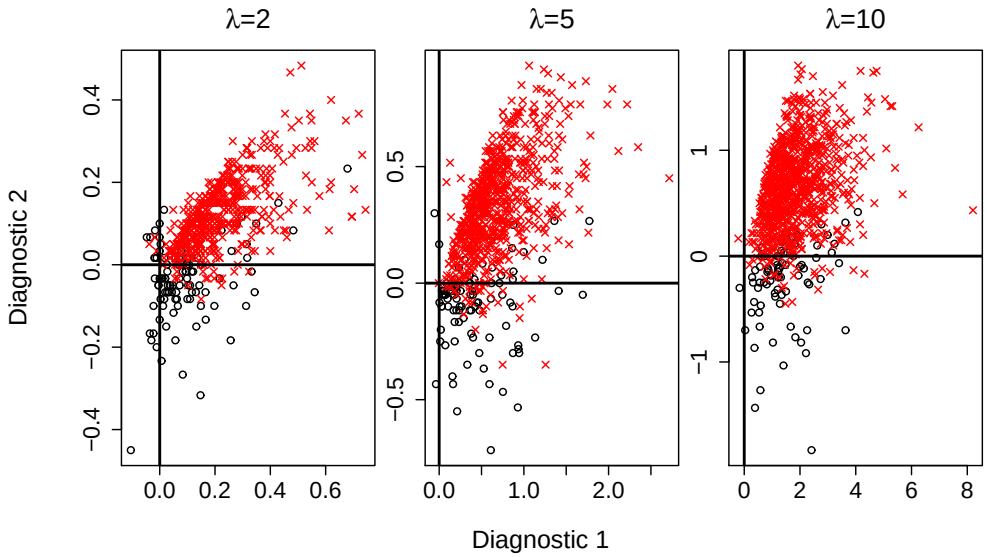

Figure 3.10: Diagnostic 1 (3.13) versus diagnostic 2 (3.14) from the multivariate negative-binomial model when $T = 3$, based upon 1000 simulated datasets for $S = 20$, $\lambda = 2, 5, 10$, $\alpha = 5$ and $p = 0.25$. Values where $\hat{\lambda} > 500$ and $\hat{\lambda} \leq 500$ are shown by black circles and red crosses, respectively.

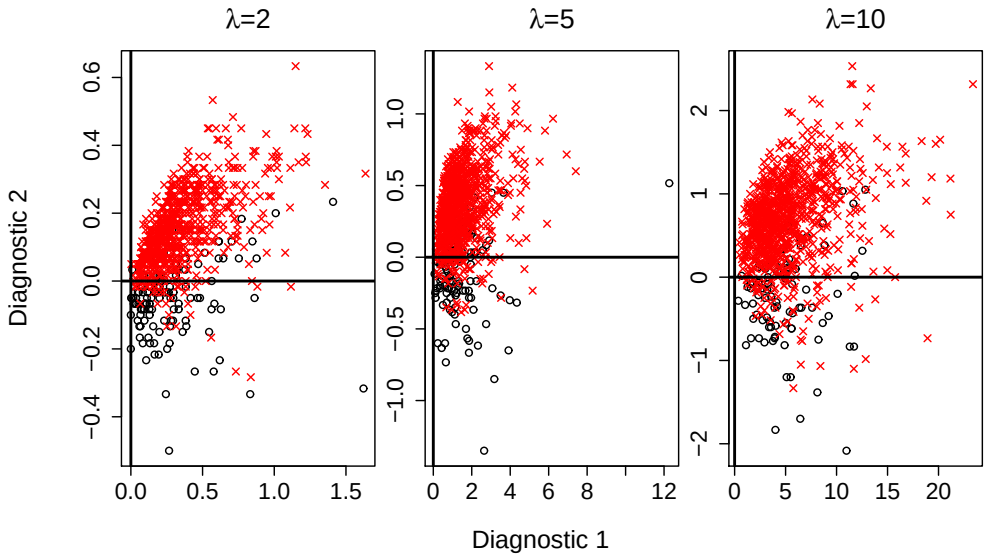

Figure 3.11: Diagnostic 1 (3.13) versus diagnostic 2 (3.14) from the multivariate negative-binomial model when $T = 3$, based upon 1000 simulated datasets for $S = 20$, $\lambda = 2, 5, 10$, $\alpha = 1.25$ and $p = 0.25$. Values where $\hat{\lambda} > 500$ and $\hat{\lambda} \leq 500$ are shown by black circles and red crosses, respectively.

3.7 Application to Hermann's Tortoise Data

In this section we analyse data from a study of the threatened Hermann's tortoise *Testudo hermanni* in southeastern France. One hundred and eighteen sites were each surveyed three times during a period when the species is most active. Full details are provided in Couturier et al. (2013), and we briefly reassess the conclusions drawn in their paper and demonstrate the effect of study design on results.

For the tortoise data, optimisation of the negative-binomial model confirms that $\hat{\lambda}$ is infinite in the negative binomial model for these data; after 500 iterations, the estimates had reached

$$\hat{\lambda} = 39616973, \qquad \hat{p} = 3.322971 \times 10^{-8}, \qquad \hat{\alpha} = 1.506465.$$

As noted in Couturier et al. (2013), the fit is much improved compared to the Poisson case, with - maximum log-likelihood values of 540.34 versus 576.27, but at the expense of $\hat{\lambda}$ becoming infinite. Hence for this dataset a finite estimate of mean abundance can be obtained for the Poisson but not for the negative-binomial. Whilst the first diagnostic (3.13) is positive, $m_{12} - m_1^2 = 1.05$, so that the Poisson estimate is finite, the additional diagnostic (3.14) is negative, as $m_1 - m_2 + m_{12} = -0.2655$.

The zero-inflated Poisson is an intermediate model between the Poisson and negative-binomial, with a - maximum log-likelihood value of 562.13 for these data. The zero-inflated Poisson therefore provides an improvement upon the Poisson case, but still yields the finite parameter estimate $\hat{\lambda} = 7.58$.

To show the potential effect of study design on model performance, we inspect the sample covariance diagnostic (3.13) for this dataset for the Poisson case for a reduced number of sites and/or visits. Taking two of the three visits made at all sites, the diagnostic was always positive (0.97-1.17). The diagnostic based upon all three visits but a random sample of fewer sites, was negative for 1.7% and 0% of 1000 samples, respectively for $S = 20$ and $S = 50$. However for only two visits, the diagnostic was negative for 9.0%

and 0.8% of 1000 samples, respectively for $S = 20$ and $S = 50$.

3.8 Discussion and recommendations

In this chapter we have shown that the N-mixture model can produce infinite estimates of abundance, particularly when working with a limited number of sampling occasions and/or low detection probability. The equivalence of the N-mixture model with the multivariate Poisson has been demonstrated, allowing us to understand and diagnose poor behaviour of the N-mixture model.

We believe the equivalence of the Poisson N-mixture model to the multivariate Poisson distribution to be previously largely unknown, especially in statistical ecology. The multivariate Poisson model conveniently avoids the requirement to select an upper bound K. We provide `R` code for fitting the multivariate Poisson and negative-binomial models, for any T, as an electronic appendix to this thesis. Due to the complexity of the multivariate Poisson and negative-binomial models, the associated computation time increases with T and the size of the counts, and is greater than the computation time for the N-mixture models. We have fitted these models for up to $T = 5$, which in our experience covers most practical applications of the models, although computation time will of course be dependent upon both the data being analysed and the computing system being used. Possible alternative techniques for fitting the multivariate distributions include using the EM algorithm (Karlis 2003), a composite likelihood (Jost et al. 2006) or a symbolic computation approach (Sontag and Zeilberger 2010). Consequently this equivalence could also have the alternative purpose of using the N-mixture model to provide simple fitting of the multivariate Poisson and negative-binomial models for particular covariance structures.

Since development by Royle (2004a), various extensions have been made to the N-mixture model, many of which were reviewed in Dénes et al. (2015). In each case we anticipate that without sufficient information from the available data, similar issues with estimating finite λ to those demonstrated in

this chapter may be encountered.

A zero-inflated Poisson or zero-inflated negative-binomial distribution can be used to allow for excess zeros in the abundance distribution (Wenger and Freeman 2008), and Joseph et al. (2009) suggest that the zero-inflated Poisson may be preferable to negative-binomial distributions. Application to the data for Hermann's tortoise in Section 3.7 suggested that the zero-inflated Poisson may provide a better fit than a standard Poisson whilst estimating finite λ, when that was not possible in the negative binomial case. Further work could be undertaken to explore the prevalence of this effect.

An extension of the N-mixture model to open populations by including population dynamics parameters offers great potential but also requires many upper bounds to be set (Dail and Madsen 2011), hence further work could explore the computational performance of this model. Kéry et al. (2009) extended the N-mixture model to allow for analysis of data resulting from closed sampling periods connected by open periods and the multivariate formulations also apply in that case. Dorazio et al. (2013) provide an extension in which p is given a distribution at each visit. The binomial distribution in (3.1) is then replaced by a beta-binomial. This has also been considered in a Bayesian context by Martin et al. (2011). For the multivariate Poisson case this extension is dealt with by appropriate numerical integration of the probability of (3.4). An increasing number of studies use a Bayesian approach for parameter estimation (Kéry et al. 2009; Graves et al. 2011). Further simulation study comparing a Bayesian approach with maximum likelihood estimation could show whether this approach can also produce poor estimates in some scenarios. Some comparisons have been made by Toribio et al. (2012), based upon parameter values from Royle (2004a).

In practice, covariates are frequently used to describe variation in abundance and detection parameters. Further analysis could determine how the inclusion of covariates might affect instances where a finite abundance estimate cannot be obtained for a model with constant abundance and detec-

tion. In particular with the addition of covariates parameters may become identifiable (Cole and Morgan 2010), as we find for stopover models in Section 4.2, where abundance and detection probabilities become separable via the inclusion of a covariate for the detection probability. The effect of including covariates will clearly be scenario dependent and will not always allow for λ and p to be separated, as was not the case in Knape and Korner-Nievergelt (2015), where the N-mixture model with covariates was sensitive to the choice of K.

Although not considered in this thesis, the N-mixture model has also been considered for the case of only one visit, where $T = 1$ (Sólymos et al. 2012), which might be applicable in situations where the closure assumption is violated. Sólymos et al. (2012) suggested that abundance and detection can be correctly identified when appropriate covariates are incorporated, although simulations were based on a minimum of 100 sites. However the ability to separate abundance and detection from single-visit data has been contested by Knape and Korner-Nievergelt (2015), who suggest that in this particular case estimates are sensitive to the choice of link function, and also refer to the similar arguments made by Hastie and Fithian (2013) in the context of the presence-only model (Royle et al. 2012), as discussed in Section 2.1 of this thesis.

Good experimental design is vital for occupancy studies; see for example Guillera-Arroita et al. (2010, 2014). The same issues apply for N-mixture work, though with the different perspective of avoiding poor model-fitting behaviour. If possible, study design effort should be distributed to ensure more than two visits are made to each site (in addition to including a reasonable number of sites). Alternatively a study design where more visits are made to a subset of the sites is worth exploring.

For maximum-likelihood estimation, we recommend using MOM estimates to start the iterative search for MLEs. In the Poisson case the covariance diagnostic may be used to determine when infinite estimates of abundance may arise. Infinite estimates of abundance may occur for some model choices but not others, as for the Hermann's Tortoise case study.

Hence we advise fitting the model for multiple distribution choices, to identify which may provide finite estimates of abundance. An `R` program which allows for covariates in the detection and abundance parameters is available in the electronic appendices that accompany this thesis.

Despite having applicability to many different taxa, the N-mixture model is not directly suitable for modelling butterfly transect data, such as from the UKBMS, due to a lack of closure in abundance across visits. Although Pellet et al. (2012) suggest that repeated visits could be made on a single day, for example by repeating counts by walking the transect back and forth. Given the lack of closure between visits, the open N-mixture model may be suitable for butterfly data (Dail and Madsen 2011). The issue of a lack a closure between visits within the season was also discussed in Section 2.5, in the context of estimating abundance from only presence-absence data using the Royle-Nichols model (Royle and Nichols 2003), which is associated with the N-mixture model (Dorazio 2007).

The standard N-mixture model requires only two parameters to be estimated and is a classic example of hierarchical modelling, which has received increasing popularity and application (Royle and Dorazio 2008). In Chapter 4 we describe recent approaches for modelling butterfly abundance which involve many parameters, due to requiring a parameter to be estimated for each site. New models with fewer parameters are developed in Chapter 5, and in Section 5.4 we incorporate ideas from N-mixture models, by testing a hierarchical approach for describing the site parameters.

Appendix A: Performance of method-of-moments estimation

We assess the performance of MOM estimation as a simple method for parameter estimation compared to maximum likelihood estimation (MLE) from the N-mixture model. The upper bound K for the MLE was automatically selected such that the tail proportion was 10^{-10}: see Section 3.5.2. For the Poisson case, estimates for where the covariance diagnostic is negative were excluded in this comparison. Correspondingly, estimates for the negative-binomial were excluded when one or more of the diagnostics was negative. Additionally, for both the Poisson and negative-binomial, cases where either the MLE or MOM estimate of λ is finite but large ($\hat{\lambda} > 100$) were excluded to provide a fair comparison.

For the Poisson case, when $p = 0.25$, the MOM approach only performs better than MLE based upon RMSE when $T = 2$ (Table A.1). However for smaller $p = 0.10$, MOM estimation performs better for almost all cases (Table A.2). In the negative-binomial case, results are not greatly affected by varying α (Tables A.3-A.6). As in the Poisson case, when $p = 0.25$, MOM only outperforms MLE when few visits are made, which is emphasised when λ is small. For smaller $p = 0.10$, MOM often performed better than MLE in terms of RMSE, although the difference was reduced for increasing T and λ.

Method of moments can quickly provide good estimates of λ and p, but it does not consistently outperform MLE. We suggest using MOM estimates as sensible starting values for optimisation of the N-mixture likelihood.

Table A.1: Comparison of estimation via method-of-moments (MOM) and the N-mixture model (MLE) for the Poisson case with $\lambda = 2, 5, 10$, $p = 0.25$ and $S = 20$. RMSE is the root mean-squared error for λ. EPD is the proportion of simulations discarded when the covariance diagnostic was negative or either estimate of $\hat{\lambda} > 100$. EPN is the proportion of simulations when the covariance diagnostic was negative.

a) $\lambda = 2$

T	Method	Mean	Median	RMSE	EPD	EPN
2	MLE	2.28	1.58	2.49	0.312	0.219
	MOM	1.9	1.41	1.5		
3	MLE	2.53	1.89	2.66	0.18	0.098
	MOM	2.43	1.63	2.61		
4	MLE	2.73	2.01	3.19	0.091	0.033
	MOM	2.97	1.82	4.03		
5	MLE	2.7	2.04	3.11	0.055	0.012
	MOM	2.93	1.93	4.37		

b) $\lambda = 5$

T	Method	Mean	Median	RMSE	EPD	EPN
2	MLE	5.97	3.87	7.92	0.258	0.171
	MOM	5.45	3.64	5.72		
3	MLE	6.95	4.74	7.97	0.152	0.083
	MOM	6.68	4.27	9.01		
4	MLE	6.44	4.93	6.74	0.081	0.017
	MOM	6.97	4.57	8.29		
5	MLE	6.47	5.04	6.03	0.046	0.008
	MOM	6.59	4.8	6.63		

c) $\lambda = 10$

T	Method	Mean	Median	RMSE	EPD	EPN
2	MLE	11.5	8.07	11.52	0.255	0.157
	MOM	9.96	7.21	8.79		
3	MLE	12.89	9.51	11.72	0.147	0.072
	MOM	12.39	8.76	11.82		
4	MLE	12.89	9.87	10.72	0.094	0.029
	MOM	12.78	9.34	11.44		
5	MLE	12.14	10.08	7.82	0.055	0.016
	MOM	12.42	9.53	9.87		

Table A.2: Comparison of estimation via method-of-moments (MOM) and the N-mixture model (MLE) for the Poisson case with $\lambda = 2, 5, 10$, $p = 0.1$ and $S = 20$. RMSE is the root mean-squared error for λ. EPD is the proportion of simulations discarded when the covariance diagnostic was negative or either estimate of $\hat{\lambda} > 100$. EPN is the proportion of simulations when the covariance diagnostic was negative.

a) $\lambda = 2$

T	Method	Mean	Median	RMSE	EPD	EPN
2	MLE	1.1	0.77	1.51	0.61	0.52
	MOM	0.71	0.61	1.36		
3	MLE	1.87	1.12	2.41	0.506	0.377
	MOM	1.25	0.94	1.22		
4	MLE	2.43	1.4	3.4	0.444	0.283
	MOM	1.58	0.98	1.51		
5	MLE	2.65	1.58	3.97	0.356	0.214
	MOM	1.94	1.21	2.27		

b) $\lambda = 5$

T	Method	Mean	Median	RMSE	EPD	EPN
2	MLE	3.19	1.97	5.62	0.52	0.424
	MOM	2.25	1.67	3.31		
3	MLE	4.6	2.84	5.79	0.467	0.331
	MOM	3.53	2.18	4.09		
4	MLE	6.33	3.63	9.04	0.387	0.235
	MOM	5.42	2.7	7.45		
5	MLE	6.71	4.08	8.64	0.364	0.203
	MOM	5.39	3.09	7.92		

c) $\lambda = 10$

T	Method	Mean	Median	RMSE	EPD	EPN
2	MLE	6.72	4.01	8.8	0.527	0.451
	MOM	4.73	3.17	6.82		
3	MLE	10.16	6	12.5	0.433	0.299
	MOM	8.21	4.55	11		
4	MLE	12.5	7.96	13.99	0.387	0.223
	MOM	9.72	5.85	11.73		
5	MLE	11.59	7.69	11.78	0.384	0.174
	MOM	10.53	6.76	12.59		

Table A.3: Comparison of estimation via method-of-moments (MOM) and the N-mixture model (MLE) for the negative-binomial case with $\lambda = 2, 5, 10$, $p = 0.25$, $\alpha = 1.25$, and $S = 20$. RMSE is the root mean-squared error for λ. EPD is the proportion of simulations discarded when either covariance diagnostic was negative or either estimate of $\hat{\lambda} > 100$. EPN is the proportion of simulations when both diagnostics were negative.

a) $\lambda = 2$

T	Method	Mean	Median	RMSE	EPD	EPN
2	MLE	2.24	1.44	4.22	0.256	0.058
	MOM	1.81	1.3	1.67		
3	MLE	2.52	1.72	3.52	0.185	0.013
	MOM	2.49	1.57	3.33		
4	MLE	2.64	1.78	3.6	0.129	0
	MOM	2.84	1.71	5.37		
5	MLE	2.7	1.84	4.1	0.093	0
	MOM	2.89	1.79	5.31		

b) $\lambda = 5$

T	Method	Mean	Median	RMSE	EPD	EPN
2	MLE	5.42	3.44	8.58	0.258	0.009
	MOM	5.2	3.16	7.67		
3	MLE	6.43	4.35	8.13	0.192	0
	MOM	6.14	3.93	7.8		
4	MLE	5.99	4.32	5.82	0.151	0
	MOM	6.82	4.34	8.25		
5	MLE	5.88	4.56	5.49	0.1	0
	MOM	6.63	4.52	7.56		

c) $\lambda = 10$

T	Method	Mean	Median	RMSE	EPD	EPN
2	MLE	10.66	7.07	11.3	0.287	0.001
	MOM	9.32	6.36	9.11		
3	MLE	11.49	8.55	9.29	0.207	0
	MOM	11.74	7.92	12.1		
4	MLE	11.76	8.79	10.52	0.135	0
	MOM	11.45	8.38	10.24		
5	MLE	11.68	9.12	9.08	0.106	0
	MOM	11.44	8.4	10.2		

Table A.4: Comparison of estimation via method-of-moments (MOM) and the N-mixture model (MLE) for the negative-binomial case with $\lambda = 2, 5, 10$, $p = 0.1$, $\alpha = 1.25$, and $S = 20$. RMSE is the root mean-squared error for λ. EPD is the proportion of simulations discarded when either covariance diagnostic was negative or either estimate of $\hat{\lambda} > 100$. EPN is the proportion of simulations when both diagnostics were negative.

a) $\lambda = 2$

T	Method	Mean	Median	RMSE	EPD	EPN
2	MLE	1.02	0.64	1.92	0.565	0.401
	MOM	0.67	0.51	1.4		
3	MLE	1.48	0.91	2.38	0.45	0.187
	MOM	1.1	0.8	1.35		
4	MLE	1.7	1.06	2.48	0.425	0.097
	MOM	1.36	0.9	1.55		
5	MLE	2.58	1.38	6.25	0.349	0.044
	MOM	1.7	1.08	1.92		

b) $\lambda = 5$

T	Method	Mean	Median	RMSE	EPD	EPN
2	MLE	2.69	1.68	5.13	0.455	0.161
	MOM	1.96	1.41	3.51		
3	MLE	3.74	2.29	5.51	0.405	0.048
	MOM	3.32	2	4.51		
4	MLE	5.19	2.73	8.69	0.364	0.012
	MOM	4.47	2.36	6.91		
5	MLE	5.46	2.95	8.93	0.348	0.002
	MOM	4.53	2.67	7.88		

c) $\lambda = 10$

T	Method	Mean	Median	RMSE	EPD	EPN
2	MLE	5.79	3.36	9.68	0.439	0.037
	MOM	4.28	2.89	7.02		
3	MLE	7.63	4.24	11.08	0.373	0.002
	MOM	6.13	3.94	7.75		
4	MLE	8.84	5.47	10.57	0.373	0
	MOM	8.64	5.1	11.67		
5	MLE	8.73	5.7	10.27	0.35	0
	MOM	8.3	5.14	9.72		

Table A.5: Comparison of estimation via method-of-moments (MOM) and the N-mixture model (MLE) for the negative-binomial case with $\lambda = 2, 5, 10$, $p = 0.25$, $\alpha = 5$, and $S = 20$. RMSE is the root mean-squared error for λ. EPD is the proportion of simulations discarded when either covariance diagnostic was negative or either estimate of $\hat{\lambda} > 100$. EPN is the proportion of simulations when both diagnostics were negative.

a) $\lambda = 2$

T	Method	Mean	Median	RMSE	EPD	EPN
2	MLE	2.38	1.6	2.88	0.301	0.151
	MOM	1.79	1.32	1.57		
3	MLE	2.62	1.88	3.1	0.195	0.052
	MOM	2.33	1.67	2.36		
4	MLE	2.91	1.95	4.74	0.098	0.011
	MOM	2.9	1.91	4.05		
5	MLE	2.5	1.98	2.49	0.052	0.003
	MOM	2.85	1.86	4.28		

b) $\lambda = 5$

T	Method	Mean	Median	RMSE	EPD	EPN
2	MLE	6.25	3.89	7.86	0.243	0.065
	MOM	5.6	3.6	7.07		
3	MLE	6.51	4.47	7.77	0.129	0.01
	MOM	6.41	4.13	8.62		
4	MLE	6.6	4.86	6.48	0.094	0.001
	MOM	6.93	4.67	8.21		
5	MLE	6.58	4.88	7.44	0.07	0.001
	MOM	6.92	4.64	8.15		

c) $\lambda = 10$

T	Method	Mean	Median	RMSE	EPD	EPN
2	MLE	11.11	7.55	10.41	0.235	0.02
	MOM	10.45	7	10.94		
3	MLE	12.08	8.8	11.23	0.153	0
	MOM	12.52	8.57	12.35		
4	MLE	12.34	9.45	10.68	0.091	0
	MOM	12.29	9.01	10.74		
5	MLE	11.84	9.51	8.03	0.053	0
	MOM	12.44	9.33	10.08		

Table A.6: Comparison of estimation via method-of-moments (MOM) and the N-mixture model (MLE) for the negative-binomial case with $\lambda = 2, 5, 10$, $p = 0.1$, $\alpha = 5$, and $S = 20$. RMSE is the root mean-squared error for λ. EPD is the proportion of simulations discarded when either covariance diagnostic was negative or either estimate of $\hat{\lambda} > 100$. EPN is the proportion of simulations when both diagnostics were negative.

a) $\lambda = 2$

T	Method	Mean	Median	RMSE	EPD	EPN
2	MLE	1	0.65	1.44	0.605	0.497
	MOM	0.7	0.6	1.4		
3	MLE	1.56	1.04	2.15	0.482	0.291
	MOM	1.18	0.82	1.28		
4	MLE	2.25	1.31	3.45	0.454	0.187
	MOM	1.6	1.06	1.62		
5	MLE	2.75	1.56	5.47	0.393	0.139
	MOM	1.81	1.17	2.05		

b) $\lambda = 5$

T	Method	Mean	Median	RMSE	EPD	EPN
2	MLE	3.39	1.86	6.29	0.517	0.301
	MOM	2.19	1.56	3.32		
3	MLE	4.73	2.61	7.9	0.449	0.174
	MOM	3.45	2.18	4.17		
4	MLE	5.4	3.34	8.1	0.384	0.092
	MOM	4.36	2.73	5.7		
5	MLE	5.82	3.64	7.9	0.342	0.063
	MOM	5.66	2.99	10.01		

c) $\lambda = 10$

T	Method	Mean	Median	RMSE	EPD	EPN
2	MLE	7.09	4.13	9.52	0.466	0.171
	MOM	5.51	3.61	6.99		
3	MLE	8.42	5.19	10	0.393	0.075
	MOM	7.34	4.55	9.28		
4	MLE	9.72	5.96	10.9	0.36	0.045
	MOM	9.13	5.55	10.7		
5	MLE	9.76	6.65	10.56	0.343	0.015
	MOM	9.94	5.85	11.41		

Chapter 4

Recent models for butterfly abundance

The remaining core chapters of this thesis deal with modelling the abundance of UK butterflies. In this chapter we review past and present methods for modelling butterfly abundance from UKBMS data, which was described in Section 1.3.1. In Section 4.1 we discuss recent approaches for deriving indices of abundance, using generalised additive models (GAMs). The development of the two-stage GAM approach described in Section 4.1.3 was undertaken for my dissertation as part of an MRes at the University of York. During my PhD, the applications of the model were extended and the approach was published in *Methods in Ecology and Evolution* (Dennis et al. 2013).

Secondly, in Section 4.2 we describe a 'stopover' model approach for describing butterfly count data, which includes the estimation of survival parameters, and is different from the typically empirical model descriptions of these data. The methods described in this chapter provide foundations for comparison with the new models which we will present in the later core chapters of this thesis.

4.1 Generalised additive models

Abundance indices produced from UKBMS data are vital for assessing trends in the abundance of UK butterflies. Appropriate modelling approaches must account for the highly variable numbers within a season, in accordance with differing seasonal patterns of emergence. A further challenge proposed by these data is the substantial proportion of proposed visits not made by recorders, which we will now briefly describe.

4.1.1 Missing data

Within the UKBMS, typically fewer than the optimal 26 weekly counts are made at each site per year, and across the dataset, considering all sites, years and species, approximately 29% of counts are missed, equivalent to approximately 8 out of 26 weeks of the transect season. There is no evidence of a trend over time in the proportion of missed counts ($p = 0.69$) although there is a latitudinal gradient in the proportion of missed counts ($p < 0.001$), which tends to increase the further north sites are located. Dividing the data crudely into three regional areas, corresponding to low (below 250 km), mid (between 250 km and 625 km) and high (above 625 km) northings in the UK, the average percentage of counts missed are approximately 26%, 32% and 46%, respectively. The frequency of missing counts is also not uniform across the transect season, with an increase in missing counts at the ends of the season. Given these trends, it is likely that many missed counts are due to unsuitable weather conditions, rather than just recorder unavailability.

4.1.2 Original GAM approach

Estimates of missing counts for butterfly monitoring schemes were originally obtained using linear interpolation of the counts either side of the missing value. The use of generalized additive models (GAM, Hastie and Tibshirani 1990; Wood 2006) as an alternative method was introduced by Rothery and Roy (2001), who applied the models to both UKBMS and simulated data with varying flight periods. This procedure has been adopted for annual

reporting of the UKBMS since 2002 (Greatorex-Davies and Roy 2003), and still remains the method employed for habitat-specialist species (Brereton et al. 2014).

A GAM is a generalized linear model (GLM) where part of the linear predictor contains one or more smooth functions of predictor variables (Wood 2006), hence it is more flexible than the linear approach, but requires more data to avoid the potential for erratic behaviour. Here we outline the original GAM approach (Rothery and Roy 2001), where values for weeks with missing counts are imputed by fitting a GAM with Poisson distribution and a log link function to the observed counts at individual sites and years. GAMs can be fitted using the `mgcv` package in `R` (Wood 2000, 2006; R Core Team 2015), which selects the level of smoothing internally using generalized cross-validation (GCV).

If y_t represents the count at a site on day t in an example year, then

$$\mathbb{E}[y_t] = \mu_t = \exp[s(t; f)], \tag{4.1}$$

where the function $s(t; f)$ denotes a cubic regression spline, for a given monitored site and year, with f degrees of freedom. Here, $t \in (1, 182)$ represents each day in the monitoring season from April to September. Thereafter, real counts are used where taken and the weeks with missing counts are allocated imputed values, $\hat{\mu}_t$, from the GAM for the middle day of that week. The result is a flight period curve corresponding to the seasonal variation in counts, which may be real or imputed for each week.

Annual site indices of abundance (an index value for each site and year recorded) are then calculated by an estimate of the area under the flight period curve. For a series of T counts $y_1, y_2, \ldots, y_T$ (which may be real or imputed) at times $t_1, t_2, \ldots, t_T$, as in Rothery and Roy (2001), the trapezoidal rule is used to approximate the integral of the curve to give the index

$$\text{Index} = \sum_{j=2}^{T} \frac{(y_j + y_{j-1})(t_j - t_{j-1})}{2}. \tag{4.2}$$

Across-site, collated indices are then derived by fitting a single log-linear regression model to the annual indices at all sites, with site and year as

additive predictors (Roy et al. 2007). This can be fitted using any of the widely-available software packages for GLM (van Strien et al. 2001). The model accounts for the fact that some years yield higher counts than others, and also that the population varies geographically, across sites. Collated indices are derived from the indices at all sites and hence describe national trends in abundance.

For this GAM approach, where a high proportion of weeks or the peak of the flight period is missed (defined where the maximum prediction of a missed count exceeds the maximum of the observed counts), data for that particular site and year are excluded from analysis, since prediction from the GAM is likely to be poor in these instances. Under these criteria, on average across the species monitored by the UKBMS 38% of transect visits made do not contribute to reported population indices. This represents a substantial quantity of data not utilised, and in the interest of the optimal use of the volunteer-collected records, a new approach, which also uses GAMs, was developed with the aim of allowing for more efficient analysis of the UKBMS data and hence more robust estimates of changes in butterfly abundance.

4.1.3 Two-stage GAM approach

Whilst the previous strategy involves fitting a GAM to counts on an individual site/year basis, here a GAM is applied across all sites within a year, to estimate the average annual seasonal flight curve. In this case all incomplete series of recordings may be included. This approach is published in Dennis et al. (2013).

A GAM with Poisson distribution and a log link function is used to estimate the annual seasonal pattern (which is assumed to the same across S sites) as follows. If $y_{i,t}$ represents the count at site $i = 1, \ldots, S$ on day $t \in (1, 182)$ in an example year, then

$$\mathbb{E}[y_{i,t}] = \mu_{i,t} = \exp[\eta_i + s(t; f)], \tag{4.3}$$

where η_i represents a site effect and $s(t; f)$ denotes a smoothing function with f degrees of freedom. This creates a flight period curve which is

common for all sites for that year, but varies (via η_i) in magnitude between sites with respect to varying abundance between sites. Estimation of an average seasonal pattern across sites for each year allows for even those with a high proportion of missing counts to be included in abundance estimation.

Studies of butterfly phenology confirm that butterfly flight periods vary from year-to-year (Roy and Sparks 2000). Hence, due to an interaction between the day and the year, a single-stage extension of equation (4.3) for the full dataset with an additional simple year effect would be too restrictive, since this would only estimate a single flight period across all years. A direct comparison of total annual abundances, obtained by summing the expected values at all sites, which can each be estimated via equation (4.3), cannot be made due to the variation in the set of sites covered each year. Therefore an additional stage to the model is introduced.

If $y_{i,t,k}$ represents the count of a species at site $i = 1, , S$ in year $k = 1, \ldots, Y$ on day $t \in (1, 182)$, then the mean count is given by

$$\mathbb{E}[y_{i,t,k}] = \mu_{i,k}(t) = \exp[\alpha_i + \beta_k + \gamma_k(t)], \tag{4.4}$$

where α_i and β_k represent effects for the ith site and the kth year respectively and $\gamma_k(t)$ allows for the seasonal pattern, which can vary between years, but not over sites. A site index, $M_{i,k}$ for site i and year k, can be calculated as the sum of the expected counts for that season, which is given by summing (4.4) over t as follows

$$\begin{aligned} M_{i,k} = \sum_t \mu_{i,k}(t) &= \sum_t \exp[\alpha_i + \beta_k + \gamma_k(t)] \\ &= \exp[\alpha_i + \beta_k] \sum_t \exp[\gamma_k(t)]. \end{aligned} \tag{4.5}$$

Since both the annual effects and seasonal effects in the model vary with respect to year, we constrain $\gamma_k(t)$ so that $\sum_t \exp[\gamma_k(t)] = 1$. The annual effects, β_k, provide an index proportional to total abundance provided that the $\exp[\gamma_k(t)]$ sum to one. Hence equation (4.4) is fitted to the counts for all years as a Poisson GLM with the values of $\gamma_k(t)$ as an offset, where $\gamma_k(t)$ represent the annual seasonal pattern and were obtained by scaling

the output from the first stage (equation 4.3). Missing values can also be estimated from equation (4.4) and thereafter the approach is the same as for the original GAM approach, as site indices are derived from formula (4.2). Collated indices are then estimated, and β_k taken as an index of abundance, as before, via a further GLM with site and year as multi-level factors.

4.1.4 Comparison of the two GAM methods

The two GAM approaches described in Sections 4.1.2 and 4.1.3 are compared in Dennis et al. (2013), via an extensive simulation study and application to UKBMS data. In this chapter, we briefly outline these results.

Simulation study

The two GAM approaches and linear interpolation approach were compared for simulated data. Figure 4.1 shows the flight periods of three species with different levels of voltinism. Data were simulated based on UKBMS data for these three species, generating weekly counts for 100 sites with seasonal variation corresponding to the season flight curves in Figure 4.1. Linear trends in abundance were imposed to simulate varying declines over a period of ten years, and 30% of records were discarded to resemble the missing data in the real data.

The percentage of simulations that detected a significant trend was used to assess the statistical performance of the models (Elston et al. 2011). The simulation study showed that compared to the original GAM and linear interpolation approaches, the two-stage GAM approach had greater power to detect trends, particularly for smaller declines (Figure 4.2). For no change in abundance over ten years, the percentage of simulations that incorrectly predict significant trends lies reasonably close to 5% in all cases. In addition, trend estimates from the original GAM are less accurate than from the two-stage GAM, and accompanied by larger standard errors.

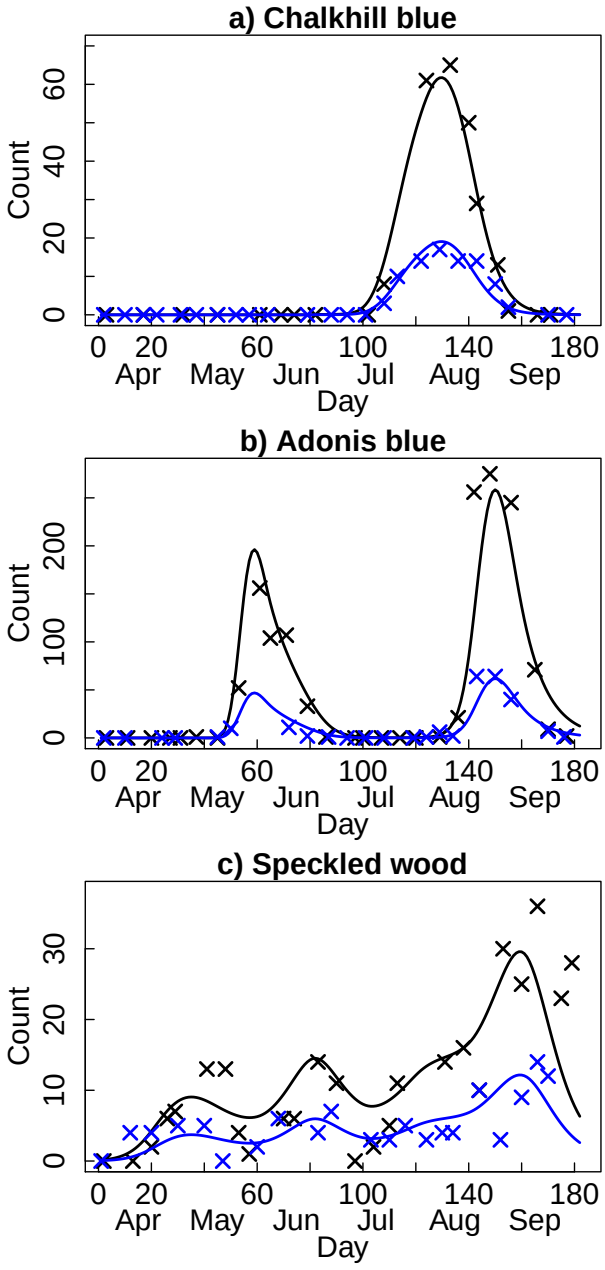

Figure 4.1: Real weekly counts at two example UKBMS sites in 2005 for three species, with the corresponding GAM (blue/black correspond to different sites). This figure appears in Dennis et al. (2013).

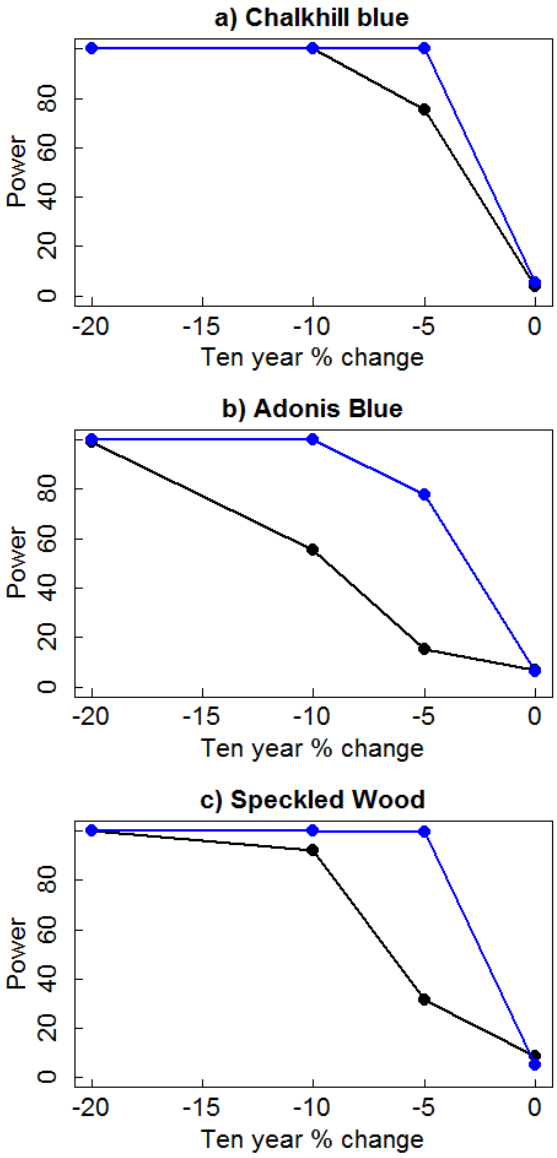

Figure 4.2: Estimated power (the percentage of simulations that detected a significant linear time trend) for the original (black) and two-stage (blue) GAM approaches. This figure appears in Dennis et al. (2013).

4.1.5 Application to UKBMS data

Collated indices were calculated from UKBMS data for 46 butterfly species, using both the original and two-stage GAM models. Confidence intervals for both GAM approaches require a bootstrapping approach, which involves drawing a random sample, with replacement, from the set of sites, for a given number of replicates (in this case 100 replicates was judged to be sufficient for each species, for each model). Collated indices are estimated for the sites in each bootstrap sample and then ordered to derive approximate 95% confidence intervals for each species (Fewster et al. 2000). By applying all stages of each model to each bootstrap sample, error propagation is accounted for. However, bootstrapping requires a high level of computational effort, hence in Dennis et al. (2013) for species with many sites the analysis was restricted to the last ten years and a random subsample of 300 sites.

The mean number of sites per year that contribute to the two GAM-based models highlights the substantial improvement in data efficiency of the two-stage GAM approach (Figure 4.3a). The two-stage GAM approach makes full use of the data available, whilst the original GAM approach discards a proportion of the data. For all species, fewer data were used under the original GAM approach and hence a reduced geographical coverage was represented, whereas results from the two-stage GAM approach are fully representative of the area for which data have been collected. The mean percentage of 10 km grid squares which contain at least one monitored site that were retained under the original GAM approach was approximately 63% (Figure 4.3b).

The collated indices for the 46 species from the two models are generally highly correlated and produce similar estimated linear trends in abundance (Figure 4.4a). The majority of points fall near the line of equality; although predictions from the two-stage GAM approach tend to be greater, especially for the larger changes (i.e. estimation of large increases is more pronounced for the two-stage GAM approach). Confidence intervals are in general narrower for the two-stage GAM approach (Figure 4.4b). This is

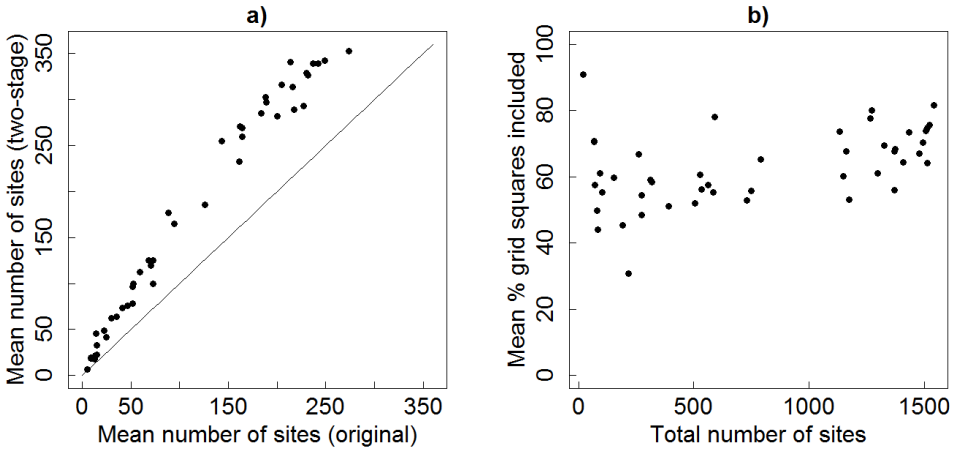

Figure 4.3: a) Comparison of the mean number of sites included (averaged by year) by each model for each species. The solid line is the 1-1 line. b) Mean percentage of total monitored 10 km grid squares retained under the original GAM approach (averaged by year) against the total number of sites for each species. These figures appear in Dennis et al. (2013).

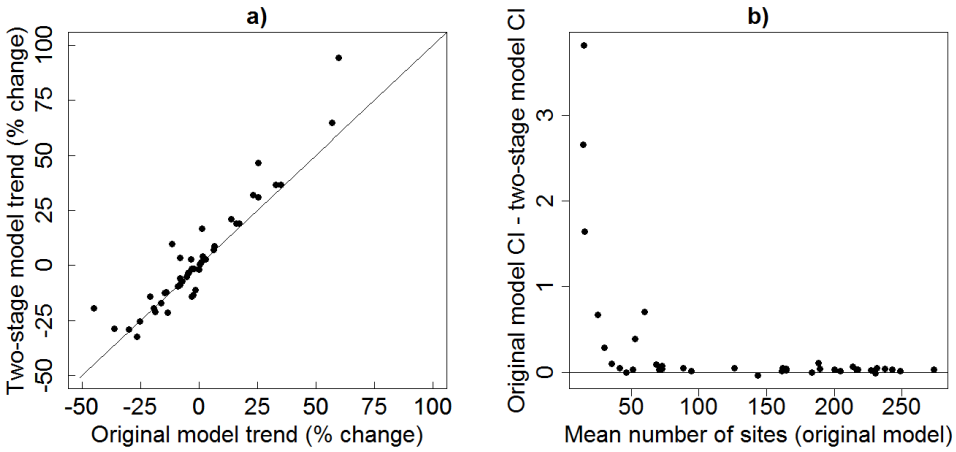

Figure 4.4: a) Comparison of the estimated percentage trends of the collated indices for the two GAM approaches for each species. The solid line is the 1-1 line. b) The difference in mean width (over years) of the confidence intervals from the two GAM approaches compared to the mean number of sites (averaged by year) for each species. These figures appear in Dennis et al. (2013).

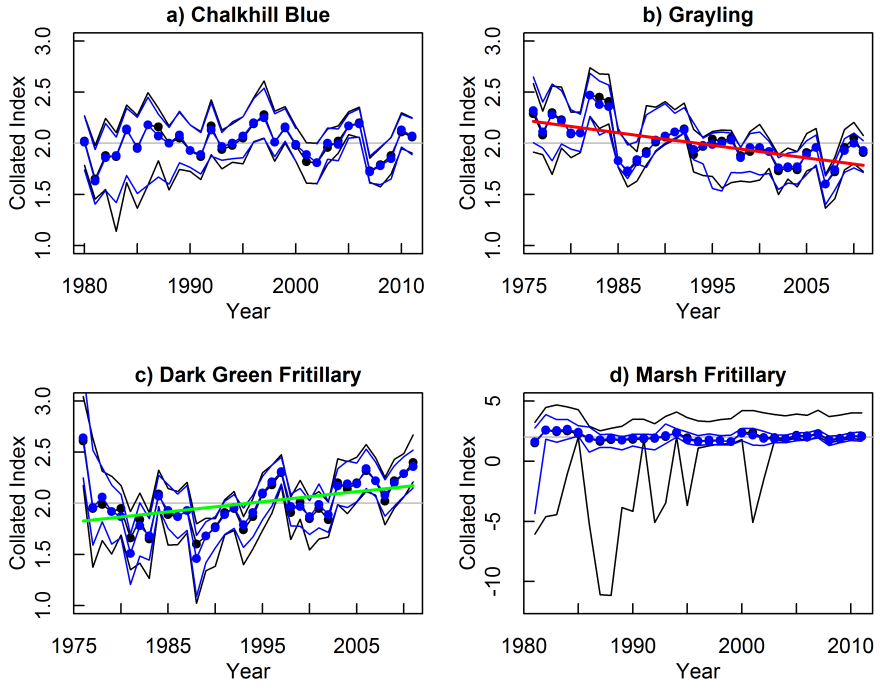

Figure 4.5: Collated indices for the original (black) and two-stage (blue) GAM approaches, with corresponding confidence intervals. Indices are scaled relative to a value of 2.0 in the initial year, as in UKBMS reports. Red/green lines indicate significant decrease/increase from linear regressions (p-value ≤ 0.05).

more pronounced for species recorded at fewer sites. For illustration, Figure 4.5 shows the two collated indices for selected species and displays the close correspondence between the indices. For the Marsh Fritillary, a localised species with relatively few records, the confidence interval is considerably narrower under the two-stage GAM approach compared to the original GAM approach model which shows particularly wide intervals for some years. However, as discussed in Section 1.3.1, alternative sampling methods not included here are utilised by the UKBMS to increase the sample size of monitoring sites for priorities species, such as Marsh Fritillary.

4.1.6 Improving efficiency

As mentioned in the previous section, a disadvantage of the two-stage GAM approach is that computation times may be long for species with many

sites. In this section we assess two potential approaches for reducing the time taken to fit these models. All comparisons in computation time are based on fitting models using a University of Kent server (64 bit Intel Xeon E5540 x 2, 2.53GHz, 32GB). In each case for illustration we fit the models to data for the four example species in Figure 4.5. The main computational burden arises from the need to perform bootstrapping to obtain estimates of error. In this section we only assess how the time taken to fit the model to the original data may be reduced, but any benefits would also apply to reducing the time taken to bootstrap.

Limiting the number of years

A potential disadvantage of the two-stage GAM approach is that the second stage requires a GLM with offset to be fitted to all the data, which may be time-consuming. For annual reporting of UKBMS data, the models require refitting annually with the addition of new data for each year. In this section we investigate whether the computation time may be reduced by fitting the second stage of the model to only a subsection of the data, without sacrificing the precision of the estimates of abundance. For each of the last 12 years (2000-2011), we fit the second stage of the model (equation 4.4) to data from only the previous ten years. The site indices were then estimated and taken for only the most recent year, before being combined with site indices from the previous years to estimate the collated index.

On average across the 12 years and four species, using only ten years in the second stage of the model reduced the computation time of this stage by 56%, with the average for each species ranging between 52% and 61%, and an overall range of 30-72%. Figure 4.6 shows that there are minimal differences between the estimated collated indices, which is further demonstrated in Table 4.1, which compares estimated percentage trends in abundance from the two approaches.

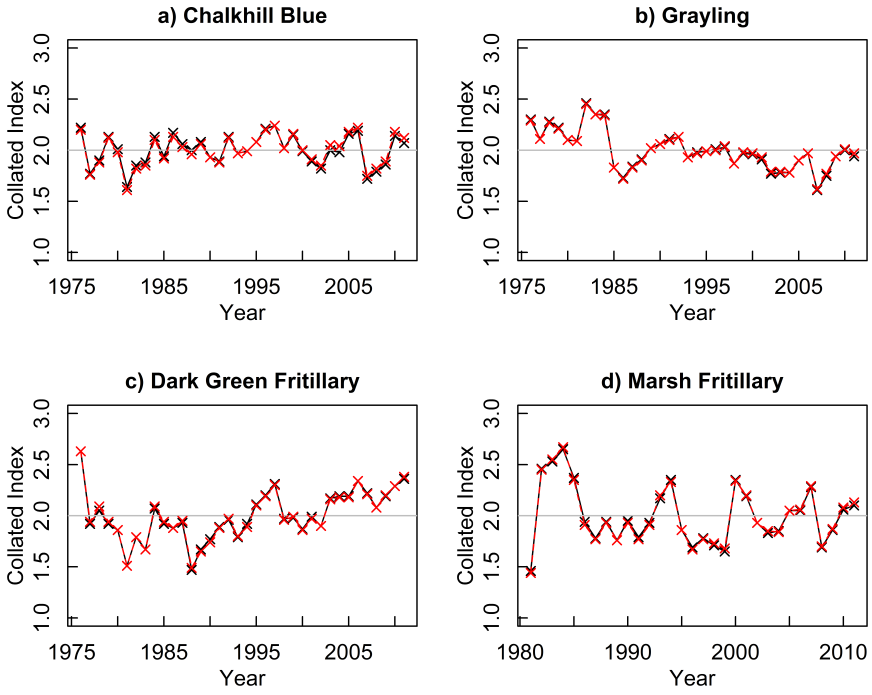

Figure 4.6: Collated indices for the two-stage GAM approach, using all years (black), and only the last 10 years (red) in the second stage of the model. Indices are scaled relative to a value of 2.0 in the initial year, as in UKBMS reports.

Table 4.1: Comparison of model trends (percentage change of the linear trend of the index) when fitting the two-stage GAM approach. 10-year refers to fitting only the last ten years in the second stage of the model, from 2000-2011. Significant trends are represented by $^{*}p \leq 0.05$, $^{**}p \leq 0.01$ and $^{***}p \leq 0.001$.

	Series trend (%)			
Species	Full		10-year	
Chalkhill Blue	1.39		5.47	
Grayling	-18.57	***	-17.60	***
Dark Green Fritillary	19.53	**	18.51	*
Marsh Fritillary	-7.72		-6.45	

Treating counts as daily or weekly

Within the GAM approaches, the count data are typically treated as daily, with $s(t; f)$ a smoothing function of $t \in (1, 182)$ days in the transect season. Given that only one count is made per week in accordance with the UKBMS design, in this section we fit the two-stage GAM approach but treat the data as weekly. Hence we instead fit $s(w; f)$, where $w \in (1, 26)$ is the week number in the season. We explore whether taking a weekly approach can effect the computation time required to fit the GAM, and how the estimated collated index might be effected.

Treating the data as daily or weekly has minimal effect on the predicted shape of the seasonal pattern (Figure 4.7). Furthermore, Figure 4.8 shows that there are minimal differences between the estimated collated indices. This is supported by Table 4.2, which compares estimated percentage trends in abundance from the two approaches. However, computation times between the two approaches were variable and for two of the four species, the weekly GAM approach took significantly longer than the daily GAM. Closer inspection suggests that the computations times are influenced by a small number of years where there may be issues with model fitting, and that on the whole for the other years the computation times are fairly similar between fitting a weekly or daily model.

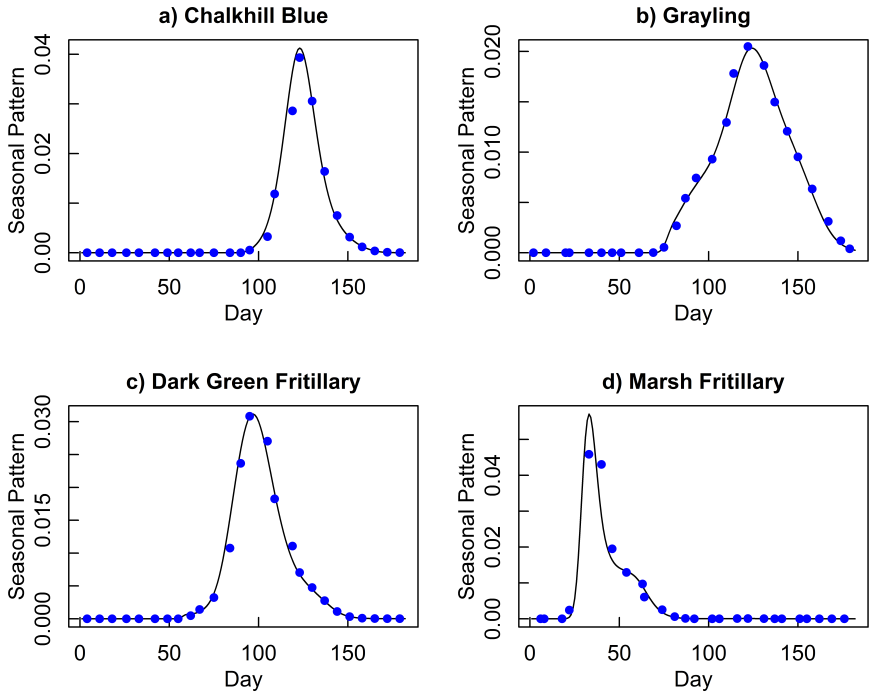

Figure 4.7: Predicted seasonal pattern from the two-stage GAM approach for each species in 2011, treating the counts as daily (solid black line) and weekly (blue dots).

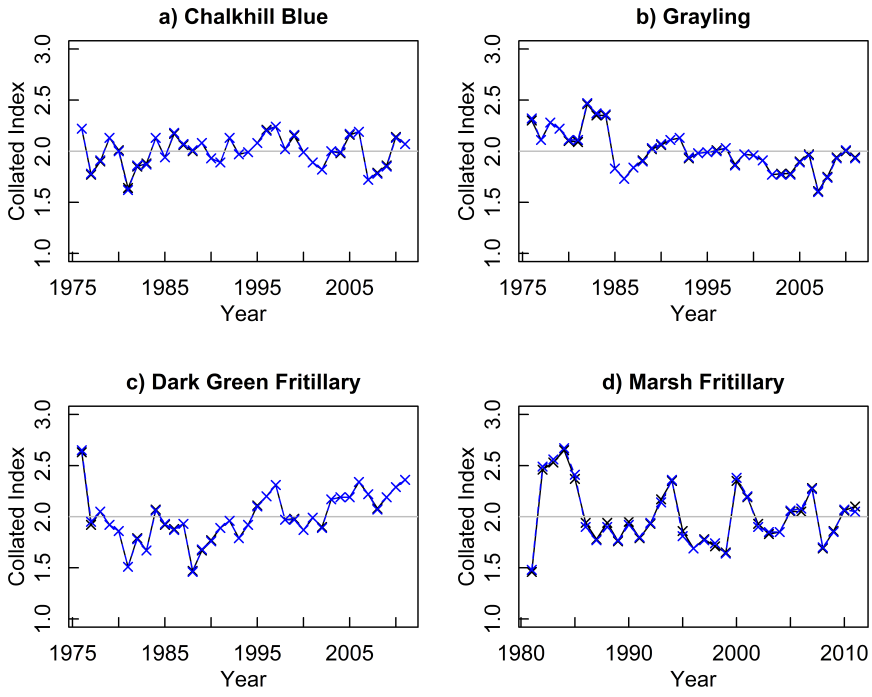

Figure 4.8: Collated indices for the two-stage GAM approach, treating the counts as daily (black), and weekly (blue). Indices are scaled relative to a value of 2.0 in the initial year, as in UKBMS reports.

Table 4.2: Comparison of model trends (percentage change of the linear trend of the index) when fitting the two-stage GAM approach, treating the data as either daily or weekly. Significant trends are represented by $^{*}p \leq 0.05$, $^{**}p \leq 0.01$ and $^{***}p \leq 0.001$. Time represents the percentage difference in computation time of the weekly approach relative to the daily approach.

	Series trend (%)				
Species	Daily		Weekly		Time
Chalkhill Blue	1.39		1.23		83
Grayling	-18.57	***	-19.35	***	-2
Dark Green Fritillary	19.53	**	19.05	**	114
Marsh Fritillary	-7.72		-8.29		-43

4.1.7 Discussion

In this section of Chapter 4, we have described the primary recent modelling approaches for deriving indices of butterfly abundance, using GAMs. The UKBMS provides a large-scale source of butterfly population data for assessing the status and trends in abundance for species which serve as key indicators for change in biodiversity (Brereton et al. 2011b). The full potential of these data had not previously been realised due to limitations in the original GAM approach, particularly due to the substantial proportion excluded from analysis (approximately 38% visited sites per year).

The two-stage GAM approach addresses the implications of this in documenting annual change, firstly by estimating an annual seasonal pattern and then using this to adjust for incomplete series when modelling changes between years. This approach produces more precise trend estimates and allows all volunteer records to contribute to the indices and thus incorporates data from more populations within the geographic range of a species, providing full coverage at least of the monitored area.

Application of the two models to the UKBMS data showed predictions of

large changes in abundance were generally greater for the two-stage GAM approach, which may suggest that the original GAM approach underestimates the magnitude of the change in abundance for some species with such changes. This could have important implications for conclusions drawn from abundance indices for UKBMS data, for example in the classification of Red Lists (Fox et al. 2011c). Bootstrapped confidence intervals for the collated indices indicate that estimates from the two-stage GAM approach have greater precision than the original GAM approach. The confidence intervals tend to be wider for earlier years in the dataset, probably due to the smaller number of sites available to sample from. The confidence intervals are particularly narrower from the two-stage GAM approach for species with fewer sites, which reinforces that such species may benefit from the greater usage of data.

Further extensions for the two-stage GAM approach could be undertaken. A possible drawback of the approach is that the seasonal pattern is assumed to be the same across sites within each year. In come cases a geographically varying approach to the model may improve missing count estimates, since for some species flight periods vary regionally. For example, as we will see in Section 4.2, Common Blue populations are known to exhibit different levels of voltinism with latitude across the UK. Additionally, some species, especially those with a large latitudinal and altitudinal range, exhibit spatial variation in phenology, for example in their date of emergence (Roy and Asher 2003). Hence the seasonal pattern estimation may be over-simplified by the two-stage GAM approach, although variation will generally be greater from year to year than within years. In this chapter seasonal patterns were considered to be consistent at all sites (within a year) for ease of illustration. Spatial variation in the flight period may be incorporated in GAMs using covariates, but may not be straightforward computationally. This matter is not explored further in this thesis, since the new methods proposed in Chapters 5 and 6 provide a simpler and more informative way to allow for spatial variation in flight periods.

The two-stage GAM approach has the benefit of all volunteer input

contributing to the abundance indices, thus providing confidence that their efforts are valuable and hence aiding the retention of volunteers (Bell et al. 2008), therefore allowing the scheme to continue at its current level and making further expansion more likely. Additionally, using the two-stage GAM approach to estimate population trends for wider countryside species has allowed for WCBS data to be incorporated (Brereton et al. 2014), thus providing more representative indices by reducing the current bias from uneven sampling of wider countryside species (Brereton et al. 2011a).

Despite the apparent benefits of the two-stage GAM approach, application to species with many sites can be slow, particularly given the need to perform bootstrapping to obtain estimates of error. In Section 4.1.6, exploratory analyses suggest that fitting the second-stage of the model to data from only ten years was effective in reducing computation time without greatly influencing the estimated abundance indices. Further analysis is required to assess the relative effect this may have on computation time and precision when bootstrapping is performed. Furthermore, it is unclear how these results might vary for species with many more sites, since we anticipate that reducing the number of years may have minimal impact on computation time when there are many site effects to estimate. An iterative approach to model-fitting may be possible for species with appreciable data (Wood et al. 2015).

4.2 Stopover models

The GAM-based methods described in Section 4.1 estimate abundance indices for butterflies, but only describe seasonal variation in counts empirically. As discussed in Section 1.1.4, alternative methods for describing butterfly counts have been proposed, but not applied widely due to a lack of flexibility in assumptions.

A new so-called 'stopover' modelling approach for describing butterfly counts borrows ideas from stopover capture-recapture literature. In doing so parameters of interest are estimated, such as mean arrival times and survival probability. Data for multivoltine species are described by a novel mixture model, which provides estimates of relative brood sizes.

The new approach for modelling butterfly abundance was published in Matechou et al. (2014), for which I performed the application to UKBMS data. In this chapter the model is described and the results from the paper are outlined.

Stopover models were originally developed in a capture-recapture modelling context (Matechou et al. 2013), where individuals within a population can be uniquely marked or identified, which is not the case for typical count data for butterflies. The unknown times of arrival and departures of individuals to a site are modelled, and the average duration of the stay of the individuals can be indirectly estimated. The stopover model proposed in Matechou et al. (2014) explains seasonal variation in butterfly counts in terms of arrival (emergence) and survival. Relatively little is known regarding butterfly survival, and what is known results from short-term mark-recapture programs, which are expensive and only local, hence these models may provide valuable new information on butterfly lifespans, and how they may vary.

4.2.1 Model description

Suppose counts of adult butterflies are recorded at S sites, each visited on T occasions, within a given year. We assume that the T possible sampling

occasions are equally spaced. Each count, $y_{i,j}$, for the ith site and jth visit, can be treated as the realisation of a random variable from a suitable discrete distribution, which, for example, is often taken as Poisson. In this case for expectation $\lambda_{i,j}$ at site i and visit j, made at time $t_{i,j}$ (e.g. week number in the season), the model likelihood has the form

$$\mathrm{L}(\boldsymbol{N}, \boldsymbol{\beta}, \boldsymbol{\phi}; \boldsymbol{y}) = \prod_{i=1}^{S} \prod_{j=1}^{T} \left[\frac{\exp(-\lambda_{i,j}) \lambda_{i,j}^{y_{i,j}}}{y_{i,j}!} \right], \tag{4.6}$$

where

$$\lambda_{i,j} = N_i \sum_{d=1}^{j} \beta_{i,d-1} \left(\prod_{m=d}^{j-1} \phi_{m,c} \right), \tag{4.7}$$

for $j = 1, \ldots, T$ and $c = m - d + 1$, is the unknown number of occasions that an individual has been present at the site, where $d = 1, \ldots, j$ are the possible times of emergence for an individual detected on visit j. The parameters $\{\beta_{i,d-1}\}$ describe the proportions of the 'super-population' N_i emerging at site i and visit d, such that $\sum_{d=1}^{T} \beta_{i,d-1} = 1$ for each site i. These emergence parameters are modelled using a mixture of B normal distributions to represent B broods, so that

$$\beta_{i,d-1} = \sum_{b=1}^{B} w_{i,b} \{ F_{i,b}(t_{i,d}) - F_{i,b}(t_{i,d} - 1) \},$$

where $w_{i,b}$ represent the relative weights of each brood, and $F_{i,b}(t_{i,d}) = \Pr(X \leq t_{i,d})$, for $X \sim N(\mu_{i,b}, \sigma_{i,b}^2)$, where $\mu_{i,b}$ is the mean date of emergence for brood b and $\sigma_{i,b}^2$ the associated variance. Given that $F_{i,b}(0) = 0$ and $F_{i,b}(T) = 1$ for each i and b, then $\beta_{i,0} = \sum_{b=1}^{B} w_{i,b}[F_{i,b}(1)]$ and $\beta_{i,T-1} = 1 - \sum_{b=1}^{B} w_{i,b}[F_{i,b}(T-1)]$. We define $\phi_{m,c}$ as the probability that an individual which has been at a site for c occasions and is present at visit m will remain until $m + 1$. So, for example if $j = 3$, then for a particular site i, $\lambda_{i,3} = N_i(\beta_{i,0}\phi_{1,1}\phi_{2,2} + \beta_{i,1}\phi_{2,1} + \beta_{i,2})$.

In Matechou et al. (2014), variation in survival is demonstrated with respect to time and age, such that for time variation

$$\mathrm{logit}(\phi_{m,c}) = \alpha_{\phi,0} + \alpha_{\phi,1} x_m,$$

for all c, where x_m is a time-varying covariate such as calendar time, or alternatively for age variation

$$\text{logit}(\phi_{m,c}) = \alpha_{\phi,0} + \alpha_{\phi,1}c,$$

for all m, where age is defined as the unknown time since entry to the site, c.

The mean emergence times and relative weights of each brood may be modelled in terms of a site-specific covariate to account for spatial variation in emergence and relative brood sizes.

In theory, imperfect detection may be incorporated into the model, such that

$$\lambda_{i,j} = N_i \left[\sum_{d=1}^{j} \beta_{i,d-1} \left(\prod_{m=d}^{j-1} \phi_{m,c} \right) \right] p_{i,j}, \tag{4.8}$$

where $p_{i,j}$ represents the probability of detecting an individual that is present at site i on occasion j. If p is assumed to be constant, only the product $N_i p$ is estimable. However when p is allowed to vary with a time-varying covariate, such as temperature, Matechou et al. (2014) suggest that N and p may be estimated separately provided sufficient information is available from the data. These findings were discussed in the context of parameter redundancy: a model is termed parameter redundant when one or more parameters cannot be estimated (Catchpole and Morgan 1997). In this stopover model approach, if the covariate for p does not vary considerably across visits, or the effect on p is not statistically significant, then the model will behave like a parameter-redundant model, where each N_i cannot be separated from p.

Matechou et al. (2014) conducted an extensive simulation study of the stopover model approach for butterflies, which we do not describe in depth here. The model was found to perform well for multiple scenarios for $S = 10$, $T = 15$ and up to 20% missing data, for up to $M = 3$ broods.

4.2.2 Application to UKBMS data

The stopover model approach was demonstrated with UKBMS data for a single butterfly species, the Common Blue, for data collected in 2010. In this section we provide an outline of these results.

Data were limited to a random sample of 50 monitored sites, excluding sites where more than 6 counts were missing from the season or the sum of the counts made was less than 10. Common Blue is known to exhibit bivoltine populations in the south of the UK, while populations become single-brooded in the north. However, a precise latitude at which this occurs or knowledge of how this boundary may have changed over time are both unknown (Asher et al. 2001). Hodgson et al. (2011) demonstrate the change from two broods in the south to one brood in the north using GAMs, and found that the best fitting model for Common Blue did not include temporal variation, which was included by using growing degree-days as a covariate.

Normal mixture distributions with two components, such that $B = 2$, were used to describe the emergence pattern of the butterflies. Common Blue overwinters as a caterpillar and is therefore not seen in flight until late spring. The start of the season was defined as the week with the first positive count, with season length totalling 21 weeks.

A model comparison was undertaken for varying parameter assumptions using AIC. Detection probabilities were set either as constant and common across sites or as logistically dependent on temperature at the site on the day of sampling, which is usually recorded by the observer. Missing temperature records were replaced by the average of neighbouring sites.

The two models with the lowest AIC values had w and μ dependent on northing and the survival probabilities dependent quadratically on calendar time (week number in the season). The most favoured model had detection probability dependent on temperature, such that p increased with temperature, whereas the second most favoured model had constant detection probability. Table 4.3 shows the parameter estimates for the favoured model, which had 61 parameters in total corresponding to the eleven parameters given in Table 4.3, plus the estimated $\{N_i\}$ for each of $S = 50$ sites.

The weighting of the first normal distribution with respect to the second increases with northing, with the second brood almost disappearing in the north as w approaches unity (Figure 4.9a). The means of the two normal

distributions suggest a later time of emergence in the north (Figure 4.9b). This is also demonstrated by the entry parameters: two relatively even broods at southern sites, with the first brood dominating at high northing, in addition to a later emergence (Figure 4.10). At high northing values, when Common Blue are univoltine, Figure 4.10 shows a small peak at the end of the season, which is similarly found in Figure 4.9b, where μ_2 extends beyond T. This issue may be resolved by suitably constraining μ.

The estimated survival probabilities, shown in Figure 4.9c, peak around week 11 of 21, before dropping off towards the ends of the season. They are estimated as approximately zero for the initial weeks of the season.

Table 4.3: Parameter estimates from the most favoured (in terms of AIC) stopover model applied to UKBMS data for Common Blue. Est and SE represent the parameter estimates and standard error, respectively. All covariates were standardised to have zero mean and unit variance. All estimates are on the log scale, except those relating to p and ϕ which are on the logit scale. The results in this table appear in Matechou et al. (2014).

Parameter	Est	SE
p_j(intercept)	-4.600	1.769
p_j(temperature)	5.522	2.170
$w_{i,1}$(intercept)	1.186	0.160
$w_{i,1}$(northing)	1.101	0.150
$\mu_{i,1}$(intercept)	1.688	0.023
$\mu_{i,2}$(intercept)	2.748	0.013
$\mu_{i,1}$(northing)	0.209	0.010
σ	1.251	0.055
ϕ_j(intercept)	1.743	0.193
ϕ_j(week)	1.562	0.266
ϕ_j(week^2)	-3.200	0.297

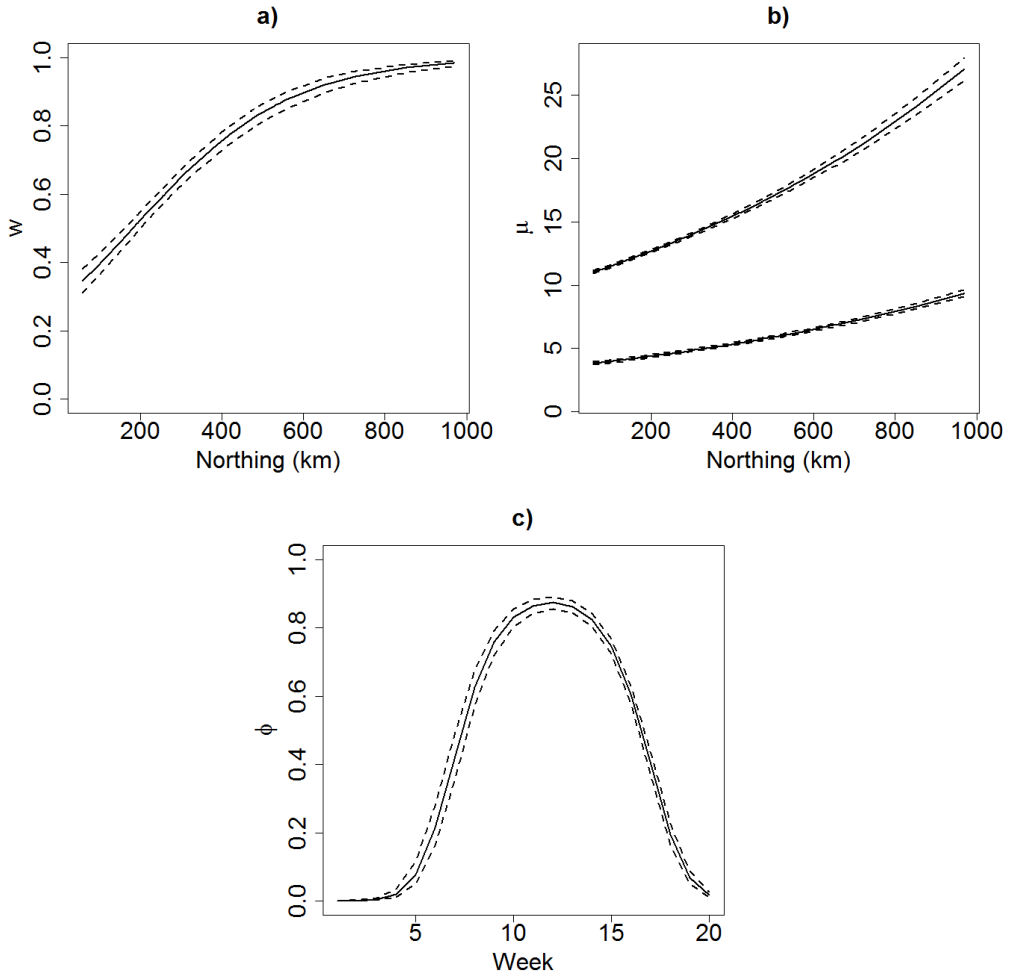

Figure 4.9: Parameter estimates (with 95% confidence intervals) from the stopover model for Common Blue. a) Relative size of the first brood, w, b) mean emergence times of the two broods, μ, with northing, and c) estimated survival probabilities, ϕ, with week in the season. These figures appear in Matechou et al. (2014).

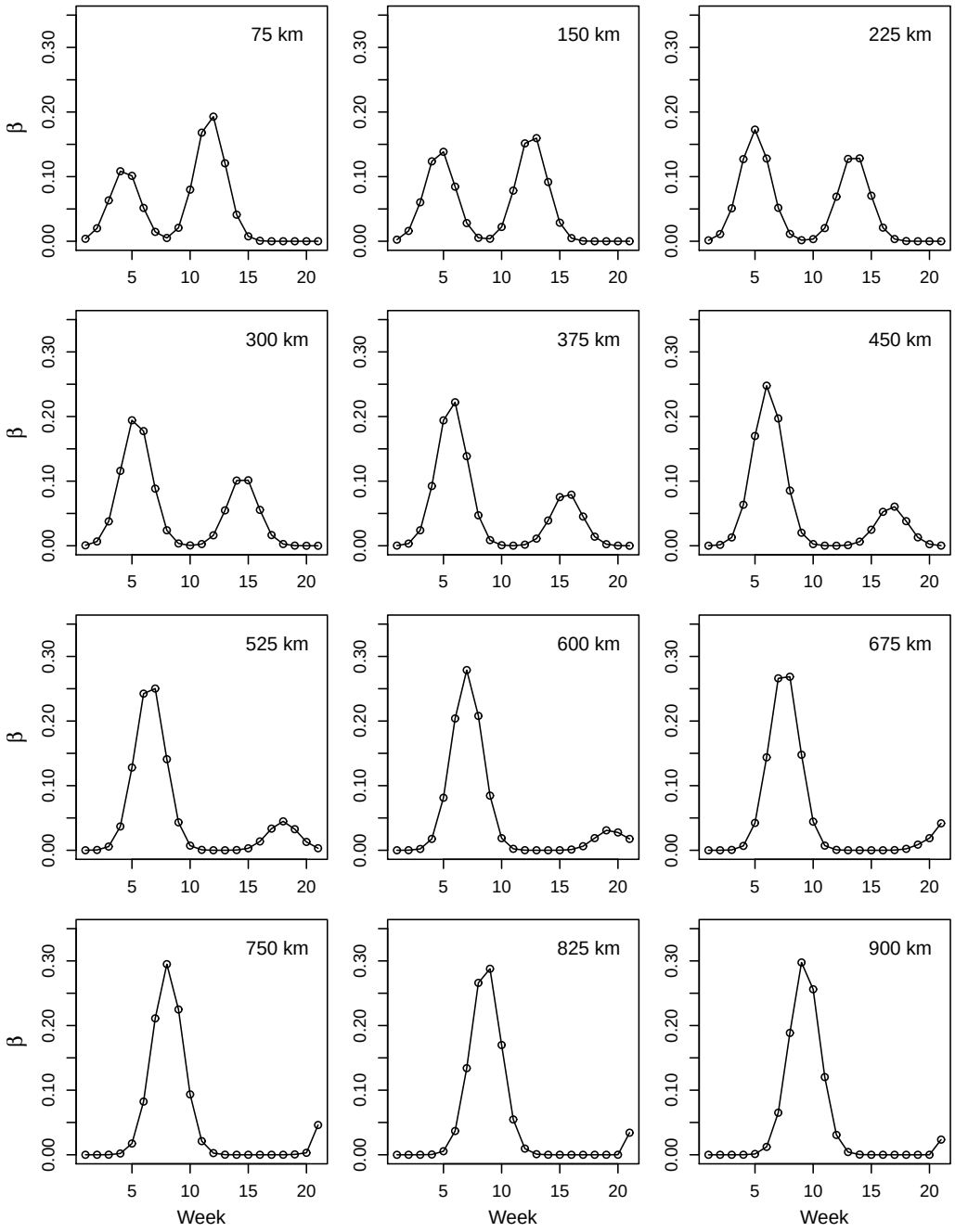

Figure 4.10: Estimated arrival proportions for Common Blue at a sample of northing values. This figure appears in Matechou et al. (2014).

4.2.3 Discussion

Prior to the development of stopover models for describing butterfly count data in Matechou et al. (2014), the main approaches for indexing abundance were non-parametric and empirical. The GAM approaches described in Section 4.1 involve interpolating missing values, and do not account for potentially counting the same individual on separate occasions within the season. Consequently, estimates of the total number of sightings rather than individuals are made.

The stopover model can estimate indices of abundance that are more representative of the actual number of individuals than the GAM approaches, by implicitly accounting for possible repeat sightings of individuals during a season. Describing the seasonal variation in counts parametrically provides estimates of new and valuable parameters, which are likely to be informative for studying phenological change, as well as potential changes in the relative sizes of two (or more) broods. The novel mixture element in the stopover model approach also allows data for bivoltine (and multivoltine) species to be modelling parametrically.

The stopover approach is related to the pioneering work of Zonneveld (1991), which we described in Chapter 1, as a special case, in which data from single sites are modelled individually with a constant rate of survival. The capacity for useful inference was limited by data from only a single site and season. By simultaneously analysing data from multiple, potentially many, sites, in Matechou et al. (2014) the stopover model demonstrates improved inference on key ecological parameters, and that assumptions may be tested, for example whether survival is constant or varying.

Matechou et al. (2014) demonstrates the potential of stopover modelling for butterfly count data, and using northing as a covariate, confirms and quantifies, the long-standing field experience that Common Blue is effectively single-brooded in the far north of its range and bivoltine at southern sites, and that emergence is later with increasing northing.

We will provide further applications of stopover models in this thesis,

for example in Chapter 5 they form part of a general framework that we develop for modelling butterfly count data. Furthermore, in Chapter 6, we describe stopover models within a slightly different formulation, in the context of dynamic models. In both of these chapters comparisons are also made with the two-stage GAM approach from Section 4.1.

Although beyond the scope of this thesis, wider application of the stopover approach is needed to confirm performance of the model for more extensive data, specifically for multiple years and for more species, with varying numbers of broods per season. This may be particularly relevant for species with fewer sites or low counts, which may not provide enough information to robustly estimate survival.

Previously, a need for capture-recapture data has been advised to obtain robust estimates of butterfly survival (Gross et al. 2007; Haddad et al. 2008; Nowicki et al. 2008). Comparison of survival estimates from the stopover model with estimates from mark-recapture studies could confirm whether the stopover model can offer a valid alternative, by estimating survival from only count data. Additionally, application and model-selection for more species could examine whether variation in survival, for example with time or age, is consistent or variable across different species.

Various extensions or modifications to the approach are possible. For example, alternatives to the Normal distributions for the emergence times could be explored, for instance Calabrese (2012) generalised Zonneveld (1991) to consider asymmetric distributions. Cornulier et al. (2009) also used asymmetric distributions within mixture models to permit a degree of skewness in the hatching dates of birds from monitored nests. Allowing for more flexible distributions may, for example, accommodate a scenario where most butterflies emerge at once in accordance with suitable climatic conditions.

In other contexts, stopover models use analogous methods to describe the arrival and departure of (marked) individuals from a location, which are usually considered as immigration and emigration, and absolute abundance may be estimated. Butterflies are not individually identifiable from

count data, which thus prohibits the estimation of true abundance when detection probability is assumed constant. For butterfly transect data, such as from the UKBMS, which are collected under standardised protocols, it is typical to assume detectability to be constant, and consequently measures of relative rather than absolute abundance are used in management and monitoring. Given the large-scale and long-term nature of the data, variation in detection is assumed to be minimal compared to variation in abundance (van Swaay et al. 2008). A distance-sampling study by Isaac et al. (2011a) suggested that "UKBMS data provide a good reflection of relative abundance for most species", despite variation in detectability among species. In Matechou et al. (2014), detectability was modelled as a function of temperature at the site on the day of sampling. If available, other covariates such as habitat type, recorder effort, experience or age could also be incorporated, but might not necessarily provide sufficient information to separate $\{N_i\}$ and p. Where possible, further analysis could be undertaken to compare the impacts of allowing variation in detectability upon indices of abundance and their associated trends.

Chapter 5

A generalised abundance index

In producing indices for insects such as butterflies it is important to account for variation in counts within seasons, and in the previous chapter two recent methods were described: one non-parametric, using generalised additive models, and the other parametric, based on stopover models. In this chapter we present a novel generalised abundance index which encompasses both parametric and non-parametric approaches. We will see that it is extremely efficient due to the use of concentrated likelihood techniques. This has particular relevance for the analysis of data from long-term extensive monitoring schemes with records for many species and sites, for which the existing modelling techniques can be time consuming. Performance of the index is demonstrated by several applications to UK Butterfly Monitoring Scheme data. We demonstrate the potential for new insights into both phenology and spatial variation in seasonal patterns from parametric modelling and the incorporation of covariate dependence, which is relevant for both monitoring and conservation. This chapter is based upon a paper that is under review by the *Annals of Applied Statistics*.

5.1 Background

As discussed already in Chapter 1, abundance indices for butterflies are vital for monitoring the population status of species and contribute to the assessment of trends in biodiversity. Novel methods for deriving indices

accurately and efficiently are continually sought.

The GAM and stopover model approaches described in Chapter 4 each have advantages for modelling butterfly count data, but both require optimisation of a likelihood with potentially many parameters corresponding to the relative abundance for each site. Given the often large amount of data available from monitoring schemes such as the UKBMS, fitting these models for hundreds or thousands of sites over many years, for multiple species, is computer-intensive and challenging. Long-term monitoring schemes require annual updates, and time-consuming methods, particularly the non-parametric bootstrapping required for error estimation, lead to appreciable lags in data processing. The need for more efficient data analysis methods motivates the model developments in this chapter.

The new generalised abundance index (GAI) is described in Section 5.2. A concentrated likelihood approach is given for the Poisson case, followed by an iterative concentrated likelihood method for the negative-binomial and zero-inflated Poisson distributions. The derivation of the index is given in Section 5.2.5, followed by three possible options for describing seasonal variation, including a novel phenomenological model. In Section 5.3 we demonstrate the efficiency of the concentrated likelihood approach via simulation. Section 5.4 describes an alternative hierarchical model approach and then in Section 5.5 model comparisons are made for the stopover model, with real and simulated data. Section 5.6 presents a series of examples of the GAI applied to UKBMS data, chosen to illustrate the flexibility of the approach. The last example indicates how a multi-year model can be formed, and the chapter ends with a discussion in Section 5.7.

5.2 Generalised abundance index

Suppose counts are recorded at S sites, each visited on T occasions, within a single year. We treat each count, $y_{i,j}$, for the ith site and jth visit, as an appropriate discrete random variable. As noted in Chapter 3, particularly useful are Poisson, negative-binomial and zero-inflated Poisson distri-

butions. The expectation of the distribution, $\lambda_{i,j}$, is modelled as a product of site parameters, N_i, which represent the relative abundance for the ith site, and general $a_{i,j} = a_i(t_{i,j}, \boldsymbol{\eta})$, which denotes a function for describing the seasonal variation in counts in terms of a small set of parameters $\boldsymbol{\eta}$, where $t_{i,j}$ is the time (e.g. week number in the season) of the jth visit to site i. The $a_{i,j}$ is thus not forced to be the same across all sites, which allows for greater flexibility and realism compared to the currently adopted two-stage GAM approach (Section 4.1.3). Both non-parametric and parametric functions for $a_{i,j}$ are possible, as we will demonstrate in Section 5.2.6.

5.2.1 Concentrated likelihood for the Poisson case

The Poisson distribution with expectation $\lambda_{i,j} = N_i a_{i,j}$ gives the likelihood

$$\mathrm{L}(\mathbf{N}, \boldsymbol{\eta}; \mathbf{y}) = \prod_{i=1}^{S} \prod_{j=1}^{T} \frac{\exp(-N_i a_{i,j})(N_i a_{i,j})^{y_{i,j}}}{y_{i,j}!}. \tag{5.1}$$

Maximisation of this likelihood is straightforward but cumbersome when data arise from many sites, where S could be over 1000 for some common species. For instance in Matechou et al. (2014), as described in Section 4.2.2, a random sample of 50 sites was taken, but Common Blue have been monitored at 1448 sites as of 2013 (Brereton et al. 2014). However, the number of parameters to estimate can be reduced appreciably by optimising a concentrated (or profile) likelihood as follows. Using the notation $a_{i,\cdot} = \sum_{j=1}^{T} a_{i,j}$,

$$\begin{aligned}\ell = \mathrm{Log}(\mathrm{L}) = &-\sum_{i=1}^{S} N_i a_{i,\cdot} + \sum_{i=1}^{S} y_{i,\cdot} \log(N_i) \\ &+ \sum_{i=1}^{S} \sum_{j=1}^{T} y_{i,j} \log(a_{i,j}) - \sum_{i=1}^{S} \sum_{j=1}^{T} \log(y_{i,j}!).\end{aligned}$$

Then

$$\frac{\partial \ell}{\partial N_i} = -a_{i,\cdot} + \frac{y_{i,\cdot}}{N_i},$$

and equating to zero we obtain

$$N_i = \frac{y_{i,\cdot}}{a_{i,\cdot}}, \tag{5.2}$$

which evidently estimates $\{N_i\}$ by scaled site totals. Substituting this expression for $\{N_i\}$ in (5.1) results in a Poisson likelihood with expectation $\lambda_{i,j} = \frac{y_{i,.}}{a_{i,.}} a_{i,j}$, which we refer to as a concentrated likelihood, which is maximised with respect to only the parameters, $\boldsymbol{\eta}$, associated with $\{a_{i,j}\}$. Estimation of $\{N_i\}$ is then straightforward, by deriving $\hat{a}_{i,.}$, and substituting into (5.2). An alternative approach for reducing the number of parameters, by treating the site parameters as random effects, is shown to generalise (5.2) in Section 5.4.

5.2.2 Negative-binomial case

For the negative-binomial case, we take the NB-2 form (Hilbe 2011, p187)

$$\Pr(Y = y) = \binom{y + r - 1}{y} \left(\frac{m}{r+m}\right)^y \left(\frac{r}{r+m}\right)^r, \tag{5.3}$$

which is parameterised by r, the negative-binomial dispersion parameter, and $p = \frac{m}{r+m}$, where m is the expectation of the negative-binomial. Hence the negative-binomial likelihood is given by

$$\mathrm{L}(\mathbf{N}, \boldsymbol{\eta}, r; \mathbf{y}) = \prod_{i=1}^{S} \prod_{j=1}^{T} \frac{\Gamma(y_{i,j} + r)}{\Gamma(r) y_{i,j}!} \left(\frac{N_i a_{i,j}}{r + N_i a_{i,j}}\right)^{y_{i,j}} \left(\frac{r}{r + N_i a_{i,j}}\right)^r, \tag{5.4}$$

where the expectation of $y_{i,j}$ is $N_i a_{i,j}$, as in the Poisson case. Hence

$$\begin{aligned} \ell = \mathrm{Log}(\mathrm{L}) = \sum_{i=1}^{S} \sum_{j=1}^{T} \Bigg[& \log\left\{\frac{\Gamma(y_{i,j} + r)}{\Gamma(r) y_{i,j}!}\right\} + y_{i,j} \log(N_i a_{i,j}) \\ & - (r + y_{i,j}) \log(r + N_i a_{i,j}) + r \log r \Bigg], \end{aligned} \tag{5.5}$$

leading to

$$\frac{\partial \ell}{\partial N_i} = \sum_{j=1}^{T} \left\{ \frac{y_{i,j}}{N_i} - \frac{(r + y_{i,j}) a_{i,j}}{r + N_i a_{i,j}} \right\}. \tag{5.6}$$

An exact solution for N_i does not result in this case from equating $\frac{\partial \ell}{\partial N_i}$ to zero. However, given that $\mathbb{E}(y_{i,.}) = N_i a_{i,.}$, if we make the approximation $y_{i,j} \approx N_i a_{i,j}$, then (5.6) reduces to

$$N_i = \frac{y_{i,.}}{a_{i,.}},$$

as in (5.2), which provides an approximation for a concentrated likelihood, which can be fitted as for the Poisson case. Exact maximum-likelihood parameter estimates can then be obtained as follows:

(i) Maximise the approximate concentrated likelihood from (5.5) with $N_{i,} = \frac{y_{i,\cdot}}{a_{i,\cdot}}$ to give parameter estimates for $\hat{a}_{i,j}$.

(ii) Based on $\hat{a}_{i,j}$, solve $\frac{\partial \ell}{\partial N_i} = 0$ in (5.6) numerically for N_i.

(iii) Insert the N_i from (ii) into (5.5) and optimise for the parameters of $\hat{a}_{i,j}$.

(iv) Iterate steps (ii)-(iii) until convergence.

5.2.3 Zero-inflated Poisson case

The approach for the negative binomial applies also for the zero-inflated Poisson. In this case the likelihood is

$$\mathrm{L}(\mathbf{N}, \boldsymbol{\eta}, \psi; \mathbf{y}) = \prod_{i=1}^{S} \prod_{j=1}^{T} \left\{1 - \psi + \psi e^{-N_i a_{i,j}}\right\}^{1-b_{i,j}} \left\{ \frac{\psi e^{-N_i a_{i,j}} \left(N_i a_{i,j}\right)^{y_{i,j}}}{y_{i,j}!} \right\}^{b_{i,j}},$$

where $1 - \psi$ accounts for additional zeros, and

$$b_{i,j} = \begin{cases} 1 & \text{if } y_{i,j} > 0 \\ 0 & \text{if } y_{i,j} = 0. \end{cases}$$

Then

$$\ell = \mathrm{Log}(\mathrm{L}) = \sum_{i=1}^{S} \sum_{j=1}^{T} \left\{ (1 - b_{i,j}) \log\left(1 - \psi + \psi e^{-N_i a_{i,j}}\right) + b_{i,j} \log\left(\frac{\psi}{y_{i,j}!}\right) \right.$$
$$\left. - b_{i,j} N_i a_{i,j} + b_{i,j} y_{i,j} \log\left(N_i a_{i,j}\right) \right\}, \tag{5.7}$$

and differentiating with respect to N_i gives

$$\frac{\partial \ell}{\partial N_i} = \sum_{j=1}^{T} \left\{ \frac{-\psi a_{i,j} (1 - b_{i,j}) e^{-N_i a_{i,j}}}{1 - \psi + \psi e^{-N_i a_{i,j}}} - b_{i,j} a_{i,j} + \frac{b_{i,j} y_{i,j}}{N_i} \right\}. \tag{5.8}$$

Steps (i)-(iv) in Section 5.2.2 can then be applied to obtain maximum-likelihood parameter estimates, but replacing (5.5) and (5.6) with (5.7) and (5.8), respectively.

5.2.4 Increased efficiency

Step (ii) of Section 5.2.2 is easily achieved using the `uniroot` function in `R` and only a few iterations of steps (ii)-(iii) are generally needed. The concentrated likelihoods are functions of S fewer parameters than the original likelihoods. Substantial reductions in computation time are then made, which we demonstrate via simulation in Section 5.3. An `R` program for the GAI, which incorporates the concentrated likelihoods with iteration where required, is provided as an electronic appendix to this thesis.

5.2.5 Generalised abundance index

For each year for any particular model we use the average of the estimated site parameters, $\{\hat{N}_i\}$, as a measure of abundance, given by

$$G = \frac{1}{S}\sum_{i=1}^{S}\hat{N}_i. \tag{5.9}$$

The model is fitted separately for each year, G is calculated in each case and the results are plotted against time to provide an index of abundance. As in Section 4.1.5 for the two-stage GAM approach, errors are derived by non-parametric bootstrapping, where for each replicate the GAI is fitted to data for a random sample of sites, drawn with replacement.

We specify a particular GAI using the x/z notation, with x denoting the distribution and z the choice for $a_{i,j}$. In this paper we consider x as P, ZIP and NB for the Poisson, zero-inflated Poisson, and negative-binomial distributions, respectively. In the following section possible options for z are described.

5.2.6 Functions for $a_{i,j}$

The function $a_{i,j}$ may be any general function which describes the seasonal variation in counts over the monitoring period. Here we present both non-parametric and parametric options.

Splines

For illustration we adopt simple cubic B-splines (Chambers and Hastie 1991), such that

$$a_{i,j} = \exp\left\{\alpha_0 + \sum_{d=1}^{f} \alpha_d B_d(t_{i,j})\right\},$$

where $t_{i,j}$ is the time of the jth visit to the ith site, $B_d(t_{i,j})$ are the basis functions and f is the degrees of freedom, defined as the sum of the degree of the spline (in this case 3 for cubic splines) and the number of knots. The estimated seasonal pattern is the same across sites, as for the GAM approach (Section 4.1.3). Model notation is x/S. We compare the P/S GAI with the two-stage GAM approach in Section 5.6.1.

Phenomenological model

The seasonal variation in counts tends to reflect the emergence of B broods. In this case $a_{i,j}$ is taken as a mixture of B Normal probability density functions so that

$$a_{i,j} = \sum_{b=1}^{B} w_{i,b} \frac{1}{\sigma_{i,b}\sqrt{2\pi}} \exp\left\{-\frac{(t_{i,j} - \mu_{i,b})^2}{2\sigma_{i,b}^2}\right\}, \tag{5.10}$$

where $w_{i,b}$, $\mu_{i,b}$ and $\sigma_{i,b}$ correspond to the weight, mean and standard deviation, respectively, for the ith site and bth brood. For a univoltine species, where $B = 1$, $a_{i,j}$ would be the single Normal probability density function

$$a_{i,j} = \frac{1}{\sigma_i\sqrt{2\pi}} \exp\left\{-\frac{(t_{i,j} - \mu_i)^2}{2\sigma_i^2}\right\}. \tag{5.11}$$

We denote these models by x/N$_B$.

Stopover model

The functions for $a_{i,j}$ presented above are solely descriptive, fitting appropriate curves (non-parametrically or parametrically) through counts. The stopover model described in Section 4.2 of this thesis explains seasonal variation via specific parameters relating to the butterfly life-cycle. Based upon

(4.7), in this case

$$a_{i,j} = \sum_{d=1}^{j} \beta_{i,d-1} \left(\prod_{m=d}^{j-1} \phi_{m,c} \right), \tag{5.12}$$

for $j = 1, \ldots, T$ and $c = m - d + 1$, where $d = 1, \ldots, j$ are the possible times of emergence for an individual detected on visit j. As defined in Section 4.2.1, the parameters $\{\beta_{i,d-1}\}$ describe the proportions N_i emerging at site i and visit d, and are modelled using a mixture of B normal distributions. We again define $\phi_{m,c}$ as the probability that an individual which has been at a site for c occasions and is present at visit m will remain until $m + 1$.

We denote these models by x/SO$_B$. Whereas previously in Section 4.2 estimation of potentially many $\{N_i\}$ is required, using the concentrated likelihood approach for the stopover model means that estimation of only parameters within the expression of (5.12) is necessary. We demonstrate the reductions in computation time that arise from fitting the concentrated likelihood approach in Section 5.3. In Section 5.5 we compare stopover and phenomenological models for simulated and UKBMS data from 2010, and a further application to data for multiple years is made in Section 5.6.3.

5.3 Demonstration of efficiency via simulation

In this section we compare the performance of optimising a full versus a concentrated likelihood for simulated data for Poisson, negative-binomial and zero-inflated Poisson GAI, for both phenomenological and stopover models. Data were simulated from the relevant fitted model, based on a single year for $S = 50$ sites and $T = 26$ visits, where for illustration the parameter values used were based upon reasonable values that might be applicable for data for a real species. For the negative-binomial and zero-inflated Poisson cases, we set $r = 0.75$ and $\psi = 0.75$, respectively. For the stopover models, we set $\phi = 0.5$. We assume a univoltine species where the counts arise from a Normal distribution with $\mu = 10$ and $\sigma = 2.5$, and N_i for each site was drawn from a Poisson distribution with an expectation of 150.

For the simplest P/N$_1$ GAI, the concentrated likelihood has just two parameters to estimate, and for the full likelihood, with the addition of a

parameter for each site, there are 52 parameters to estimate. The negative-binomial and zero-inflated Poisson phenomenological models each required one additional parameter to be estimated. Similarly where the stopover model formulation was used, an additional parameter, ϕ, was estimated.

The concentrated likelihoods were maximised using the `optim` function in the `R` software package (R Core Team 2015) with the default Nelder-Mead algorithm, as were all of the analyses in this chapter except where specified. The full likelihoods were maximised using the BFGS algorithm, since the Nelder-Mead algorithm did not always optimise. The computation times are based on the simulations performed on a University of Kent server (64 bit Intel Xeon E5540 x 2, 2.53GHz, 32GB). Similarly the timing comparisons made throughout this chapter were performed on this server. Iterative likelihood optimisation for the negative-binomial and zero-inflated Poisson cases, as described in Sections 5.2.2 and 5.2.3, was performed until the difference in the current and previous log-likelihood value was < 0.001.

Based on the average time taken to fit each model to one simulated dataset, using a concentrated likelihood approach showed very large reduc-

Table 5.1: Average computation times (in seconds) from 20 simulated datasets, fitting the full and concentrated likelihood approach for the phenomenological and stopover models. The mean and maximum number of iterations are given for the ZIP and NB iterative concentrated likelihood approach.

	Computation time		No. of iterations	
Model	Full	Concentrated	Mean	Max
P/N_1	8.6	0.1	-	-
ZIP/N_1	18.3	0.7	3	3
NB/N_1	20.3	0.7	4	5
P/SO_1	66.9	0.6	-	-
ZIP/SO_1	101.5	9.8	11	23
NB/SO_1	93.9	5.2	6	7

tions in computation time (Table 5.1). In particular for the Poisson case, fitting the full parameter model took over 100 times longer than fitting the concentrated likelihood model for both the phenomenological and stopover models. Despite requiring iterative likelihood optimisation, the concentrated approach was also faster than optimising the full likelihood in the zero-inflated Poisson and negative-binomial cases. The zero-inflated Poisson and negative-binomial phenomenological models always each converged within 3 and 5 iterations through steps (ii)-(iv) of Section 5.2.2, respectively, whereas for the stopover model formulation the zero-inflated Poisson model took a maximum of 23 iterations, and hence took the longest time to fit. In all cases the stopover model took longer than the phenomenological model to fit, which would be anticipated given the greater complexity of the model, which also has an additional parameter to estimate.

5.4 A hierarchical model approach

An alternative approach to optimising a concentrated likelihood involves treating the individual site effects as random effects. Using a hierarchical approach, we assume the site parameters, N_i, to be independent random variables with a particular probability density function $f(N_i, \boldsymbol{\theta})$, as in the N-mixture model (Section 3.2).

5.4.1 Poisson-gamma model

It is natural in this instance for $f(N_i, \boldsymbol{\theta})$ to be a continuous distribution, where N_i can take any non-negative value. The gamma distribution is a sensible choice, since the Poisson-gamma mixture is well known to produce a negative-binomial distribution, as shown below. Here we explore the gamma distribution with shape parameter α and rate parameter β. The likelihood for site i and visit j will be based upon

$$\Pr(Y = y_{i,j}) = \int_0^\infty \frac{e^{-a_{i,j}N_i}(a_{i,j}N_i)^{y_{i,j}}}{y_{i,j}!} \frac{\beta^\alpha}{\Gamma(\alpha)} N_i^{\alpha-1} e^{-\beta N_i} \, \mathrm{d}N_i,$$

which simplifies to

$$\Pr(Y = y_{i,j}) = \binom{y_{i,j} + \alpha - 1}{y_{i,j}} \left(\frac{a_{i,j}}{a_{i,j} + \beta}\right)^{y} \left(\frac{\beta}{a_{i,j} + \beta}\right)^{\alpha}.$$

Hence, a Poisson-gamma mixture where the Poisson expectation is the scalar product, $a_{i,j}N_i$, is a negative-binomial distribution as in expression (5.3), parameterised by $r = \alpha$ and $p = \frac{a_{i,j}}{a_{i,j}+\beta}$.

Consequently, the likelihood over S sites and T visits for the Poisson-gamma model is

$$\mathrm{L}(\boldsymbol{\eta}, \alpha, \beta; \boldsymbol{y}) = \prod_{i=1}^{S} \prod_{j=1}^{T} \binom{y_{i,j} + \alpha - 1}{y_{i,j}} \left(\frac{a_{i,j}}{a_{i,j} + \beta}\right)^{y_{i,j}} \left(\frac{\beta}{a_{i,j} + \beta}\right)^{\alpha}, \quad (5.13)$$

where $\boldsymbol{\eta}$ is the set of parameters associated with $\{a_{i,j}\}$. Incorporating the hierarchical aspect into the model increases the number of parameters relative to the GAI, by the addition of parameters for the gamma distribution.

We note the similarity of the Poisson-gamma likelihood in (5.13) with the negative-binomial likelihood in (5.4), but with an absence of $\{N_i\}$. Whereas in (5.4) the expectation is $N_i a_{i,j}$, the expectation of the Poisson-gamma model is $\frac{\alpha}{\beta} a_{i,j}$, which corresponds to the product of $a_{i,j}$ and the expectation of the gamma distribution for N_i. Moreover, in (5.13), the dispersion parameter r in (5.4) is replaced by α. Overdispersion is accounted for in two different ways: in (5.4) via r, and in (5.13) only via the gamma distribution for N_i.

The conditional probability density of N_i is derived by Bayes theorem as

$$\begin{aligned} f_{N_i}(n_i | y_{i,j}, a_{i,j}, \alpha, \beta) &= \frac{\Pr(y_{i,j} | n_i, a_{i,j}) f(n_i | \alpha, \beta)}{\int \Pr(y_{i,j} | n_i, a_{i,j}) f(n_i | \alpha, \beta) \mathrm{d}n_i} \\ &\propto \Pr(y_{i,j} | n_i, a_{i,j}) \Pr(n_i | \alpha, \beta) \\ &\propto n_i^{y_{i,j}+\alpha-1} e^{-(a_{i,j}+\beta)n_i}, \end{aligned}$$

which is a gamma distribution with shape parameter $y_{i,j} + \alpha$ and rate parameter $a_{i,j} + \beta$. Hence

$$\mathbb{E}(N_i) = \frac{y_{i,j} + \alpha}{a_{i,j} + \beta},$$

and, averaging over j, we can estimate each N_i by

$$\mathbb{E}(N_i) = \frac{y_{i,\cdot} + \alpha}{a_{i,\cdot} + \beta}. \tag{5.14}$$

This expression generalises the expression of (5.2), and as $\alpha, \beta \to 0$, keeping the ratio constant results in (5.2).

In other scenarios, a discrete distribution for N_i may be more appropriate. For example in Royle (2004a) and Chapter 3, the Poisson and negative-binomial distributions are mixed with the Binomial distribution.

5.4.2 Negative-binomial-gamma model

As for the GAI in Section 5.2.2, the negative-binomial provides an alternative to the Poisson model. We again take the negative-binomial defined by (5.3), parameterised by the dispersion parameter r and expectation $Na_{i,j}$. The negative-binomial-gamma likelihood is

$$\mathrm{L}(\alpha, \beta, \boldsymbol{\eta}; \boldsymbol{y}) = \prod_{i=1}^{S} \prod_{j=1}^{T} \int_0^\infty \frac{\Gamma(r + y_{i,j})}{y_{i,j}!\Gamma(r)} \left(\frac{r}{r + a_{i,j}N}\right)^r \left(\frac{a_{i,j}N}{r + a_{i,j}N}\right)^{y_{i,j}} \times \frac{\beta^\alpha}{\Gamma(\alpha)} N^{\alpha-1} e^{-\beta N} \, \mathrm{d}N. \tag{5.15}$$

The integral in (5.15) does not have a simple solution as in the Poisson-gamma case, hence evaluation of the likelihood requires numerical integration. In `R`, we use the standard `integrate` function (with a tolerance of 10^{-4}). Due to this need for numerical integration, fitting the negative-binomial-gamma model is difficult and only limited results have been obtained. The negative-binomial-gamma model is also much more time-consuming to fit compared to the Poisson-gamma.

5.4.3 Comparison of the hierarchical model and GAI

For illustration we compare model performance for the P/N_2 GAI, the analogous hierarchical Poisson-gamma model, and the NB/N_2 GAI, for a sample of five bivoltine species for UKBMS data from 2010, although univoltine species or alternatives for $\{a_{i,j}\}$ could have also been taken. The following aspects of the model fitting apply also for later applications of the GAI in

this chapter, except where specified. Where a species has been observed at more than 100 sites within a given year (this is true of all five species except Small Blue which was observed at 41 sites per year on average), each model was fitted to a common random sample of 100 sites. Due to the mixture model aspect of the bivoltine phenomenological models, different starting values for the parameters could yield different local maxima (Matechou et al. 2014; McLachlan and Peel 2004), therefore each model was run from five random starting values and in each case results are only presented for the fitted model with the highest likelihood value. We let $\mu_2 = \mu_1 + \mu_d$, where $\mu_1, \mu_d \geq 0$ to ensure $\mu_2 \geq \mu_1$, and consider the homoscedastic case where $\sigma_1 = \sigma_2$. Despite possible spatial variation in seasonal pattern (for example as demonstrated for Common Blue in Section 4.2), since the focus here was on model comparison, all parameters in $\boldsymbol{\eta}$ were assumed to be constant (w, μ_1, μ_d and σ). This resulted in four, five and six model parameters for the P/N_2 GAI, NB/N_2 GAI and Poisson-gamma model, respectively.

The Poisson-gamma model has lower AIC values than the P/N_2 GAI for four out of the five species, but the NB/N_2 GAI consistently has AIC values that are the lowest (Table 5.2). Given that the models are applied to large, noisy data sets, there are often large differences in AIC as each model describes the data, particularly in terms of overdispersion, differently. The Poisson-gamma model is an intermediate option between the two GAIs: it allows for variation in $\{N_i\}$, whereas the NB/N_2 GAI estimates the appreciable additional variation in the raw data with respect to the Poisson.

Estimates of the four parameters associated with the mixture components show minimal differences between the three models. The associated standard errors are consistently smallest for the P/N_2 GAI, and are larger from the NB/N_2 GAI and Poisson-gamma model, which may be anticipated as a consequence of accounting for overdispersion. Estimates of the average abundance, $\hat{G}$, which were estimated by the expression in (5.9), are similar for the different methods, as well as the associated 95% confidence intervals, which were estimated via a bootstrapping approach (Section 5.2.5). For the hierarchical Poisson-gamma model, $\hat{G}$ could also be estimated simply by

$\hat{G} = \hat{\alpha}/\hat{\beta}$. Individually, comparison of the $\{\hat{N}_i\}$ from the P/N_2 GAI, estimated from (5.2), and from the Poisson-gamma model, derived from (5.14), also correspond well (Figure 5.1).

The computation times for the P/N_2 GAI are lower than for the hierarchical Poisson-gamma model and NB/N_2 GAI. Computation times for the NB/N_2 GAI are longer than for the Poisson case due to the iterative concentrated likelihood approach (Section 5.2.2). The differences in computation time for the hierarchical model compared to the GAIs would be more significant for the negative-binomial-gamma models, which are not straightforward to fit, as discussed in Section 5.4.2. We conclude that the GAI is preferable to the hierarchical models as it is simpler and more efficient, whilst producing similar results, and the negative-binomial GAI performs best. Consequently we focus on the GAI in the remainder of this chapter.

Table 5.2: Model comparison for a) the P/N_2 GAI, b) the hierarchical Poisson-gamma model and c) the NB/N_2 GAI. The computation time is given in seconds. $\hat{G}$ is the index of abundance from the expression of (5.9), with a 95% confidence interval estimated via bootstrapping. Parameter estimates are given with the associated standard errors in brackets.

	Species	Time	Log(L)	AIC	$\hat{G}$	$\hat{w}$	$\hat{\mu}_1$	$\hat{\mu}_d$	$\hat{\sigma}$
	Holly Blue	0.34	-2115	4238	21.8 (14.4, 32.9)	0.29 (0.011)	7.42 (0.107)	11.38 (0.123)	2.31 (0.042)
	Small Blue	0.31	-2263	4535	60.3 (47.5, 77.7)	0.77 (0.008)	5.24 (0.033)	7.74 (0.069)	1.57 (0.022)
a)	Wall Brown	0.39	-2532	5073	28.5 (23.4, 32.8)	0.36 (0.010)	7.25 (0.070)	10.84 (0.084)	1.86 (0.030)
	Small White	0.57	-4421	8850	73.5 (60.3, 87.9)	0.11 (0.004)	8.05 (0.121)	10.55 (0.123)	2.63 (0.028)
	Common Blue	0.37	-6925	13857	190.6 (138, 233.8)	0.25 (0.004)	6.10 (0.028)	8.94 (0.031)	1.67 (0.010)

	Species	Time	Log(L)	AIC	$\hat{G}$	$\hat{w}$	$\hat{\mu}_1$	$\hat{\mu}_d$	$\hat{\sigma}$	$\hat{\alpha}$	$\hat{\beta}$
	Holly Blue	4.61	-2113	4238	21.7 (14.3, 33.2)	0.31 (0.023)	7.40 (0.162)	11.50 (0.197)	2.37 (0.071)	0.28 (0.019)	0.014 (0.001)
	Small Blue	0.80	-1664	3340	61.7 (47.6, 78.7)	0.68 (0.049)	5.22 (0.071)	8.13 (0.136)	1.32 (0.038)	0.29 (0.024)	0.003 (5e-04)
b)	Wall Brown	1.25	-2175	4362	28.4 (23.3, 32.9)	0.36 (0.027)	7.44 (0.153)	10.68 (0.175)	2.05 (0.053)	0.29 (0.019)	0.011 (0.001)
	Small White	4.44	-3431	6874	73.9 (60.6, 88.2)	0.11 (0.009)	8.10 (0.179)	10.88 (0.195)	2.62 (0.060)	0.46 (0.023)	0.006 (4e-04)
	Common Blue	1.96	-3979	7969	192.7 (137.2, 233.3)	0.23 (0.019)	6.43 (0.112)	9.02 (0.128)	1.79 (0.038)	0.25 (0.011)	0.001 (1e-04)

	Species	Time	Log(L)	AIC	$\hat{G}$	$\hat{w}$	$\hat{\mu}_1$	$\hat{\mu}_d$	$\hat{\sigma}$	$\hat{r}$
	Holly Blue	2.51	-1826	3661	21.8 (14.4, 33.3)	0.27 (0.018)	6.90 (0.145)	11.62 (0.168)	2.22 (0.053)	0.81 (0.077)
	Small Blue	1.56	-1475	2961	60.5 (48.0, 78.3)	0.75 (0.021)	5.30 (0.079)	7.94 (0.135)	1.54 (0.040)	0.64 (0.057)
c)	Wall Brown	3.31	-1965	3940	28.6 (23.5, 32.8)	0.31 (0.020)	7.28 (0.117)	10.93 (0.141)	1.87 (0.039)	0.55 (0.042)
	Small White	3.22	-3144	6298	73.9 (60.4, 88.1)	0.12 (0.008)	8.24 (0.164)	10.72 (0.176)	2.62 (0.050)	0.88 (0.054)
	Common Blue	3.79	-3429	6869	192.6 (139.8, 237.5)	0.22 (0.012)	6.53 (0.082)	8.78 (0.096)	1.76 (0.026)	0.75 (0.042)

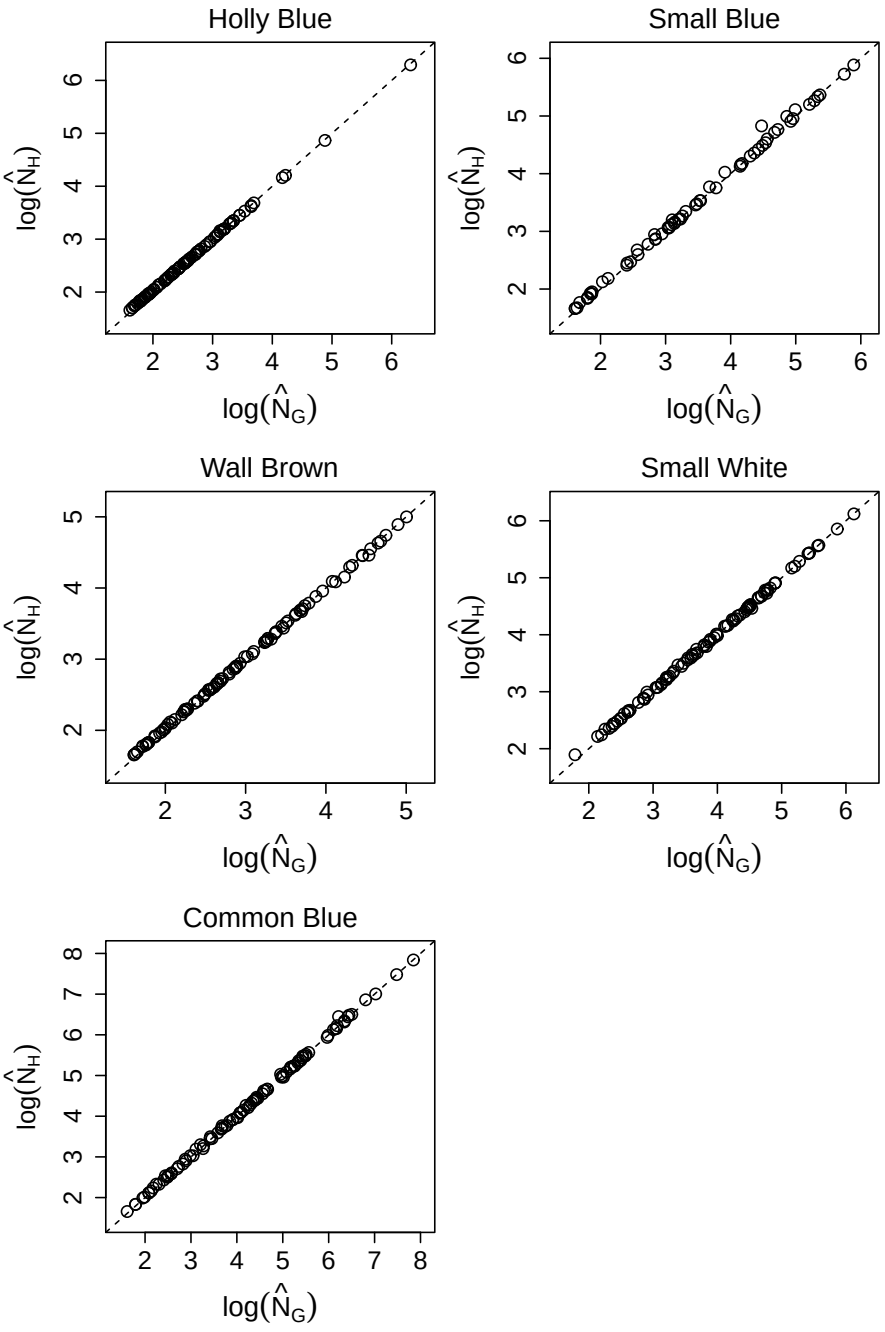

Figure 5.1: Comparison of estimated site parameters, $\hat{N}_G$, from the P/N_2 GAI and $\hat{N}_H$ from the hierarchical Poisson-gamma model. Both axes are displayed on the log scale and the dashed line indicates the 1-1 line.

5.5 Comparison of the SO_B and N_B GAIs

In the following section we compare the phenomenological and stopover GAI. The P/N_B GAI can be viewed as an approximation to the P/SO_B GAIs. In the stopover model, P/SO_1, assuming ϕ to be constant,

$$\lambda_{i,j} = N_{i,SO}(\alpha_{i,j} + \alpha_{i,j-1}\phi + \alpha_{i,j-2}\phi^2 + \cdots + \alpha_{i,0}\phi^{j-1}), \tag{5.16}$$

where $N_{i,SO}$ denotes the site parameter from the stopover model for a given site i, and for a given occasion, j, $\alpha_{i,j} = F(t_{i,j}) - F(t_{i,j}-1)$, where $F(t_{i,j}) = \Pr(X \leq t_{i,j})$, for $X \sim N(\mu_i, \sigma_i^2)$. Comparatively, for the P/N_1 GAI,

$$\lambda_{i,j} = N_{i,G}\alpha_{i,j}, \tag{5.17}$$

where $\{N_{i,G}\}$ are the site parameters for the phenomenological model and $\alpha_{i,j} = f(t_{i,j}) = \frac{1}{\sigma_i\sqrt{2\pi}}\exp\left\{-\frac{(t_{i,j}-\mu_i)^2}{2\sigma_i^2}\right\}$, from equation (5.11). Since the multiplier of $N_{i,SO}$ is greater than that for $N_{i,G}$, if we equate (5.16) and (5.17), then we find that

$$N_{i,G} > N_{i,SO}. \tag{5.18}$$

If we consider the sum of $\lambda_{i,j}$ over j, the coefficients of ϕ in the stopover model will sum approximately to unity as they form the area under a density. An approximate geometric sum for ϕ ($\phi < 1$) remains which will produce $1/(1-\phi)$. This suggests that the site estimates will differ between the two models by a scaling factor of approximately $1 - \phi$.

Similar theory applies for the $B = 2$ case, and the x/N_B GAI will similarly approximate the x/SO_B GAI for alternative distributions to the Poisson.

5.5.1 Simulation study

In Matechou et al. (2014) the stopover model was shown to perform well for data simulated from the stopover model. In this section we consider how the stopover might perform if data are simulated under a different scenario. In particular we simulated data from the P/N_B GAI, for $B = 1, 2$, and then compare the model fit from the P/SO_B and P/N_B GAI.

For $B = 1, 2$, we simulated 100 datasets for $T = 26$ and varying numbers of sites and proportions, c, of missing counts. Based upon reasonable values that might be applicable for data for a real species, we set $\mu = 10$, $\sigma = 2.5$, and for the bivoltine case $w = 0.6$, $\mu_d = 8$ and assumed the same variances for the two broods such that $\sigma_1 = \sigma_2 = 2.5$. The N_i for each site was drawn from a Poisson distribution with an expectation of 150. The $\mathrm{P/N}_B$ GAI has two and four parameters for the univoltine and bivoltine case, respectively, and in each case the corresponding $\mathrm{P/SO}_B$ has one additional parameter, ϕ.

Typically the $\mathrm{P/N}_1$ GAI produces accurate parameter estimates, with increasing precision for more sites and/or fewer missing counts (Table 5.3). Despite being different from the simulated model, fitting the $\mathrm{P/SO}_1$ produces reasonable parameter estimates. As expected given the results of (5.18), the estimates of G, which are the average of $\{\hat{N}_i\}$, are lower from the stopover model by a factor of roughly $1 - \hat{\phi}$, as discussed in Section 5.5.

Estimates of μ are earlier from the stopover model, which could be anticipated since μ in the stopover model represents the mean date of emergence of individuals into the population, whereas the corresponding parameter in the phenomenological model represents the mean flight date, consisting of both individuals that have entered the population and those that have survived from previous weeks. Estimates of σ are consistently smaller for the $\mathrm{SO/N}_2$ GAI. In this case σ represents the length of the emergence period, whereas in the phenomenological model σ describes the length of the flight period. Estimates of ϕ are relatively close to zero, which suggests that the stopover model tries to estimate the underlying phenomenological model, given that the two models are approximately the same when survival probability is zero.

Accuracy and precision of the parameter estimates improves with increasing S, but the effect of c is less apparent. Similar conclusions can be made for the $B = 2$ case (Table 5.4). Note that the root-mean-square error (RMSE) could not be calculated for $\hat{\phi}$ because a true value of ϕ does not exist, given that the data were simulated from the phenomenological model.

Fitting the stopover model to data generated by the phenomenological model produces biased and imprecise estimates of G, and small estimates of survival probability, which in some scenarios could be credible. Hence stopover models should only be used when there is confidence that it is the correct model.

Table 5.3: Summary of simulation output from fitting a) P/SO_1 and b) P/N_1 GAIs. S is the number of sites and c is the proportion of missing counts. We denote the mean estimate of a parameter by $\hat{}$ and SE and RMSE are the associated standard error and root-mean-square error, respectively.

	S	c	$\hat{G}$	SE	RMSE	$\hat{\mu}$	SE	RMSE	$\hat{\sigma}$	SE	RMSE	$\hat{\phi}$	SE
	20	0.0	136.5	1.75	22.02	9.37	0.017	0.65	2.45	0.006	0.08	0.10	0.012
	50	0.0	136.8	1.31	18.55	9.40	0.011	0.61	2.45	0.003	0.06	0.08	0.009
	100	0.0	140.5	1.15	14.89	9.43	0.010	0.58	2.47	0.003	0.04	0.06	0.008
	20	0.3	134.6	1.85	33.95	9.36	0.017	0.94	2.44	0.006	0.12	0.11	0.012
a)	50	0.3	138.1	1.40	25.96	9.40	0.012	0.87	2.45	0.004	0.08	0.08	0.009
	100	0.3	141.0	1.08	19.89	9.43	0.009	0.82	2.47	0.003	0.06	0.06	0.007
	20	0.5	135.1	1.94	42.38	9.35	0.018	1.16	2.44	0.007	0.15	0.11	0.012
	50	0.5	137.0	1.50	34.36	9.39	0.013	1.08	2.45	0.004	0.11	0.09	0.010
	100	0.5	140.4	1.15	25.92	9.42	0.010	1.01	2.46	0.003	0.08	0.06	0.008
	20	0.0	151.8	0.31	3.56	10.00	0.004	0.04	2.50	0.003	0.08		
	50	0.0	149.3	0.17	1.78	10.00	0.003	0.03	2.50	0.002	0.06		
	100	0.0	150.0	0.11	1.08	10.00	0.002	0.02	2.50	0.001	0.04		
	20	0.3	150.7	0.35	5.08	10.00	0.005	0.07	2.50	0.004	0.12		
b)	50	0.3	150.1	0.20	2.89	10.00	0.003	0.05	2.50	0.002	0.08		
	100	0.3	150.2	0.13	1.81	10.00	0.002	0.03	2.50	0.002	0.06		
	20	0.5	151.8	0.41	7.74	10.00	0.006	0.10	2.50	0.004	0.15		
	50	0.5	149.9	0.23	3.91	10.00	0.004	0.06	2.50	0.002	0.11		
	100	0.5	150.0	0.14	2.48	10.00	0.002	0.04	2.50	0.002	0.08		

Table 5.4: Summary of simulation output from fitting a) P/SO_2 and b) P/N_2 GAIs. S is the number of sites and c is the proportion of missing counts. We denote the mean estimate of a parameter by $\hat{}$ and SE and RMSE are the associated standard error and root-mean-square error, respectively.

	S	c	$\hat{G}$	SE	RMSE	$\hat{w}$	SE	RMSE	$\hat{\mu_1}$	SE	RMSE	$\hat{\mu_d}$	SE	RMSE	$\hat{\sigma}$	SE	RMSE	$\hat{\phi}$	SE
	20	0.0	128.9	1.85	28.01	0.60	0.001	0.01	9.30	0.018	0.73	7.99	0.010	0.10	2.43	0.006	0.094	0.15	0.012
	50	0.0	130.7	1.54	24.64	0.60	0.001	0.01	9.35	0.015	0.67	7.99	0.007	0.07	2.44	0.004	0.072	0.13	0.010
	100	0.0	128.4	1.57	26.62	0.60	0.002	0.02	9.32	0.022	0.72	7.92	0.077	0.77	2.44	0.005	0.082	0.14	0.011
	20	0.3	126.7	2.00	43.46	0.60	0.004	0.06	9.28	0.034	1.12	7.96	0.043	0.60	2.42	0.007	0.151	0.15	0.013
a)	50	0.3	129.9	2.07	40.77	0.59	0.006	0.09	9.27	0.061	1.34	7.91	0.061	0.87	2.43	0.011	0.191	0.14	0.014
	100	0.3	128.7	1.77	39.15	0.60	0.004	0.05	9.31	0.029	1.06	7.89	0.087	1.23	2.44	0.006	0.128	0.14	0.012
	20	0.5	127.2	2.13	54.03	0.60	0.004	0.08	9.27	0.042	1.46	7.96	0.044	0.76	2.42	0.010	0.219	0.15	0.014
	50	0.5	128.6	2.11	52.06	0.59	0.006	0.10	9.27	0.057	1.60	7.92	0.058	1.01	2.42	0.011	0.237	0.15	0.014
	100	0.5	128.5	1.64	46.78	0.60	0.003	0.05	9.31	0.025	1.26	7.93	0.071	1.23	2.43	0.006	0.151	0.14	0.011
	20	0.0	151.6	0.22	2.68	0.60	0.001	0.01	9.99	0.007	0.07	8.00	0.010	0.10	2.50	0.004	0.037		
	50	0.0	149.5	0.18	1.82	0.60	0.001	0.01	10.01	0.004	0.04	7.99	0.007	0.07	2.50	0.003	0.027		
	100	0.0	150.0	0.13	1.32	0.59	0.006	0.06	10.03	0.029	0.29	7.92	0.076	0.77	2.52	0.023	0.230		
	20	0.3	149.7	0.33	4.71	0.60	0.001	0.02	10.00	0.008	0.11	7.99	0.011	0.16	2.50	0.004	0.060		
b)	50	0.3	151.3	0.27	4.29	0.60	0.001	0.01	10.00	0.005	0.07	7.99	0.008	0.11	2.50	0.003	0.040		
	100	0.3	150.0	0.14	1.98	0.60	0.004	0.06	10.01	0.020	0.29	7.97	0.054	0.77	2.51	0.016	0.231		
	20	0.5	150.3	0.36	6.21	0.60	0.001	0.02	10.00	0.009	0.15	8.00	0.012	0.21	2.50	0.005	0.088		
	50	0.5	150.9	0.27	4.91	0.60	0.001	0.01	10.00	0.006	0.11	8.00	0.008	0.14	2.50	0.003	0.054		
	100	0.5	150.0	0.16	2.74	0.60	0.003	0.06	10.01	0.017	0.29	7.98	0.044	0.77	2.51	0.013	0.233		

5.5.2 Comparison for UKBMS data

For illustration we now compare model performance for the P/N_2 and P/SO_2 GAIs for five bivoltine butterfly species from UKBMS data for 2010, as in Section 5.4.3. All parameters in $\boldsymbol{\eta}$ were again assumed to be constant, therefore there were four and five model parameters for the P/N_2 and P/SO_2 GAI, respectively, where ϕ is the additional parameter.

Figure 5.2 demonstrates empirically that the estimates of $\{N_i\}$ differ between the P/SO_2 and P/N_2 GAIs by a scaling factor of approximately $1-\phi$, as described in Section 5.5. The stopover model is generally favoured in terms of AIC and overdispersion (Table 5.5). We find similar differences in the parameters to those shown in the simulation study in Section 5.5.1. Estimates of μ_1 and μ_2 are again earlier for the P/SO_2 GAI than for the P/N_2 GAI, and estimates of σ, which are consistently greater for the P/N_2 GAI, for reasons described in Section 5.5.1. The parameter ϕ from the stopover model provides additional information compared to the P/N_2 GAI, but the stopover model takes an average of seven times longer to run. We revisit the stopover model in Section 5.6.3, where for the first time we fit the stopover model to data for multiple years.

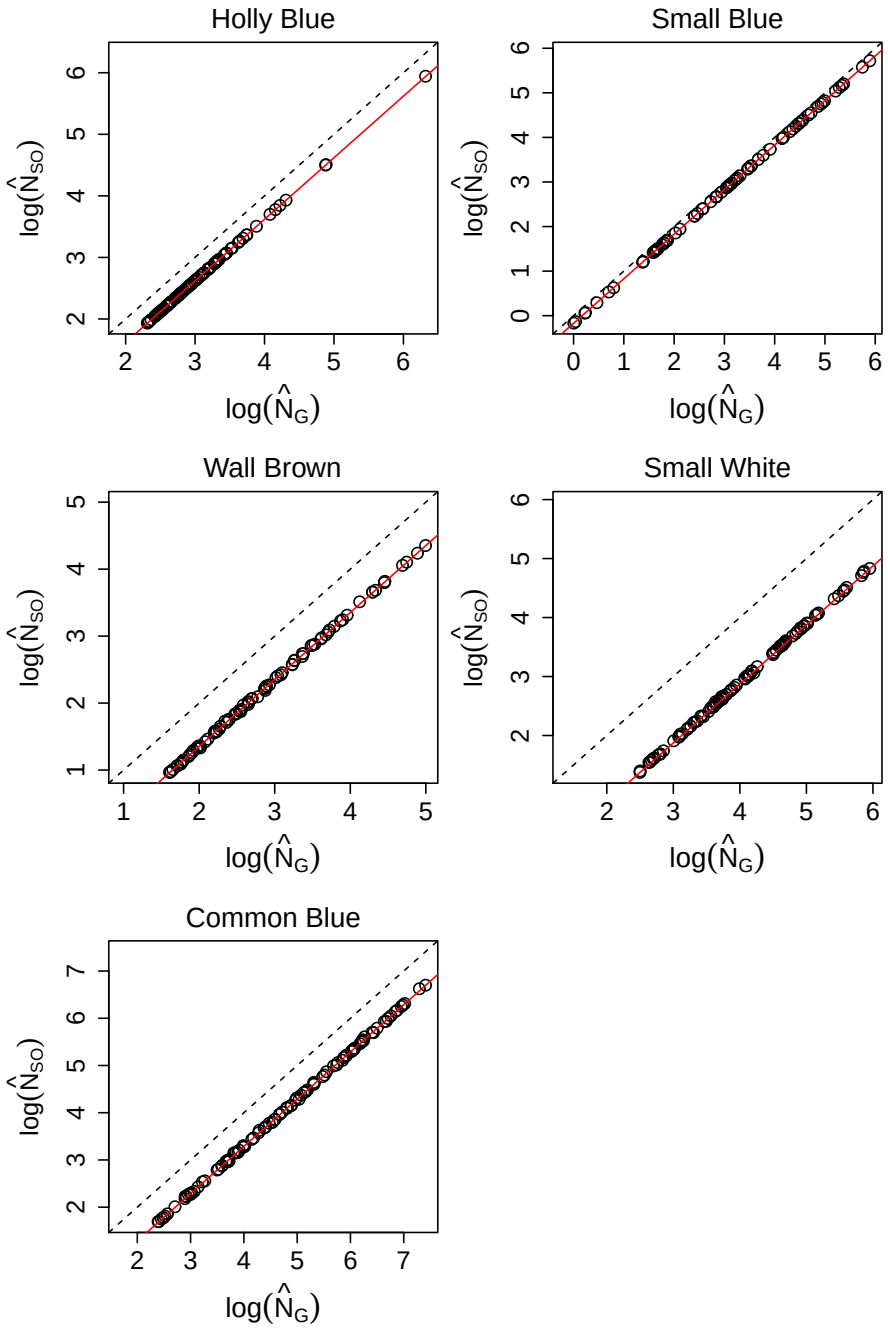

Figure 5.2: Comparison of estimated site parameters, $\hat{N}_G$ from the P/N_2 GAI and $\hat{N}_{SO}$ from the P/SO_2 GAI. Both axes are displayed on the log scale. The dashed line indicates the 1-1 line and the red line indicates the line with offset $\log(1-\hat{\phi})$.

Table 5.5: Parameter estimates from a) the P/SO_2 and b) the P/N_2 GAIs. The computation time is given in seconds. D is the dispersion estimate (residual deviance/degrees of freedom). Note that the results in b) were also presented in Table 5.2a.

a) P/SO_2 GAI													
Species	Time	Log(L)	AIC	$\hat{w}$		$\hat{\mu}_1$		$\hat{\mu}_d$		$\hat{\sigma}$		D	$\hat{\phi}$
Holly Blue	3.23	-2114.3	4238.6	0.287	(0.011)	6.372	(0.263)	11.379	(0.123)	2.102	(0.109)	1.325	0.376 (0.107)
Small Blue	2.72	-2262.6	4535.2	0.767	(0.008)	4.577	(0.117)	7.756	(0.070)	1.478	(0.054)	3.144	0.149 (0.087)
Wall Brown	3.62	-2500.3	5010.7	0.372	(0.010)	5.950	(0.085)	10.888	(0.080)	1.286	(0.051)	1.844	0.507 (0.021)
Small White	4.89	-4343.0	8696.1	0.120	(0.005)	6.205	(0.130)	10.286	(0.112)	1.825	(0.056)	3.005	0.653 (0.015)
Common Blue	3.28	-6677.3	13364.6	0.260	(0.004)	4.948	(0.032)	8.858	(0.029)	1.189	(0.019)	5.958	0.447 (0.009)
b) P/N_2 GAI													
Species	Time	Log(L)	AIC	$\hat{w}$		$\hat{\mu}_1$		$\hat{\mu}_d$		$\hat{\sigma}$		D	
Holly Blue	0.34	-2115.0	4238.0	0.286	(0.011)	7.424	(0.107)	11.382	(0.123)	2.308	(0.042)	1.325	
Small Blue	0.31	-2263.3	4534.6	0.766	(0.008)	5.242	(0.033)	7.743	(0.069)	1.573	(0.022)	3.142	
Wall Brown	0.39	-2532.3	5072.7	0.363	(0.010)	7.251	(0.070)	10.839	(0.084)	1.856	(0.030)	1.877	
Small White	0.57	-4421.1	8850.1	0.110	(0.004)	8.048	(0.121)	10.550	(0.123)	2.626	(0.028)	3.085	
Common Blue	0.37	-6924.6	13857.2	0.253	(0.004)	6.103	(0.028)	8.943	(0.031)	1.665	(0.010)	6.244	

5.6 Examples

To illustrate the range of modelling options, we now apply the GAI for a series of examples of butterfly transect counts from the UKBMS.

5.6.1 Splines

A spline is advised for species with complex seasonal flight patterns, which may not be modelled parametrically with ease. We demonstrate the P/S GAI, and make comparisons with output from a two-stage GAM (Section 4.1.3), for Speckled Wood, a multivoltine species whose flight pattern tends to exhibit three overlapping broods per year. The flight period may be further complicated since the Speckled Wood overwinters as both caterpillar and pupa, which may emerge at difference times. The models were fitted to data for a subset of 100 sites.

To formulate the B-spline basis matrix in the GAI, we use the `splines` package in `R` (R Core Team 2015). Six knots were used for this example, but other choices had minimal effect on the results. The optimal number of knots could be selected automatically, for example using cross validation as in GAM approaches. The Nelder-Mead algorithm in `optim` did not always optimise the likelihood for the P/S GAI, therefore the BFGS algorithm was used instead.

Comparable seasonal pattern curves are predicted from the GAM and P/S GAI (Figure 5.3), as well as similar relative indices of abundance (Figure 5.4), despite the simplicity and greater speed of fitting the GAI, compared to the GAM approach, which we demonstrate for the phenomenological GAI in the next section. In order to compare the GAI and GAM approaches, each index was standardised to have zero mean and unit variance. Confidence intervals were derived for each index via bootstrapping, using 100 replicates. Figure 5.3 shows confidence intervals that are slightly wider from the P/S GAI than the GAM, this may be because the GAI does not account for variation in sites between years, or the choice of spline may be modified, for example in terms of the number of knots used. In the next

section further comparisons of model accuracy will be made, based on the phenomenological GAI.

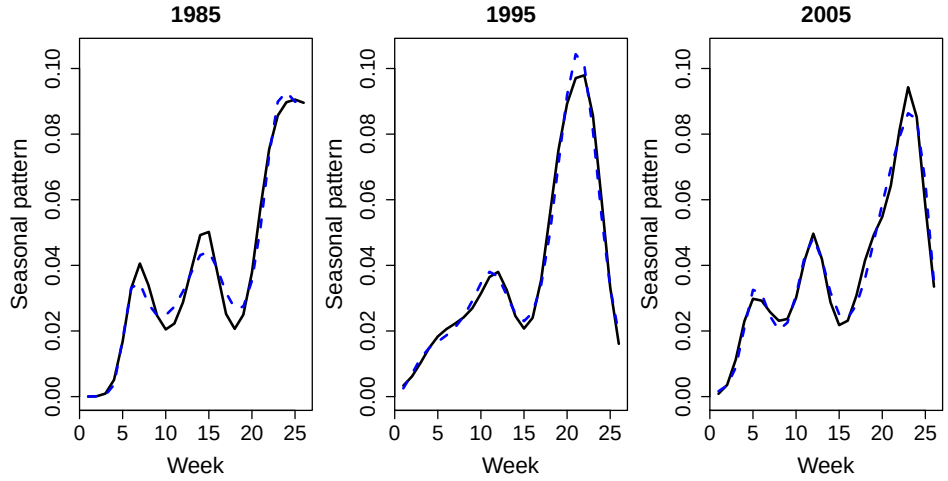

Figure 5.3: Predicted seasonal pattern for each week since the start of the season for the GAM approach (black solid) and P/S GAI (blue dashed) for Speckled Wood. The middle day for each week was taken for the GAM.

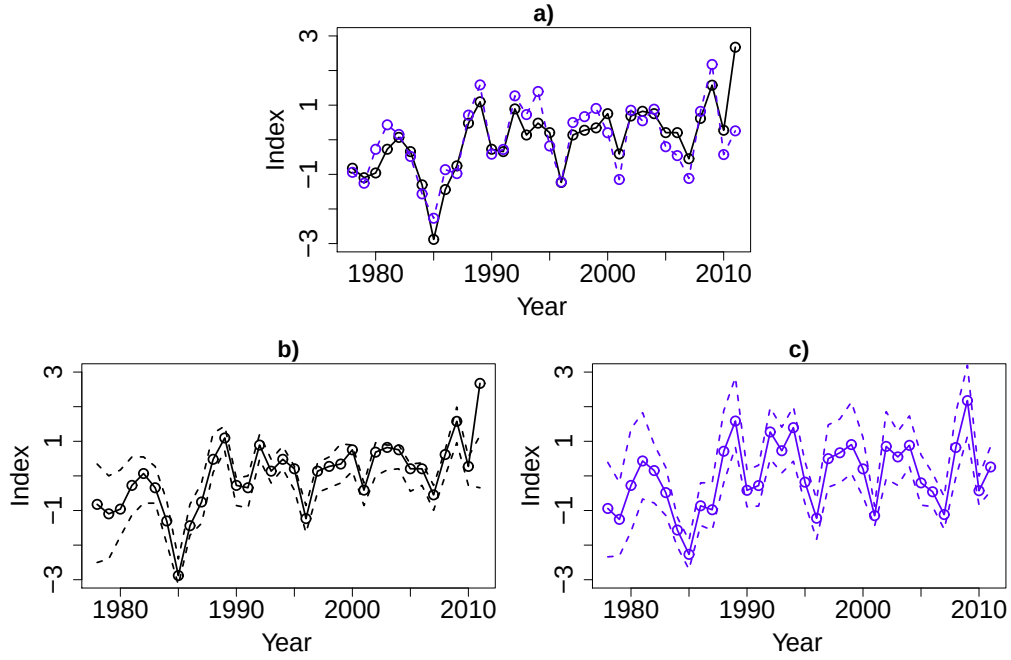

Figure 5.4: a) Relative abundance indices for the GAM approach (black solid) and P/S GAI (blue dashed) for Speckled Wood. Indices from a) are shown with associated bootstrapped intervals for the two-stage GAM and P/S GAI in b) and c), respectively.

5.6.2 Indices from the phenomenological model

We examine the performance of the x/N_2 GAI in producing indices of abundance for multiple years for five bivoltine UK butterfly species. For demonstration, we fit the model where x is Poisson, zero-inflated Poisson and negative-binomial for each species and make comparisons with the two-stage GAM approach (Section 4.1.3). For each species, each model was fitted to data for each year from 1978-2011 separately, and an index of abundance then formed as defined in Section 5.2.5. Confidence intervals were derived via bootstrapping, using 100 replicates. In order to compare the GAI and GAM approaches, each index was standardised to have zero mean and unit variance.

There were minimal differences in the indices derived from the P, ZIP and NB GAIs, but NB performed best in terms of AIC and dispersion, where dispersion values closer to unity indicate a better model (Figures 5.5 and 5.6). The latter is unavailable for ZIP since the deviance is not directly estimable for distributions not within the generalised linear model family. The indices of abundance from the GAM and NB/N_2 GAI show similar patterns (Figure 5.7). The greatest difference is for the Small Blue, particularly for earlier years in the index, which may be due to the lack of sites available for this habitat-specialist species, as described in Section 5.4.3.

The confidence intervals for the GAI are narrower than those for the GAM for three of the five species, and are never greatly wider (Table 5.6 and Figure 5.8). The GAI is substantially quicker than the GAM (Table 5.6).

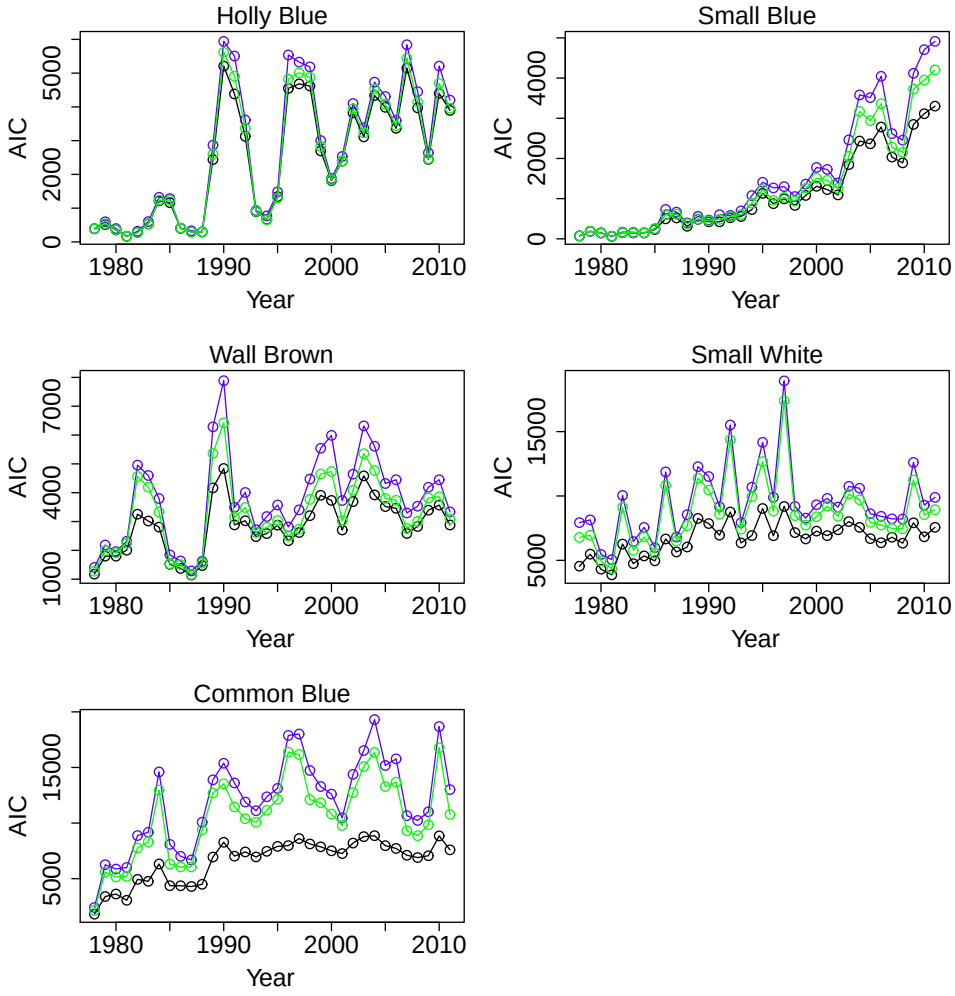

Figure 5.5: AIC values from the P/N_2 (blue), ZIP/N_2 (green) and NB/N_2 (black) GAIs.

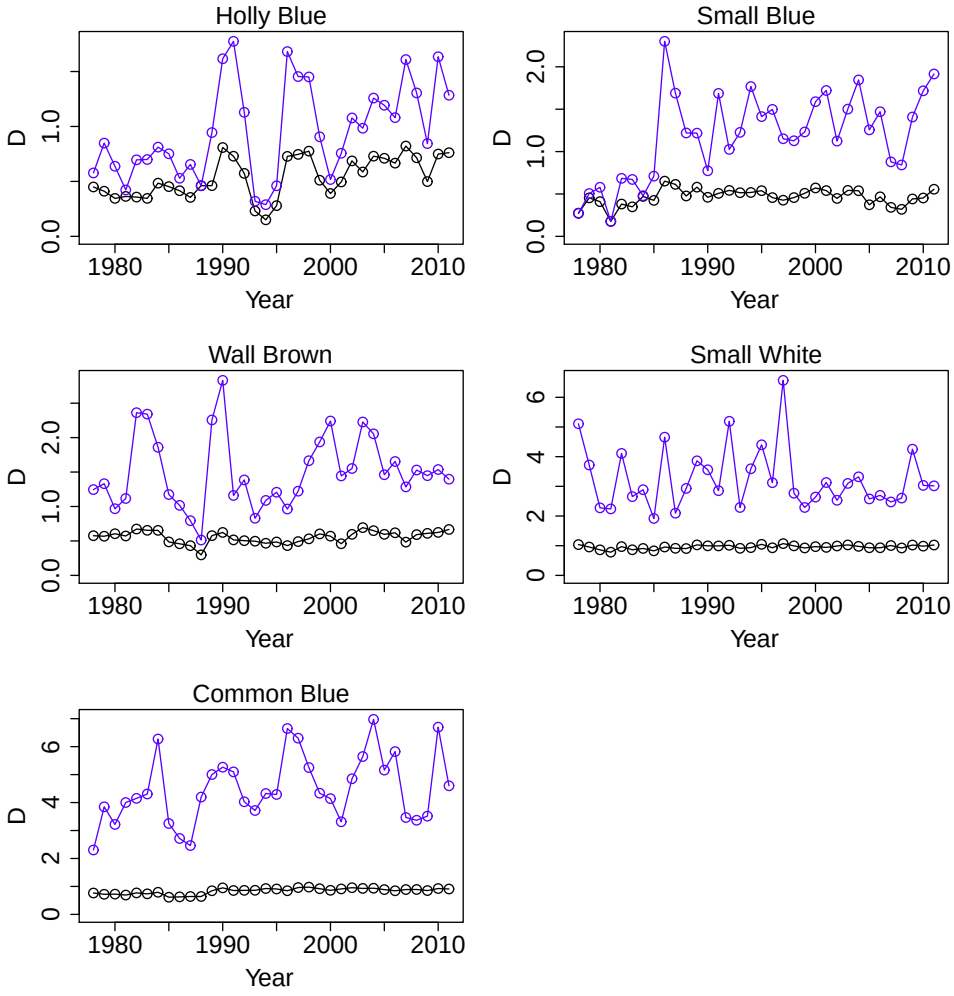

Figure 5.6: Dispersion values (residual deviance/degrees of freedom) from the P/N_2 (blue), and NB/N_2 (black) GAIs.

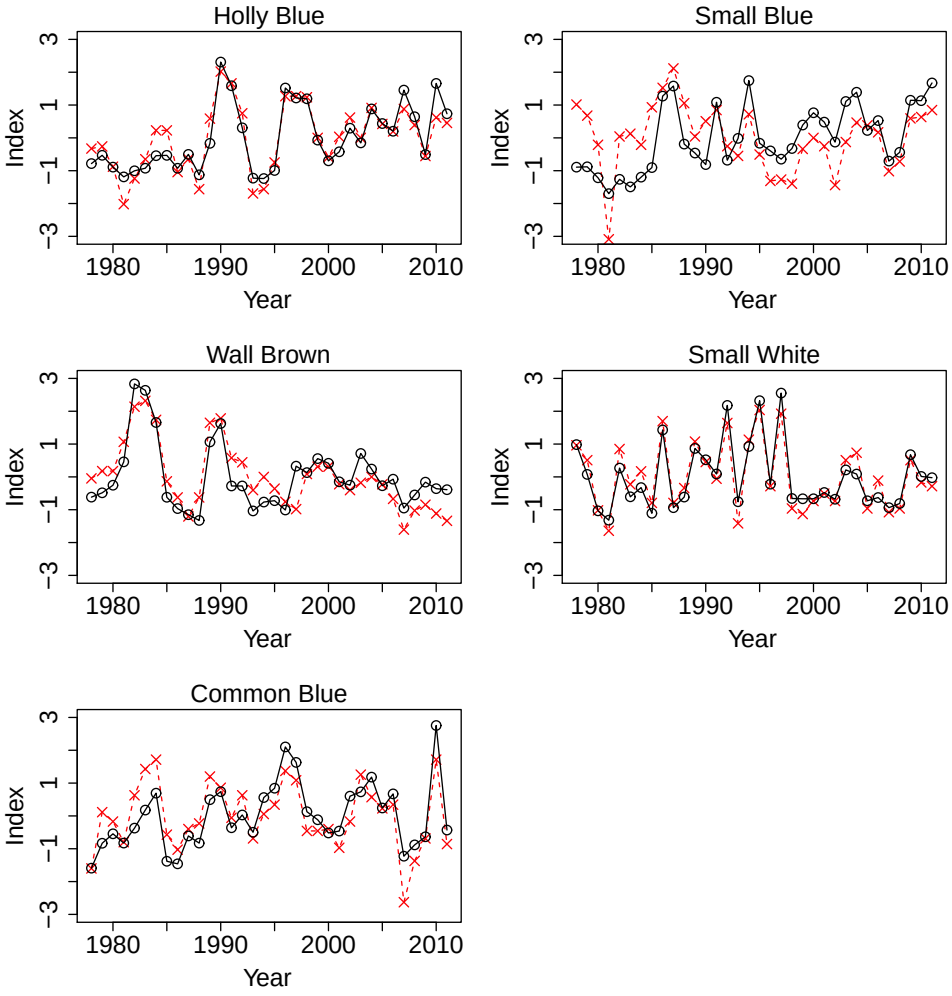

Figure 5.7: Relative abundances indices from the NB/N_2 GAI (black, solid line, circles) and two-stage GAM approach (red, dashed line, crosses).

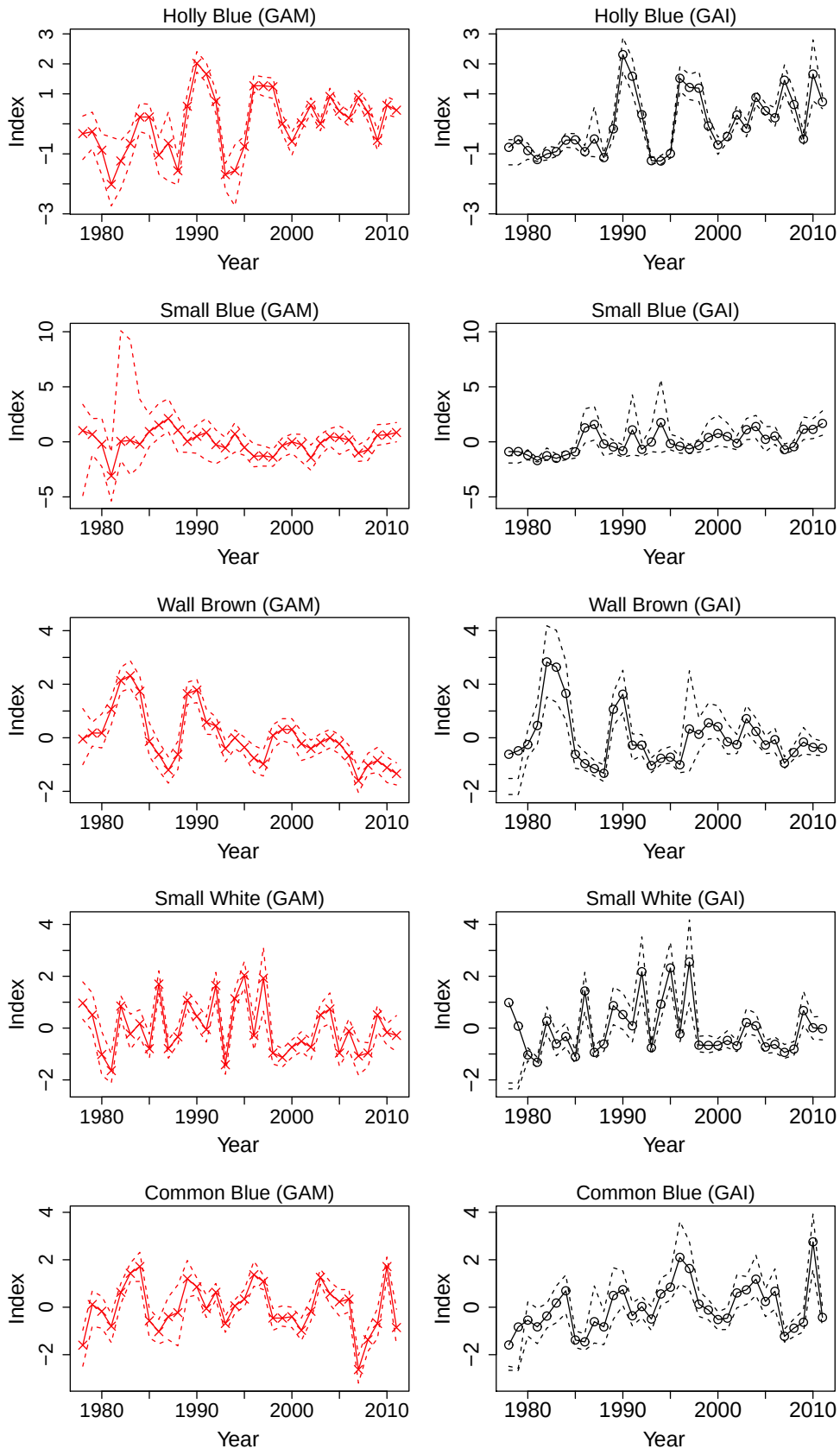

Figure 5.8: Comparison of indices with bootstrapped intervals derived from the two-stage GAM (red) and NB/N_2 GAI (black).

Table 5.6: Comparison of efficiency and accuracy for the GAM and P/N_2, ZIP/N_2 and NB/N_2 GAIs. Computation times are given in minutes.

Species	Time for a single run				Mean CI width			
	GAM	GAI			GAM	GAI		
		P	ZIP	NB		P	ZIP	NB
Holly Blue	9	0.3	3	1	0.862	0.664	0.703	0.627
Small Blue	32	0.2	2	1	3.091	1.892	1.949	1.871
Wall Brown	39	0.4	3	2	0.860	1.089	1.147	1.096
Small White	23	0.5	3	3	0.998	0.954	0.954	0.938
Common Blue	22	0.4	3	2	1.066	1.305	1.328	1.338

5.6.3 Stopover model

For illustration we apply the P/SO_1 GAI to data for two univoltine species to assess changes in survival probability ϕ over time. As discussed in Chapter 4, in Matechou et al. (2014) models were fitted where ϕ varied with time or age, but data were only considered for Common Blue in a single year. In this chapter only constant ϕ (within each year) is considered to look at variation over many years. In the absence of the concentrated likelihood approach fitting the stopover model to data for multiple years would have previously been more time-consuming.

The stopover model requires more data than the simpler phenomenological or spline models, and hence analysis was restricted to start from the first year where at least 30 sites were monitored. Figure 5.9 shows annual variation in predicted survival probability for the two species, but without obvious trends. In Figure 5.10 we see that higher estimates of survival are correlated with earlier emergence in the season, which generates an hypothesis for further investigation. In Chapter 6 we develop dynamic models for butterfly abundance, which includes further investigations of variation butterfly survival in Section 6.2.3.

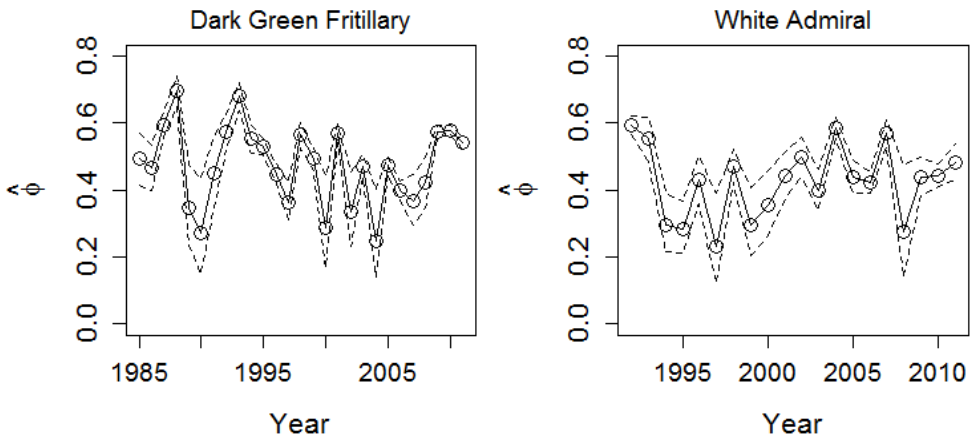

Figure 5.9: Predicted weekly survival probability, $\hat{\phi}$, from fitting a P/SO_1 GAI for two univoltine species.

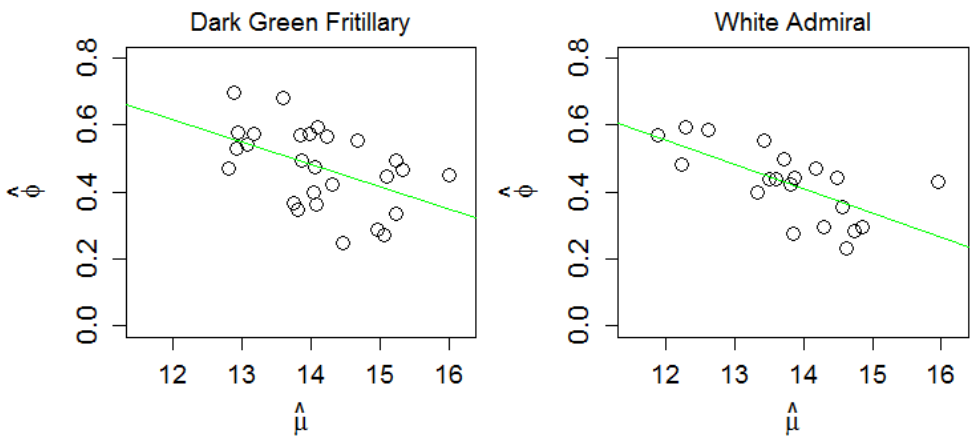

Figure 5.10: Average week of emergence, $\hat{\mu}$, versus weekly predicted survival probability, $\hat{\phi}$, from fitting a P/SO$_1$ GAI to data for two univoltine species. The green lines show the fitted linear trend, which was significant for both species ($p \leq 0.05$).

5.6.4 Regressing parameters on year and northing

In this section we demonstrate the flexibility of the GAI for the inclusion of covariates, which would not be as straightforward with previous modelling approaches. Rather than fitting the model separately to data for each year, a single concentrated likelihood can be maximised over multiple years. The number of parameters can be reduced by restricting appropriate parameters over time, for example to be constant or linearly time-varying.

For demonstration, we apply models to data for Wall Brown, which is one of the five bivoltine species considered in this chapter. We use the P/N$_2$ GAI, but now fit a single multi-year model. A similar approach could be undertaken for variations of the GAI, for example with the stopover model description for $\{a_{i,j}\}$, or with an alternative distribution to the Poisson, such as the negative-binomial which was favoured in Section 5.6.2. The parameters w, μ_1 and μ_d could vary linearly with year, or an additive or multiplicative combination of year and northing. We allowed the standard deviation σ to be constant or linearly varying with year but consider only the homoscedastic case where $\sigma_1 = \sigma_2$.

The most complex model, which had 14 parameters and included an interaction between northing and year for w, μ_1 and μ_d, was favoured in terms of AIC. The top five favoured models are given in Table 5.7, where the second most favoured model had 13 parameters, with no interaction between year and northing for μ_d.

Parameter estimates from the favoured model are given in Table 5.8, and the estimated seasonal pattern is provided for three years in Figure 5.11, each for a sample of northing values. The positive value of the slope for year for w suggests an overall trend for an increase in size of the first brood relative to the second brood over time (Table 5.8). The timing of the first brood is later further north, but has become earlier over time, and the difference in the timing of the two broods has increased over time. The standard deviation has changed minimally with time.

Table 5.7: Model comparison for the multi-year P/N_2 GAI for Wall Brown. The number of model parameters is denoted by np. AIC and ΔAIC are presented for the five most-favoured models, where ΔAIC is the difference between the AIC and the minimum AIC. year×north denotes that a parameter was described by year, northing, and their multiplicative interaction.

Model	np	AIC	ΔAIC
w(year×north)μ_1(year×north)μ_d(year×north)σ(year)	14	143831.3	-
w(year×north)μ_1(year×north)μ_d(year+north)σ(year)	13	143838.9	7.6
w(year×north)μ_1(year×north)μ_d(year)σ(year)	12	143845.8	14.5
w(year×north)μ_1(year×north)μ_d(year×north)σ(.)	13	143872.8	41.5
w(year×north)μ_1(year×north)μ_d(year+north)σ(.)	12	143879.1	47.8

Table 5.8: Parameter estimates for the most favoured (in terms of AIC) multi-year P/N_2 GAI for Wall Brown. Est and SE represent the parameter estimates and standard error, respectively. All covariates were standardised to have zero mean and unit variance. All estimates are on the log scale, except those relating to w which are on the logit scale. Interaction terms are indicated by $\times$.

Parameter	Est	SE
w(intercept)	-0.899	0.002
w(northing)	-0.027	0.002
w(year)	0.229	0.002
w(year$\times$northing)	-0.122	0.001
μ_1(intercept)	2.134	0.001
μ_1(northing)	0.059	0.002
μ_1(year)	-0.086	0.002
μ_1(year$\times$northing)	0.011	0.003
μ_d(intercept)	2.464	0.003
μ_d(northing)	-0.005	0.009
μ_d(year)	0.036	0.011
σ(intercept)	0.613	0.010
σ(year)	0.020	0.010

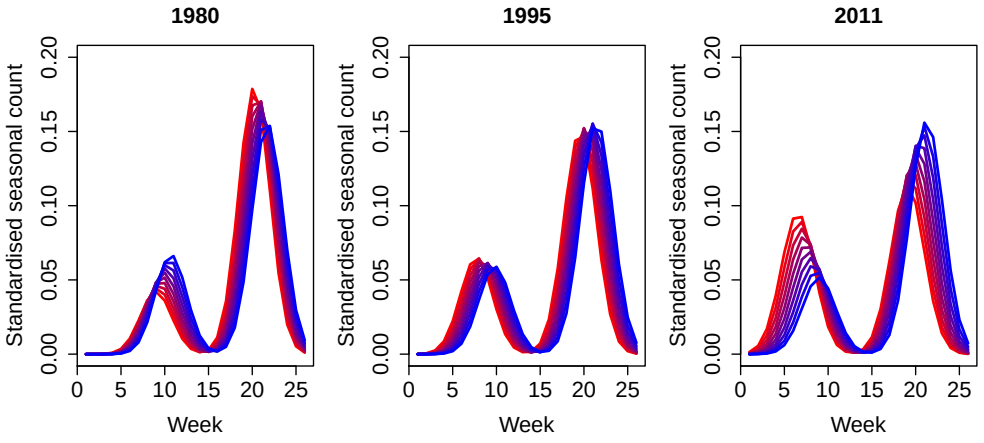

Figure 5.11: Predicted seasonal pattern (standardised seasonal count) for each week since the start of the season for the multi-year P/N_2 GAI (1980-2011) for Wall Brown for three years. Each line represents one of ten equally-spaced Northing values between 17 km (red) and 667 km (blue).

5.7 Discussion

This chapter has presented a generalised abundance index which unifies and extends exisiting methods for estimating abundance of seasonal insects. The GAI is suitably general for parametric or non-parametric functions to be chosen specific to the study species and scenario. Splines may be preferable for some species with complex flight periods, such as migrants. The newly proposed phenomenological model is a simplification of the stopover model. The stopover model provides additional insights via the estimates of survival. However, for wider-scale analysis, the phenomenological model is more efficient and akin to the GAM-based methods currently used for deriving abundance indices. The phenomenological model is also expected to be more robust than the stopover model which makes more assumptions, and the phenomenological model may also be more suitable in cases with limited data, since the stopover model has greater demands on data in order to estimate survival.

When spatio-temporal models are fitted to long-term data for many species and sites an important consideration is the computational effort required. Model fitting is very time-consuming for the GAM approach. When there are many sites, bootstrapping can take weeks for a single UKBMS species. Approaches for reducing the computation time from the GAM approach, such as those explored in Section 4.1.6, are unlikely to be matched by the substantial improvements in computation time made by the GAI. The efficiency of the GAI will reduce the time and resources required for data processing, leading to faster outputs and feedback of results to recorders and policy makers. The provision of feedback to recorders is essential for the motivation and retention of participants in citizen science projects, particularly schemes such as the UKBMS, which require high levels of commitment than opportunistic schemes such as the BNM (Chapter 2).

The GAM approach assumes the seasonal pattern to be static across sites within each year. Geographic variation could be incorporated in the smoothing component but that does not appear to be straightforward and

robust, particularly compared to the parametric approaches within the GAI which can readily incorporate available covariates, such as northing, land cover, weather or growing degree days (Hodgson et al. 2011). Novel description of spatial and temporal variation in seasonal pattern will benefit phenological studies, which for butterfly data have involved measures such as mean first appearance, mean peak appearance and mean length of the flight period (Roy and Sparks 2000; Karlsson 2014). Hodgson et al. (2011) utilised GAMs for studying spatio-temporal variation in phenology, but changes in phenology and voltinism can be studied more flexibly through the GAI, extending the capacity to study the non-uniform effects of climate change.

As demonstrated in Section 5.6.4, the GAI can also be applied to data across multiple years, which could be valuable for exploring phenological hypotheses. In Chapter 6, we build upon fitting models to data for multiple years by developing dynamic models which describe data from multiple years consecutively.

The GAM approach accounts for turnover in sites between years. This is not included in the GAI, but comparable results to the GAM are produced despite the simplicity of the model. Time variation in sites may need to be accounted for when there is a limited number of sites. Trends in relative abundance for individual sites can be estimated by the GAI, which may be of interest for conservation and monitoring of certain locations. For the GAM approach trends in abundance are assumed to be spatially constant, which may be an unrealistic assumption.

In this chapter the relative abundance parameters $\{N_i\}$ are confounded by imperfect detection. As discussed in Section 4.2.3, the study of UKBMS data is typically in terms of relative, rather than absolute, indices of abundance. As in Section 4.2.1 some variability in detection can be accounted for in the stopover model by incorporating a suitable covariate to separate detection probability p from $\{N_i\}$. In this chapter we did not explore the separation of abundance and detection probability, but further study in this area could be valuable to ascertain the effects of allowing variation in detectability.

The examples presented in this chapter demonstrate the generality of the GAI framework, and application of models other than GAMs to multiple years and species for the first time. In practice, wider model selection would be required in any application of the GAI. As for the stopover model, alternatives to the Normal distribution in the parametric approaches, such as asymmetric distributions to account for skewness in emergence are also possible. Clearly the "best" model choice will be dependent on both the purpose of the study and the species of interest.

The gains in efficiency achieved by the GAI arise from maximising a concentrated likelihood. The proposed iterative concentrated likelihood approach for negative-binomial and zero-inflated Poisson is effective and still considerably quicker than previous methods. The Poisson distribution may be sufficient if an index is the required output of a study, since it is quick with minimal differences in accuracy. Using random effects to describe $\{N_i\}$ is slower and less straightforward than the concentrated likelihood method, but could be valuable in particular modelling contexts. Random effects may also be more suitably incorporated within a Bayesian framework.

The GAI is a robust and flexible framework that can produce new insights relevant to the monitoring and conservation of invertebrates with both efficiency and accuracy. An `R` program for the GAI is provided as an electronic appendix to this thesis.

Chapter 6

Dynamic models

The methods for modelling butterfly abundance described in Chapters 4 and 5 do not impose any relationship between counts from one year to the next, which is the topic of this chapter. Causes of variation in both abundance and seasonal pattern from one year to the next are multi-faceted, relating to population numbers during the previous year, as well as other factors driving the unobserved stages of the life-cycle, such as weather. Building upon the GAI framework in the previous chapter, we now present models which provide succinct descriptions of longitudinal butterfly data across multiple sites from consecutive years. This approach produces, for the first time, estimates of the key parameters of brood productivities, which are included in a deterministic, auto-regressive manner, allowing the data from each year and/or brood to feed into those of the following year and/or brood.

We describe the formulation for these new dynamic models for univoltine and bivoltine species in Sections 6.1.1 and 6.1.2, respectively. In Section 6.1.3 we present a novel stopover model formulation, that differs from that of Section 4.2 and Chapter 5 of this thesis. As in Chapter 5, in Section 6.1.4 we develop a concentrated likelihood approach which results in appreciable efficiency gains. We provide formulae for deriving indices of abundance in Section 6.1.5. In the bivoltine case separate estimates of productivity for each brood results in new indices, which indicate the contributions from different generations. Both phenomenological and stopover

models are demonstrated using UKBMS data (Section 6.2). Comparisons are made with abundance indices generated from GAMs, and the incorporation of covariates is also explored. In Section 6.2.5 we make comparisons with the GAI approach from Chapter 5, and finally this chapter concludes with a discussion. This chapter is based upon a paper that is under review by the *Journal of Agricultural, Biological, and Environmental Statistics*.

6.1 Dynamic model formulation

For a given species, suppose counts of adults are recorded at S sites, each visited on T occasions, over Y years. As in Chapter 5, each count can be treated as the realisation of a random variable from a suitable discrete distribution. For example, if this is taken as Poisson, with expectation $\lambda_{i,j,k}$ for site i, visit j, and year k, the likelihood has the form

$$\mathrm{L}(\boldsymbol{\rho}, \boldsymbol{\eta}, \boldsymbol{N}_1; \boldsymbol{y}) = \prod_{i=1}^{S} \prod_{j=1}^{T} \prod_{k=1}^{Y} \frac{\exp(-\lambda_{i,j,k}) \lambda_{i,j,k}^{y_{i,j,k}}}{y_{i,j,k}!},$$

where $\{y_{i,j,k}\}$ are the counts and $\boldsymbol{\rho}$, $\boldsymbol{\eta}$, and $\boldsymbol{N}_1$, are the model parameters which we describe in the next sections, representing productivity, the set of parameters that describe seasonal variation in counts, and relative abundance in the first year, respectively. We adopt the Poisson distribution throughout this chapter, but there are other possibilities, such as the negative-binomial and zero-inflated Poisson, which were explored in the previous chapter and Chapter 3.

As in Section 5.2, but with an additional subscript for year, we write $\lambda_{i,j,k} = N_{i,k} a_{i,j,k}$, where $a_{i,j,k} = a_{i,k}(t_{i,j,k}, \boldsymbol{\eta})$, which denotes a function for describing the seasonal variation in counts, in terms of $\boldsymbol{\eta}$, where $t_{i,j,k}$ is the time of the jth visit to site i in year k (e.g. week number in the season). The methods of this chapter are applied to both a phenomenological model based on Normal probability density functions and stopover models which involve mechanisms allowing for estimation of survival.

6.1.1 Phenomenological model for univoltine species

For a univoltine species the counts within a season generally increase from zero and then decrease to zero corresponding to the emergence and death of adult butterflies over the season. Extending the univoltine phenomenological GAI, which is given in equation (5.11), to multiple years, this seasonal variation may be described by Normal probability density functions $\mathrm{N}(\mu_{i,k}, \sigma^2_{i,k})$, corresponding to site i and year k, so that for the jth visit at time $t_{i,j,k}$ we have

$$\lambda_{i,j,k} = N_{i,k} a_{i,j,k} = N_{i,k} \frac{1}{\sigma_{i,k}\sqrt{2\pi}} \exp\left\{ -\frac{(t_{i,j,k} - \mu_{i,k})^2}{2\sigma^2_{i,k}} \right\}, \tag{6.1}$$

where $N_{i,k}$ provides an estimate of relative abundance for site i in a given year, k.

In the GAI (Chapter 5), the models were mostly fitted separately to data for each year, and hence there was no linkage between the relative abundance estimates in different years. Even when the GAI is fitted as a single model in Section 5.6.4, the estimates of abundance are not linked, and only $\{a_{i,j,k}\}$ were regressed on year, to reduced the number of parameters. In contrast, here we allow the relative abundance $N_{i,k+1}$, for site i and year $k+1$, to depend upon the value at that site in the previous year, $N_{i,k}$, in a deterministic first-order autoregressive manner by a population growth rate, $\rho_{i,k}$ which, assuming the species does not overwinter as an adult, we define as "productivity", i.e. $N_{i,k+1} = \rho_{i,k} N_{i,k}$. Developing the recursion over time provides

$$\lambda_{i,j,1} = N_{i,1} a_{i,j,1} \tag{6.2a}$$

and

$$\lambda_{i,j,k} = N_{i,k} a_{i,j,k} = \left(N_{i,1} \prod_{m=1}^{k-1} \rho_{i,m} \right) a_{i,j,k}, \tag{6.2b}$$

which is similar to the model in Freeman and Newson (2008), but with a seasonal component. The productivities, $\{\rho_{i,m}\}$, describe the successes of a given generation over sites for each year and represent products of the number of eggs laid per adult and the probability of each egg reaching the

adult stage in the next generation. The expressions of equations (6.2a) and (6.2b) characterise the univoltine models of this chapter, with different formulations for the seasonal pattern, $\{a_{i,j,k}\}$, providing different models, as we shall see for a stopover model formulation in Section 6.1.3.

6.1.2 Phenomenological model for bivoltine species

We may extend the model above to describe counts from two annual broods by incorporating two Normal distributions as follows (where extra, final, subscripts designate brood):

$$\lambda_{i,j,k} = N_{i,k,1}\frac{1}{\sigma_{i,k,1}\sqrt{2\pi}}\exp\left\{-\frac{(t_j-\mu_{i,k,1})^2}{2\sigma^2_{i,k,1}}\right\} + N_{i,k,2}\frac{1}{\sigma_{i,k,2}\sqrt{2\pi}}\exp\left\{-\frac{(t_j-\mu_{i,k,2})^2}{2\sigma^2_{i,k,2}}\right\},$$

which we may write as

$$\lambda_{i,j,k} \equiv N_{i,k,1}a_{i,j,k,1} + N_{i,k,2}a_{i,j,k,2},$$

where at site i in year k the relative abundance for the first brood is given by $N_{i,k,1}$ and for the second brood by $N_{i,k,2}$.

Whereas in the GAI (Chapter 5) two broods are described by a mixture of probability density functions, here the relative abundance of a second brood in each year is assumed to depend on that of the first brood that year. Dependence between the two broods in any year is introduced by defining $N_{i,k,2} = \rho_{i,k,1}N_{i,k,1}$, in addition to the between-year dependence. So that we write

$$\begin{aligned}\lambda_{i,j,1} &= N_{i,1,1}a_{i,j,1,1} + N_{i,1,2}a_{i,j,1,2}\\ &= N_{i,1,1}a_{i,j,1,1} + \rho_{i,1,1}N_{i,1,1}a_{i,j,1,2}\\ &= N_{i,1,1}(a_{i,j,1,1} + \rho_{i,1,1}a_{i,j,1,2}),\end{aligned} \tag{6.3a}$$

and

$$\begin{aligned}\lambda_{i,j,k} &= N_{i,k,1}a_{i,j,k,1} + N_{i,k,2}a_{i,j,k,2} \\ &= \left(N_{i,1,1}\prod_{m=1}^{k-1}\prod_{b=1}^{2}\rho_{i,m,b}\right)a_{i,j,k,1} + \left(N_{i,1,1}\rho_{i,k,1}\prod_{m=1}^{k-1}\prod_{b=1}^{2}\rho_{i,m,b}\right)a_{i,j,k,2} \\ &= N_{i,1,1}\left(a_{i,j,k,1} + \rho_{i,k,1}a_{i,j,k,2}\right)\prod_{m=1}^{k-1}\prod_{b=1}^{2}\rho_{i,m,b}, \qquad (6.3b)\end{aligned}$$

where $\rho_{i,k,1}$ represents the productivity of the first brood in a given year k, and correspondingly $\rho_{i,k,2}$ represents the productivity of the second brood, which feeds into the abundance of the first brood of the following year, $N_{i,k+1,1}$. Thus the new development for bivoltine species is naturally based on the fact that the relative size of a given brood depends on the productivity of the previous brood, including within each year. In this chapter we denote the phenomenological models by N_B, where B is the number of broods.

6.1.3 Stopover models

An attraction of a stopover model is that it incorporates adult survival. The dynamic models in this chapter which incorporate a stopover model formulation use a new approach for describing data for species with multiple broods, and hence the formulation in this case is novel, and differs from that of Section 4.2 and Chapter 5 of this thesis.

As described in Section 4.2.1, the previous methods consider a site abundance $N_{i,k}$ in year k, referred to as a super-population by Matechou et al. (2014), which is distributed across multiple broods by a mixture of B normal distributions, each with a relative weight, $w_{i,k,b}$. Hence the expected number of individuals at site i at time $t_{i,j,k}$ in year k is given by

$$\lambda_{i,j,k} = N_{i,k}\left\{\sum_{d=1}^{j}\beta_{i,d-1,k}\left(\prod_{m=d}^{j-1}\phi_{i,m,k}\right)\right\},$$

and the proportion of $N_{i,k}$ arriving at time $t_{i,d,k}$ is modelled by setting

$$\beta_{i,d-1,k} = \sum_{b=1}^{B} w_{i,k,b}\left\{F_{i,k,b}(t_{i,d,k}) - F_{i,k,b}(t_{i,d,k}-1)\right\}, \qquad (6.4)$$

where $F_{i,k,b}(t_{i,d,k}) = P(X \leq t_{i,d,k})$ when $X \sim N(\mu_{i,k,b}, \sigma^2_{i,k,b})$. In this typical stopover model formulation the mixture of equation (6.4) is used to describe multiple brood sizes.

In the univoltine dynamic stopover model, $B = 1$, and $w_{i,k,1} = 1$, and the recursion of equations (6.2a) and (6.2b) applies, but now with a different specification of $\{a_{i,j,k}\}$. For the bivoltine case in the dynamic stopover model we assign a separate site abundance to each brood in a year, as for the bivoltine phenomenological model in Section 6.1.2. Thus we assume the two broods for bivoltine species to be separate such that, for site i, visit j and brood b, in year k,

$$a_{i,j,k,b} = \sum_{d=1}^{j} \beta_{i,d-1,k,b} \left(\prod_{m=d}^{j-1} \phi_{i,d,k,b} \right), \tag{6.5}$$

where we define $\{\phi_{i,d,k,b}\}$ as the appropriate survival probabilities of an individual from one week to the next, which are now estimated separately for each brood. This was not considered in the original specification of the stopover model (Section 4.2 and Chapter 5). The parameters $\{\beta_{i,d-1,k,b}\}$ describe the proportions of $N_{i,k,b}$ arriving at visit d, and are modelled using Normal distributions, so that

$$\beta_{i,d-1,k,b} = F_{i,k,b}(t_{i,d,k}) - F_{i,k,b}(t_{i,d,k} - 1),$$

where $F_{i,k,b}(t_{i,d,k}) = \Pr(X \leq t_{i,d,k})$, for $X \sim N(\mu_{i,k,b}, \sigma^2_{i,k,b})$, and $\mu_{i,k,b}$ is now the appropriate mean date of emergence for brood b. The recursion of equations (6.3a) and (6.3b) then applies, with the new specification of $\{a_{i,j,k,b}\}$ from equation (6.5).

We specify the dynamic stopover model by SO_B, where B is the number of broods.

6.1.4 Concentrated likelihood

As for all of the models in this thesis, we fit the dynamic models by maximum likelihood. As in Chapter 5, the number of parameters in the likelihood maximisation can be reduced by S, using a concentrated likelihood approach as follows. S is typically large and so computational efficiency is

substantially increased. We consider first the univoltine case. Using equations (6.2a) and (6.2b), apart from an additive constant, the log-likelihood for site i may be written as

$$\ell_i = \mathrm{Log}(\mathrm{L}_i) = \sum_{j=1}^{T} \left[-N_{i,1}a_{i,j,1} + y_{i,j,1}\log\left(N_{i,1}a_{i,j,1}\right) + \sum_{k=2}^{Y} \left\{ -N_{i,1}a_{i,j,1} \prod_{m=1}^{k-1} \rho_{i,m} + y_{i,j,k}\log\left(N_{i,1}a_{i,j,k} \prod_{m=1}^{k-1} \rho_{i,m} \right) \right\} \right]. \tag{6.6}$$

For all data the log-likelihood is $\ell = \mathrm{Log}(\mathrm{L}) = \sum_{i=1}^{S} \ell_i$. Using equation (6.6) we obtain

$$\frac{\partial \ell_i}{\partial N_{i,1}} = \sum_{j=1}^{T} \left\{ -a_{i,j,1} + \frac{y_{i,j,1}}{N_{i,1}} + \sum_{k=2}^{Y} \left(-a_{i,j,1} \prod_{m=1}^{k-1} \rho_{i,m} + \frac{y_{i,j,k}}{N_{i,1}} \right) \right\},$$

and equating to zero we find

$$N_{i,1} = \sum_{j=1}^{T} \frac{\sum_{k=1}^{Y} y_{i,j,k}}{a_{i,j,1} + \sum_{k=2}^{Y} a_{i,j,k} \prod_{m=1}^{k-1} \rho_{i,m}}. \tag{6.7}$$

Thus despite an apparent strong dependence of $\{N_{i,k}\}$ on $\{N_{i,1}\}$ in equation (6.2b), this is only a consequence of the deterministic links between each $N_{i,k}$, and all data contribute to the estimation of $\{N_{i,1}\}$, and hence $\{N_{i,k}\}$. Substitution of the expressions for $\{N_{i,1}\}$ from (6.7) in (6.6), results in a concentrated likelihood, which is maximised with respect to only the parameters associated with $\boldsymbol{\rho}$ and $\mathbf{a}$. Estimation of $\{N_{i,1}\}$ is made by substituting estimates of $\{a_{i,j,k}\}$ and $\{\rho_{i,m}\}$ into (6.7). The above approach holds for both phenomenological and stopover models.

The concentrated likelihood for the bivoltine case is given similarly as follows. Using equations (6.3a) and (6.3b), the log-likelihood for site i is

given, apart from an additive constant, by

$$\begin{aligned}\ell_i = \mathrm{Log}(\mathrm{L}_i) = \sum_{j=1}^{T} \Bigg\{ & - N_{i,1,1}\left(a_{i,j,1,1} + \rho_{i,1,1}a_{i,j,1,2}\right) \\ & + y_{i,j,1}\log\left\{N_{i,1,1}\left(a_{i,j,1,1} + \rho_{i,1,1}a_{i,j,1,2}\right)\right\} \\ & + \sum_{k=2}^{Y}\Bigg[-N_{i,1,1}\left(a_{i,j,k,1} + \rho_{i,k,1}a_{i,j,k,2}\right)\prod_{m=1}^{k-1}\prod_{b=1}^{2}\rho_{i,m,b} \\ & \quad + y_{i,j,k}\log\left\{N_{i,1,1}\left(a_{i,j,k,1} + \rho_{i,k,1}a_{i,j,k,2}\right)\prod_{m=1}^{k-1}\prod_{b=1}^{2}\rho_{i,m,b}\right\}\Bigg]\Bigg\},\end{aligned} \tag{6.8}$$

where we have defined $\{a_{i,j,k,b}\}$ and $\{\rho_{i,k,b}\}$, for site i, visit j and brood b, in year k in Section 6.1.2. This gives

$$\begin{aligned}\frac{\partial \ell_i}{\partial N_{i,1,1}} = \sum_{j=1}^{T}\Bigg[& - \left(a_{i,j,1,1} + \rho_{i,1,1}a_{i,j,1,2}\right) + \frac{y_{i,j,1}}{N_{i,1,1}} \\ & + \sum_{k=2}^{Y}\left\{- \left(a_{i,j,k,1} + \rho_{i,k,1}a_{i,j,k,2}\right)\prod_{m=1}^{k-1}\prod_{b=1}^{2}\rho_{i,m,b} + \frac{y_{i,j,k}}{N_{i,1,1}}\right\}\Bigg],\end{aligned}$$

and equating to zero we find

$$N_{i,1,1} = \sum_{j=1}^{T}\frac{\sum_{k=1}^{Y} y_{i,j,k}}{a_{i,j,1,1} + \rho_{i,j,1}a_{i,j,1,2} + \sum_{k=2}^{Y}\left\{\left(a_{i,j,k,1} + \rho_{i,m,1}a_{i,j,k,2}\right)\prod_{m=1}^{k-1}\prod_{b=1}^{2}\rho_{i,m,b}\right\}}. \tag{6.9}$$

We note how $N_{i,1,1}$ is a weighted sum over visits of totals at site i across years. As in the univoltine case, we substitute the expressions for $\{N_{i,1,1}\}$ from (6.9) into (6.8) and maximise the overall concentrated likelihood, ℓ, with respect to parameters associated with $\boldsymbol{\rho}$ and $\boldsymbol{a}$. Estimation of $\{N_{i,1,1}\}$ is obtained by substituting estimates of $\{a_{i,j,k,b}\}$ and $\{\rho_{i,k,b}\}$ into (6.9).

This concentrated likelihood approach applies for both the phenomenological and stopover models for bivoltine species, with variation only in the specification of $\{a_{i,j,k,b}\}$.

All applications of the dynamic models in this chapter were made using the above concentrated likelihood approach.

6.1.5 Annual index of abundance

The averages of the site abundance estimates, for each year k, are used to create an index of abundance for year k. For a univoltine species we set

$$G_k = \frac{1}{S}\sum_{i=1}^{S}\widehat{N}_{i,k} = \begin{cases} \dfrac{1}{S}\displaystyle\sum_{i=1}^{S}\widehat{N}_{i,1} & \text{if } k = 1 \\ \dfrac{1}{S}\displaystyle\sum_{i=1}^{S}\left(\widehat{N}_{i,1}\prod_{m=1}^{k-1}\widehat{\rho}_{i,m}\right) & \text{if } k > 1, \end{cases} \tag{6.10}$$

for $k = 1, \ldots, Y$, from equations (6.2a) and (6.2b). Similarly for the bivoltine case we estimate an index $G_{k,b}$ for each brood, $b = 1, 2$, as

$$G_{k,1} = \frac{1}{S}\sum_{i=1}^{S}\widehat{N}_{i,k,1} = \begin{cases} \dfrac{1}{S}\displaystyle\sum_{i=1}^{S}\widehat{N}_{i,1,1} & \text{if } k = 1 \\ \dfrac{1}{S}\displaystyle\sum_{i=1}^{S}\left(\widehat{N}_{i,1,1}\prod_{m=1}^{k-1}\prod_{b=1}^{2}\widehat{\rho}_{i,m,b}\right) & \text{if } k > 1, \end{cases} \tag{6.11}$$

and

$$G_{k,2} = \frac{1}{S}\sum_{i=1}^{S}\widehat{N}_{i,k,2} = \begin{cases} \dfrac{1}{S}\displaystyle\sum_{i=1}^{S}\widehat{N}_{i,1,1}\widehat{\rho}_{i,k,1} & \text{if } k = 1 \\ \dfrac{1}{S}\displaystyle\sum_{i=1}^{S}\left(\widehat{N}_{i,1,1}\widehat{\rho}_{i,k,1}\prod_{m=1}^{k-1}\prod_{b=1}^{2}\widehat{\rho}_{i,m,b}\right) & \text{if } k > 1, \end{cases} \tag{6.12}$$

for $k = 1, \ldots, Y$, making use of the recursions demonstrated in (6.3a) and (6.3b).

6.2 Application

We apply the dynamic models to UKBMS data for an illustrative subset of univoltine and bivoltine UK butterfly species. Each model was fitted to data for 1978-2011. Sites at which the species of interest was never recorded or at which monitoring was undertaken for fewer than five years were excluded from this analysis. As for the applications of the GAI in Chapter 5, a subset of 100 monitored sites was randomly selected for each species, with the exception of Holly Blue, which required samples of up to 200 sites to obtain reasonable estimates of productivity.

The concentrated likelihoods were maximised using the `optim` function in `R` (R Core Team 2015). Given the application to data across many years, the dynamic models in this chapter are more complicated than the GAI in Chapter 5, with more parameters to estimate. We found that the default Nelder-Mead algorithm in `optim` could not optimise the likelihood for the dyamic models, particularly for bivoltine species, and therefore the limited-memory BFGS algorithm (Byrd et al. 1995) was used instead. Associated `R` code for the dynamic models is provided as an electronic appendix to this thesis. Estimates of error for the abundance index can be obtained via bootstrapping, as for other methods (Sections 4.1.5 and 5.2.5), but error bars have not been presented in this chapter, for clarity of presentation.

We illustrate the performance of the dynamic models in terms of indices, productivity, survival and phenology, with and without the addition of covariates. Where parameters were assumed to be constant spatially the subscript for site, i, is omitted. We compare indices of abundance with those derived from the two-stage GAM approach (Section 4.1.3). Comparisons are also made later to the GAI approach (Chapter 5) in Section 6.2.5.

As in Chapter 5, note that in all models for bivoltine species, we let $\mu_2 = \mu_1 + \mu_d$, where $\mu_1, \mu_d \geq 0$, to ensure that $\mu_2 \geq \mu_1$.

The covariates we select are northing and temperature, and were selected to demonstrate the potential of the models, so that they may not be optimal. The average minimum daily temperature during October-March was used as a covariate for overwinter productivity. For bivoltine species, the mean temperature within the flight period of the first brood was used to describe productivity of the first brood. Productivities were regressed on the log scale. Survival in stopover models was logistically regressed on mean temperature within the flight period of the brood of interest. Approximate flight periods for the sample species are provided in Table 6.1, and were used for the relevant temperature covariates. We use monthly mean and minimum Central England Temperature data (Parker et al. 1992). All covariates were standardised to have zero mean and unit variance. Due to interest in

the possible effect of covariates on estimates of survival, we primarily use stopover models when covariates are employed and phenomenological models otherwise.

The phenomenological dynamic models discussed in the context of indices in Sections 6.2.1 and 6.2.2 have 35 and 71 parameters for $B = 1, 2$, respectively. Given that $Y = 34$, in the univoltine case there are 33 annual estimates of ρ_k, as well as estimates of μ and σ, and in the bivoltine case, there are 34 parameters for $\rho_{k,1}$ and 33 parameters for $\rho_{k,2}$, in addition to μ_1, μ_d, σ_1, and σ_2.

Table 6.1: Approximate flight periods for the sample of butterfly species studied, which are used for the relevant temperature covariates. The flight periods were specified as the first/last month for which the average weekly count was positive (> 0.1). For bivoltine species, we defined the mid point between the two generations by the month with the minimum weekly count between the two peaks in counts, and hence assumed the break between two generations to always be less than one month.

Species	Flight period
Chalkhill Blue	July-September
Small Skipper	June-September
Green Hairstreak	April-July
White Admiral	June-August
Gatekeeper	June-September
Marbled White	June-August
Wall Brown	April-July-September
Holly Blue	April-June-September
Small White	April-June-September
Brown Argus	April-July-September
Green-veined White	April-June-September

6.2.1 Indices

We compare relative abundance indices for model N_1 and the two-stage GAM approach (Section 4.1.3). As in the previous chapter, we use the GAM approach as a benchmark for comparison, since it is the method currently adopted by the UKBMS for most species. Estimates of abundance from the dynamic model are derived from estimates of annual productivity and estimates of initial abundance, as described in Section 6.1.5. In this section we allow productivity to vary with each brood and year, but μ and σ are considered as constant. Varying these parameters between years provides useful information and we shall see examples of this in Sections 6.2.4, but these parameters had no distinguishable effect on indices of abundance.

Figure 6.1a gives a comparison between annual indices of abundance for the six univoltine species. There is very good agreement between the indices resulting from the dynamic model and the two-stage GAM approach (Section 4.1.3). Dynamic models allow us to add more information to indices for bivoltine species, which we illustrate in Figures 6.2a and 6.3, where the same information is presented, but in two different ways. We can see how the dynamic model allows us to extend the indices produced by the GAM approach by providing separate indices for each brood.

6.2.2 Productivity

Figure 6.1b presents annual estimates of productivity for the illustrative univoltine species, from fitting model N_1 as in Section 6.2.1. Values of $\rho_{k,}$ greater than unity indicate years of growth compared to the previous year. Hence as anticipated we see a tendency for growth rates less than unity for species in decline, such as Small Skipper, while for Marbled White growth rates tend to be above unity during the initial period of growth, followed by fluctuations about unity in more recent years, when the population appears to be relatively stable.

Figure 6.2b presents estimated annual productivities for each brood for the bivoltine species, using model N_2 as fitted in Section 6.2.1. Values above

unity now represent growth relative to the previous brood. In Figure 6.4 we see how the productivities reflect the relative sizes of the fitted seasonal curves, for which the average over the series is shown. The relative sizes of the broods will actually vary with productivity each year.

Figure 6.5 shows the results of including covariates for these species, in this case for model SO_1 with $\rho_{i,k}$ and $\phi_{i,k}$ varying with temperature and northing, which we revisit in Section 6.2.3. It is interesting that with the exception of Gatekeeper, higher productivity is associated with cooler winters and in all cases with more Northerly latitudes.

Figure 6.6 shows the effect of adding covariates to the data for bivoltine species, in this case for model SO_2 with productivity varying with temperature and northing, and survival varying with temperature, which we discuss further in Section 6.2.3. Associations of first-brood productivity, $\rho_{i,k,1}$, with northing and weather varied between the five species, which may be associated with different species' traits. The association of higher productivity with cooler winters, which was shown for univoltine species in Figure 6.5, is also found for three of the five bivoltine species, with the primary exception of Holly Blue, which unlike the other species does not favour grasslands.

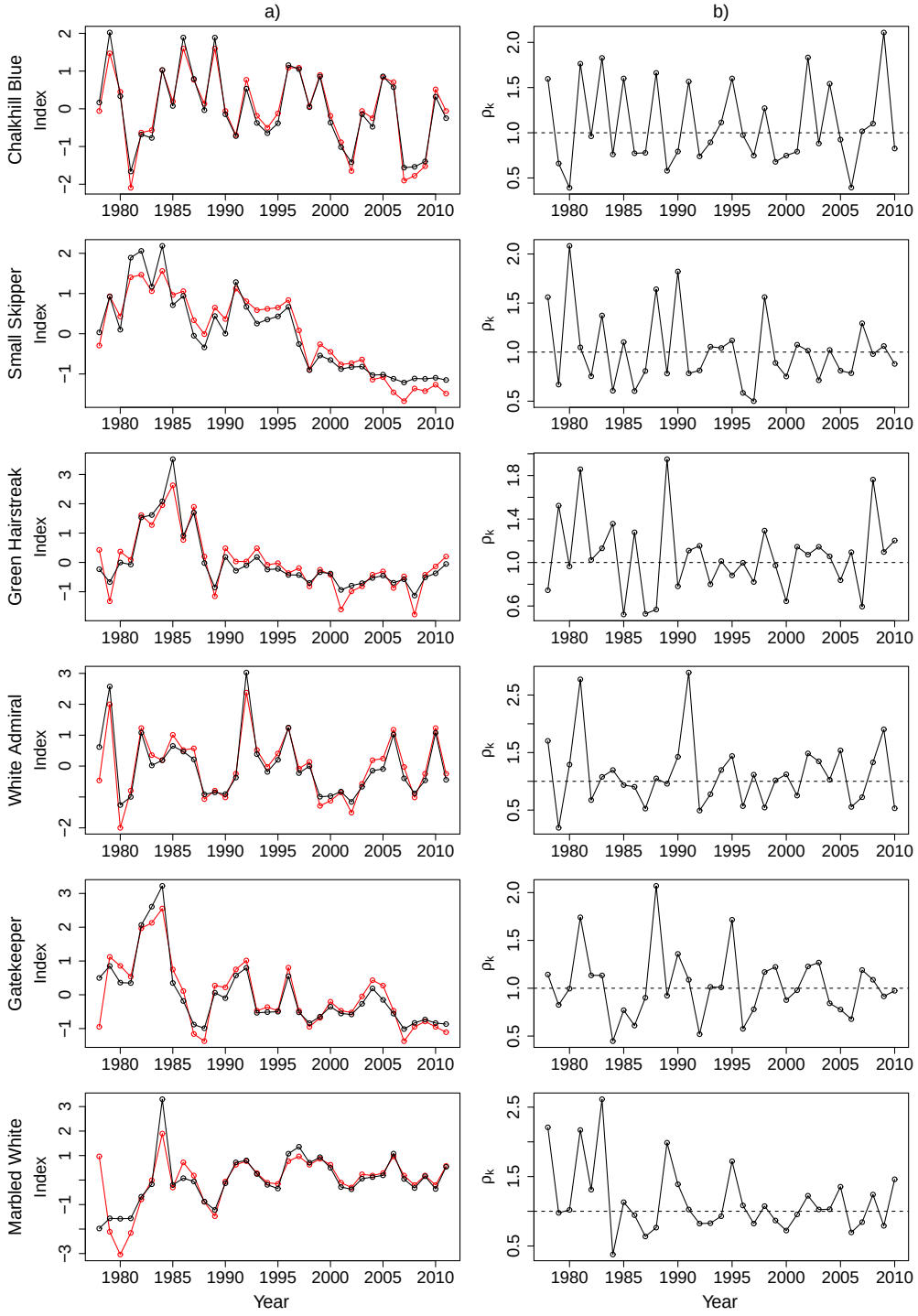

Figure 6.1: a) Relative abundance indices from model N_1 (black) and the GAM approach (red) and b) annual estimates of productivity, ρ_k, from model N_1, which was fitted to estimate ρ_k across sites for each year. The dashed line in b) separates productivities above/below unity, corresponding to growth/decline compared to the previous year.

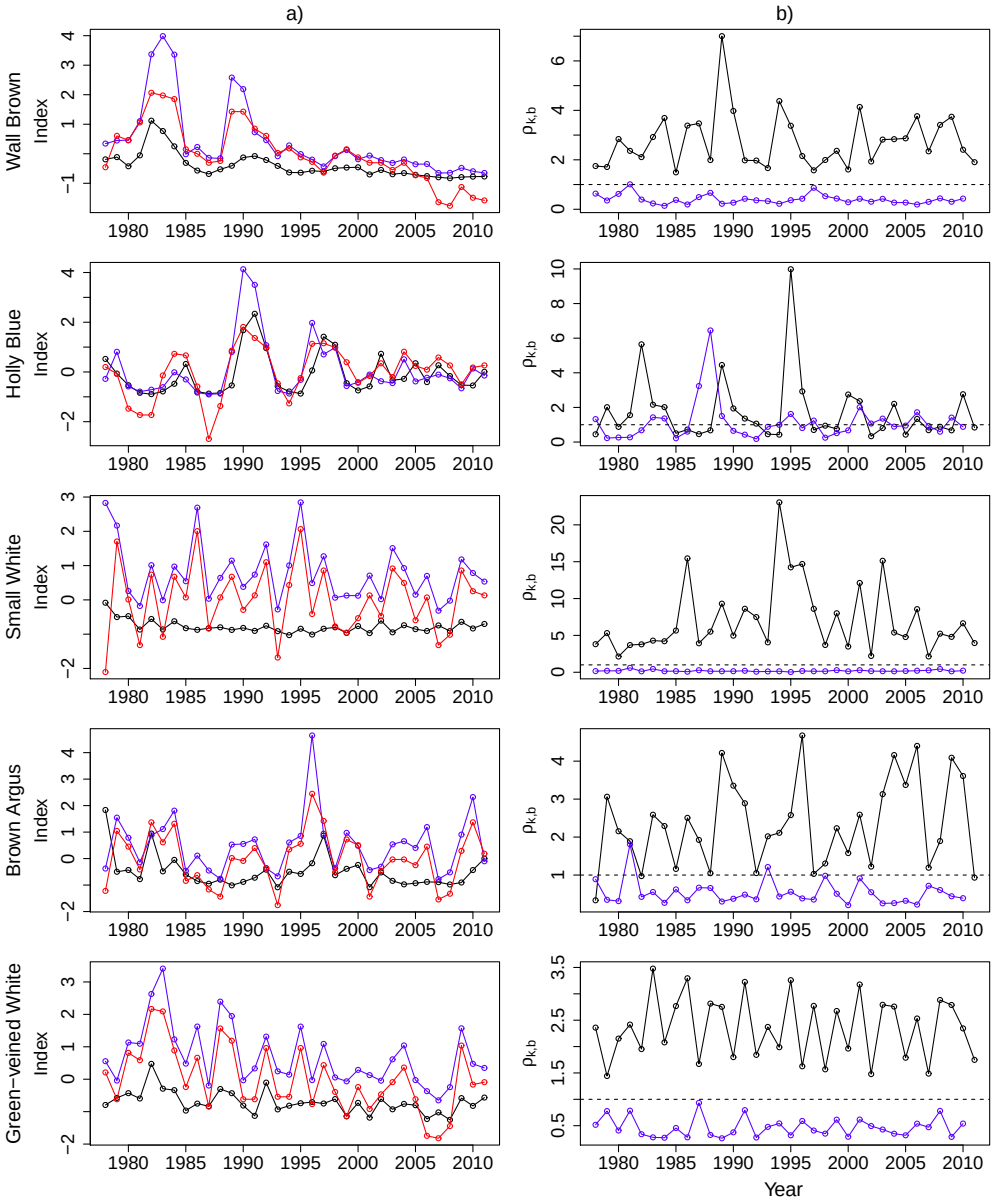

Figure 6.2: a) Relative abundance indices for the first (black) and second (blue) broods from model N_2 and the GAM approach (red). b) annual estimates of productivity for the first ($\rho_{k,1}$, black) and second ($\rho_{k,2}$, blue) brood from model N_2, which was fitted to estimate $\rho_{k,b}$ across sites for each brood and year. The dashed line in b) separates productivities above/below unity, corresponding to growth/decline compared to the previous brood.

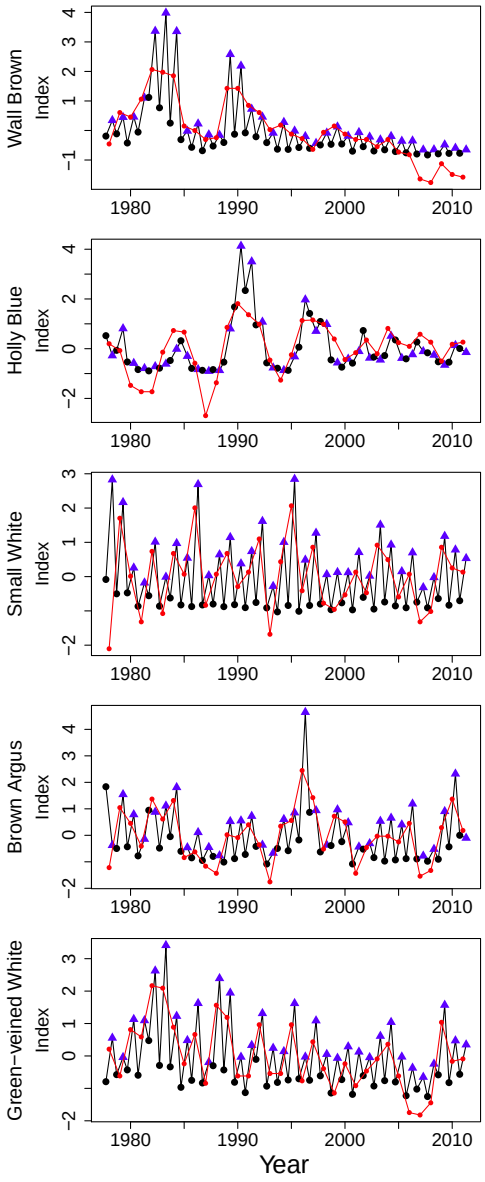

Figure 6.3: Alternative representation of relative abundance indices for the first (black circles) and second (blue triangles) broods from model N_2 and the GAM approach (red).

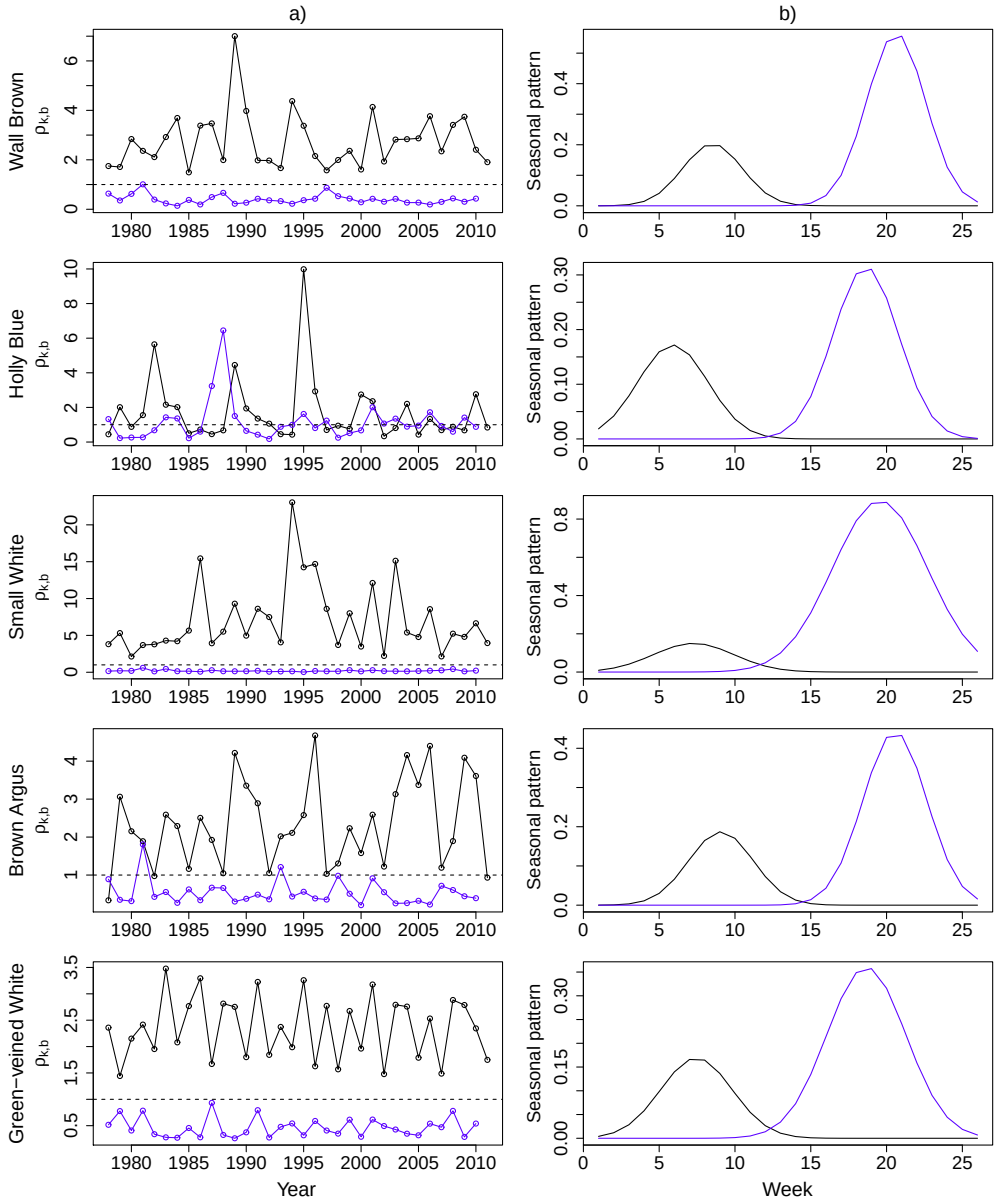

Figure 6.4: a) Annual estimates of productivity for the first ($\rho_{k,1}$, black) and second ($\rho_{k,2}$, blue) brood for each bivoltine species. Model N_2 was fitted to estimate $\rho_{k,b}$ across sites for each brood and year. b) the corresponding average seasonal patterns. The dashed line in a) separates productivities above/below unity, corresponding to growth/decline compared to the previous brood. Note that the productivities in a) were given in Figure 6.2b.

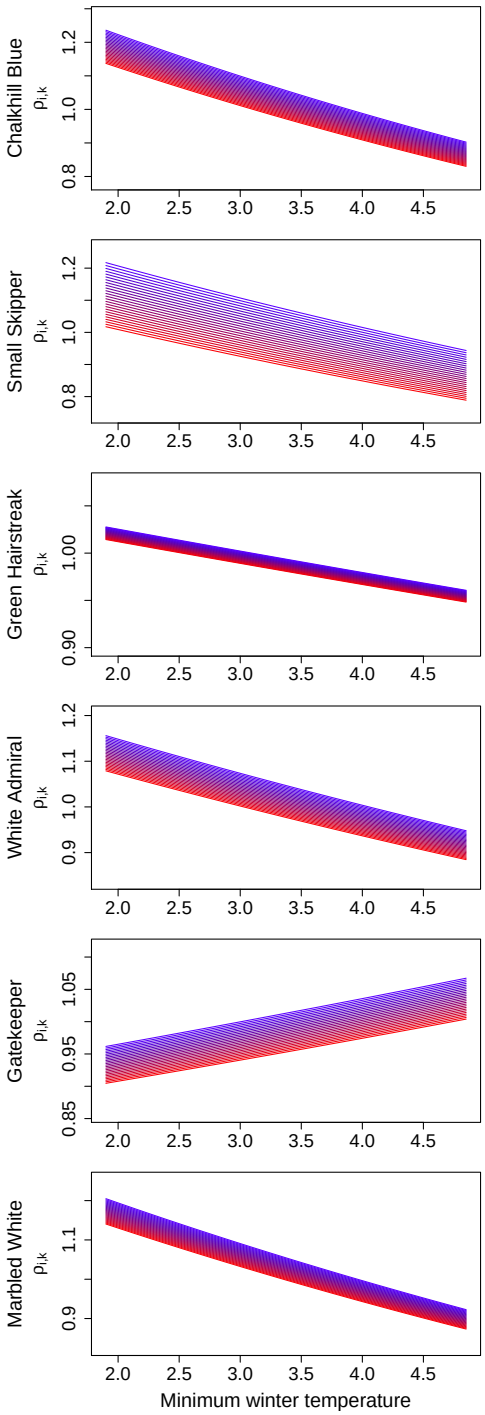

Figure 6.5: Predicted productivity with varying temperature from model SO_1. Each line represents one of 25 equally-spaced northing values within the species range (red at southern sites and blue at northern sites). Model SO_1 was fitted with $\rho_{i,k}$ and $\phi_{i,k}$ regressed on temperature and northing.

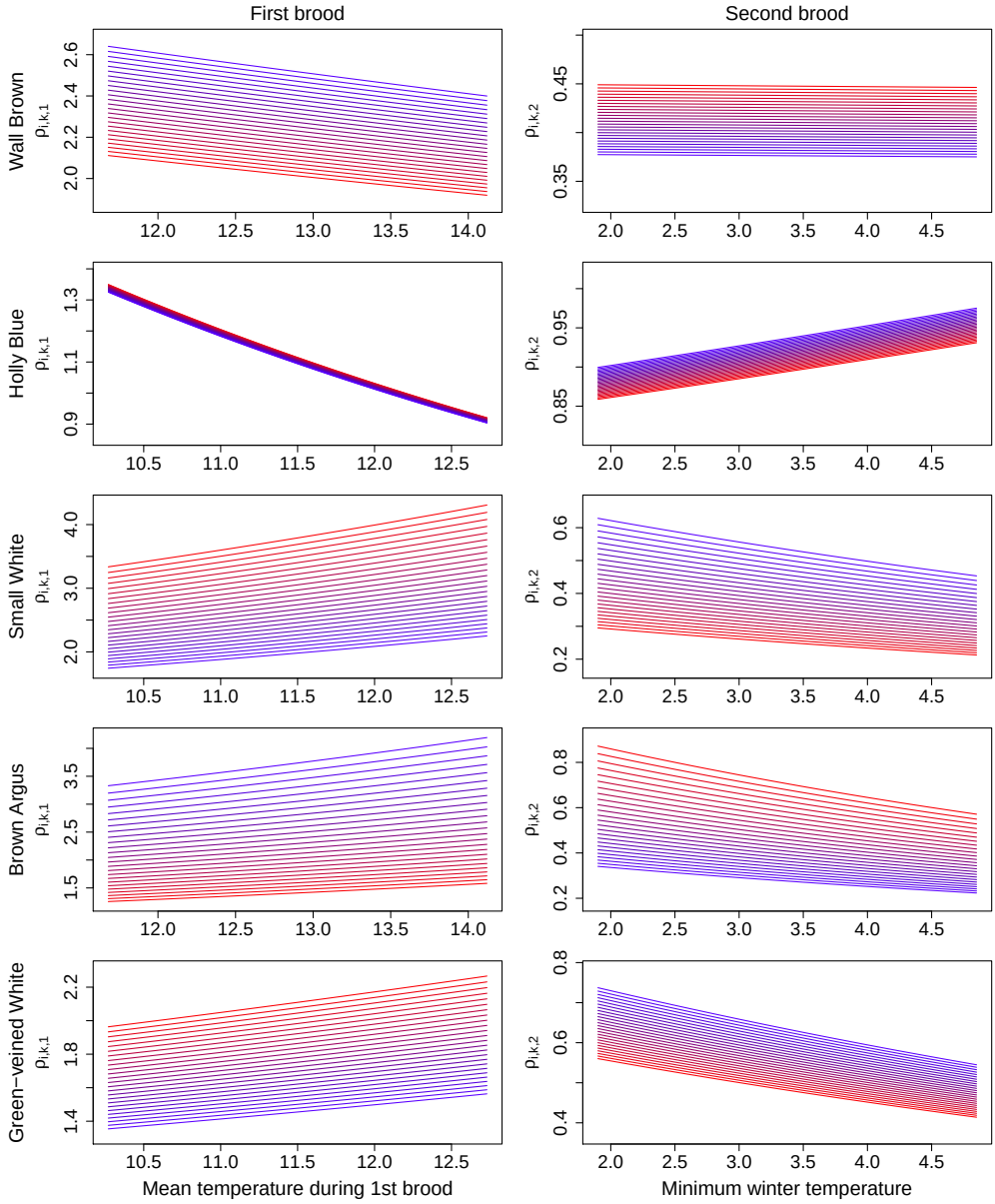

Figure 6.6: Predicted productivity with varying temperature from model SO_2. Each line represents one of 25 equally-spaced Northing values within the species range (red at southern sites and blue at northern sites). Model SO_2 was fitted with $\rho_{i,k,b}$ for each brood regressed on temperature and northing and $\phi_{i,k,b}$ for each brood regressed on temperature.

6.2.3 Survival

The stopover models allow estimation of weekly survival of butterflies, from which adult life expectancies (in weeks) can be estimated by expressions such as $1/(1-\phi)$. Variation in life expectancy with temperature and northing is displayed for univoltine species in Figure 6.7, based on the model with covariates, fitted in the previous section. For these univoltine species, there was generally a negative association of life expectancy with higher average temperature during the flight period. Four out of the six univoltine species indicated greater survival at southerly sites.

Variation in life expectancy with temperature is shown for bivoltine species in Figure 6.8. As for the associations of first brood productivity with weather, we find that the variation in first brood life expectancy with temperature differs between the species sampled. With the exception of Holly Blue, life expectancy for the second brood of the bivoltine species increases with temperature. Fitting model SO_2 with covariates for both northing and temperature on ρ and ϕ for each brood produced unrealistic estimates of lifespan for Brown Argus and Holly Blue, hence in Figure 6.8 we allow ϕ in the SO_2 to vary with temperature and brood only. This requires further investigation, but is likely to be due to the relatively large number of parameters in model SO_2 and/or relatively small size of the sample.

Tables 6.2, 6.3a and 6.4b show the parameter estimates and associated standard errors from the SO_B models with covariates. For comparison estimates are also included for the N_1 and N_2 models with covariates for ρ, which are not presented in the figures. The SO_B models with covariates have 8 and 14 parameters for $B = 1, 2$, respectively, compared to the N_B models with 5 and 10 parameters for $B = 1, 2$, respectively.

Standard errors in Table 6.2a are generally small, but are large for two instances for Green Hairstreak, which exhibit flatness in the associated plots (Figures 6.5 and 6.7). Estimates of the parameters relating to ρ and their associated errors are very similar from SO_1 and N_1. There are differences in μ and σ since in the stopover model μ represents the mean date of emergence

which will be earlier than the mean flight date, and σ relates to the length of the period of emergence, which will be shorter the length of the flight period in the N_1 model. This was also described and shown in Sections 5.5.1 and 5.5.2. The associated errors for μ and σ are smaller for the N_1 than for the SO_1 model.

For the bivoltine species there is more variation in the estimates from N_2 and SO_2. As in the univoltine case, standard errors from the phenomenological model tend to be smaller than those from the stopover model.

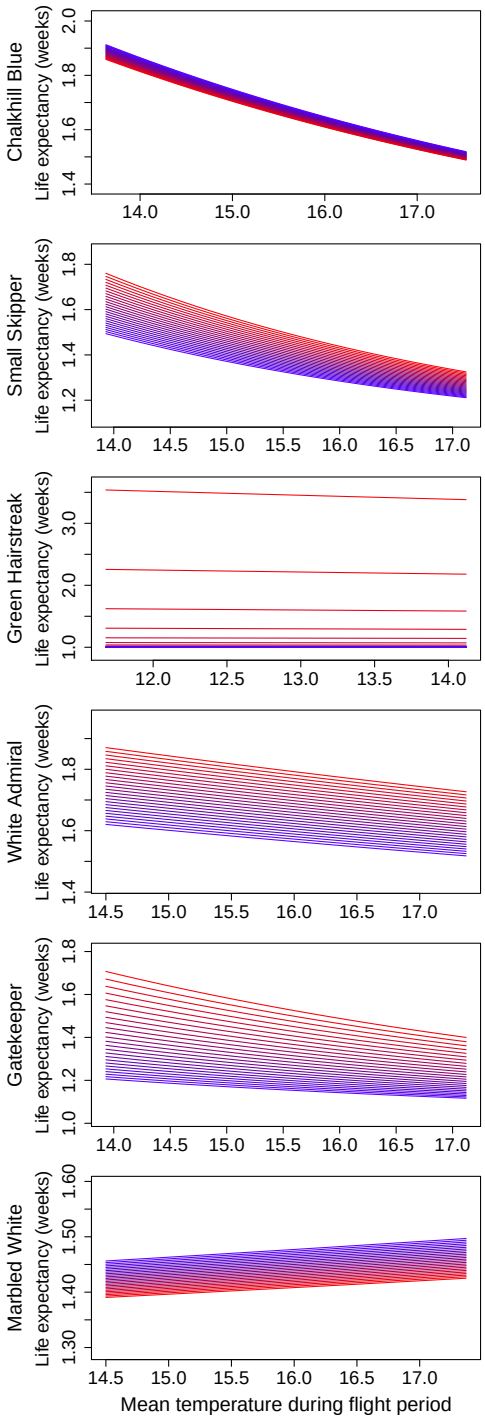

Figure 6.7: Predicted life expectancy (in weeks) with varying temperature from model SO_1. Each line represents one of 25 equally-spaced northing values within the species range (red at southern sites and blue at northern sites). Model SO_1 was fitted with $\rho_{i,k}$ and $\phi_{i,k}$ regressed on temperature and northing.

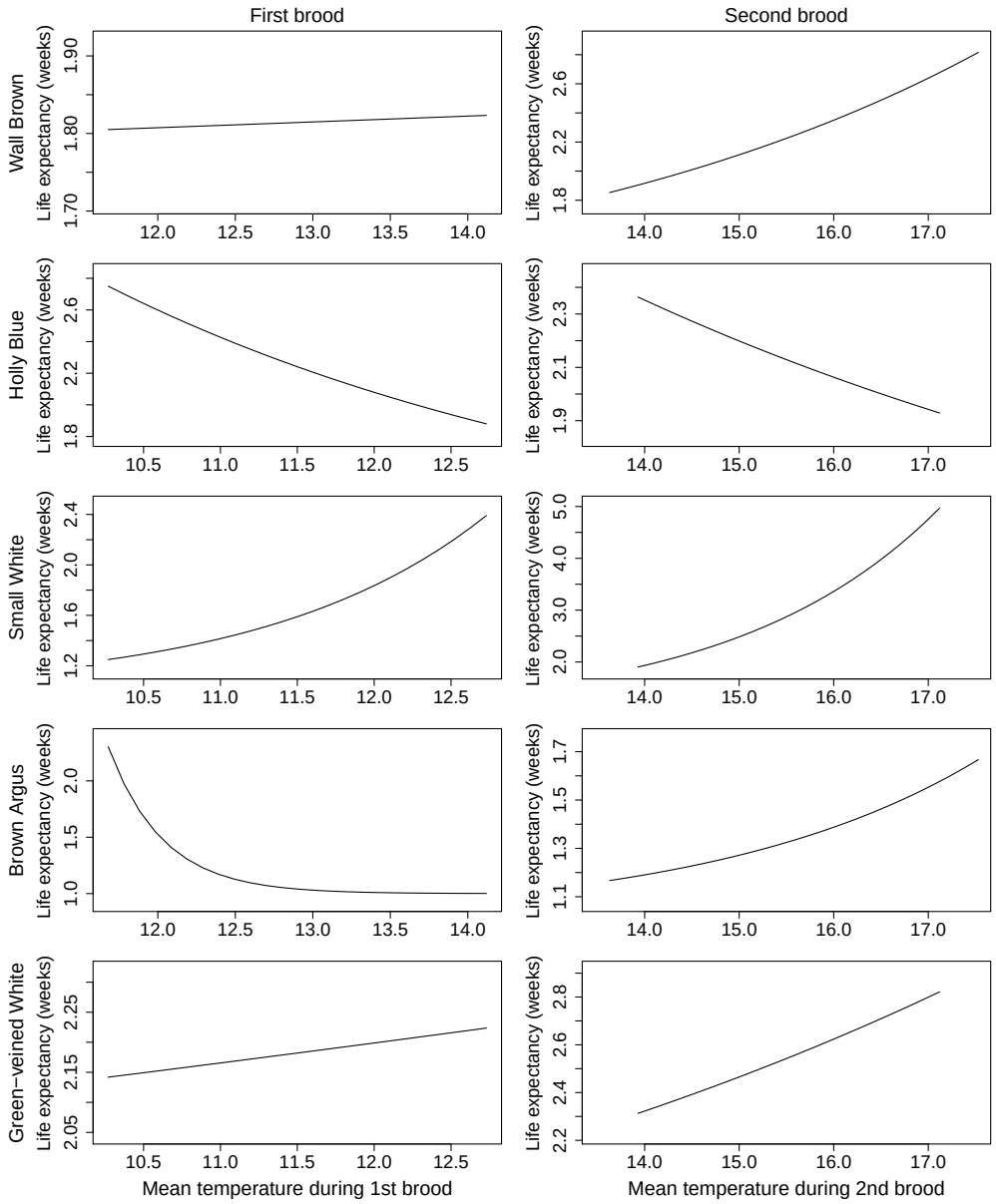

Figure 6.8: Predicted life expectancy for each brood (in weeks) with varying temperature from model SO_2. Model SO_2 was fitted with $\rho_{i,k,b}$ for each brood regressed on temperature and northing and $\phi_{i,k,b}$ for each brood regressed on temperature.

Table 6.2: Parameter estimates from the a) SO_1 and b) N_1 models with covariates. Est and SE represent the parameter estimate and standard error, respectively. All estimates are on the log scale, except those relating to ϕ which are on the logit scale.

		Chalkhill Blue		Small Skipper		Green Hairstreak		White Admiral		Gatekeeper		Marbled White	
	Parameter	Est	SE	Est	SE	Est	SE	Est	SE	Est	SE	Est	SE
a)	$\rho_{i,k}$(intercept)	0.0194	0.0004	-0.0455	0.0008	-0.0140	0.0023	0.0094	0.0025	-0.0365	0.0005	0.0255	0.0011
	$\rho_{i,k}$(wtemp)	-0.0772	0.0011	-0.0624	0.0021	-0.0165	0.0056	-0.0487	0.0059	0.0256	0.0012	-0.0655	0.0023
	$\rho_{i,k}$(north)	0.0199	0.0004	0.0399	0.0010	0.0029	0.0016	0.0158	0.0015	0.0108	0.0003	0.0107	0.0009
	$\phi_{i,k}$(intercept)	-0.4161	0.0109	-0.7725	0.0423	-2.3267	0.2276	-0.3347	0.0399	-0.9194	0.0175	-0.8585	0.0234
	$\phi_{i,k}$(temp)	-0.1246	0.0038	-0.1893	0.0107	-0.0155	0.0205	-0.0513	0.0151	-0.1270	0.0054	0.0242	0.0075
	$\phi_{i,k}$(north)	0.0145	0.0056	-0.0960	0.0214	-3.8071	0.3083	-0.0776	0.0220	-0.2185	0.0087	0.0304	0.0128
	μ(emergence)	2.8857	0.0004	2.7588	0.0013	1.8340	0.0048	2.6408	0.0021	2.8375	0.0004	2.6362	0.0007
	σ(emergence)	0.3704	0.0028	0.5488	0.0060	0.7506	0.0090	0.4023	0.0120	0.3391	0.0028	0.2842	0.0046
b)	$\rho_{i,k}$(intercept)	0.0192	0.0004	-0.0472	0.0008	-0.0151	0.0023	0.0092	0.0025	-0.0377	0.0005	0.0256	0.0011
	$\rho_{i,k}$(wtemp)	-0.0763	0.0011	-0.0662	0.0021	-0.0157	0.0056	-0.0492	0.0059	0.0270	0.0012	-0.0660	0.0023
	$\rho_{i,k}$(north)	0.0209	0.0004	0.0410	0.0010	0.0037	0.0016	0.0158	0.0015	0.0109	0.0003	0.0109	0.0009
	μ(flight period)	2.9473	0.0002	2.8188	0.0005	2.0007	0.0033	2.7227	0.0010	2.8892	0.0002	2.7001	0.0003
	σ(flight period)	0.5797	0.0013	0.6690	0.0029	0.9534	0.0071	0.6291	0.0056	0.4834	0.0014	0.4458	0.0022

Table 6.3a: Parameter estimates from the SO_2 model with covariates. Est and SE represent the parameter estimate and standard error, respectively. All estimates are on the log scale, except those relating to ϕ which are on the logit scale.

	Wall Brown		Holly Blue		Small White		Brown Argus		Green-veined White	
Parameter	Est	SE	Est	SE	Est	SE	Est	SE	Est	SE
$\rho_{i,k,1}$(intercept)	0.7869	0.0436	0.1003	0.0755	1.1730	0.1016	0.6211	0.0474	0.6392	0.0415
$\rho_{i,k,1}$(temp)	-0.0234	0.0048	-0.1089	0.0068	0.0727	0.0022	0.0564	0.0033	0.0408	0.0018
$\rho_{i,k,1}$(north)	0.0674	0.0175	-0.0038	0.0284	-0.1312	0.0138	0.1596	0.0153	-0.1012	0.0088
$\rho_{i,k,2}$(intercept)	-0.8674	0.0436	-0.1021	0.0756	-1.1815	0.1017	-0.6095	0.0475	-0.6374	0.0416
$\rho_{i,k,2}$(wtemp)	-0.0015	0.0059	0.0198	0.0102	-0.0801	0.0032	-0.1037	0.0049	-0.0742	0.0026
$\rho_{i,k,2}$(north)	-0.0524	0.0176	0.0094	0.0285	0.1529	0.0138	-0.1537	0.0154	0.0748	0.0089
$\phi_{k,1}$(intercept)	-0.2068	0.0940	0.2106	0.1182	-0.5156	0.3086	-2.8444	0.6983	0.1678	0.0888
$\phi_{k,1}$(temp)	0.0055	0.0239	-0.1956	0.0334	0.4891	0.0701	-1.7035	0.4374	0.0197	0.0136
$\phi_{k,2}$(intercept)	0.2277	0.0121	0.1430	0.0265	0.5430	0.0086	-1.0809	0.0296	0.4148	0.0064
$\phi_{k,2}$(temp)	0.1667	0.0327	-0.0855	0.0918	0.3297	0.0559	0.3056	0.1391	0.0730	0.0234
μ_1(emergence)	2.0203	0.0090	1.4842	0.0271	1.8331	0.0243	2.1331	0.0046	1.8044	0.0124
μ_d(emergence)	2.4234	0.0063	2.5370	0.0115	2.4170	0.0141	2.4201	0.0054	2.3789	0.0073
σ_1(emergence)	0.5647	0.0207	0.6306	0.0380	0.9677	0.0182	0.7065	0.0105	0.7482	0.0166
σ_2(emergence)	0.3105	0.0159	0.5797	0.0333	0.9116	0.0170	0.6887	0.0098	0.6179	0.0119

Table 6.4b: Parameter estimates from the N_2 model with covariates. Est and SE represent the parameter estimate and standard error, respectively. All estimates are on the log scale.

	Wall Brown		Holly Blue		Small White		Brown Argus		Green-veined White	
Parameter	Est	SE	Est	SE	Est	SE	Est	SE	Est	SE
$\rho_{i,k,1}$(intercept)	-1.0292	0.0176	-0.1019	0.0243	-1.7222	0.0129	-0.8385	0.0143	-0.8373	0.0084
$\rho_{i,k,1}$(temp)	-0.0447	0.0053	-0.0985	0.0066	0.0470	0.0021	0.0643	0.0032	0.0374	0.0018
$\rho_{i,k,1}$(north)	0.0591	0.0153	-0.0130	0.0282	-0.1257	0.0141	0.1605	0.0153	-0.1017	0.0088
$\rho_{i,k,2}$(intercept)	0.9542	0.0177	0.0968	0.0245	1.7188	0.0129	0.8466	0.0144	0.8396	0.0084
$\rho_{i,k,2}$(wtemp)	0.0326	0.0069	0.0113	0.0101	-0.0604	0.0031	-0.1090	0.0045	-0.0703	0.0025
$\rho_{i,k,2}$(north)	-0.0664	0.0154	0.0187	0.0282	0.1459	0.0142	-0.1544	0.0153	0.0752	0.0088
μ_1(flight period)	2.1423	0.0034	1.7744	0.0078	1.9703	0.0047	2.2037	0.0026	2.0105	0.0023
μ_d(flight period)	2.4924	0.0028	2.5391	0.0047	2.5157	0.0029	2.4419	0.0024	2.4152	0.0018
σ_1(flight period)	0.6731	0.0109	0.8727	0.0157	0.9510	0.0113	0.7457	0.0084	0.8616	0.0061
σ_2(flight period)	0.6640	0.0067	0.8497	0.0130	1.1478	0.0044	0.7496	0.0057	0.9529	0.0038

6.2.4 Phenology

In this section we demonstrate the potential to produce estimates of phenology using the dynamic models. The N_1 and N_2 models were fitted with $\boldsymbol{\rho}$, $\boldsymbol{\mu}$ and $\boldsymbol{\sigma}$ each varying with year. Hence the N_1 requires 101 parameters to be estimated, corresponding to 33 parameters for ρ_k, and 34 parameters each for μ_k and σ_k. Similarly the N_2 model has 203 parameters: 34 for $\rho_{k,1}$, 33 for $\rho_{k,2}$, and 34 each for $\mu_{k,1}$, $\mu_{k,d}$, $\sigma_{k,1}$ and $\sigma_{k,2}$. To identify potential phenological trends, simple linear regressions were performed post-model fitting and green lines indicate significant regressions (p-value ≤ 0.05). This could also be examined by building regressions within the model.

Figures 6.9a and 6.10 suggest that the mean flight period date, μ, has advanced for all species and broods, which is consistent with what is expected, and was also found in Section 5.6.4. From Figures 6.9b and 6.11 we see that the length of the flight period/brood has increased significantly for 3 out of 6 univoltine and 4 out of 5 bivoltine species studied, which is in agreement with previous findings (Roy and Sparks 2000). Figures 6.10 and 6.11 show the presence of a small number of outliers which provides further evidence that the dynamic models for the bivoltine species may be difficult to fit or require more data. This requires further investigation.

With the exception of Green Hairstreak, for the six univoltine species there was no clear relationship between μ_k and ρ_k (Figure 6.12). For Green Hairstreak, which emerges early in the season, lower productivities are associated with an earlier flight period, which may lead to declines if advances in phenology continue with changes in climate. For most of the five bivoltine species, significant patterns between the mean flight period for each generation and the associated productivity were not found (Figure 6.13). However for Brown Argus and Green-veined White, productivity of the second generation was lower when $\mu_{k,2}$ was advanced.

These results show that the dynamic models frequently predict phenological changes consistent with expected patterns. The improved estimates of phenology may be studied in combination with demographic parameters,

to reveal potential novel insights. Subject to producing robust estimates, changes in phenology may also be modelled using the stopover models, in order to separate changes in emergence from changes in survival.

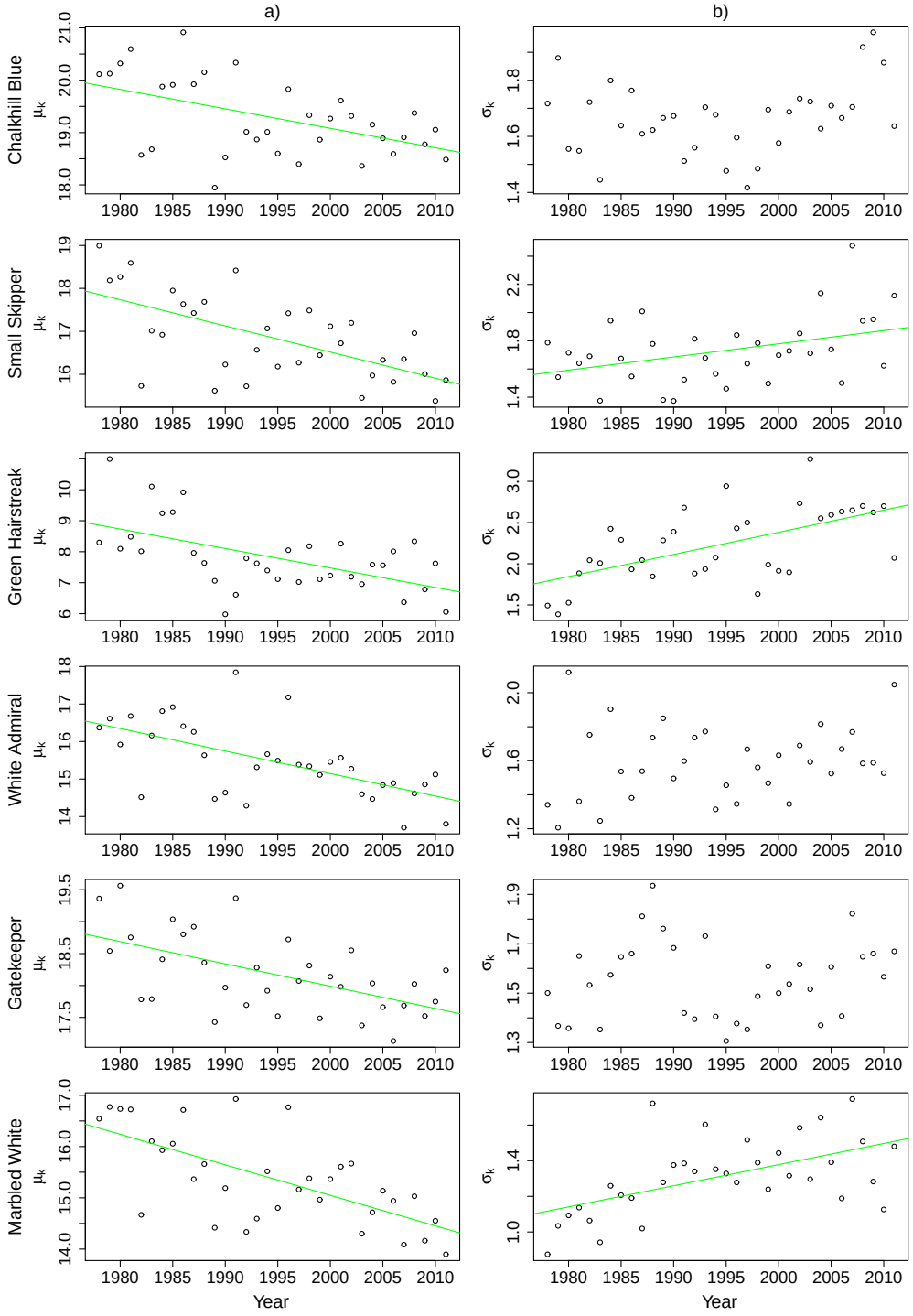

Figure 6.9: Annual estimates of a) μ_k and b) σ_k from model N_1, which was fitted to estimate ρ_k, μ_k and σ_k across sites for each year. Green lines indicate significant linear regressions (p-value ≤ 0.05).

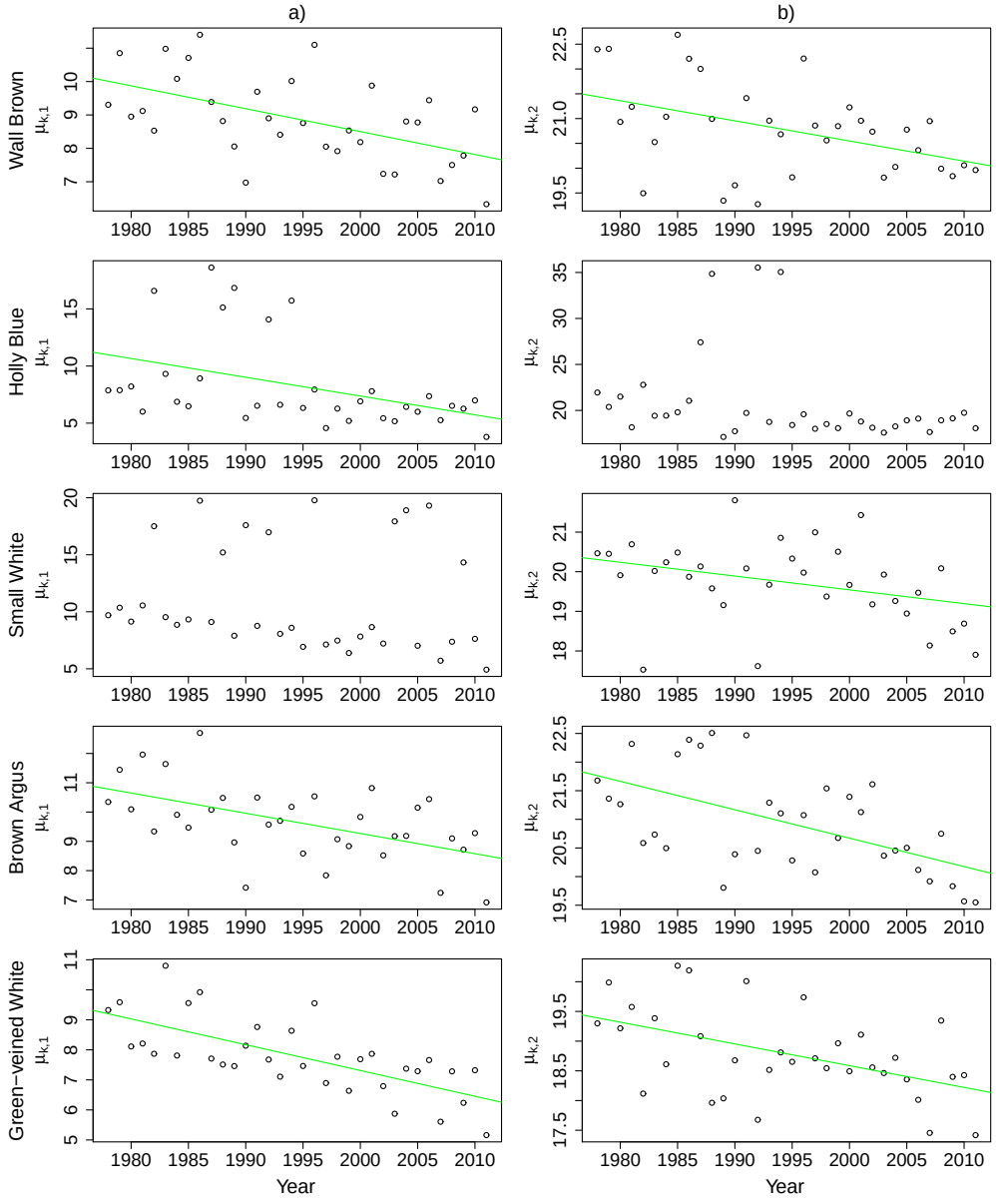

Figure 6.10: Annual estimates of a) $\mu_{k,1}$ and b) $\mu_{k,2}$ from model N_2, which was fitted to estimate $\rho_{k,b}$, $\mu_{k,b}$ and $\sigma_{k,b}$ across sites for each brood and year. Green lines indicate significant linear regressions (p-value ≤ 0.05).

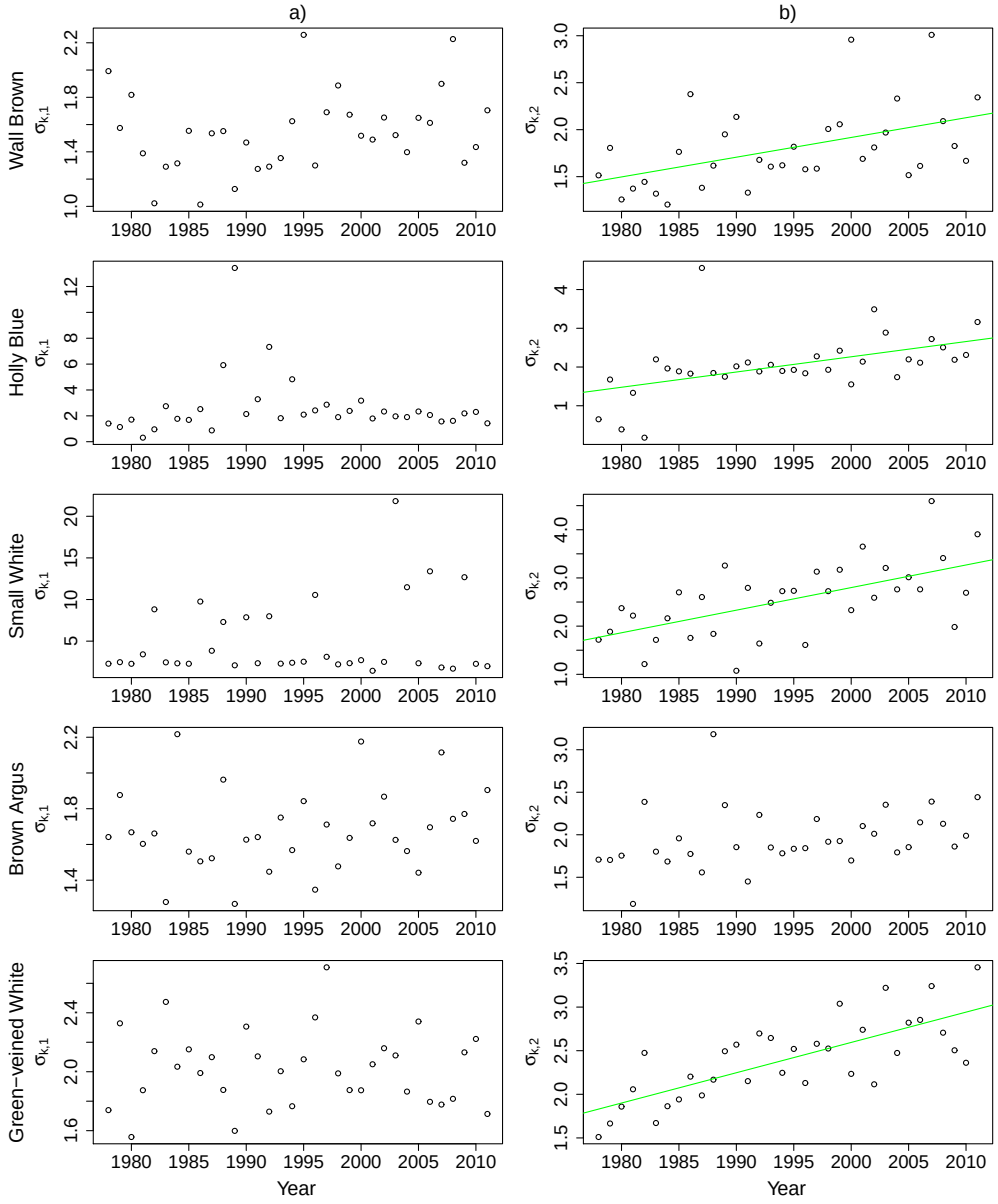

Figure 6.11: Annual estimates of a) $\sigma_{k,1}$ and b) $\sigma_{k,2}$ from model N_2, which was fitted to estimate $\rho_{k,b}$, $\mu_{k,b}$ and $\sigma_{k,b}$ across sites for each brood and year. Green lines indicate significant linear regressions (p-value ≤ 0.05).

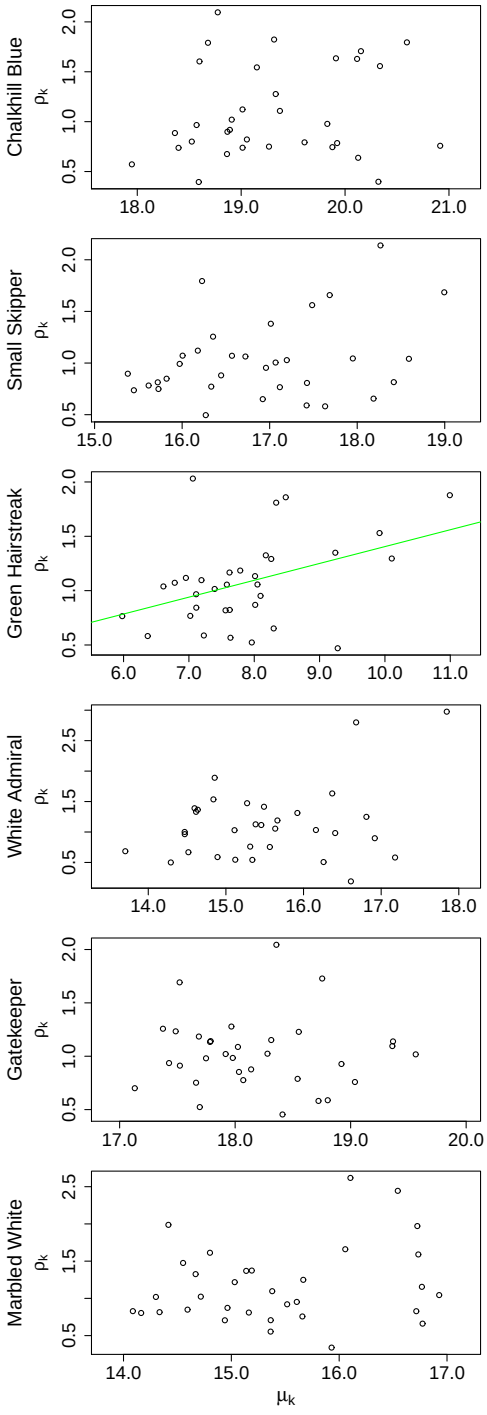

Figure 6.12: Annual estimates of μ_k versus productivity ρ_k from model N_1, which was fitted to estimate ρ_k, μ_k and σ_k across sites for each year. Green lines indicate significant linear regressions (p-value ≤ 0.05).

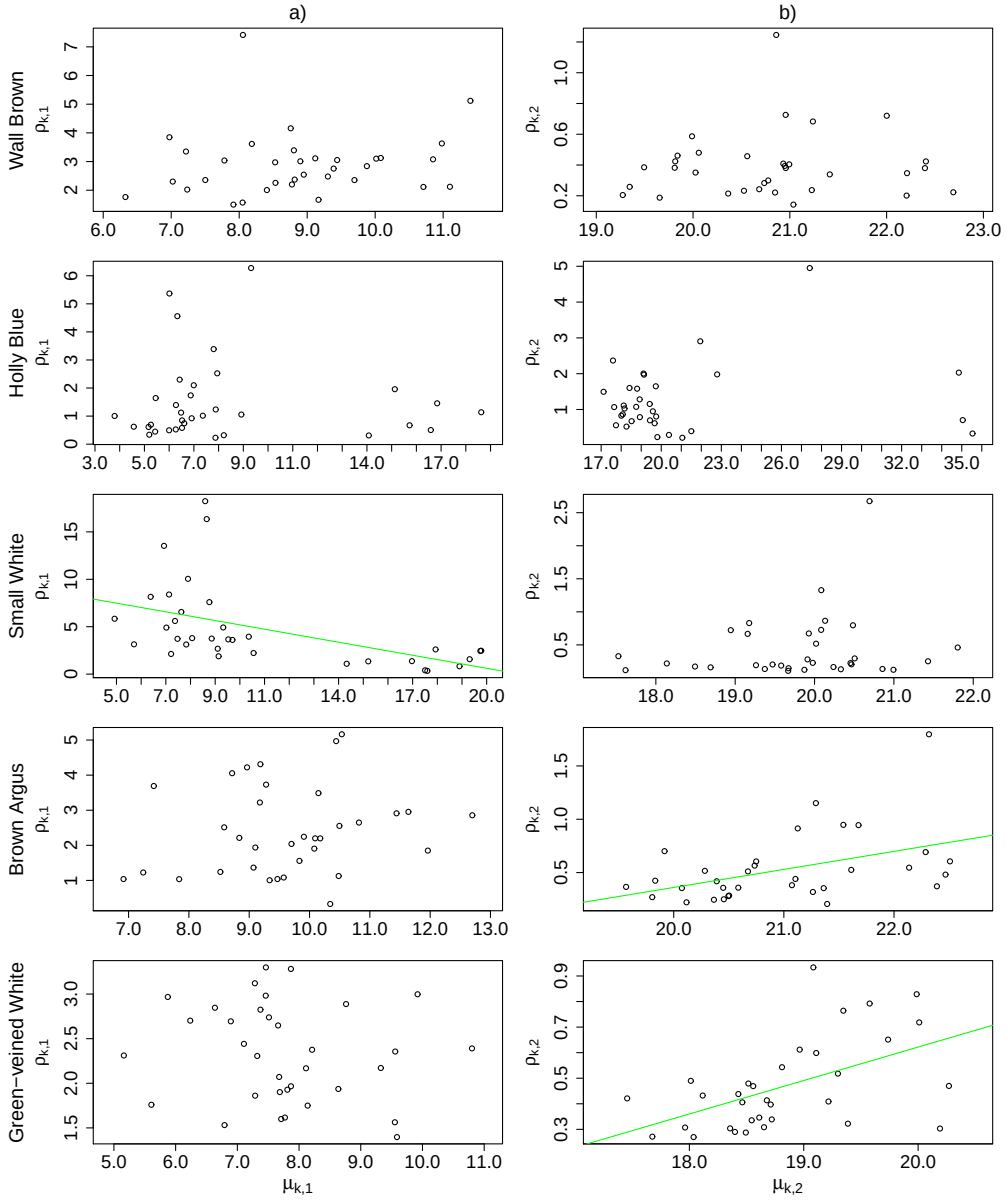

Figure 6.13: Annual estimates of a) $\mu_{k,1}$ versus $\rho_{k,1}$ and b) $\mu_{k,2}$ versus $\rho_{k,2}$ from model N_2, which was fitted to estimate $\rho_{k,b}$, $\mu_{k,b}$ and $\sigma_{k,b}$ across sites for each brood and year. Green lines indicate significant linear regressions (p-value ≤ 0.05).

6.2.5 Comparison to the GAI approach

In this section we discuss how the dynamic models compare with the GAI presented in Chapter 5. The GAI approach was presented in a more general context than the dynamic models, and provides a broad framework for modelling butterfly count data for any given year, encompassing a range of possible discrete distributions as well as phenomenological, stopover and spline alternatives for modelling the seasonal variation in counts. The GAI models have structural similarities to the dynamic models, but, aside from regressions on $\{a_{i,j,k}\}$, abundance from different years is analysed separately, and hence unlike the dynamic models do not produce estimates of productivity.

We compare output from the dynamic model N_1 and the P/N_1 GAI (Section 5.2). In this comparison we regressed μ and σ on year, therefore for the GAI there were four parameters to estimate, corresponding to an intercept and slope parameter each for μ and σ. The dynamic model N_1 was also fitted with μ and σ regressed on year, with the addition of annual estimates for productivity.

The estimates and associated standard errors are generally similar from the two models (Table 6.5). The estimates of dispersion suggest overdispersion in some cases. The standard errors could be suitably inflated to deal with this, or, as demonstrated in Section 5.6.2, a negative-binomial model may be preferred. Figure 6.14 compares estimates of site abundance from the two methods.

Indices of abundance from the dynamic model and GAI show good agreement with the index resulting from the GAM approach (Section 4.1.3) in Figure 6.15. The index from the dynamic model is often closer to the GAM index than the GAI, for example in some years for Gatekeeper and Marbled White. This could be a result of site variation between years, which is accounted for by the GAM approach, as well as in the dynamic model, where G (Section 6.1.5) can be estimated from every site for each year (and brood). In contrast, for the GAI only sites visited in a given year contribute to the

index G (equation 5.9). On average across the six species, the GAI took 15 seconds, whereas the dynamic model took 87 minutes. The GAI performs hugely better than the alternative approaches in terms of efficiency, which is an important consideration when indices require evaluation every year for all species. Differences between the indices produced from different methods are fairly small. The dynamic model can provide estimates of productivity, as well as separate indices for different broods, but with greater computational requirements.

Table 6.5: Comparison of a) the dynamic N_1 model and b) the P/N_1 GAI with log-linear regressions on year. Est and SE represent the parameter estimate and standard error, respectively. All estimates are on the log scale. To reduce bias, estimates for σ are based on models with time-varying μ. D is the dispersion (residual deviance/degrees of freedom) and T is the approximate computation time in minutes.

	Species	μ(intercept)		μ(slope)		σ(intercept)		σ(slope)		D	T
		Est	SE	Est	SE	Est	SE	Est	SE		
a)	Chalkhill Blue	2.9555	0.0002	-0.0168	0.0002	0.4999	0.0013	0.0310	0.0020	9.4	91
	Small Skipper	2.8203	0.0005	-0.0309	0.0005	0.5397	0.0031	0.0542	0.0020	3.3	57
	Green Hairstreak	2.0387	0.0034	-0.0673	0.0037	0.8305	0.0275	0.0886	0.0296	1.1	35
	White Admiral	2.7439	0.0011	-0.0415	0.0012	0.4594	0.0256	0.0331	0.0172	0.8	120
	Gatekeeper	2.8980	0.0002	-0.0159	0.0002	0.4170	0.0018	0.0241	0.0018	6.5	72
	Marbled White	2.7358	0.0005	-0.0436	0.0005	0.3203	0.0114	0.0184	0.0081	4.2	147
b)	Chalkhill Blue	2.9557	0.0002	-0.0169	0.0002	0.5015	0.0014	0.0298	0.0020	4.6	0.21
	Small Skipper	2.8199	0.0005	-0.0313	0.0005	0.5372	0.0031	0.0559	0.0020	1.9	0.24
	Green Hairstreak	2.0408	0.0035	-0.0673	0.0037	0.8311	0.0278	0.0881	0.0305	0.8	0.14
	White Admiral	2.7448	0.0011	-0.0413	0.0012	0.4606	0.0261	0.0313	0.0173	0.6	0.22
	Gatekeeper	2.8980	0.0002	-0.0159	0.0002	0.4152	0.0018	0.0255	0.0018	4.5	0.21
	Marbled White	2.7359	0.0005	-0.0436	0.0005	0.3199	0.0118	0.0202	0.0080	3.0	0.24

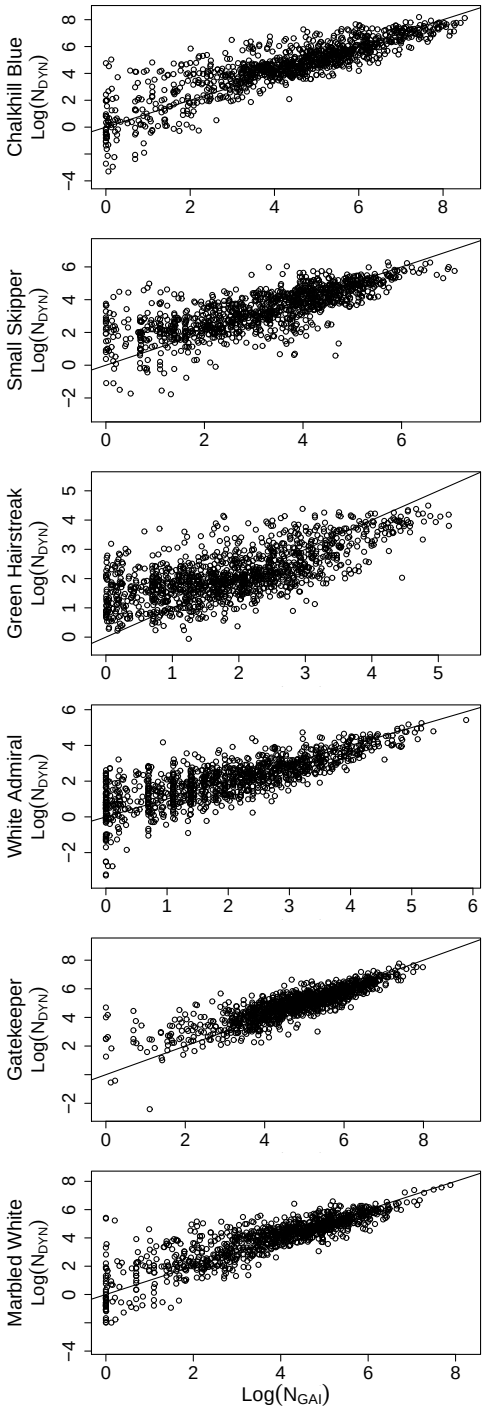

Figure 6.14: Comparison of site parameters $\{N_{i,k}\}$ from the P/N_1 GAI model (N_{GAI}) and model N_1 (N_{DYN}), as fitted in Table 6.5. Both axes are displayed on the log scale and the line indices the 1-1 line.

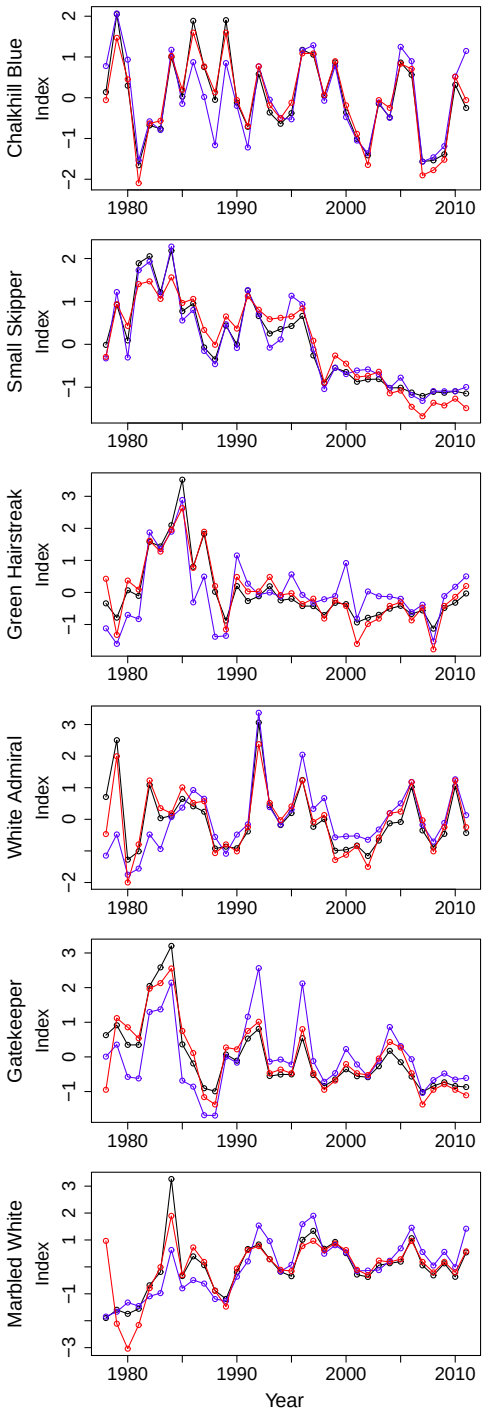

Figure 6.15: Relative abundance indices from dynamic model N_1 (black), the P/N_1 GAI model (blue) and the GAM approach (red). The GAM approach is as fitted in Section 6.2.1. The dynamic and GAI models are as fitted in Table 6.5.

6.3 Discussion

The dynamic model framework presented in this chapter allows for novel investigation of the drivers of fluctuations in butterfly abundance from year to year and provides a basis that can be adapted to both the study species and research aim. In this chapter we have presented only a preliminary application of the models. The methods of Chapter 5, which model data for each year separately, may be better suited for estimating indices of abundances most efficiently, whereas the dynamic models provide additional information of potential value for understanding butterfly demography. In particular novel estimates of productivities and abundance indices for separate broods provide new insights.

For the majority of the sample species, higher productivity was associated with cooler winters. Variability in lifespan and first brood productivity of bivoltine species differed more between species. Further application may look for trait-based variation, for example overwintering stage: egg, larva, chrysalis or adult. Diamond et al. (2011) explored relationships between changes in date of first appearance and species' traits.

Further work is needed to explore the most relevant covariates driving changes in productivity, survival and phenology. Spatial covariates such as habitat/land-cover variables may describe additional variation in the model parameters. The inclusion of local-scale weather could identify the period within the life-cycle for which weather has the most impact on abundance of the adult stage. Growing degree-days may also be explored (Hodgson et al. 2011; Cayton et al. 2015). Here covariates were included only additively on a logistic linear scale, whereas true relationships may be non-linear, for example productivity/survival might be limited by extremes in weather; models with thresholds could be employed (Besbeas and Morgan 2012). The models could also be extended to describe variation in productivity stochastically.

Many of the possible model variations from previous chapters also apply here. In this chapter we have considered the data to arise only from a

Poisson distribution. In Chapter 5 the negative-binomial and zero-inflated Poisson were also considered, and approximate concentrated likelihood approaches derived, which could similarly be done for the dynamic models in this chapter. Alternatively, Pagel et al. (2014) accounted for overdispersion by a mixed log-normal-Poisson distribution within a Bayesian framework. As suggested for the stopover model in Section 4.2.3 and for the GAI in Section 5.7, alternatives to the Normal distribution for describing seasonal variation could be explored, for example to describe skewness.

This study has only accounted for species which are distinctly univoltine or bivoltine. A spline may be used to define complex seasonal patterns as shown in Chapter 5, and the models could be extended to allow more than two broods each year. The models may be developed to accommodate variation in voltinism, where the first generation contributes to both the second generation within the same year and first generation the following year.

Given the greater complexity of the dynamic models, which unlike the GAI in Chapter 5 model data from multiple years simultaneously, it is understandable that model fitting becomes increasingly difficult as the complexity increases, particularly for species with multiple broods. Hence many of the proposed extensions and avenues for further work would most likely be subject to this restraint, which may be related to the amount of information available from the data.

The dynamic models produce realistic estimates of parameters relevant to phenology, providing further validation of the models. As discussed already in Section 1.1.2, phenological studies have typically involved measures such as mean first appearance, mean peak appearance and mean length of the flight period, which may be driven by observer behaviour. The improved estimates of phenology from dynamic models provide the opportunity to study linkages between changes in phenology and demographic changes in abundance and/or productivity, for example possible phenological mismatch (Hindle et al. 2014).

Using a phenomenological model may be optimal in scenarios with lim-

ited data, but the stopover model allows for additional insights by estimating survival. Spatio-temporal variation in the lifespans of butterflies has had limited attention, as have potential linkages with other parameters, for example to explore how phenology affects survival, or whether variation in survival can influence productivity. Using a stopover model separates relevant parameters, for example to determine whether an increase in flight period length is due to an extended period of emergence, or increased lifespan.

Density dependence, which has been highlighted for some butterflies (Nowicki et al. 2009), may be incorporated here in productivity and/or survival by introducing a dependency on the relative abundance. Additionally, allowing for spatial dependence of ρ and autocorrelation in abundance may be advantageous (Johnson et al. 2012). Pagel et al. (2014) included spatially autocorrelated random effects when modelling mean population density, but did not account for the within-year variability in counts.

For some threatened, conservation-priority UK butterflies, such as Large Blue and Marsh Fritillary data are available on other stages of the butterfly life-cycle, such as counts of caterpillars or eggs. An attraction of the model framework proposed here is the potential for the incorporation of data from multiple stages of the life-cycle, which could aid the monitoring and conservation of rarer species for which coverage from standard monitoring schemes can be limited.

The new dynamic models may address the "lack of mechanistic understanding about factors driving butterfly population dynamics" (Isaac et al. 2011b), which we previously referred to in Chapter 1. Further application of the models will generate a variety of hypotheses for future investigation, which have the potential to illuminate complex features of butterfly phenology and demography which are at present poorly understood. The potential of the dynamic models, as well as areas for future work, will be revisited in Chapter 7, within the context of other approaches for modelling butterfly abundance.

Although we have presented the dynamic models in the context of but-

terflies, it may be applied to other insect species, possibly after modification appropriate to their ecology. For example, adaptation of the models to flightless longhorn beetles, *Dorcadion fuliginator*, which take two years to reach maturity (Baur et al. 2005), is in progress. Other examples are many dragonflies and some crickets. The models may also be adapted for the study of migrant bird and reptile populations.

Chapter 7

Discussion and future work

In this thesis we have developed new approaches for modelling the abundance and distribution of butterflies. During a period of habitat loss, climate change and loss of biodiversity, the availability of accurate and efficient modelling techniques is crucial for monitoring and understanding changes in species' population and distribution. The novel models described in this thesis provide a basis for new and exciting future studies, generating hypotheses for further investigation, which will lead to better understanding of the drivers of changes in butterfly populations.

The models developed in this thesis have primarily been applicable for count data, from which indices of abundance can be derived. Indices play an important rôle in monitoring changes in biodiversity and progress towards biodiversity targets. As the most comprehensively monitored insect taxon, known to respond rapidly and sensitively to change, indices for butterflies are particularly valuable, but devising methods that can be fitted to large data sets is challenging and they can be computer intensive.

As described in Section 1.1, butterfly populations in the UK and beyond are undergoing various changes in their abundance, range, phenology and in some cases voltinism. Of particular note is that three-quarters of UK butterfly species have shown declines in their distribution, abundance, or both over a ten-year period (Fox et al. 2011a). The new methods described in this thesis will aid the monitoring of these changes in the form of accurate

and efficient indices for abundance, as well as completely novel occupancy indices for butterflies, both of which may guide future conservation and management.

Both the UKBMS and BNM, which were the primary datasets considered in the thesis, consist of data gathered by volunteers/citizen scientists, amounting to millions of records which were previously not exploited fully. The original GAM approach involved discarding data for sites where a high proportion of weeks or the peak of the flight period is missed (Section 4.1.2). The new methods developed for modelling butterfly abundance, including the two-stage GAM approach, have the benefit of being possible to apply to all available data, which is essential for both the motivation and retention of volunteer participants, as well as the production of accurate indices.

In terms of studying changes in butterfly distributions, the BNM records were previously only used to map butterfly distributions superficially, by comparing changes over limited multi-year time periods. New analyses are possible using the occupancy approach described in Chapter 2, which demonstrates the formulation of annual occupancy maps and new associated indices for occupancy, at both the UK and regional scale. With further development and application, this approach may advance the study of changes in distribution and range dynamics, and allow for improved and more regular reporting of such changes than previously.

In Chapter 3 it was shown that the popular N-mixture model, which is used for modelling abundance and detection probability from count data, can produce infinite estimates of abundance in some scenarios. The equivalent multivariate Poisson and negative-binomial models provide alternative approaches for model fitting which avoid the need to select an upper bound K. It is hoped that the results in this chapter will increase awareness among practitioners of the potential issues associated with fitting these popular models to data where detection probability is low and/or the number of sampling occasions is small. Aspects of the models in Chapter 3 were also relevant in the development of models suitable for describing butterfly abundance in Chapters 5 and 6.

A key challenge when modelling butterfly count data, such as the UKBMS, is the large amount of information available, where counts have been made from multiple visits, over many sites and years, for many species, which show much variation, for example in population size, range, overwintering stage and foodplants. An additional complicating feature of the data is the seasonal nature of the counts, and for some species the presence of multiple broods per year. In Chapters 4-6 we have considered a variety of approaches for modelling butterfly abundance, within a range of different contexts. The different methods were designed to be broadly applicable to various types of species, and each have associated advantages and disadvantages. Given the variation between different butterfly species, we anticipate that the best modelling approach may vary according to individual species, as well as the data available and study purpose. This thesis provide a greater choice of methods, which may be tailored to the demands of different species, and which we hope may lead to interesting and influential applications in the future.

Given the demonstrated efficiency and flexibility, we would recommend that the phenomenological GAI presented in Chapter 5 may be best suited for estimating indices of abundance, where a suitable choice of function for the seasonal variation in counts can be made on an individual species basis. In particular the GAI is very efficient compared to the two-stage GAM approach and dynamic models, which would lead to faster outputs and feedback of results to recorders, as well as policy makers. Improved reporting may enhance the experience of the citizen scientists involved, which is important for retaining volunteers on schemes such as the UKBMS which require considerable effort from participants.

One feature for further consideration is the influence of variation in sites sampled between years, which is not currently accounted for by the GAI. The two-stage GAM approach and dynamic models incorporate this aspect, although this is typically based upon the assumption that trends in abundance are the same across sites. However trends may vary among sites within the dynamic models by allowing the productivities to vary spatially,

for example with suitable covariates (Section 6.2.2).

The GAM-based approaches that have been typically used to model UKBMS data describe the seasonal pattern non-parametrically as a means to impute missing records. The parametric descriptions of seasonal variation proposed in this thesis go beyond solely empirical descriptions and provided new and meaningful mechanistic parameters from only count data, such as survival and productivity. This has particular relevance for species with multiple broods per year, as studying the population dynamics of individual broods has typically not been previously possible. Although less efficient than the GAI, the dynamic models in Chapter 6 consider both within- and between-year population changes simultaneously, as well as explicitly modelling separate broods and their dependence. Hence the dynamic models have the potential to improve our understanding of the complex processes underlying butterfly population dynamics over large spatial and temporal scales, in particular through the study of the new and informative parameters that explain aspects of phenology and demography.

The stopover models for butterfly abundance can provide new insights into both spatial and temporal variation in the survival of adult butterflies, and how survival may link with other features such as phenology. Butterfly lifespans have previously received limited attention, and in particular their study has mostly been restricted to small-scale studies of mark-release-recapture (MRR) data, often for a single species, since an effective method for estimating survival from only count data was lacking (Nowicki et al. 2008). Hence from the stopover models survival can be estimated for various species, and also compared between broods for bi- or multivoltine species, although comparison with estimates from MRR data is needed to confirm the validity of the survival estimates from stopover models. Estimates of abundance from stopover models could be used to produce indices that separate the emergence pattern and lifespans, in order to estimate an index that is more representative of the actual butterfly population, rather than the number observed, which is not possible for GAMs and phenomenological models. Pollard and Yates (1993) and Nowicki et al. (2008) advised

that effects of variation in lifespans on indices of abundance are likely to be small, but Nowicki et al. (2008) also suggested that abundance indices may be "overestimated in good weather seasons, and underestimated in bad ones". By estimating survival, the stopover models provide the opportunity to determine whether declines in species' abundance are accompanied by changes in the lifespan of adult butterflies, or if the changes are a result of other factors, for example relating to productivity.

By providing new opportunities for describing various aspects of butterfly populations, the new modelling approaches devised in this thesis can aid our understanding of the many threats to butterfly populations. There is wider scope to study the impacts of weather and climate, for example weather extremes (Oliver et al. 2013), on particular features of the butterfly life cycle, at different times of the year, and for different broods for multivoltine species. The influences of species' traits, such as overwintering stage and the number of host plant species, on aspects of butterfly population dynamics may also be investigated (Diamond et al. 2011).

The interesting new parameters that relate to phenology and voltinism also present the possibility for more detailed studies on these features which, as discussed in Chapter 1, were previously based on naïve measures which may be prone to bias, or in the case of voltinism often not considered. In particular this may be relevant for revealing potential damaging effects of changes in phenology in response to climate change, such as phenological mismatch between species' emergence and food sources (Hindle et al. 2014), or so-called lost generations (Van Dyck et al. 2015), where a species might respond to increased temperatures by producing an additional brood towards the end of the season, which could be detrimental if there is insufficient time to complete the full life-cycle.

Given the breadth of this thesis, applications in each chapter are only demonstrative and in each case there is scope for future work, which has mostly been described in the relevant discussions at the end of each chapter. In particular, further study is required to determine the robustness and potential limitations of the new methods, particularly in the context of

limited data, and/or for more complex model descriptions, for example for the dynamic models, especially for bivoltine species with a stopover model formulation.

Given the large and increasing number of butterfly and other insect schemes (Tables 1.1 and 1.2), we anticipate that the models presented in this thesis may also prove useful beyond the application to UKBMS data, to monitoring schemes for butterflies in other countries, as well as data for other insects, such as moths, possibly with adaptation where required. The occupancy approaches devised in Chapter 2 may also be used to study annual changes in the distributions of other taxa with opportunistic observation records, for example the National Moth Recording Scheme (NMRS) consists of distribution records for UK moths, and has reached over 15 millions record since its introduction in 2007 (Fox et al. 2013).

In this thesis applications were limited to only the UKBMS and BNM data for UK butterflies, but as described in Section 1.3.3, the WCBS also exists to improve monitoring of the wider countryside and could be used in combination with the other schemes. The WCBS data are currently incorporated with UKBMS data for wider countryside species using the two-stage GAM approach (Brereton et al. 2014), and trends in abundance from the WCBS have been shown to correlate with those from the UKBMS (Roy et al. 2014). As mentioned in Section 2.5, combining multiple sources of information, for example count data with opportunistic records as in Pagel et al. (2014), is also an avenue for further work.

In Chapter 2, dynamic occupancy maps were proposed as a tool for visualising spatio-temporal change in butterfly distributions. Further work could be undertaken to ascertain the performance of site-occupancy models and the associated dynamic maps for more habitat-specialist species with limited ranges. Similarly, applications of the models for abundance in this thesis require testing for habitat-specialist species, which often have limited data.

For some habitat-specialist species additional methods are used to monitor abundance: adult timed counts, larval web counts and egg counts (Br-

ereton et al. 2014). There is potential to adapt the dynamic models to incorporate data on other stages of the butterfly life-cycle, as discussed in Section 6.3, which could lead to stage-specific parameter estimates such as survival (Manly 1974), and hence aid the monitoring and conservation of rarer species. Another possible adaptation of the dynamic models is to the study of possible drivers for the timing and magnitude of annual influxes of migratory species such as Painted Lady and Red Admiral, including measures of climate (Sparks et al. 2005). Similarly, population dynamics for species which overwinter in the adult stage, such as Brimstone and Small Tortoiseshell, could be studied.

Temporal changes in abundance have been the focus in Chapters 4-6, but spatial variation in abundance could be investigated and visualised using maps or regional indices, as for the occupancy models in Chapter 2. It will also be valuable to model changes in occupancy and abundance at more local scales, for example at sites of particular conservation interest, and in this case using the UKBMS data at the site section level may be valuable. There is also potential to account for spatial autocorrelation in butterfly occupancy and or abundance, as discussed in Sections 2.5 and 6.3. Density-dependence is another factor that could be explored, as advocated in Nowicki et al. (2009). The models in this thesis could also be adapted to explore synchrony in populations (Sutcliffe et al. 1996; Powney et al. 2010), either between sites for a given species or across sites but between multiple species, by incorporating random effects (Lahoz-Monfort et al. 2011, 2013), for example in the ρ parameter for productivity in the dynamic models. A preliminary study has been performed, exploring synchrony between similar species using occupancy models.

Many of these modelling suggestions may be most feasible within a Bayesian framework, which can readily incorporate hierarchical models. All analyses in this thesis were made using maximum-likelihood estimation. Random effects were used to describe many abundance parameters in Chapter 3 and Section 5.4, but, as discussed, this may be more straightforward in a Bayesian context. Despite this, classical inference may be favoured: meth-

ods of model selection and goodness-of-fit are better established and there is no need to choose suitable priors and undertake prior sensitivity studies. Moreover, when describing methods for producing indices of abundance which are used for reporting trends, it is possible that classical approaches may be more interpretable to non-experts, such as citizen scientists. In the context of modelling large datasets, for many species, Bayesian methods can be highly computer intensive, which could be prohibitive when indices require annual updates, although this is likely to become less restrictive in future.

Although associated `R` code is provided in an electronic appendix to this thesis, the possibility of developing a free, easy to use, statistical package in `R`, which incorporates general frameworks for modelling the abundance of seasonal insects of butterflies, could encourage the wider application of these methods by producing more accessible tools for users.

Bibliography

Aarts, G., Fieberg, J. and Matthiopoulos, J. (2012). Comparative interpretation of count, presence–absence and point methods for species distribution models. *Methods in Ecology and Evolution*, **3**, 177–187.

Altermatt, F. (2010a). Climatic warming increases voltinism in European butterflies and moths. *Proceedings of the Royal Society B: Biological Sciences*, **277**, 1281–1287.

Altermatt, F. (2010b). Tell me what you eat and I'll tell you when you fly: diet can predict phenological changes in response to climate change. *Ecology Letters*, **13**, 1475–1484.

Asher, J., Fox, R. and Warren, M. S. (2011). British butterfly distributions and the 2010 target. *Journal of Insect Conservation*, **15**, 291–299.

Asher, J., Warren, M., Fox, R., Harding, P., Jeffcoate, G. and Jeffcoate, S. (2001). *The Millennium Atlas of Butterflies in Britain and Ireland*. Oxford University Press.

Barnosky, A. D., Matzke, N., Tomiya, S., Wogan, G. O., Swartz, B., Quental, T. B., Marshall, C., McGuire, J. L., Lindsey, E. L., Maguire, K. C., Mersey, B. and Ferrer, E. A. (2011). Has the Earth's sixth mass extinction already arrived? *Nature*, **471**, 51–57.

Bates, A. J., Sadler, J. P., Everett, G., Grundy, D., Lowe, N., Davis, G., Baker, D., Bridge, M., Clifton, J., Freestone, R. et al. (2013). Assessing the value of the Garden Moth Scheme citizen science dataset: how does

light trap type affect catch? *Entomologia Experimentalis et Applicata*, **146**, 386–397.

Baur, B., Coray, A., Minoretti, N. and Zschokke, S. (2005). Dispersal of the endangered flightless beetle *Dorcadion fuliginator* (Coleoptera: Cerambycidae) in spatially realistic landscapes. *Biological Conservation*, **124**, 49–61.

Bell, S., Marzano, M., Cent, J., Kobierska, H., Podjed, D., Vandzinskaite, D., Reinert, H., Armaitiene, A., Grodzińska-Jurczak, M. and Muršič, R. (2008). What counts? Volunteers and their organisations in the recording and monitoring of biodiversity. *Biodiversity and Conservation*, **17**, 3443–3454.

Besbeas, P. and Morgan, B. J. T. (2012). A threshold model for heron productivity. *Journal of Agricultural, Biological, and Environmental Statistics*, **17**, 128–141.

Bishop, T. R., Botham, M. S., Fox, R., Leather, S. R., Chapman, D. S. and Oliver, T. H. (2013). The utility of distribution data in predicting phenology. *Methods in Ecology and Evolution*, **4**, 1024–1032.

Bled, F., Royle, J. A. and Cam, E. (2011). Hierarchical modeling of an invasive spread: the Eurasian Collared-Dove *Streptopelia decaocto* in the United States. *Ecological Applications*, **21**, 290–302.

Botham, M. S., Brereton, T. M., Middlebrook, I., Cruickshanks, K. L., Harrower, C., Beckmann, B. and Roy, D. B. (2008). United Kingdom Butterfly Monitoring Scheme report for 2008. CEH Wallingford.

Botham, M. S., Brereton, T. M., Middlebrook, I., Randle, Z. and Roy, D. B. (2013a). United Kingdom Butterfly Monitoring Scheme report for 2011. Centre for Ecology & Hydrology.

Botham, M. S., Brereton, T. M., Middlebrook, I., Randle, Z. and Roy, D. B. (2013b). United Kingdom Butterfly Monitoring Scheme report for 2012. Centre for Ecology & Hydrology.

Brereton, T. M., Botham, M. S., Middlebrook, I., Randle, Z., Noble, D. G. and Roy, D. B. (2014). United Kingdom Butterfly Monitoring Scheme report for 2013. Centre for Ecology and Hydrology and Butterfly Conservation.

Brereton, T. M., Cruickshanks, K. L., Risely, K., Noble, D. G. and Roy, D. B. (2011a). Developing and launching a wider countryside butterfly survey across the United Kingdom. *Journal of Insect Conservation*, **15**, 279–290.

Brereton, T. M., Roy, D. B., Middlebrook, I., Botham, M. S. and Warren, M. S. (2011b). The development of butterfly indicators in the United Kingdom and assessments in 2010. *Journal of Insect Conservation*, **15**, 139–151.

Brewer, C. (2008). Using generalized estimating equations with regression splines to improve analysis of butterfly transect data. MPhil thesis, University of St. Andrews.

Bried, J. T. and Pellet, J. (2011). Optimal design of butterfly occupancy surveys and testing if occupancy converts to abundance for sparse populations. *Journal of Insect Conservation*, pp. 1–11.

Buckland, S., Magurran, A., Green, R. and Fewster, R. (2005). Monitoring change in biodiversity through composite indices. *Philosophical Transactions of the Royal Society B: Biological Sciences*, **360**, 243–254.

Butchart, S. H., Walpole, M., Collen, B., van Strien, A., Scharlemann, J. P., Almond, R. E., Baillie, J. E., Bomhard, B., Brown, C., Bruno, J. et al. (2010). Global biodiversity: indicators of recent declines. *Science*, **328**, 1164–1168.

Byrd, R. H., Lu, P., Nocedal, J. and Zhu, C. (1995). A limited memory algorithm for bound constrained optimization. *SIAM Journal on Scientific Computing*, **16**, 1190–1208.

Calabrese, J. M. (2012). How emergence and death assumptions affect count-based estimates of butterfly abundance and lifespan. *Population Ecology*, **54**, 431–442.

Catchpole, E. A., Kgosi, P. M. and Morgan, B. J. T. (2001). On the near-singularity of models for animal recovery data. *Biometrics*, **57**, 720–726.

Catchpole, E. A. and Morgan, B. J. T. (1997). Detecting parameter redundancy. *Biometrika*, **84**, 187–196.

Cayton, H. L., Haddad, N. M., Gross, K., Diamond, S. E. and Ries, L. (2015). Do growing degree days predict phenology across butterfly species?. *Ecology*, DOI: http://dx.doi.org/10.1890/15-0131.1.

Chakraborty, A., Gelfand, A. E., Wilson, A. M., Latimer, A. M. and Silander, J. A. (2011). Point pattern modelling for degraded presence-only data over large regions. *Journal of the Royal Statistical Society: Series C (Applied Statistics)*, **60**, 757–776.

Chambers, J. M. and Hastie, T. J. (1991). *Statistical models in S*. Chapman & Hall/CRC, Boca Raton.

Chambert, T., Kendall, W. L., Hines, J. E., Nichols, J. D., Pedrini, P., Waddle, J. H., Tavecchia, G., Walls, S. C. and Tenan, S. (2015). Testing hypotheses on distribution shifts and changes in phenology of imperfectly detectable species. *Methods in Ecology and Evolution*, DOI: 10.1111/2041-210X.12362.

Chapin III, F. S., Zavaleta, E. S., Eviner, V. T., Naylor, R. L., Vitousek, P. M., Reynolds, H. L., Hooper, D. U., Lavorel, S., Sala, O. E., Hobbie, S. E. et al. (2000). Consequences of changing biodiversity. *Nature*, **405**, 234–242.

Cole, D. J. and Morgan, B. J. T. (2010). Parameter redundancy with covariates. *Biometrika*, **97**, 1002–1005.

Conrad, K. F., Warren, M. S., Fox, R., Parsons, M. S. and Woiwod, I. P. (2006). Rapid declines of common, widespread British moths provide evidence of an insect biodiversity crisis. *Biological Conservation*, **132**, 279–291.

Convention on Biological Diversity (2006). Framework for monitoring implementation of the achievement of the 2010 target and integration of targets into the thematic programmes of work, COP 8 Decision VIII/15. `www.cbd.int/decisions`.

Cormack, R. M. (1989). Log-linear models for capture-recapture. *Biometrics*, **45**, 395–413.

Cornulier, T., Elston, D. A., Arcese, P., Benton, T. G., Douglas, D. J., Lambin, X., Reid, J., Robinson, R. A. and Sutherland, W. J. (2009). Estimating the annual number of breeding attempts from breeding dates using mixture models. *Ecology Letters*, **12**, 1184–1193.

Couturier, T., Cheylan, M., Bertolero, A., Astruc, G. and Besnard, A. (2013). Estimating abundance and population trends when detection is low and highly variable: A comparison of three methods for the Hermann's tortoise. *The Journal of Wildlife Management*, **77**, 454–462.

Cowley, M. J. R., Thomas, C. D., Thomas, J. A. and Warren, M. S. (1999). Flight areas of British butterflies: assessing species status and decline. *Proceedings of the Royal Society of London. Series B: Biological Sciences*, **266**, 1587–1592.

Dail, D. and Madsen, L. (2011). Models for estimating abundance from repeated counts of an open metapopulation. *Biometrics*, **67**, 577–587.

Dapporto, L. and Dennis, R. L. H. (2013). The generalist–specialist continuum: testing predictions for distribution and trends in British butterflies. *Biological Conservation*, **157**, 229–236.

Defra (2013). UK Biodiversity indicators in your pocket 2013. Published by Defra on Behalf of the UK Biodiversity Partnership, Defra, London.

Dénes, F. V., Silveira, L. F. and Beissinger, S. R. (2015). Estimating abundance of unmarked animal populations: accounting for imperfect detection and other sources of zero inflation. *Methods in Ecology and Evolution*, DOI: 10.1111/2041-210X.12333.

Dennis, E. B., Freeman, S. N., Brereton, T. and Roy, D. B. (2013). Indexing butterfly abundance whilst accounting for missing counts and variability in seasonal pattern. *Methods in Ecology and Evolution*, **4**, 637–645.

Dennis, E. B., Morgan, B. J. T., Freeman, S. N., Brereton, T. and Roy, D. B. (2014). A generalised abundance index for seasonal invertebrates. Technical report UKC/SMSAS/14/006, University of Kent. Submitted to the *Annals of Applied Statistics*.

Dennis, E. B., Morgan, B. J. T., Freeman, S. N., Roy, D. B. and Brereton, T. (2015a). Dynamic models for longitudinal butterfly data. Technical report `https://kar.kent.ac.uk/id/eprint/46264`, University of Kent. Submitted to the *Journal of Agricultural, Biological, and Environmental Statistics*.

Dennis, E. B., Morgan, B. J. T. and Ridout, M. S. (2015b). Computational aspects of N-mixture models. *Biometrics*, DOI: 10.1111/biom.12246.

Dennis, R. L. H., Shreeve, T. G., Arnold, H. R. and Roy, D. B. (2005). Does diet breadth control herbivorous insect distribution size? Life history and resource outlets for specialist butterflies. *Journal of Insect Conservation*, **9**, 187–200.

Dennis, R. L. H. and Sparks, T. H. (2007). Climate signals are reflected in an 89 year series of British Lepidoptera records. *European Journal of Entomology*, **104**, 763–767.

Devictor, V., Whittaker, R. J. and Beltrame, C. (2010). Beyond scarcity: citizen science programmes as useful tools for conservation biogeography. *Diversity and Distributions*, **16**, 354–362.

Diamond, S. E., Frame, A. M., Martin, R. A. and Buckley, L. B. (2011). Species' traits predict phenological responses to climate change in butterflies. *Ecology*, **92**, 1005–1012.

Díaz, S., Fargione, J., Chapin III, F. S. and Tilman, D. (2006). Biodiversity loss threatens human well-being. *PLoS Biology*, **4**, e277.

Dodd, C. K. and Dorazio, R. M. (2004). Using counts to simultaneously estimate abundance and detection probabilities in a salamander community. *Herpetologica*, **60**, 468–478.

Dorazio, R. M. (2007). On the choice of statistical models for estimating occurrence and extinction from animal surveys. *Ecology*, **88**, 2773–2782.

Dorazio, R. M., Martin, J. and Edwards, H. H. (2013). Estimating abundance while accounting for rarity, correlated behavior, and other sources of variation in counts. *Ecology*, **94**, 1472–1478.

Elith, J., H. Graham, C., P. Anderson, R., Dudk, M., Ferrier, S., Guisan, A., J. Hijmans, R., Huettmann, F., R. Leathwick, J., Lehmann, A., Li, J., G. Lohmann, L., A. Loiselle, B., Manion, G., Moritz, C., Nakamura, M., Nakazawa, Y., McC. M. Overton, J., Townsend Peterson, A., J. Phillips, S., Richardson, K., Scachetti-Pereira, R., E. Schapire, R., Sobern, J., Williams, S., S. Wisz, M. and E. Zimmermann, N. (2006). Novel methods improve prediction of species' distributions from occurrence data. *Ecography*, **29**, 129–151.

Elith, J., Phillips, S. J., Hastie, T. J., Dudík, M., Chee, Y. E. and Yates, C. J. (2011). A statistical explanation of MaxEnt for ecologists. *Diversity and Distributions*, **17**, 43–57.

Elston, D. A., Nevison, I. M., Scott, W. A., Sier, A. R. J. and Morecroft, M. D. (2011). Power calculations for monitoring studies: a case study with alternative models for random variation. *Environmetrics*, **22**, 618–625.

Ferrer-Paris, J. R., Sánchez-Mercado, A., Rodríguez-Clark, K. M., Rodríguez, J. P. and Rodríguez, G. A. (2014). Using limited data to

detect changes in species distributions: insights from Amazon parrots in Venezuela. *Biological Conservation*, **173**, 133–143.

Fewster, R. M., Buckland, S. T., Siriwardena, G. M., Baillie, S. R. and Wilson, J. D. (2000). Analysis of population trends for farmland birds using generalized additive models. *Ecology*, **81**, 1970–1984.

Fielding, A. H. and Bell, J. F. (1997). A review of methods for the assessment of prediction errors in conservation presence/absence models. *Environmental Conservation*, **24**, 38–49.

Fiske, I. and Chandler, R. B. (2011). `unmarked`: An R package for fitting hierarchical models of wildlife occurrence and abundance. *Journal of Statistical Software*, **43**, 1–23.

Fithian, W., Hastie, T. et al. (2013). Finite-sample equivalence in statistical models for presence-only data. *Annals of Applied Statistics*, **7**, 1917–1939.

Fitzpatrick, M. C., Gotelli, N. J. and Ellison, A. M. (2013). MaxEnt versus MaxLike: empirical comparisons with ant species distributions. *Ecosphere*, **4**, art55.

Flockhart, D. T. T., Wassenaar, L. I., Martin, T. G., Hobson, K. A., Wunder, M. B. and Norris, D. R. (2013). Tracking multi-generational colonization of the breeding grounds by monarch butterflies in eastern North America. *Proceedings of the Royal Society B: Biological Sciences*, **280**, 20131087.

Forister, M. L. and Shapiro, A. M. (2003). Climatic trends and advancing spring flight of butterflies in lowland California. *Global Change Biology*, **9**, 1130–1135.

Fox, R., Brereton, T. M., Botham, M. S., Middlebrook, I., Roy, D. B. and Warren, M. S. (2011a). The state of the UK's Butterflies 2011. Butterfly Conservation and the Centre for Ecology & Hydrology, Dorset.

Fox, R., Parsons, M. S., Chapman, J. W., Woiwod, I. P., Warren, M. S. and Brooks, D. R. (2013). The state of Britain's larger moths 2013. Butterfly Conservation and Rothamstead Research, Dorset.

Fox, R., Randle, Z., Hill, L., Anders, S., Wiffen, L. and Parsons, M. (2011b). Moths count: recording moths for conservation in the UK. *Journal of Insect Conservation*, **15**, 55–68.

Fox, R., Warren, M. S., Asher, J., Brereton, T. M. and Roy, D. B. (2007). The state of Britain's butterflies 2007. Butterfly Conservation and the Centre for Ecology & Hydrology, Dorset.

Fox, R., Warren, M. S., Brereton, T. M., Roy, D. B. and Robinson, A. (2011c). A new Red List of British butterflies. *Insect Conservation and Diversity*, **4**, 159–172.

Franco, A., Hill, J. K., Kitschke, C., Collingham, Y. C., Roy, D. B., Fox, R., Huntley, B. and Thomas, C. D. (2006). Impacts of climate warming and habitat loss on extinctions at species' low-latitude range boundaries. *Global Change Biology*, **12**, 1545–1553.

Freeman, S. N. and Newson, S. E. (2008). On a log-linear approach to detecting ecological interactions in monitored populations. *Ibis*, **150**, 250–258.

Gaston, K. J. (1991). The magnitude of global insect species richness. *Conservation Biology*, **5**, 283–296.

Gillingham, P. K., Alison, J., Roy, D. B., Fox, R. and Thomas, C. D. (2014). High abundances of species in protected areas in parts of their geographic distributions colonised during a recent period of climatic change. *Conservation Letters*, DOI: 10.1111/conl.12118.

Glowka, L., Burhenne-Guilmin, F. and Synge, H. (1994). Guide to the convention on biological diversity. IUCN, Gland.

Graves, T. A., Kendall, K. C., Royle, J. A., Stetz, J. B. and Macleod, A. C. (2011). Linking landscape characteristics to local grizzly bear abundance using multiple detection methods in a hierarchical model. *Animal Conservation*, **14**, 652–664.

Greatorex-Davies, J. N. and Roy, D. B. (2003). The Butterfly Monitoring Scheme: Report to recorders 2002. CEH Monks Wood.

Green, P. J. and Silverman, B. W. (1994). *Nonparametric Regression and Generalized Linear Models*. Chapman & Hall, London.

Gross, K., Kalendra, E. J., Hudgens, B. R. and Haddad, N. M. (2007). Robustness and uncertainty in estimates of butterfly abundance from transect counts. *Population Ecology*, **49**, 191–200.

Guillera-Arroita, G., Lahoz-Monfort, J. J. and Elith, J. (2014a). Maxent is not a presence-absence method: a comment on Thibaud et al.. *Methods in Ecology and Evolution*, **5**, 1192–1197.

Guillera-Arroita, G., Lahoz-Monfort, J. J., MacKenzie, D. I., Wintle, B. A. and McCarthy, M. A. (2014b). Ignoring imperfect detection in biological surveys is dangerous: A response to 'Fitting and Interpreting Occupancy Models'. *PloS one*, **9**, e99571.

Guillera-Arroita, G., Ridout, M. S. and Morgan, B. J. T. (2010). Design of occupancy studies with imperfect detection. *Methods in Ecology and Evolution*, **1**, 131–139.

Guillera-Arroita, G., Ridout, M. S. and Morgan, B. J. T. (2014). Two-stage Bayesian study design for species occupancy estimation. *Journal of Agricultural, Biological, and Environmental Statistics*, **19**, 278–291.

Guillera-Arroita, G., Ridout, M. S., Morgan, B. J. T. and Linkie, M. (2012). Models for species-detection data collected along transects in the presence of abundance-induced heterogeneity and clustering in the detection process. *Methods in Ecology and Evolution*, **3**, 358–367.

Haddad, N. M., Hudgens, B., Damiani, C., Gross, K., Kuefler, D. and Pollock, K. (2008). Determining optimal population monitoring for rare butterflies. *Conservation Biology*, **22**, 929–940.

Hanczar, B., Hua, J., Sima, C., Weinstein, J., Bittner, M. and Dougherty, E. R. (2010). Small-sample precision of ROC-related estimates. *Bioinformatics*, **26**, 822–830.

Harrison, P. J., Buckland, S. T., Yuan, Y., Elston, D. A., Brewer, M. J., Johnston, A. and Pearce-Higgins, J. W. (2014). Assessing trends in biodiversity over space and time using the example of British breeding birds. *Journal of Applied Ecology*, **51**, 1650–1660.

Hastie, T. J. and Fithian, W. (2013). Inference from presence-only data; the ongoing controversy. *Ecography*, **36**, 864–867.

Hastie, T. J. and Tibshirani, R. J. (1990). *Generalized Additive Models*. Chapman & Hall/CRC, London.

Hickling, R., Roy, D. B., Hill, J. K., Fox, R. and Thomas, C. D. (2006). The distributions of a wide range of taxonomic groups are expanding polewards. *Global Change Biology*, **12**, 450–455.

Hickling, R., Roy, D. B., Hill, J. K. and Thomas, C. D. (2005). A northward shift of range margins in British Odonata. *Global Change Biology*, **11**, 502–506.

Higa, M., Yamaura, Y., Koizumi, I., Yabuhara, Y., Senzaki, M. and Ono, S. (2015). Mapping large-scale bird distributions using occupancy models and citizen data with spatially biased sampling effort. *Diversity and Distributions*, **21**, 46–54.

Hilbe, J. M. (2011). *Negative Binomial Regression*. Cambridge University Press, New York.

Hill, J. K., Thomas, C. D., Fox, R., Telfer, M. G., Willis, S. G., Asher, J. and Huntley, B. (2002). Responses of butterflies to twentieth century

climate warming: implications for future ranges. *Proceedings of the Royal Society of London. Series B: Biological Sciences*, **269**, 2163–2171.

Hill, M. O. (2011). Local frequency as a key to interpreting species occurrence data when recording effort is not known. *Methods in Ecology and Evolution*, **3**, 195–205.

Hindle, B. J., Kerr, C. L., Richards, S. A. and Willis, S. G. (2014). Topographical variation reduces phenological mismatch between a butterfly and its nectar source. *Journal of Insect Conservation*, DOI: 10.1007/s10841-014-9713-x.

Hines, J. E. (2011). Program `presence` 4.1–software to estimate patch occupancy and related parameters. U.S. Geological Survey Patuxent Wildlife Research Center, Maryland. `www.mbrpwrc.usgs.gov/software/presence.html`.

Hochachka, W. M., Fink, D., Hutchinson, R. A., Sheldon, D., Wong, W. K. and Kelling, S. (2012). Data-intensive science applied to broad-scale citizen science. *Trends in Ecology & Evolution*, **27**, 130–137.

Hodgson, J. A., Thomas, C. D., Oliver, T. H., Anderson, B. J., Brereton, T. M. and Crone, E. E. (2011). Predicting insect phenology across space and time. *Global Change Biology*, **17**, 1289–1300.

Hunt, J. W., Weckerly, F. W. and Ott, J. R. (2012). Reliability of occupancy and binomial mixture models for estimating abundance of golden-cheeked warblers (*Setophaga chrysoparia*). *The Auk*, **129**, 105–114.

Insect Count Analyzer (INCA) (2011). A user-friendly program to analyze transect count data. The Urban Wildlands Group, `http://www.urbanwildlands.org/INCA`.

Isaac, N. J. B., Cruickshanks, K. L., Weddle, A. M., Rowcliffe, J. M., Brereton, T. M., Dennis, R. L. H., Shuker, D. M. and Thomas, C. D. (2011a). Distance sampling and the challenge of monitoring butterfly populations. *Methods in Ecology and Evolution*, **2**, 585–594.

Isaac, N. J. B., Girardello, M., Brereton, T. M. and Roy, D. B. (2011b). Butterfly abundance in a warming climate: patterns in space and time are not congruent. *Journal of Insect Conservation*, **15**, 233–240.

Isaac, N. J. B., Strien, A. J., August, T. A., Zeeuw, M. P. and Roy, D. B. (2014). Statistics for citizen science: extracting signals of change from noisy ecological data. *Methods in Ecology and Evolution*, **5**, 1052–1060.

Jackson, C. H. (2011). Multi-state models for panel data: The msm package for R. *Journal of Statistical Software*, **38**, 1–29.
URL: *http://www.jstatsoft.org/v38/i08/*

Johnson, D. S., Conn, P., Hooten, M., Ray, J. and Pond, B. A. (2012). Spatial occupancy models for large data sets. *Ecology*, **94**, 801–808.

Johnson, N. L., Kotz, S. and Balakrishnan, N. (1997). *Discrete Multivariate Distributions*. Wiley, New York.

Joseph, L. N., Elkin, C., Martin, T. G. and Possingham, H. P. (2009). Modeling abundance using N-mixture models: the importance of considering ecological mechanisms. *Ecological Applications*, **19**, 631–642.

Jost, T. A., Brcich, R. F. and Zoubir, A. M. (2006). Estimating the parameters of the multivariate Poisson distribution using the composite likelihood concept. *in* 'The Proceedings of the 31st IEEE International Conference on Acoustics, Speech and Signal Processing'. Toulouse, France.

Karlis, D. (2003). An EM algorithm for multivariate Poisson distribution and related models. *Journal of Applied Statistics*, **30**, 63–77.

Karlsson, B. (2014). Extended season for northern butterflies. *International Journal of Biometeorology*, **58**, 691–701.

Kendall, W. L., Hines, J. E., Nichols, J. D. and Grant, E. H. C. (2013). Relaxing the closure assumption in occupancy models: staggered arrival and departure times. *Ecology*, **94**, 610–617.

Kéry, M. (2008). Estimating abundance from bird counts: binomial mixture models uncover complex covariate relationships. *The Auk*, **125**, 336–345.

Kéry, M. (2011). Towards the modelling of true species distributions. *Journal of Biogeography*, **38**, 617–618.

Kéry, M., Dorazio, R. M., Soldaat, L., Van Strien, A., Zuiderwijk, A. and Royle, J. A. (2009). Trend estimation in populations with imperfect detection. *Journal of Applied Ecology*, **46**, 1163–1172.

Kéry, M., Gardner, B. and Monnerat, C. (2010a). Predicting species distributions from checklist data using site-occupancy models. *Journal of Biogeography*, **37**, 1851–1862.

Kéry, M., Guillera-Arroita, G. and Lahoz-Monfort, J. J. (2013). Analysing and mapping species range dynamics using occupancy models. *Journal of Biogeography*, **40**, 1463–1474.

Kéry, M., Royle, J. A. and Schmid, H. (2005). Modeling avian abundance from replicated counts using binomial mixture models. *Ecological Applications*, **15**, 1450–1461.

Kéry, M., Royle, J. A., Schmid, H., Schaub, M., Volet, B., Häfliger, G. and Zbinden, N. (2010b). Site–occupancy distribution modeling to correct population–trend estimates derived from opportunistic observations. *Conservation Biology*, **24**, 1388–1397.

King, R. (2014). Statistical ecology. *Annual Review of Statistics and its Application*, **1**, 401–426.

Knape, J. and Korner-Nievergelt, F. (2015). Estimates from non-replicated population surveys rely on critical assumptions. *Methods in Ecology and Evolution*, DOI: 10.1111/2041-210X.12329.

Lahoz-Monfort, J. J., Guillera-Arroita, G. and Wintle, B. A. (2014). Imperfect detection impacts the performance of species distribution models. *Global Ecology and Biogeography*, **23**, 504–515.

Lahoz-Monfort, J. J., Morgan, B. J. T., Harris, M. P., Daunt, F., Wanless, S. and Freeman, S. N. (2013). Breeding together: modeling synchrony in productivity in a seabird community. *Ecology*, **94**, 3–10.

Lahoz-Monfort, J. J., Morgan, B. J. T., Harris, M. P., Wanless, S. and Freeman, S. N. (2011). A capture–recapture model for exploring multi-species synchrony in survival. *Methods in Ecology and Evolution*, **2**, 116–124.

Liu, C., White, M. and Newell, G. (2011). Measuring and comparing the accuracy of species distribution models with presence–absence data. *Ecography*, **34**, 232–243.

Lobo, J. M., Jiménez-Valverde, A. and Real, R. (2008). AUC: a misleading measure of the performance of predictive distribution models. *Global Ecology and Biogeography*, **17**, 145–151.

MacKenzie, D. I., Nichols, J. D., Hines, J. E., Knutson, M. G. and Franklin, A. B. (2003). Estimating site occupancy, colonization, and local extinction when a species is detected imperfectly. *Ecology*, **84**, 2200–2207.

MacKenzie, D. I., Nichols, J. D., Royle, J. A., Pollock, K. H., Bailey, L. L. and Hines, J. E. (2006). *Occupancy Estimation and Modeling: Inferring Patterns and Dynamics of Species Occurrence*. Academic Press, New York.

Mair, L., Thomas, C. D., Anderson, B. J., Fox, R., Botham, M. and Hill, J. K. (2012). Temporal variation in responses of species to four decades of climate warming. *Global Change Biology*, **18**, 2439–2447.

Manly, B. F. J. (1974). Estimation of stage-specific survival rates and other parameters for insect populations developing through several stages. *Oecologia*, **15**, 277–285.

Martin, J., Royle, J. A., Mackenzie, D. I., Edwards, H. H., Kéry, M. and Gardner, B. (2011). Accounting for non-independent detection when es-

timating abundance of organisms with a Bayesian approach. *Methods in Ecology and Evolution*, **2**, 595–601.

Matechou, E., Dennis, E. B., Freeman, S. N. and Brereton, T. (2014). Monitoring abundance and phenology in (multivoltine) butterfly species: a novel mixture model. *Journal of Applied Ecology*, **51**, 766–775.

Matechou, E., Morgan, B. J. T., Pledger, S., Collazo, J. A. and Lyons, J. E. (2013). Integrated analysis of capture–recapture–resighting data and counts of unmarked birds at stop-over sites. *Journal of Agricultural, Biological, and Environmental Statistics*, **18**, 120–135.

McIntyre, A. P., Jones, J. E., Lund, E. M., Waterstrat, F. T., Giovanini, J. N., Duke, S. D., Hayes, M. P., Quinn, T. and Kroll, A. J. (2012). Empirical and simulation evaluations of an abundance estimator using unmarked individuals of cryptic forest-dwelling taxa. *Forest Ecology and Management*, **286**, 129–136.

McLachlan, G. and Peel, D. (2004). *Finite Mixture Models*. Wiley, New York.

Meier, P. (1953). Variance of a weighted mean. *Biometrics*, **9**, 59–73.

Merow, C. and Silander, J. A. (2014). A comparison of Maxlike and Maxent for modelling species distributions. *Methods in Ecology and Evolution*, **5**, 215–225.

Merow, C., Smith, M. J. and Silander, J. A. (2013). A practical guide to MaxEnt for modeling species distributions: what it does, and why inputs and settings matter. *Ecography*, **36**, 1058–1069.

Met Office (2015). UK climate - Historic station data. `http://www.metoffice.gov.uk/public/weather/climate-historic` [Accessed 21 January 2015].

Morton, R. D., Rowland, C. S., Wood, C. M., Meek, L., Marston, C. G. and Smith, G. M. (2014). Land Cover Map 2007 (1km percentage aggregate

class, GB) v1.2. NERC-Environmental Information Data Centre. DOI: 10.5285/289805c2-4be7-4fb5-b6ec-1539ed88c43d.

Nowicki, P., Bonelli, S., Barbero, F. and Balletto, E. (2009). Relative importance of density-dependent regulation and environmental stochasticity for butterfly population dynamics. *Oecologia*, **161**, 227–239.

Nowicki, P., Settele, J., Henry, P.-Y. and Woyciechowski, M. (2008). Butterfly monitoring methods: the ideal and the real world. *Israel Journal of Ecology & Evolution*, **54**, 69–88.

Nychka, D., Furrer, R. and Sain, S. (2014). *fields: Tools for spatial data*. R package version 7.1. `http://CRAN.R-project.org/package=fields`.

Oliver, T. H., Brereton, T. and Roy, D. B. (2013). Population resilience to an extreme drought is influenced by habitat area and fragmentation in the local landscape. *Ecography*, **36**, 579–586.

Pagel, J., Anderson, B. J., O'Hara, R. B., Cramer, W., Fox, R., Jeltsch, F., Roy, D. B., Thomas, C. D. and Schurr, F. M. (2014). Quantifying range-wide variation in population trends from local abundance surveys and widespread opportunistic occurrence records. *Methods in Ecology and Evolution*, **5**, 751–760.

Parker, D. E., Legg, T. P. and Folland, C. K. (1992). A new daily central England temperature series, 1772–1991. *International Journal of Climatology*, **12**, 317–342.

Parmesan, C. (2007). Influences of species, latitudes and methodologies on estimates of phenological response to global warming. *Global Change Biology*, **13**, 1860–1872.

Parmesan, C., Ryrholm, N., Stefanescu, C., Hill, J. K., Thomas, C. D., Descimon, H., Huntley, B., Kaila, L., Kullberg, J., Tammaru, T. et al. (1999). Poleward shifts in geographical ranges of butterfly species associated with regional warming. *Nature*, **399**, 579–583.

Pearman, P. B. and Weber, D. (2007). Common species determine richness patterns in biodiversity indicator taxa. *Biological Conservation*, **138**, 109–119.

Pellet, J., Bried, J. T., Parietti, D., Gander, A., Heer, P. O., Cherix, D. and Arlettaz, R. (2012). Monitoring butterfly abundance: beyond Pollard walks. *PloS one*, **7**, e41396.

Pereira, H. M., Leadley, P. W., Proença, V., Alkemade, R., Scharlemann, J. P., Fernandez-Manjarrés, J. F., Araújo, M. B., Balvanera, P., Biggs, R., Cheung, W. W. et al. (2010). Scenarios for global biodiversity in the 21st century. *Science*, **330**, 1496–1501.

Phillips, S. J., Anderson, R. P. and Schapire, R. E. (2006). Maximum entropy modeling of species geographic distributions. *Ecological Modelling*, **190**, 231–259.

Pollard, E. (1988). Temperature, rainfall and butterfly numbers. *Journal of Applied Ecology*, **25**, 819–828.

Pollard, E. and Yates, T. J. (1993). *Monitoring Butterflies for Ecology and Conservation: the British Butterfly Monitoring Scheme*. Chapman & Hall, London.

Powney, G. D., Roy, D. B., Chapman, D. and Oliver, T. H. (2010). Synchrony of butterfly populations across species' geographic ranges. *Oikos*, **119**, 1690–1696.

Pöyry, J., Leinonen, R., Söderman, G., Nieminen, M., Heikkinen, R. K. and Carter, T. R. (2011). Climate-induced increase of moth multivoltinism in boreal regions. *Global Ecology and Biogeography*, **20**, 289–298.

R Core Team (2015). `R`: A Language and Environment for Statistical Computing. Vienna, Austria. `http://www.R-project.org/`.

Rands, M. R., Adams, W. M., Bennun, L., Butchart, S. H., Clements, A., Coomes, D., Entwistle, A., Hodge, I., Kapos, V., Scharlemann, J. P.

et al. (2010). Biodiversity conservation: challenges beyond 2010. *Science*, **329**, 1298–1303.

Renner, I. W. and Warton, D. I. (2013). Equivalence of MAXENT and Poisson point process models for species distribution modeling in ecology. *Biometrics*, **69**, 274–281.

Risely, K., Massimino, D., Johnston, A., Newson, S. E., Eaton, M. A., Musgrove, A. J., Noble, D. G., Procter, D. and Baillie, S. R. (2011). The Breeding Bird Survey 2011. British Trust for Ornithology, Thetford.

Roth, T., Strebel, N. and Amrhein, V. (2014). Estimating unbiased phenological trends by adapting site-occupancy models. *Ecology*, **95**, 2144–2154.

Rothery, P. and Roy, D. B. (2001). Application of generalized additive models to butterfly transect count data. *Journal of Applied Statistics*, **28**, 897–909.

Roy, D. B. and Asher, J. (2003). Spatial trends in the sighting dates of British butterflies. *International Journal of Biometeorology*, **47**, 188–192.

Roy, D. B., Ploquin, E. F., Randle, Z., Risely, K., Botham, M. S., Middlebrook, I., Noble, D., Cruickshanks, K., Freeman, S. N. and Brereton, T. M. (2014). Comparison of trends in butterfly populations between monitoring schemes. *Journal of Insect Conservation*, DOI: 10.1007/s10841-014-9739-0.

Roy, D. B., Rothery, P. and Brereton, T. (2007). Reduced-effort schemes for monitoring butterfly populations. *Journal of Applied Ecology*, **44**, 993–1000.

Roy, D. B., Rothery, P., Moss, D., Pollard, E. and Thomas, J. A. (2001). Butterfly numbers and weather: predicting historical trends in abundance and the future effects of climate change. *Journal of Animal Ecology*, **70**, 201–217.

Roy, D. B. and Sparks, T. H. (2000). Phenology of British butterflies and climate change. *Global Change Biology*, **6**, 407–416.

Royle, J. A. (2004a). N-mixture models for estimating population size from spatially replicated counts. *Biometrics*, **60**, 108–115.

Royle, J. A. (2004b). Generalized estimators of avian abundance from count survey data. *Animal Biodiversity and Conservation*, **27**, 375–386.

Royle, J. A., Chandler, R. B., Yackulic, C. and Nichols, J. D. (2012). Likelihood analysis of species occurrence probability from presence-only data for modelling species distributions. *Methods in Ecology and Evolution*, **3**, 545–554.

Royle, J. A. and Dorazio, R. M. (2008). *Hierarchical Modeling and Inference in Ecology*. Academic Press, Amsterdam.

Royle, J. A. and Kéry, M. (2007). A Bayesian state–space formulation of dynamic occupancy models. *Ecology*, **88**, 1813–1823.

Royle, J. A. and Nichols, J. D. (2003). Estimating abundance from repeated presence-absence data or point counts. *Ecology*, **84**, 777–790.

Royle, J. A., Nichols, J. D. and Kéry, M. (2005). Modelling occurrence and abundance of species when detection is imperfect. *Oikos*, **110**, 353–359.

Ruddock, J., Russell, M., Davidson, J. and Foster, A. (2007). Conserving biodiversity: the UK approach. Department for Environment, Food and Rural Affairs (DEFRA).

Sarre, S. D., MacDonald, A. J., Barclay, C., Saunders, G. R. and Ramsey, D. S. (2013). Foxes are now widespread in Tasmania: DNA detection defines the distribution of this rare but invasive carnivore. *Journal of Applied Ecology*, **50**, 459–468.

Schaub, M. and Kéry, M. (2012). Combining information in hierarchical models improves inferences in population ecology and demographic population analyses. *Animal Conservation*, **15**, 125–126.

Silvertown, J. (2009). A new dawn for citizen science. *Trends in ecology & evolution*, **24**, 467–471.

Sólymos, P., Lele, S. and Bayne, E. (2012). Conditional likelihood approach for analyzing single visit abundance survey data in the presence of zero inflation and detection error. *Environmetrics*, **23**, 197–205.

Sontag, E. D. and Zeilberger, D. (2010). A symbolic computation approach to a problem involving multivariate Poisson distributions. *Advances in Applied Mathematics*, **44**, 359–377.

Soulsby, R. L. and Thomas, J. A. (2012). Insect population curves: modelling and application to butterfly transect data. *Methods in Ecology and Evolution*, **3**, 832–841.

Sparks, T. H., Roy, D. B. and Dennis, R. L. H. (2005). The influence of temperature on migration of Lepidoptera into Britain. *Global Change Biology*, **11**, 507–514.

Sparks, T. H. and Yates, T. J. (1997). The effect of spring temperature on the appearance dates of British butterflies 1883–1993. *Ecography*, **20**, 368–374.

Stefanescu, C., Peñuelas, J. and Filella, I. (2003). Effects of climatic change on the phenology of butterflies in the northwest Mediterranean Basin. *Global Change Biology*, **9**, 1494–1506.

Strebel, N., Kéry, M., Schaub, M. and Schmid, H. (2014). Studying phenology by flexible modelling of seasonal detectability peaks. *Methods in Ecology and Evolution*, **5**, 483–490.

Sutcliffe, O. L., Thomas, C. D. and Moss, D. (1996). Spatial synchrony and asynchrony in butterfly population dynamics. *Journal of Animal Ecology*, **65**, 85–95.

Szabo, J. K., Vesk, P. A., Baxter, P. W. J. and Possingham, H. P. (2010). Regional avian species declines estimated from volunteer-collected long-

term data using List Length Analysis. *Ecological Applications*, **20**, 2157–2169.

Thomas, C. D., Cameron, A., Green, R. E., Bakkenes, M., Beaumont, L. J., Collingham, Y. C., Erasmus, B. F., De Siqueira, M. F., Grainger, A., Hannah, L. et al. (2004). Extinction risk from climate change. *Nature*, **427**, 145–148.

Thomas, C. D., Franco, A. and Hill, J. K. (2006). Range retractions and extinction in the face of climate warming. *Trends in Ecology & Evolution*, **21**, 415–416.

Thomas, C. D., Gillingham, P. K., Bradbury, R. B., Roy, D. B., Anderson, B. J., Baxter, J. M., Bourn, N. A. D., Crick, H. Q. P., Findon, R. A., Fox, R., Hodgson, J. A., Holt, A. R., Morecroft, M. D., O'Hanlon, N. J., Oliver, T. H., Pearce-Higgins, J. W., Procter, D. A., Thomas, J. A., Walker, K. J., Walmsley, C. A., Wilson, R. J. and Hill, J. K. (2012). Protected areas facilitate species range expansions. *Proceedings of the National Academy of Sciences*, **109**, 14063–14068.

Thomas, J. A. (2005). Monitoring change in the abundance and distribution of insects using butterflies and other indicator groups. *Philosophical Transactions of the Royal Society B: Biological Sciences*, **360**, 339–357.

Thomas, J. A., Telfer, M. G., Roy, D. B., Preston, C. D., Greenwood, J. J. D., Asher, J., Fox, R., Clarke, R. T. and Lawton, J. H. (2004). Comparative losses of British butterflies, birds, and plants and the global extinction crisis. *Science*, **303**, 1879–1881.

Thomas, J. and Lewington, R. (2010). *Butterflies of Britain and Ireland*. British Wildlife Publishing, Dorset.

Toribio, S., Gray, B. and Liang, S. (2012). An evaluation of the Bayesian approach to fitting the N-mixture model for use with pseudo-replicated count data. *Journal of Statistical Computation and Simulation*, **82**, 1135–1143.

Van Dyck, H., Bonte, D., Puls, R., Gotthard, K. and Maes, D. (2015). The lost generation hypothesis: could climate change drive ectotherms into a developmental trap? *Oikos*, **124**, 54–61.

van Strien, A. J., Pannekoek, J. and Gibbons, D. W. (2001). Indexing european bird population trends using results of national monitoring schemes: a trial of a new method. *Bird Study*, **48**, 200–213.

van Strien, A. J., Plantenga, W. F., Soldaat, L. L., van Swaay, C. A. M. and Wallis De Vries, M. F. (2008). Bias in phenology assessments based on first appearance data of butterflies. *Oecologia*, **156**, 227–235.

van Strien, A. J., Swaay, C. A. and Termaat, T. (2013). Opportunistic citizen science data of animal species produce reliable estimates of distribution trends if analysed with occupancy models. *Journal of Applied Ecology*, **50**, 1450–1458.

van Strien, A. J., Termaat, T., Groenendijk, D., Mensing, V. and Kéry, M. (2010). Site–occupancy models may offer new opportunities for dragonfly monitoring based on daily species lists. *Basic and Applied Ecology*, **11**, 495–503.

van Strien, A. J., van Swaay, C. A. M. and Kéry, M. (2011). Metapopulation dynamics in the butterfly *Hipparchia semele* changed decades before occupancy declined in The Netherlands. *Ecological Applications*, **21**, 2510–2520.

van Swaay, C. A. M., Nowicki, P., Settele, J. and van Strien, A. J. (2008). Butterfly monitoring in Europe: methods, applications and perspectives. *Biodiversity and Conservation*, **17**, 3455–3469.

van Swaay, C. A. M. and Warren, M. S. (2012). Developing butterflies as indicators in europe: current situation and future options. De Vlindersticht-ing/Dutch Butterfly Conservation, Butterfly Conversation UK, Butterfly Conservation Europe, Wageningen. VS2012.012.

van Swaay, C., Cuttelod, A., Collins, S., Maes, D., López Munguira, M., Šašić, M., Settele, J., Verovnik, R., Verstrael, T., Warren, M. and Wynhof, I. (2010). European Red List of Butterflies. Luxembourg: Publications Office of the European Union.

van Swaay, C., Maes, D., Collins, S., Munguira, M. L., Šašić, M., Settele, J., Verovnik, R., Warren, M., Wiemers, M., Wynhoff, I. et al. (2011). Applying IUCN criteria to invertebrates: How red is the Red List of European butterflies? *Biological Conservation*, **144**, 470–478.

Van Turnhout, C. A. M., Willems, F., Plate, C., van Strien, A., Teunissen, W., van Dijk, A. and Foppen, R. (2008). Monitoring common and scarce breeding birds in the Netherlands: applying a posthoc stratification and weighting procedure to obtain less biased population trends. *Journal of Catalan Ornithology*, **24**, 15–29.

Walther, G.-R., Post, E., Convey, P., Menzel, A., Parmesan, C., Beebee, T. J., Fromentin, J. M., Hoegh-Guldberg, O. and Bairlein, F. (2002). Ecological responses to recent climate change. *Nature*, **416**, 389–395.

Wang, J. P. Z. and Lindsay, B. G. (2005). A penalized nonparametric maximum likelihood approach to species richness estimation. *Journal of the American Statistical Association*, **100**, 942–959.

Warren, M. S., Hill, J. K., Thomas, J. A., Asher, T. J., Fox, R., Huntley, B., Roy, D. B., Telfer, M. G., Jeffcoate, S., Harding, P., Jeffcoate, G. et al. (2001). Rapid responses of British butterflies to opposing forces of climate and habitat change. *Nature*, **414**, 65–69.

Warton, D. and Aarts, G. (2013). Advancing our thinking in presence-only and used-available analysis. *Journal of Animal Ecology*, **82**, 1125–1134.

Warton, D. I. and Shepherd, L. C. (2010). Poisson point process models solve the pseudo-absence problem for presence-only data in ecology. *Annals of Applied Statistics*, **4**, 1383–1402.

Wenger, S. J. and Freeman, M. C. (2008). Estimating species occurrence, abundance, and detection probability using zero-inflated distributions. *Ecology*, **89**, 2953–2959.

Wood, S. N. (2000). Modelling and smoothing parameter estimation with multiple quadratic penalties. *Journal of the Royal Statistical Society: Series B (Statistical Methodology)*, **62**, 413–428.

Wood, S. N. (2006). *Generalized Additive Models: an introduction with R*. Chapman & Hall/CRC, Boca Raton.

Wood, S. N., Goude, Y. and Shaw, S. (2015). Generalized additive models for large data sets. *Journal of the Royal Statistical Society: Series C (Applied Statistics)*, **64**, 139–155.

Yackulic, C. B., Chandler, R., Zipkin, E. F., Royle, J. A., Nichols, J. D., Campbell Grant, E. H. and Veran, S. (2013). Presence-only modelling using MAXENT: when can we trust the inferences? *Methods in Ecology and Evolution*, **4**, 236–243.

Yamaura, Y. (2013). Confronting imperfect detection: behavior of binomial mixture models under varying circumstances of visits, sampling sites, detectability, and abundance, in small-sample situations. *Ornithological Science*, **12**, 73–88.

Zellweger-Fischer, J., Kéry, M. and Pasinelli, G. (2011). Population trends of brown hares in Switzerland: The role of land-use and ecological compensation areas. *Biological Conservation*, **144**, 1364–1373.

Zonneveld, C. (1991). Estimating death rates from transect counts. *Ecological Entomology*, **16**, 115–121.